



RETURNING MATERIALS:  
Place in book drop to  
remove this checkout from  
your record. FINES will  
be charged if book is  
returned after the date  
stamped below.

--	--	--



**PHOTOCHEMISTRY OF STERICALLY CONGESTED KETONES**

By

Boli Zhou

A DISSERTATION

Submitted to

Michigan State University

In partial fulfillment of the requirements

for the degree of

DOCTOR OF PHILOSOPHY

Department of Chemistry

1988



## ABSTRACT

### PHOTOCHEMISTRY OF STERICALLY CONGESTED KETONES

by

Boli Zhou

The photochemistry of various  $\alpha$ -arylacetophenone derivatives was investigated. Three types of reactions were observed with these ketones:  $\alpha$ -cleavage,  $\delta$ -hydrogen abstraction, and 1,3-aryl migration. The photoreactivity proved to be very sensitive to the substitution in the ketones - one minor structural change could lead to a completely different reaction.

Dynamic NMR studies revealed that the ketones under investigation represented a group of sterically congested ketones. Bond rotation rates in these ketones are substantially slower than the rates of the photoreactions. On the time scale of the photoreactions, the molecules are locked into conformations from which only certain reactions are allowed to occur. Since different molecules have different ground state conformations, the photoreactivity of congested ketones is very diverse.

The considerable decrease in the  $\delta$ -hydrogen abstraction rate for  $\alpha$ -monosubstituted ketones is attributed to the non-ideal geometry from which the reaction occurs. The photokinetic data and conformational analyses of the ketones allowed us to quantitatively correlate the decreased hydrogen abstraction rate to the non-ideal geometric parameters of the reacting conformations.



It  
in the c  
migrati  
complex

The  
7, a -  
a-mes:  
release  
state co

As  
ketone:  
particip

The  
the form  
hydrog  
1,2,3,4-  
formati  
quench  
product  
of the b



It was concluded that a charge transfer process from the  $\alpha$ -mesityl group to the carbonyl oxygen in the  $\alpha$ -mesityl ketones initiated the unusual 1,3-aryl migration observed. The release of steric congestion in the charge transfer complex is the driving force behind 1,3-aryl migration.

The enhancement of  $\alpha$ -cleavage rates for  $\alpha$ -mesitylisobutyrophenone **7**,  $\alpha$ -mesityl-2,4,6-trimethylacetophenone **14**, and  $\alpha$ -mesityl- $\alpha$ -phenyl-2,4,6-trimethylacetophenone **11** is due to either the release of the steric congestion during the reaction or the fact that the ground state conformation favors this reaction.

As an extension of the above studies, the photoreactions of these  $\alpha$ -aryl ketones in the solid state and the photochemistry of several  $\beta$ -arylpropiophenone derivatives were studied.

The photocyclization of the  $\beta$ -arylpropiophenone derivatives involves the formation of a 1,6-biradical via an intramolecular abstraction of an *o*-alkyl hydrogen by the excited carbonyl oxygen which cyclizes to the corresponding 1,2,3,4-tetrahydronaphthols. The low quantum efficiency of product formation is due to the competition of the well known charge transfer quenching of the triplet ketones by the  $\beta$ -aryl group. The enhancement of the product formation in methanol was attributed to an acid-catalyzed formation of the biradical from the charge transfer complex.



The  
guidance  
encourages  
pleasant

The  
State U  
assistant  
Departm

Ver  
and lov



## Acknowledgments

The author wishes to thank Professor Peter J. Wagner for his inspiring guidance throughout the course of this work. His insight, advice, encouragement, and sense of humor have made my graduate career both a pleasant and fruitful one.

The author is grateful to the National Science Foundation and Michigan State University for financial support in the form of teaching and research assistantships. The author would also like to thank the Chemistry Department for the use of its excellent facilities.

Very special thanks are extended to my family members for their support and love.



## Table of Contents

Chapter	Page
List of Tables-----	viii
List of Figures-----	xiv
Introduction-----	1
Results-----	40
I. $\alpha$ -Arylacetophenone derivatives -----	40
A. Photoreactions in Solution-----	40
1. General Preparations of the Ketones-----	40
2. Identification of Photoproducts-----	40
3. Kinetic Data-----	53
4. Dynamic NMR Studies-----	64
5. Molecular Mechanics Calculations-----	72
6. Relative Conformation of Carbonyl Aryl and Carbonyl Group-----	78
7. X-Ray Crystallography-----	79
8. Spectroscopy-----	79
a. Ultraviolet-Visible Absorption Spectra-----	79
b. Phosphorescence Spectra-----	85
B. Photoreactions in Solid State-----	85
II. $\beta$ -Arylpropiophenone Derivatives-----	89
A. Identification of Photoproducts -----	89
B. Kinetic Data-----	93



m

Disc

L

D

D

Expe

L



C. Molecular Mechanics Calculations	93
D. Spectroscopy	95
1. Ultraviolet-Visible Absorption Spectra	95
2. Phosphorescence Spectra	95
III. Representative Low Temperature NMR and Phosphorescence Spectra	96
Discussion	120
I. $\alpha$ -Arylacetophenone Derivatives	120
A. Photochemistry in Solution	120
1. Triplet Lifetimes and Reaction Rates	120
2. What Determines the Excited State Decay Mode?	127
3. $\alpha$ -Substituent Effect on $\delta$ -Hydrogen Abstraction	129
4. Formations of Aryl Vinyl Ethers	141
5. $\alpha$ -Cleavage Reactions	150
6. Kinetic Rotational Control in $\alpha$ -Mesitylvalerophenone	158
7. Possible Formation of the 1,5-Biradical via a Proton Transfer from a Charge Transfer Complex	162
8. Photoenolization of $\alpha$ -(2,4,6-Triisopropylphenyl)-acetophenone	165
B. Photochemistry in Solid State	168
II. $\beta$ -Arylpropiophenone Derivatives	172
III. Derivation of Equation (25)	178
Experimental	181
I. Purification of Chemicals	181
A. Solvents and Additives	181
B. Internal Standards	182
C. Quenchers	182



II. Equipment and Procedures	183
A. Photochemical Glassware	183
B. Sample Preparations	183
C. Degassing Procedures	184
D. Irradiation Procedures	184
E. Analysis Procedures	185
F. Calculation of Quantum Yields	185
G. Methods Used for Product Isolation	187
H. Spectroscopic Measurements	187
III. Preparation of Starting Ketones	188
IV. Isolation and Identification of Photoproducts	212
V. Irradiation in Solid State	226
A. In Powder Form	227
B. In Crystal	229
VI. Irradiation in Cyclodextrin Complexes	231
VII. Dynamic NMR Measurements	233
VIII. Molecular Mechanics Calculations	234
IX. X-Ray Crystallograpgy	235
Appendix	236
References	299



Table

1

2

3

4

5

6

7

8

9

10

11

12



## List of Tables

Table		Page
1	Lifetimes of $\alpha$ -Arylacetophenones-----	54
2	Quantum Yields of Photoproducts from $\alpha$ -Arylacetophenones--	55
3	Dependence of Z/E Ratios of Aryl Vinyl Ethers upon Relative Absorbances at 365 nm-----	63
4	Kinetic Parameters of C $_{\alpha}$ -CO Bond Rotation for $\alpha$ -(o-Tolyl)isobutyrophenone 4-----	66
5	Kinetic Parameters of C $_{\alpha}$ -Mes Bond Rotation for $\alpha$ -Mesitylpropiophenone 5-----	67
6	Kinetic Parameters of C $_{\alpha}$ -Mes Bond Rotation for $\alpha$ -Mesitylvalerophenone 6-----	68
7	Kinetic Parameters of C $_{\alpha}$ -CO Bond Rotation for $\alpha$ -Mesitylisobutyrophenone 7-----	69
8	Kinetic Parameters of C $_{\alpha}$ -Mes Bond Rotation for $\alpha$ -Mesitylisobutyrophenone 7-----	70
9	Kinetic Parameters of C $_{\alpha}$ -Mes Bond Rotation for $\alpha$ -Mesityl- $\alpha$ -Phenylacetophenone 8-----	71
10	Relative Energies of Different Conformations of $\alpha$ -Arylacetophenones-----	73
11	Spectroscopic Data Related to Ar and C=O Conjugation-----	79
12	UV Absorption Maxima and Extinction Coefficients of $\alpha$ -Arylacetophenones-----	80



13	Phosphorescence Maxima ( $\lambda_{0,0}$ ) and Triplet Energy of $\alpha$ -Arylacetophenones-----	85
14	Relative Yields of Photoproducts from Irradiation in Powder----	88
15	Relative Yields of Photoproducts from Irradiation in Crystal----	89
16	Triplet Lifetimes of $\beta$ -Arylpropiophenones in Benzene-----	92
17	Quantum Yields of Tetrahydronaphthols in various solvents---	92
18	Relative Energies of Different Conformations of $\beta$ -Arylpropiophenones-----	93
19	UV Absorption Maxima and Extinction Coefficients of $\beta$ -Arylpropiophenones-----	95
20	Phosphorescence Maxima ( $\lambda_{0,0}$ ) and Triplet Energy of $\beta$ -ArylPropiophenones-----	96
21	Quantum Yields and Rate Constants of Reactions of $\alpha$ -Arylacetophenones-----	123
22	Quantum Yields of Aryl Vinyl Ether Formations in Benzene--	142
23	Rate Constants for $\epsilon$ -Hydrogen Abstraction in Several Ketones-	174
24	Kinetic Data of $C_{\alpha}$ -CO Bond Rotation for $\alpha$ -(o-Tolyl)isobutyrophenone-----	237
25	Kinetic Data of $C_{\alpha}$ -Mes Bond Rotation for $\alpha$ -Mesitylpropiophenone-----	237
26	Kinetic Data of $C_{\alpha}$ -Mes Bond Rotation for $\alpha$ -Mesitylvalerophenone-----	238
27	Kinetic Data of $C_{\alpha}$ -CO Bond Rotation for $\alpha$ -Mesitylisobutyrophenone-----	238
28	Kinetic Data of $C_{\alpha}$ -Mes Bond Rotation for $\alpha$ -Mesitylisobutyrophenone-----	239
29	Kinetic Data of $C_{\alpha}$ -Mes Bond Rotation for	



	$\alpha$ -Mesityl- $\alpha$ -Phenylacetophenone-----	239
30	Quenching Indanol Formation from $\alpha$ -(o-Tolyl)-p-Methoxy- acetophenone with 2,5-Dimethyl-2,4-Hexadiene in Benzene at 313 nm-----	240
31	Quenching Benzaldehyde Formation from $\alpha$ -(o-Tolyl)propio- phenone with Naphthalene in Benzene with 0.007 M Dodecanthiol at 365 nm-----	240
32	Quenching Benzaldehyde Formation from $\alpha$ -(o-Tolyl)propio- phenone with Naphthalene in Benzene with 0.007 M Dodecanthiol at 365 nm-----	241
33	Quenching $\alpha$ -(o-Tolyl)acetophenone Formation from $\alpha$ -(o-Tolyl)valerophenone with 2,5-Dimethyl-2,4-Hexadiene in Benzene at 313 nm-----	241
34	Quenching $\alpha$ -(o-Tolyl)acetophenone Formation from $\alpha$ -(o-Tolyl)valerophenone with 2,5-Dimethyl-2,4-Hexadiene in Benzene at 313 nm-----	242
35	Quenching Benzaldehyde Formation from $\alpha$ -(o-Tolyl)iso- butyrophenone with Naphthalene in Benzene with 0.007 M Dodecanthiol at 365 nm-----	243
36	Quenching Benzaldehyde Formation from $\alpha$ -(o-Tolyl)iso- butyrophenone with Naphthalene in Benzene with 0.007 M Dodecanthiol at 365 nm-----	243
37	Quenching Indanol Formation from $\alpha$ -Mesityl- propiophenone with Naphthalene in Benzene at 365 nm-----	244
38	Quenching Indanol Formation from $\alpha$ -Mesityl- propiophenone with Naphthalene in Benzene at 365 nm-----	244
39	Quenching Indanol Formation from $\alpha$ -Mesityl-	



	valerophenone with Naphthalene in Benzene at 365 nm-----	245
40	Quenching Indanol Formation from $\alpha$ -Mesityl- valerophenone with Naphthalene in Benzene at 365 nm-----	246
41	Quenching Benzaldehyde Formation from $\alpha$ -Mesityliso- butyrophenone with Naphthalene in Benzene with 0.007 M Dodecanthiol at 365 nm-----	247
42	Quenching Benzaldehyde Formation from $\alpha$ -Mesityliso- butyrophenone with Naphthalene in Benzene with 0.007 M Dodecanthiol at 365 nm-----	247
43	Quenching Indanol Formation from $\alpha$ -Mesityl- $\alpha$ -Phenyl- acetophenone with 2,5-Dimethyl-2,4-Hexadiene in Benzene at 365 nm-----	248
44	Quenching Indanol Formation from $\alpha$ -Mesityl- $\alpha$ -Phenyl- acetophenone with 2,5-Dimethyl-2,4-Hexadiene in Hexane at 365 nm-----	249
45	Quenching Aryl Vinyl Ether Formation from $\alpha$ -Mesityl- $\alpha$ - Phenylacetophenone with 2,5-Dimethyl-2,4-Hexadiene in Hexane at 365 nm-----	250
46	Quenching Indanol Formation from $\alpha$ -Mesityl- $\alpha$ - Phenyl-p-Methoxyacetophenone with Naphthalene in Benzene at 365 nm-----	251
47	Quenching Indanol Formation from $\alpha$ -Mesityl- $\alpha$ - Phenyl-p-Methoxyacetophenone with Naphthalene in Benzene at 365 nm-----	251
48	Quenching Aryl Vinyl Ether Formation from $\alpha$ -Mesityl- $\alpha$ - Phenyl-p-Methoxyacetophenone with Naphthalene in Benzene at 365 nm-----	252







49	Quenching Aryl Vinyl Ether Formation from $\alpha$ -Mesityl- $\alpha$ -Phenyl-p-Methoxyacetophenone with Naphthalene in Benzene at 365 nm-----	252
50	Quenching Aryl Vinyl Ether Formation from $\alpha$ -Mesityl- $\alpha$ -Phenyl-p-Cyanoacetophenone with 2,5-Dimethyl-2,4-Hexadiene in Benzene at 365 nm-----	253
51	Quenching Mesitaldehyde Formation from $\alpha$ -Phenyl-2,4,6-Trimethylacetophenone with 2,5-Dimethyl-2,4-Hexadiene in Benzene with 0.007 M Dodecanthiol at 313 nm--	254
52	Quenching Indanol Formation from $\alpha$ -Mesityl-o-Methylacetophenone with Naphthalene in Benzene at 365 nm-----	255
53	Quenching Indanol Formation from $\alpha$ -Mesityl-o-Methylacetophenone with Naphthalene in Benzene at 365 nm-----	255
54	Quenching Mesitaldehyde Formation from $\alpha$ -Mesityl-2,4,6-Trimethylacetophenone with 2,5-Dimethyl-2,4-Hexadiene in Benzene with 0.007 M Dodecanthiol at 313 nm--	256
55	Quenching Mesitaldehyde Formation from $\alpha$ -Mesityl-2,4,6-Trimethylacetophenone with 2,5-Dimethyl-2,4-Hexadiene in Benzene with 0.007 M Dodecanthiol at 313 nm--	257
56	Quenching Mesitaldehyde Formation from $\alpha$ -Mesityl- $\alpha$ -Phenyl-2,4,6-Trimethylacetophenone with 2,5-Dimethyl-2,4-Hexadiene in Benzene with 0.007 M Dodecanthiol at 313 nm--	258
57	Quenching Mesitaldehyde Formation from $\alpha$ -Mesityl- $\alpha$ -Phenyl-2,4,6-Trimethylacetophenone with 2,5-Dimethyl-2,4-Hexadiene in Benzene with 0.007 M Dodecanthiol at 313 nm--	259
58	Quenching Tetralol Formation from $\beta$ -(o-Tolyl)isobutyrophenone with 2,5-Dimethyl-2,4-Hexadiene in Benzene	







	at 313 nm-----	259
59	Quenching Tetralol Formation from $\beta$ -Mesitylisobutyro- phenone with 2,5-Dimethyl-2,4-Hexadiene in Benzene at 313 nm-----	260
60	Quenching Tetralol Formation from $\beta$ -Mesitylisobutyro- phenone with 2,5-Dimethyl-2,4-Hexadiene in Benzene at 313 nm-----	260
61	Quenching Tetralol Formation from $\beta$ -Mesitylpropio- phenone with 2,5-Dimethyl-2,4-Hexadiene in Benzene at 313 nm-----	261
62	GC Response Factors-----	262
63	HPLC Response Factors-----	263
64	Uncorrected HPLC Z/E Ratios of Aryl Vinyl Ethers-----	265
65	Quantum Yields of Photoproducts from $\alpha$ -Aryl- acetophenone Derivatives-----	266
66	Quantum Yields of Photoproducts from $\beta$ -Aryl- propiophenone Derivatives-----	272
67	X-Ray Crystallographic Parameters for $\alpha$ -Mesityl- valerophenone-----	274
68	X-Ray Crystallographic Parameters for $\alpha$ -Mesityl-2,4,6- Trimethylacetophenone-----	286
69	X-Ray Crystallographic Parameters for $\alpha$ -Mesityl- $\alpha$ -Phenyl- acetophenone-----	292



## List of Figures

Figure		Page
1	Polar Transition State for $\alpha$ -Cleavage-----	9
2	Transition State for Hydrogen Abstraction-----	11
3	$\alpha$ -Cycloalkyl-p-Chloroacetophenones-----	31
4	2-Methyl-3-Phenyl-2,3-Dihydrobenzofurans-----	44
5	2-Methyl-1-Phenylcyclobutanols-----	44
6	2-t-Butyl-1-Phenylcyclobutanols-----	44
7	3-Hydroxy-3-Methyl-2-Phenyl-2,3-Dihydrobenzofurans-----	45
8	3,4,6-Trimethyl-2-Phenyl-2-Indanols-----	46
9	4,6-Dimethyl-2-Phenyl-3-Propyl-2-Indanols-----	47
10	4,6-Dimethyl-2,3-Diphenyl-2-Indanols-----	47
11	1-Mesitoxyl-1,2-Diphenylethylene-----	48
12	Deuterium NMR Spectrum of Reaction Mixture from $\alpha$ -(2,4,6-Triisopropylphenyl)acetophenone-d <sub>2</sub> -----	49
13	<sup>1</sup> H NMR Spectrum of Reaction Mixture from $\alpha$ -(2,4,6-Triisopropylphenyl)acetophenone-----	50
14	Stern-Volmer Plot for $\alpha$ -Mesitylvalerophenone-----	58
15	Dependence of Benzaldehyde Formation from $\alpha$ -(o-Tolyl)- propiophenone on the Concentration of Dodecanthiol-----	59
16	Dependence of Benzaldehyde Formation from $\alpha$ -(o-Tolyl)- isobutyrophenone on the Concentration on Dodecanthiol-----	60



17	Plot of $1/\Phi_{isc}$ vs. [cis-Stilbene] in Sensitized Isomerization of cis-Stilbene by $\alpha$ -Mesityl- $\alpha$ -Phenylacetophenone-----	61
18	Restricted Rotation of $C_{\alpha}$ -CO Bond in Ketone 4-----	64
19	Restricted Rotation of $C_{\alpha}$ -Mes Bond in Ketone 5, 6, 8-----	64
20	Restricted Rotations of $C_{\alpha}$ -CO and $C_{\alpha}$ -Mes Bonds in Ketone 7-----	65
21	Plot of $\ln k$ vs. $1/T$ for $C_{\alpha}$ -CO Bond in Ketone 4-----	66
22	Plot of $\ln k$ vs. $1/T$ for $C_{\alpha}$ -Mes Bond in Ketone 5-----	67
23	Plot of $\ln k$ vs. $1/T$ for $C_{\alpha}$ -Mes Bond in Ketone 6-----	68
24	Plot of $\ln k$ vs. $1/T$ for $C_{\alpha}$ -CO Bond in Ketone 7-----	69
25	Plot of $\ln k$ vs. $1/T$ for $C_{\alpha}$ -Mes Bond in Ketone 7-----	70
26	Plot of $\ln k$ vs. $1/T$ for $C_{\alpha}$ -Mes Bond in Ketone 8-----	71
27	X-Ray Structure of $\alpha$ -Mesitylvalerophenone 6-----	80
28	X-Ray Structure of $\alpha$ -Mesityl- $\alpha$ -Phenylacetophenone 8-----	81
29	X-Ray Structure of $\alpha$ -Mesityl-2,4,6-Trimethyl- acetophenone 14-----	82
30	2-Methyl-1-Phenylcyclohexanols-----	91
31	$^1H$ NMR of $\alpha$ -( <i>o</i> -Tolyl)isobutyrophenone 4 at 260 K-----	97
32	$^1H$ NMR of $\alpha$ -( <i>o</i> -Tolyl)isobutyrophenone 4 at 180 K-----	98
33	$^1H$ NMR of $\alpha$ -( <i>o</i> -Tolyl)isobutyrophenone 4 at 170 K-----	99
34	$^1H$ NMR of $\alpha$ -Mesitylpropiophenone 5 at 300 K-----	100
35	$^1H$ NMR of $\alpha$ -Mesitylpropiophenone 5 at 240 K-----	101
36	$^1H$ NMR of $\alpha$ -Mesitylpropiophenone 5 at 200 K-----	102
37	$^1H$ NMR of $\alpha$ -Mesitylvalerophenone 6 at 340 K-----	103
38	$^1H$ NMR of $\alpha$ -Mesitylvalerophenone 6 at 260 K-----	104
39	$^1H$ NMR of $\alpha$ -Mesitylvalerophenone 6 at 230 K-----	105
40	$^1H$ NMR of $\alpha$ -Mesityl- $\alpha$ -Phenylacetophenone 8 at 300 K-----	106



41

42

43

44

45

46

47

48

49

50

51

52

53

54

55

56

57

58

59



41	<sup>1</sup> H NMR of of $\alpha$ -Mesityl- $\alpha$ -Phenylacetophenone 8 at 188 K—	107
42	<sup>1</sup> H NMR of of $\alpha$ -Mesityl- $\alpha$ -Phenylacetophenone 8 at 170 K—	108
43	<sup>1</sup> H NMR of of $\alpha$ -Mesitylisobutyrophenone 7 at 300 K—	109
44	<sup>1</sup> H NMR of of $\alpha$ -Mesitylisobutyrophenone 7 at 200 K—	110
45	<sup>1</sup> H NMR of of $\alpha$ -Mesitylisobutyrophenone 7 at 185 K—	111
46	<sup>1</sup> H NMR of of $\alpha$ -Mesitylisobutyrophenone 7 at 170 K—	112
47	Phosphorescence Spectrum of $\alpha$ -Mesitylpropio- phenone 5 at 77 K—	113
48	Phosphorescence Spectrum of $\alpha$ -Mesitylvalero- phenone 6 at 77 K—	114
49	Phosphorescence Spectrum of $\alpha$ -Mesitylisobutyro- phenone 7 at 77 K—	115
50	Phosphorescence Spectrum of $\alpha$ -Mesityl- $\alpha$ -Phenylaceto- phenone 8 at 77 K—	116
51	Phosphorescence Spectrum of $\alpha$ -Mesityl- $\alpha$ -Phenyl-2,4,6- Trimethylacetophenone 11 at 77 K—	117
52	Phosphorescence Spectrum of $\alpha$ -Mesityl-2,4,6-Trimethyl- acetophenone 14 at 77 K—	118
53	Phosphorescence Spectrum of $\beta$ -Mesitylisobutyro- phenone 21 at 77 K—	119
54	Geometric Parameters for Hydrogen Abstraction—	130
55	Ideal Geometry for $\delta$ -Hydrogen Abstraction—	131
56	Restricted Bond Rotation for $\alpha$ -Memosubstituted $\alpha$ -Mesitylacetophenones—	133
57	Steric Interaction during Mesityl Rotation—	134
58	Steric Interaction in the Ideal Geometry—	135
59	Conformation for Charge Transfer—	147



60

61

62

63

64

65

66

67

68

69

70

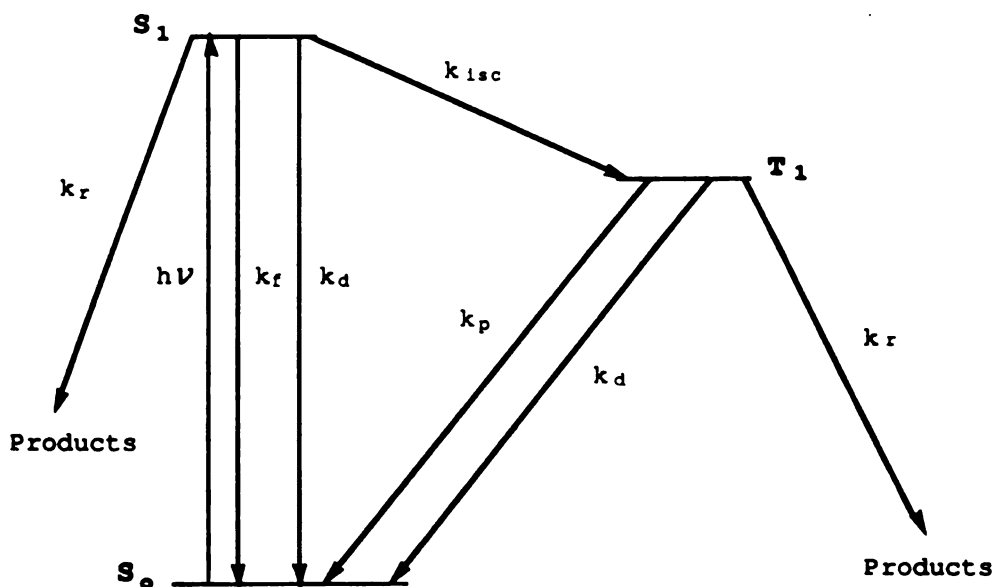


60	Conformation of 1,2,2-Trimesitylethanone-----	149
61	Restricted Rotation in $\alpha$ -Arylisobutyrophenones-----	151
62	Conformation of $\alpha$ -Arylisobutyrophenones-----	152
63	Twisted conformation of $\alpha$ -Mesitylisobutyrophenone-----	153
64	Transition State of $\alpha$ -Cleavage from $\alpha$ -Mesityl-2,4,6- Trimethylacetophenone-----	156
65	Conformation of $\alpha$ -Mesityl- $\alpha$ -Phenyl-2,4,6- Trimethylacetophenone-----	157
66	Destabilized Transition State of $\gamma$ -Hydrogen Abstraction from $\alpha$ -Mesitylvalerophenone-----	162
67	1,6-Biradical Generated in $\epsilon$ -Hydrogen Abstraction-----	172
68	Ideal Geometry for $\epsilon$ -Hydrogen Abstraction-----	173
69	Conformational Interconversion in $\beta$ -Aryl- propiophenones-----	175
70	Glassware for Irradiation in Crystal-----	227



## Introduction

Carbonyl compounds comprise a large and important class of organic substances. The chemistry of this functional group is essential to the understanding of many chemical and biochemical processes. It has been the most widely studied functional group in organic chemistry since the early stage of chemistry. Photochemistry of ketones likewise has occupied the mainstream of organic photochemistry. The study of the photochemistry of carbonyl compounds has helped in the understanding of very fundamental



Scheme 1

questions in photochemistry. These questions have to be answered to understand how light produces chemical changes in more sophisticated



chemical and biological systems.

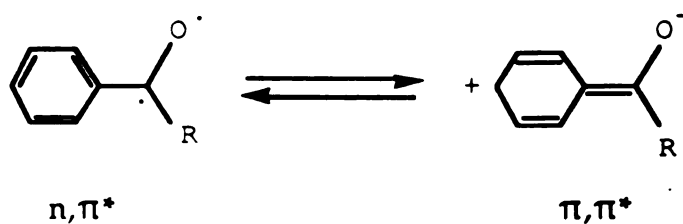
The photophysical and photochemical processes of molecules can be best described with a Jablonski<sup>1</sup> diagram (Scheme 1). Absorption of a photon promotes energetically a molecule from the ground state to the singlet excited state. The excited state molecule can decay to the ground state via emission of light (fluorescence) or radiationless decay. The former has a rate constant ( $k_f$ ) on the order of  $10^6$ - $10^9$  s<sup>-1</sup>, and the latter ( $k_d$ )  $10^5$ - $10^8$  s<sup>-1</sup>.<sup>2</sup> Photochemical reactions are possible from the excited singlet. The excited singlet can also undergo intersystem crossing to an excited triplet state. Typical rate constants for intersystem crossing ( $k_{isc}$ ) are on the order of  $10^7$ - $10^{10}$  s<sup>-1</sup>.<sup>2</sup> Direct population of the triplet state from the ground state by absorption of light is forbidden by spin selection rules. The excited triplet can decay via radiative deactivation (phosphorescence) with a rate constant,  $k_p$ , from  $10^1$ - $10^4$  s<sup>-1</sup>.<sup>2</sup> It can also undergo radiationless decay and chemical reaction. Quenching of the triplet state by energy transfer and charge transfer can occur with a rate constant as high as the rate of diffusion in a given solvent ( $<10^{10}$  M<sup>-1</sup> s<sup>-1</sup>).<sup>3</sup>

For phenyl ketones, the rate constant of intersystem crossing,  $k_{isc}$ , is about  $10^{11}$  s<sup>-1</sup>,<sup>4</sup> so fluorescence and radiationless decay are negligible. As a result, the quantum yields of intersystem crossing in phenyl ketones are close to unity.<sup>5b-c</sup> Thus irradiation of a phenyl ketone results in an indirect population of its lowest excited triplet state.

Phenyl ketones have two low lying triplets, a  $n,\pi^*$  triplet and a  $\pi,\pi^*$  triplet, whose energy levels are affected by the ring substituents. The  $n,\pi^*$  triplet comes from excitation of a nonbonding electron of the carbonyl group to a  $\pi$ -antibonding orbital, creating an electron deficient oxygen. The chemical behavior of the  $n,\pi^*$  triplet state is thus similar to that of an alkoxyl radical.  $\alpha$ -Cleavage, hydrogen abstraction, and charge transfer from an



electron donor are the reactions frequently observed.<sup>6-8</sup> The  $\pi, \pi^*$  triplet, on the other hand, arises from promotion of an electron from a  $\pi$ -bonding orbital to a  $\pi^*$ -antibonding orbital. This results in a shift of electron density from the aromatic  $\pi$ -system to the carbonyl oxygen, generating an electron rich oxygen (Scheme 2), and makes the  $\pi, \pi^*$  triplet much less reactive than the  $n, \pi^*$  triplet, or nonreactive, in the reactions mentioned above. However,



Scheme 2

thermal equilibration between the triplets can occur, if they are close enough in energy. As a result, ketones with a  $\pi, \pi^*$  lowest triplet state do undergo typical  $n, \pi^*$  triplet reactions, but with a slower rate, which is a reflection of the population of reacting  $n, \pi^*$  state in the equilibration. The reaction rate constant can be expressed as follows,

$$k_{\text{obs}} = k_r(n, \pi)X(n, \pi) \quad (1)$$

where  $k_{\text{obs}}$  is the observed rate constant,  $k_r(n, \pi)$  is the intrinsic rate constant of the  $n, \pi^*$  state, and  $X(n, \pi)$  is the percentage population of the  $n, \pi^*$  state in the equilibrium.<sup>5a, 9-11</sup>

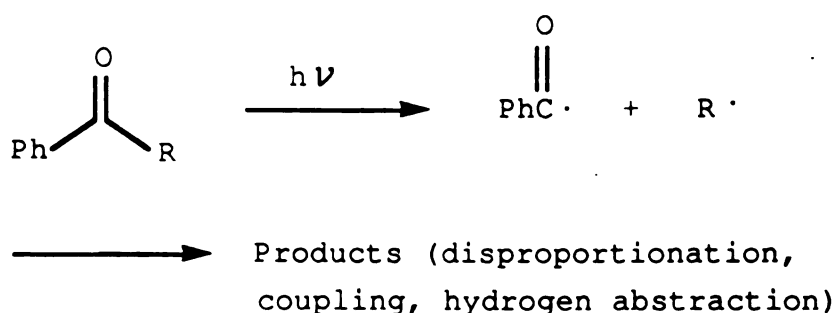
During the course of research involving the photochemistry of ketones, a wide variety of reactions have been reported. The reactions closely related



to the research presented in this thesis are summarized below.

### $\alpha$ -Cleavage Reactions

An excited ketone can undergo  $\alpha$ -cleavage reaction. The cleavage is followed by disproportionation, coupling, or hydrogen abstraction from a hydrogen donor, of the radicals generated by the cleavage. This reaction is frequently referred to as Norrish Type I reaction (Scheme 3).<sup>23a-b</sup>



Scheme 3

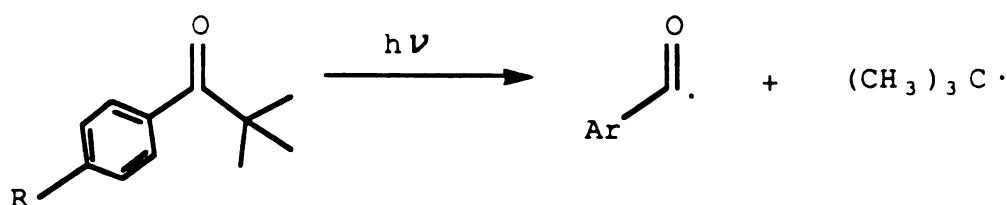
The rate constant of the reaction depends on the nature of the excited state, on the relative stability of the alkyl radicals formed, and probably on the degree of steric crowding in the reactant ketone. These points are demonstrated with the following examples.

The reaction has been generally recognized as a reaction of a  $n, \pi^*$  excitation. The simple concept of  $n, \pi^*$  excitation resulting in weakening of the  $\alpha$ -carbon bond by overlap with the vacant  $n$  orbital has been a useful theoretical model for the reaction.<sup>12</sup> This simple picture is also consistent with the well known behavior of alkoxy radicals.<sup>13-14</sup> When the excited state



configuration is  $\pi, \pi^*$ , no such overlap is possible and the reaction does not occur.

Lewis<sup>15</sup> has shown that pivalophenone, which has a lowest  $n, \pi^*$  triplet state cleaves with a rate constant of around  $10^7 \text{ s}^{-1}$ , but p-methoxypivalophenone with a  $\pi, \pi^*$  lowest triplet state has only a reaction rate constant of only  $10^5 \text{ s}^{-1}$ . Furthermore, in the same study, p-phenylpivalophenone, which also has a  $\pi, \pi^*$  lowest triplet state, is essentially stable to photolysis (Reaction 1).



R=H, pivalophenone

R=p-CH<sub>3</sub>OPh, p-methoxypivaphenone

R=Ph, p-phenylpivalophenone

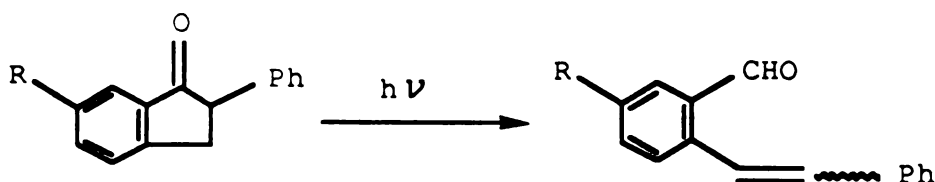
#### Reaction 1

Baum<sup>16</sup> reported a similar study with 2-phenyl-1-indanone and 2,6-diphenyl-1-indanone. Although 2-phenyl-1-indanone cleaves efficiently to isomeric products, 2,6-diphenyl-1-indanone affords little product. This observation is consistent with the fact that 2-phenyl-1-indanone has a  $n, \pi^*$  lowest triplet and 2,6-diphenyl-1-indanone has a  $\pi, \pi^*$  lowest triplet (Reaction 2).



In the case of aliphatic ketones, where both singlet and triplet state can be populated, it has been shown that the triplet state of an aliphatic ketone cleaves about 100 times faster than the first formed singlet.<sup>17-18</sup>

Turro<sup>17</sup> has estimated the  $n,\pi^*$  singlet and triplet reactivity towards  $\alpha$ -cleavage with several cyclic ketones. It was concluded that the triplet rate constant of these ketones was larger than  $5 \times 10^{10} \text{ s}^{-1}$ , and on the other hand the singlet rate constant was smaller than  $2.5 \times 10^8 \text{ s}^{-1}$ .



R=H, 2-phenyl-1-indanone

R=Ph, 2,6-diphenyl-1-indanone

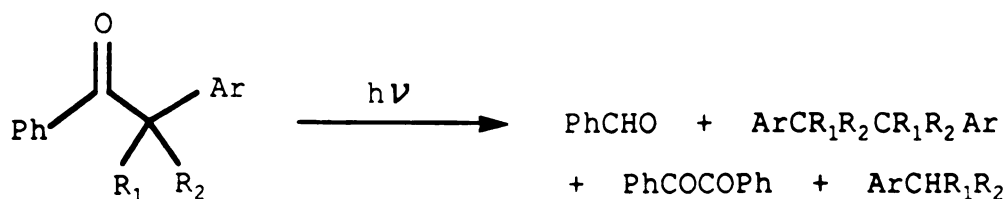
## Reaction 2

In a separate study, Yang<sup>18</sup> observed that di-tert-butyl ketone underwent the type I process with a rate of  $6 \times 10^7 \text{ s}^{-1}$  from the singlet excited state and with a rate of  $7.9 \times 10^9 \text{ s}^{-1}$  from the triplet.

While  $\alpha$ -cleavage is the major mode of deactivation for certain aliphatic ketones,<sup>19</sup> phenyl ketones undergo  $\alpha$ -cleavage at much slower rates. Even in  $\alpha,\alpha$ -dimethylvalerophenone,  $\gamma$ -hydrogen abstraction is sufficiently fast that  $\alpha$ -cleavage comprises only about 5% of the reactivity.<sup>20</sup> In fact triplet aliphatic t-butyl ketones  $\alpha$ -cleave about 4000 times faster than triplet pivalophenone.<sup>21</sup>



The triplet energy of aliphatic ketones is normally larger than 79 Kcal/mole, while that of phenyl ketones is around 74 Kcal/mole.<sup>22</sup> The energetic difference is an important factor responsible for the different activities towards  $\alpha$ -cleavage reaction between aliphatic and phenyl ketones. High triplet energy facilitates the breaking-down of the strong OC-R bond (80-90 Kcal/mole).<sup>20,24c</sup>



	$1/\tau \text{ (s}^{-1}\text{)}$
$\text{R}_1=\text{R}_2=\text{H}, \text{Ar}=\text{Ph}$	$1.6 \times 10^6$
$\text{R}_1=\text{H}, \text{R}_2=\text{CH}_3, \text{Ar}=\text{Ph}$	$2.1 \times 10^7$
$\text{R}_1=\text{R}_2=\text{CH}_3, \text{Ar}=\text{Ph}$	$1.2 \times 10^8$
$\text{R}_1=\text{H}, \text{R}_2=\text{Ph}, \text{Ar}=\text{Ph}$	$1.0 \times 10^8$
$\text{R}_1=\text{R}_2=\text{H}, \text{Ar}=\text{p-ClPh}$	$1.9 \times 10^6$
$\text{R}_1=\text{R}_2=\text{H}, \text{Ar}=\text{p-FPh}$	$2.8 \times 10^6$
$\text{R}_1=\text{R}_2=\text{H}, \text{Ar}=\text{p-MePh}$	$3.6 \times 10^6$

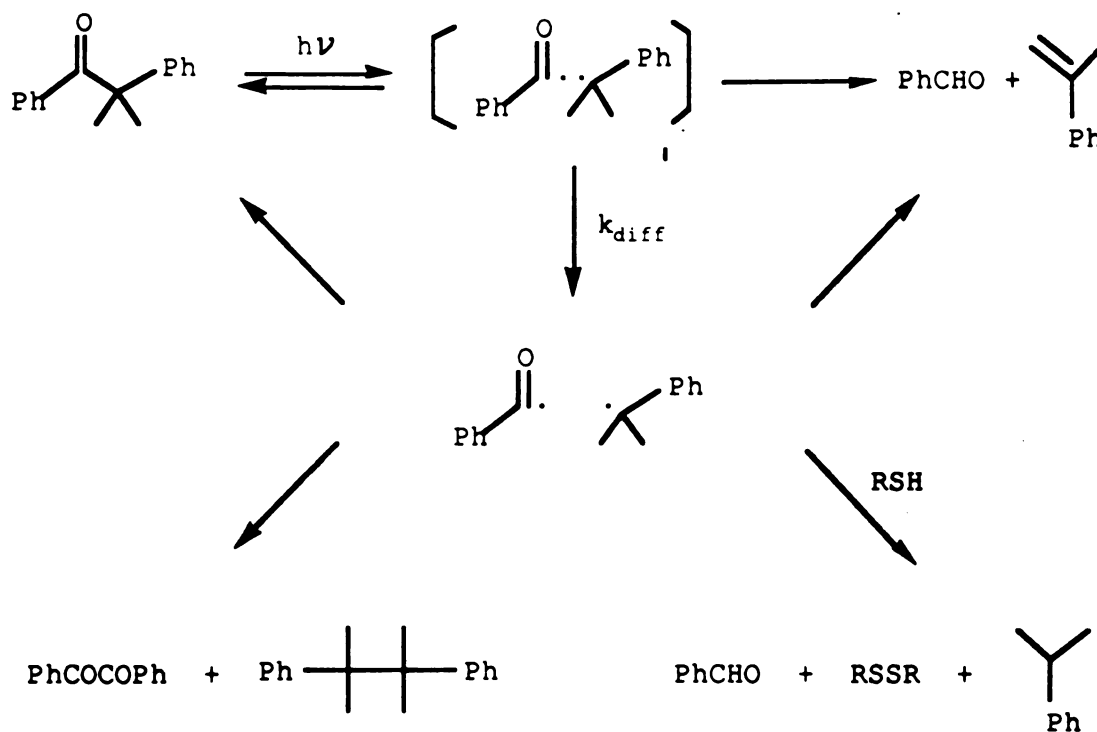
### Reaction 3

Lewis<sup>24</sup> reported a detailed study of the photochemistry of  $\alpha$ -phenylacetophenones (Reaction 3). The products observed upon the irradiation of ketones can be accounted for in terms of a general mechanism shown in scheme 4. The radicals are formed initially in a solvent cage.



Possible cage reactions of the caged radical pairs include recombination of the radicals to give ground state ketones, diffusion to separated radical pairs, and disproportionation in the cases where it is possible. Noncage reactions include recombination, coupling, hydrogen abstraction from an external hydrogen atom donor, and disproportionation where it is possible.

The formation of caged radical pairs is demonstrated by the fact that 33% of *s*-(+)- $\alpha$ -phenylpropiophenone undergoes racemization upon irradiation. The racemization arises from the recombination of the radical pairs in solvent cages.<sup>24c</sup>



Scheme 4

The separated radicals can be trapped with radical scavengers such as thiols. Lewis has shown that addition of low concentration of dodecanethiol



greatly increases the quantum yields for benzaldehyde formation. The quantum yields rise to a maximum of ca. 0.45 at  $2 \times 10^{-3}$  M thiol concentration.<sup>24a-b</sup> This is the point where all the outcage benzoyl radicals have been trapped to form benzaldehyde.

Electron donating groups on the  $\alpha$ -ring accelerate the reaction, indicating an early transition state with a moderate degree of ionic character. The transition state can be depicted as in Figure 1.<sup>24</sup>

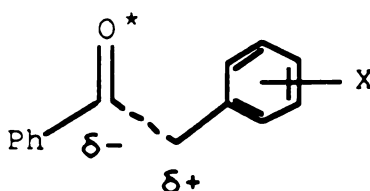


Figure 1

$\alpha$ -Substituents also speed up the cleavage. However, it was concluded that the effect of substituents upon triplet lifetimes shows that the rate constants do not depend on the stability of the resulting radicals, but rather on the ground state steric effects with these ketones.<sup>24b</sup>

### Hydrogen Abstraction Reactions

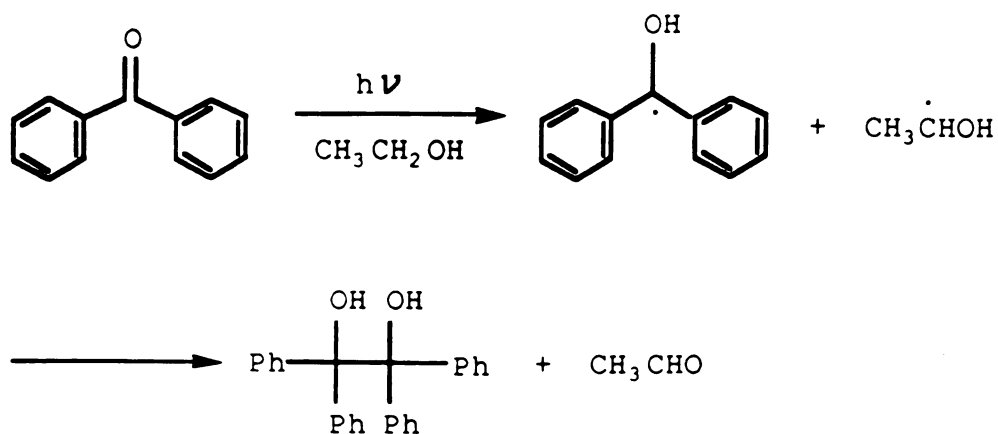
Photoexcited ketones undergo characteristic hydrogen abstraction from compounds having reactive hydrogens. This reaction was first observed by Ciamician and Silber at the beginning of this century.<sup>25</sup> When benzophenone was irradiated in ethanol, benzpinacol was formed by coupling of benzophenone ketyl radicals generated by hydrogen abstraction from ethanol



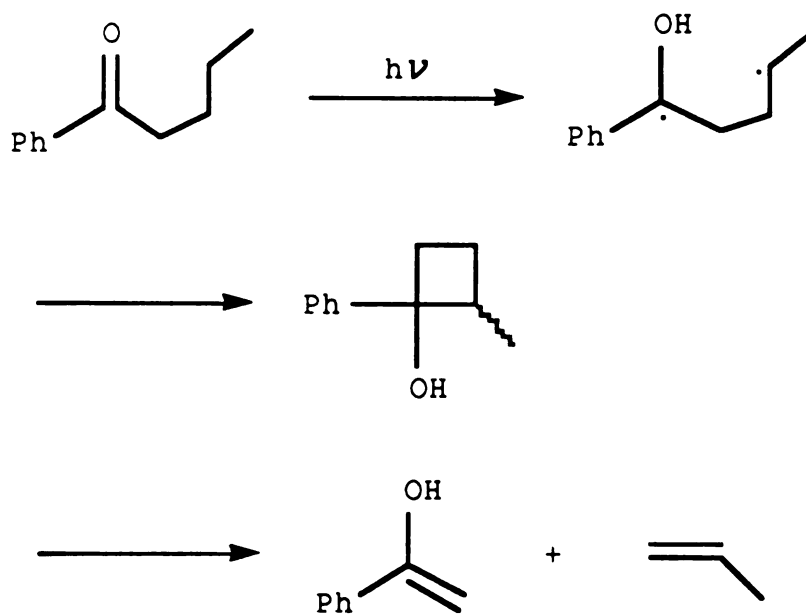




by benzophenone (Reaction 4).



Reaction 4



Scheme 5

Since then a wide variety of photochemical hydrogen abstractions have



been reported. Intramolecular hydrogen abstraction reactions are probably the most important development of the initially discovered reaction. Norrish Type II reaction is the classic example of intramolecular hydrogen abstractions.<sup>23c,5a</sup> This reaction involves formation of a 1,4-biradical via abstraction of a  $\gamma$ -hydrogen by the excited carbonyl oxygen. The biradical can either cleave into an olefin and the enol of a smaller ketone, or cyclize to a cyclobutanol (Scheme 5).

The rate constant for internal hydrogen abstraction depends on electronic configuration, on C-H bond strength, and on conformational factors. It has been well accepted that hydrogen abstractions occur from the  $n, \pi^*$  excited state of the ketones. The radical-like oxygen of a  $n, \pi^*$  excited ketone behaves in the same way as an alkoxy radical (Figure 2). Hydrogen abstraction is one of the most frequently observed reactions for an alkoxy radical.<sup>26</sup>

Simple phenyl ketones undergo hydrogen abstraction reactions from their  $n, \pi^*$  triplet states. Ring substituents that lower the  $\pi, \pi^*$  level below  $n, \pi^*$  level decrease the observed rate constants for the reactions.

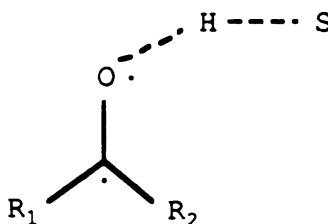
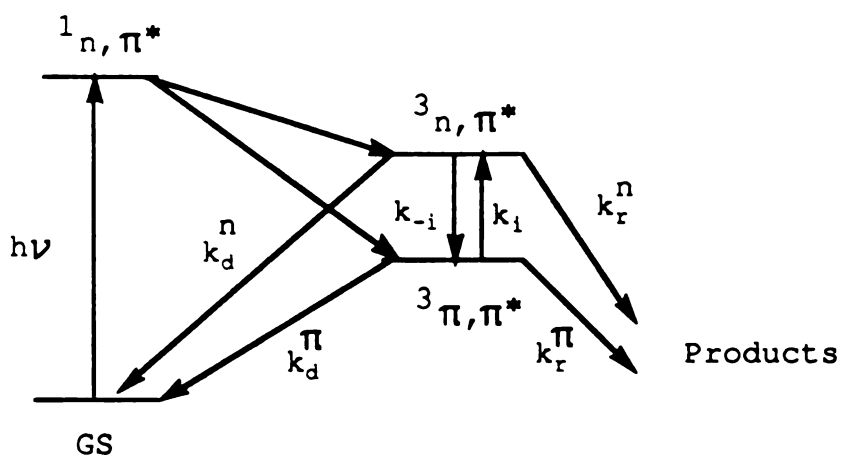


Figure 2

Yang<sup>9</sup> has shown that methyl and methoxy substituents lower the reactivity of acetophenone in its photoreduction. Wagner<sup>10-11</sup> has reported a



study of substituent effects on the photoreactivity of ring substituted valerophenones. Phenyl, methoxy, thiomethoxy, cyano, and methyl groups as well as chlorine atom alter the  $n,\pi^*$  and  $\pi,\pi^*$  energy such that the  $\pi,\pi^*$  is the lowest triplet for the phenyl ketones with such substituent. As a result, these substituents decrease the chemical reactivity of the ketone triplets. The triplet reactivity of the ketones decreases as the energy gap  $\Delta E_T$  between the  $n,\pi^*$  and  $\pi,\pi^*$  triplets increases. The following scheme (scheme 6) outlines the kinetic possibilities of the excited ketones. Population of  $n,\pi^*$  singlets is achieved by direct irradiation. The excited singlet states then undergo intersystem crossing to the triplets, which can either react, or decay to the ground states. A fast equilibrium is assumed between the two triplet states. In



Scheme 6

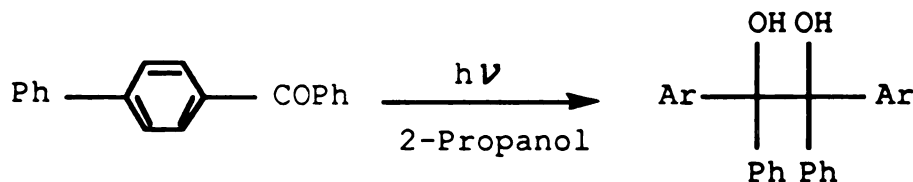
general, the possibility exists for direct decay of the  $n,\pi^*$  triplet to the ground state ketone, but for most simple ketones  $k_r^n \gg k_d^n$  with  $k_d^n$  being  $< 10^6 \text{ s}^{-1}$ .<sup>2</sup> The  $\pi,\pi^*$  triplet can decay to ground state, or possibly react slowly. However, the  $\pi,\pi^*$  triplet is frequently considered nonreactive on the



time-scale of the  $n,\pi^*$  reactions.

2-Acetonaphthone is known to have a  $\pi,\pi^*$  state so much below its  $n,\pi^*$  state that it can not be photoreduced by secondary alcohols. Although it does react with a more powerful hydrogen donor such as tri-*n*-butylstannane,<sup>27a</sup> the deactivation of the ketone towards the photoreduction is well illustrated. 2-Valeronaphthone undergoes type II reaction with very low quantum efficiency. The reaction is unquenchable by triplet quenchers, and thus is believed to occur from its singlet state, rather than from its  $n,\pi^*$  triplet.<sup>27b-c</sup>

4-Phenylbenzophenone provides another example of the reduced photoreactivity for a ketone with a  $\pi,\pi^*$  lowest triplet. The reduction of 4-phenylbenzophenone proceeds with a rate constant of  $1 \times 10^3 \text{ M}^{-1}\text{s}^{-1}$ ,  $10^{-4}$  times as great as that displayed by ketones with  $n,\pi^*$  lowest triplet (Reaction 5).<sup>28</sup>



Reaction 5

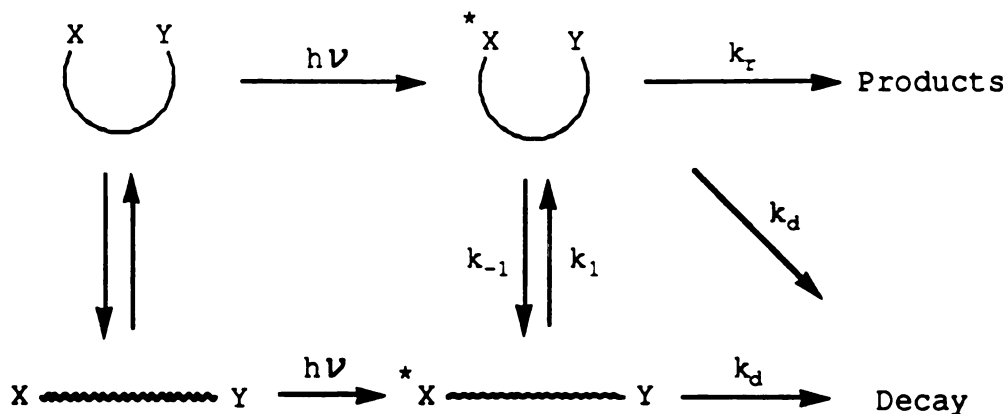
The naphyl and biphenyl ketones discussed above have  $\pi,\pi^*$  triplet levels so much below their  $n,\pi^*$  triplet states that equilibration may not be possible. The reactivity shown can be viewed as the intrinsic one for  $\pi,\pi^*$  excitation, like what is observed with  $\text{C}=\text{C}$  double bonds,<sup>29</sup> and reflects the amount of unpaired spin density on oxygen in the  $\pi,\pi^*$  triplet.

$n,\pi^*$  Singlet ketones abstract hydrogen atoms as rapidly as  $n,\pi^*$  triplet



ketones do, if the intersystem crossing is slow enough to allow a substantial population of the singlet states. In fact, the type II reaction was one of the first in which involvement of both triplets and singlets was demonstrated.<sup>30</sup> However it was noticed that the details of the singlet and triplet reactions are very different. It is now recognized that the two excited states follow different mechanisms. Although a biradical is generally involved in a triplet intramolecular hydrogen abstraction, a singlet reaction prefers non-biradical mechanisms.<sup>5a,31</sup>

Any intramolecular reaction requires the two interacting groups to get close to each other in such a way that proper orbital overlap and reaction can occur. This requirement makes photochemical intramolecular hydrogen



### Scheme 7

abstraction reactions very sensitive to conformational limitations, since the photochemical processes can occur at a competitive or faster rate with respect to the conformational motions. Scheme 7 summarizes the general problems.<sup>32</sup>

The ground state is composed of an equilibrium mixture of



conforma

X and exc

excited c

coefficien

conforma

that do

condition

1.

k

2.

k

3.

1

Ex

observed

molecul

number

In

conform

constant

abstract

reaction

reflect t

decrease

for the



conformations with generally a small fraction favorable for reactions between X and excited Y. Excitation instantaneously produces the same distribution of excited conformers modified only by any slight difference in extinction coefficients between different conformers. The competition between conformational change, reaction, and decay (all other excited state processes that do not lead to the product in question) provides three boundary conditions:

1. Excited State Conformational Equilibrium

$$k_1, k_{-1} \gg k_r, k_d$$

2. Ground State Control

$$k_1, k_{-1} \ll k_r, k_d$$

3. Rotational Control

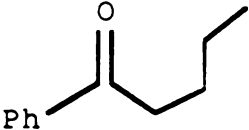
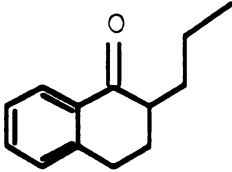
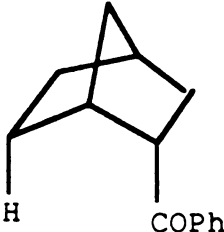
$$k_1 \sim k_d; k_{-1} < k_r$$

Excited state conformational equilibrium is the most commonly observed control factors in photochemistry, since in most sterically non-rigid molecules, conformational changes can occur prior to any photoreactions. A number of examples have been reported in literature.<sup>33-35,37</sup>

In general, the larger the fraction of excited state molecules in the conformation favorable for the photoreaction, the larger the observed rate constant for the reaction. For example, it was found that  $\gamma$ -hydrogen abstraction is more rapid in cyclic ketones than in acyclic ketones.<sup>33</sup> The reaction rates are shown above. It was suggested that the rate enhancements reflect the increased number of "frozen" C-C bonds in the reactant, i.e., a decreased probability that molecules can exist in a conformation unsuitable for the reaction. In support of this interpretation, 2-benzoylnorbornane



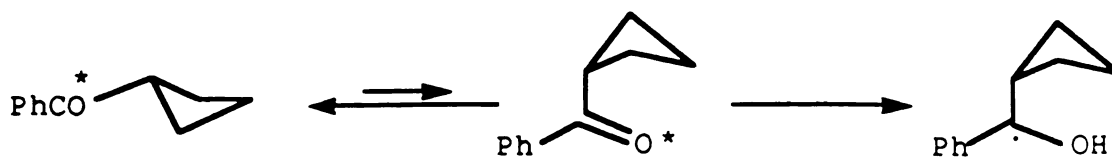
shows the same triplet activation energy as valerophenone but an activation entropy that is 8 eu less negative.

	$k_H, 10^8 \text{ s}^{-1}$	$E_a, \text{ Kcal}$	$\Delta S^\ddagger, \text{ eu}$
	1.2	3.5	-12
	6.0		
	70.0	3.7	-4

Alexander<sup>34</sup> has shown that an excited state equilibrium between the two triplet ketone conformers is an important factor in the photochemistry of cyclobutyl phenyl ketone. The rapid ring puckering motions of cyclobutane allows conformational equilibrium to be established before excited states decay. The low quantum yield of type II reaction and long triplet lifetime was ascribed to a very low equilibrium population of the pseudoaxial conformer, from which the reaction is to occur (Scheme 8).

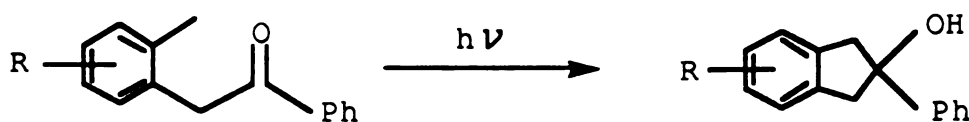
Wagner<sup>35</sup> has found that  $\alpha$ -(o-alkylphenyl)acetophenones undergo photocyclization to 2-indanols via triplet  $\delta$ -hydrogen abstraction, with the





Scheme 8

kinetic data listed below (Reaction 6). The photocyclization of the ketones is quite sensitive to the substitution on the  $\alpha$ -ring. This manifests itself in two different effects.


 $\tau^{-1} \times 10^{-9}$ 

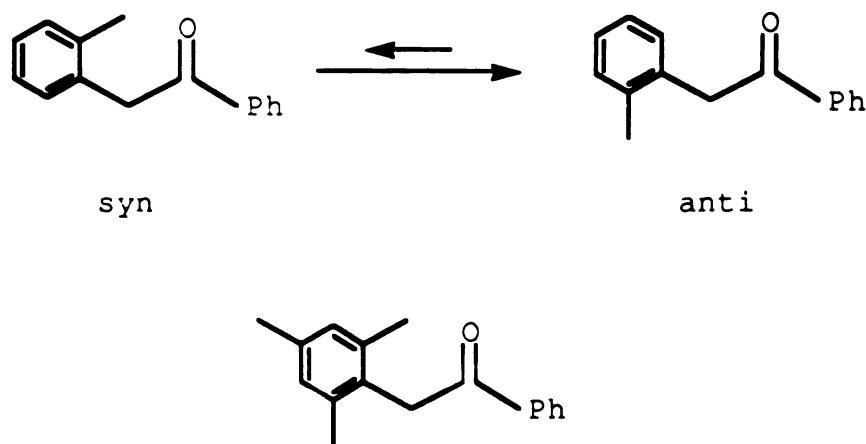
$\alpha$ -( <i>o</i> -Tolyl)acetophenone	0.16
$\alpha$ -(2,5-Dimethylphenyl)acetophenone	0.26
$\alpha$ -Mesitylacetophenone	1.1

Reaction 6

First, alkyl substituents on the  $\alpha$ -ring increase the rate of hydrogen abstraction by inductive effects. However, several literature<sup>26,36</sup> reports indicate that inductive effects result in only a 1.2 to 1.8 fold greater reactivity for mesitylene relative to toluene in benzylic hydrogen abstraction. So such inductive effects can't alone explain the observation that



$\alpha$ -mesitylacetophenone is nearly 7 times more reactive than  $\alpha$ -(o-tolyl)acetophenone.



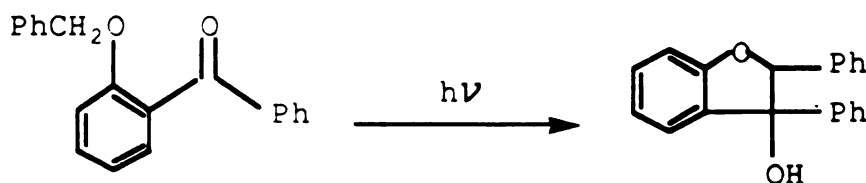
Scheme 9

A interpretation of the results based on conformational restriction was then provided by the authors.<sup>35</sup> It is assumed that there are two possible conformations for  $\alpha$ -(o-tolyl)acetophenone. Both of them have their  $C_{\alpha}$ -Ar bond eclipsing with the C=O bond. The tolyl group, however, can be oriented with the o-methyl group either on the same side (syn conformer), or different side (anti conformer) with the carbonyl group, with the latter being favored (Scheme 9).  $\delta$ -Hydrogen abstraction is not possible in the anti conformation, since the o-methyl group is not accessible to the carbonyl group. The  $\alpha$ -ring has to rotate to the less stable syn conformation in order for the reaction to occur. Symmetric 2,6-dimethyl substitution of the  $\alpha$ -phenyl group, as in  $\alpha$ -mesitylacetophenone, would eliminate the possibility of an anti conformer, leaving only the syn conformation (Scheme 9). Hence, the difference in the lifetimes for  $\alpha$ -mesitylacetophenone and



$\alpha$ -(o-tolyl)acetophenone is partially due to the lack of any unreactive anti conformer for  $\alpha$ -mesitylacetophenone.

Wagner and Meador<sup>37</sup> have estimated the excited state conformational equilibrium constant for o-(benzyloxy)benzophenone, o-(benzyloxy)benzophenone which is known to produce the corresponding dihydrobenzofuranol,<sup>38</sup> presumably by cyclization of the 1,5-biradical formed by  $\delta$ -hydrogen abstraction (Reaction 7).

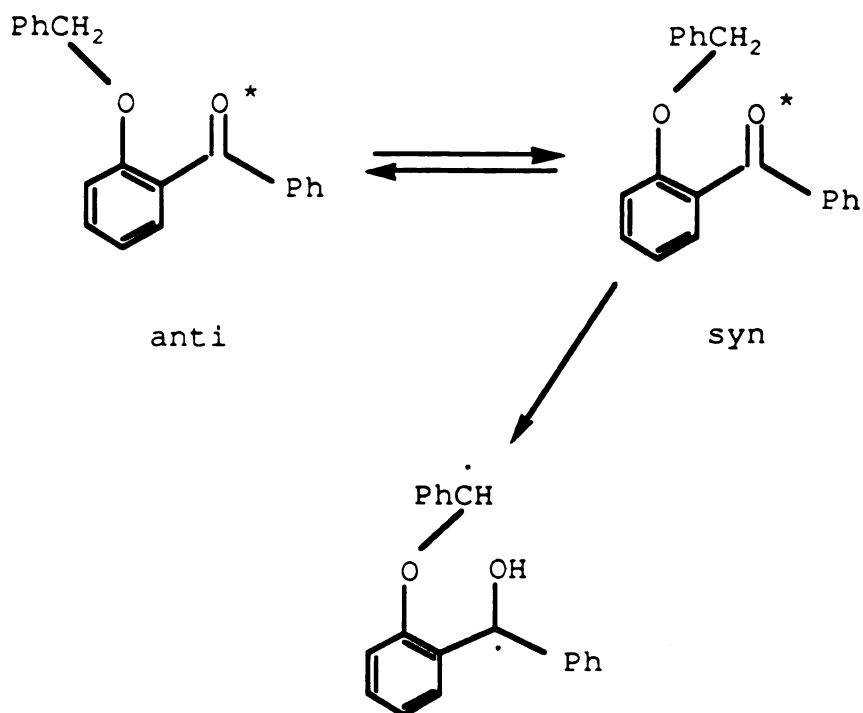


Reaction 7

The excited ketone is believed to be able to achieve a dynamic conformational equilibrium before decaying (Scheme 10). There are two different rotamers for o-(benzyloxy)benzophenone, a syn rotamer, and an anti rotamer.  $\delta$ -Hydrogen abstraction can only occur directly from the syn conformer. However, the anti rotamer can give rise to hydrogen abstraction by first rotating to the syn rotamer. In dibenzoyl ketone, there is always a carbonyl group near the benzyl C-H bonds no matter which way the alkoxy group is twisted. The 10 folds rate enhancement afforded by the extra benzoyl group suggests an equilibrium constant of 10 for rotation of the alkoxy group about the phenyl bond, with the unreactive anti rotamer favored in the monoketone.

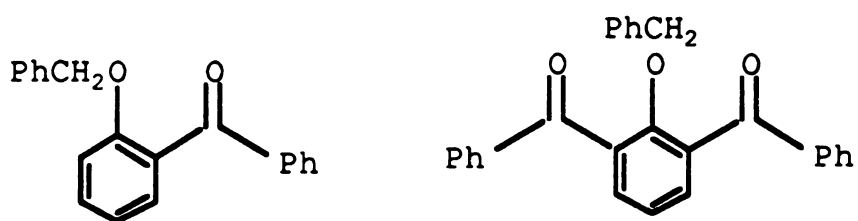
In molecules where conformational changes are comparable or slower





Scheme 10

than their photoreactions, either ground state control or rotational control may occur.


 $\tau^{-1} \times 10^{-7}$ 

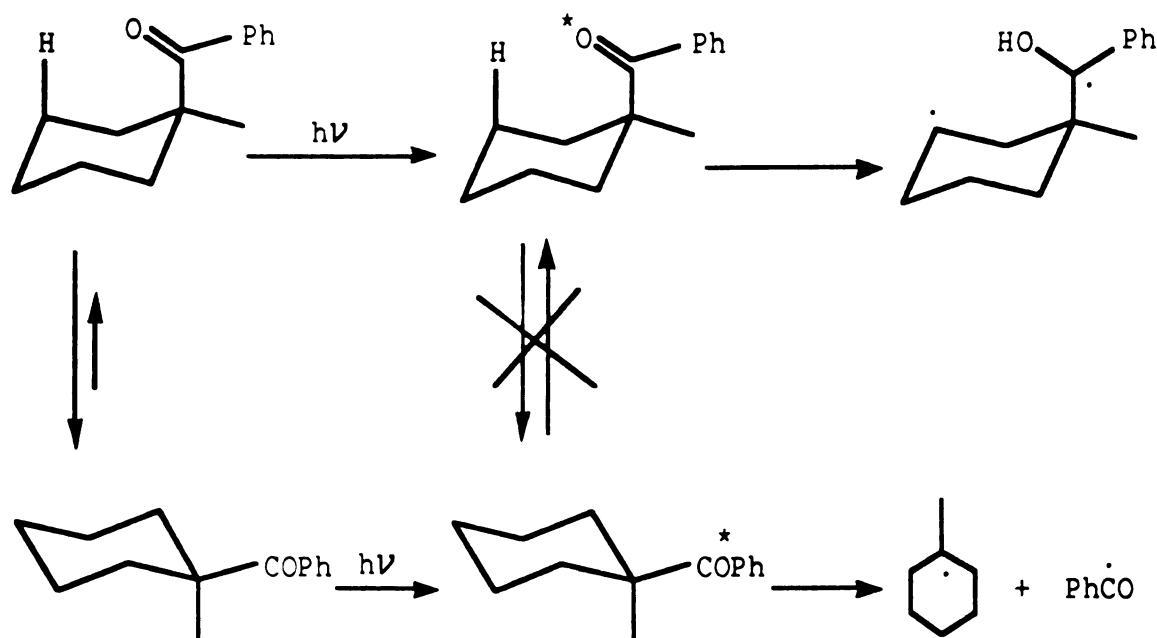
1.8

20

Several benzoylcyclohexane derivatives have provided the most clear-cut examples of ground state control in photoreactions. Lewis<sup>39</sup> has



investigated conformational effects in the photochemistry of 1-methylcyclohexyl phenyl ketone and a number of substituted analogues

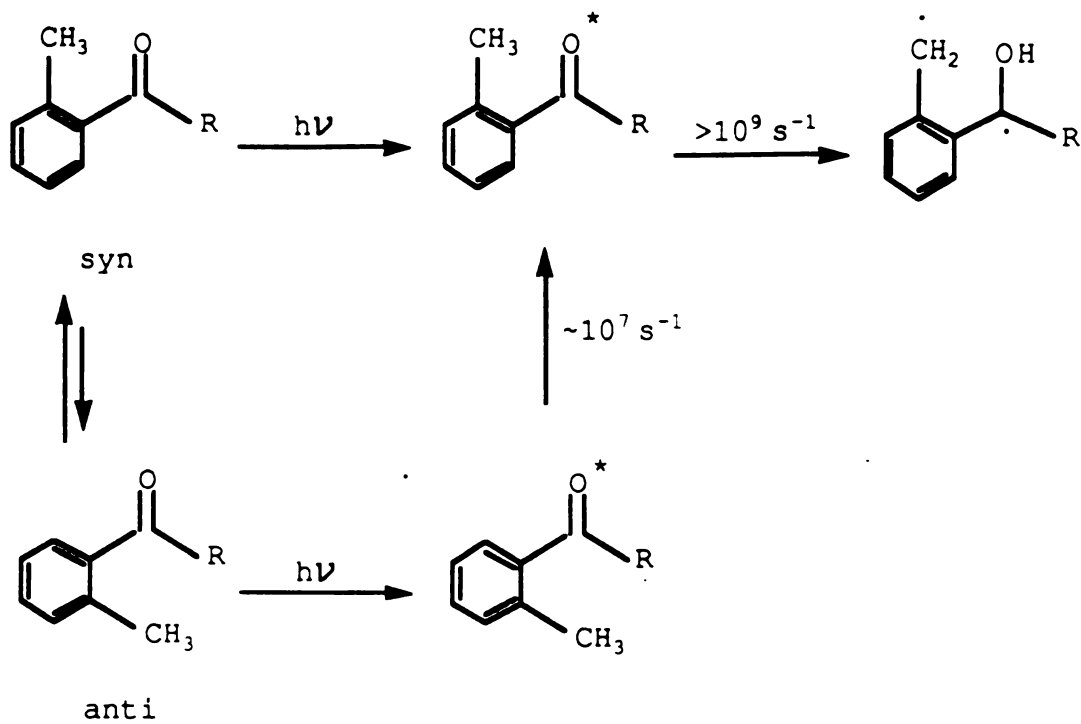


Scheme 11

(scheme 11). Lewis found that for 1-methylcyclohexylphenyl ketone, there exist two different ketone triplets each leading to different photoproducts. The ketone conformer with the benzoyl group in an axial position undergoes  $\gamma$ -hydrogen abstraction followed by cyclization to the corresponding 6-hydroxy-1-methyl-6-phenylbicyclo-[3.1.1]-heptanes. The ketone conformer having the benzoyl group in an equatorial position can not undergo hydrogen abstraction since the carbonyl group is oriented away from those hydrogens. Instead, it undergoes acyl cleavage giving rise to benzaldehyde as well as other products expected from the benzoyl and 1-methylcyclohexyl radicals. Lewis has found that the ratio of the products from the two different



pathways is entirely dependent upon the ground state population of each ketone conformer.

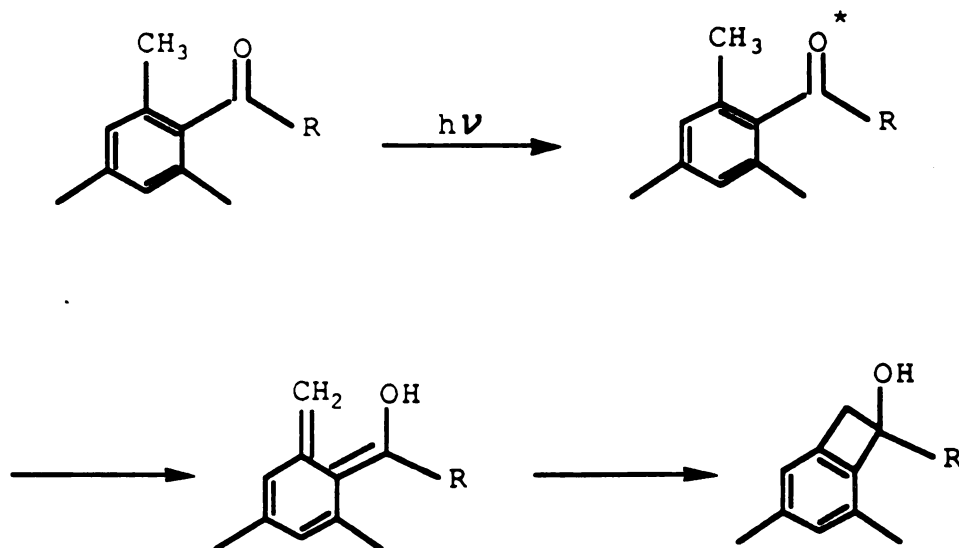


Scheme 12

A well defined example of rotational control in a photochemical reaction is provided by the photoenolization of o-alkylphenyl ketones (Scheme 12).<sup>40-42</sup> This basic photochromic system remained mechanistically confusing until it was realized that two kinetically and conformationally distinct triplets are involved.<sup>43</sup> Sensitization studies revealed that ketones such as o-methylacetophenone and o-methylbenzophenone produce two distinct triplets, one with a subnanosecond lifetime and another with a ~30 ns lifetime. Recent flash kinetic flash work has verified these conclusions.<sup>44</sup> The two triplets correspond to *syn* and *anti* conformers, which is indicated by



the behavior of 8-methyl-1-tetralone. This ketone is locked into a syn conformation and displays only a nanosecond triplet. Rapid enolization occurs from the geometrically perfect syn conformer. The decay of a longer lived triplet corresponds to anti->syn rotation.

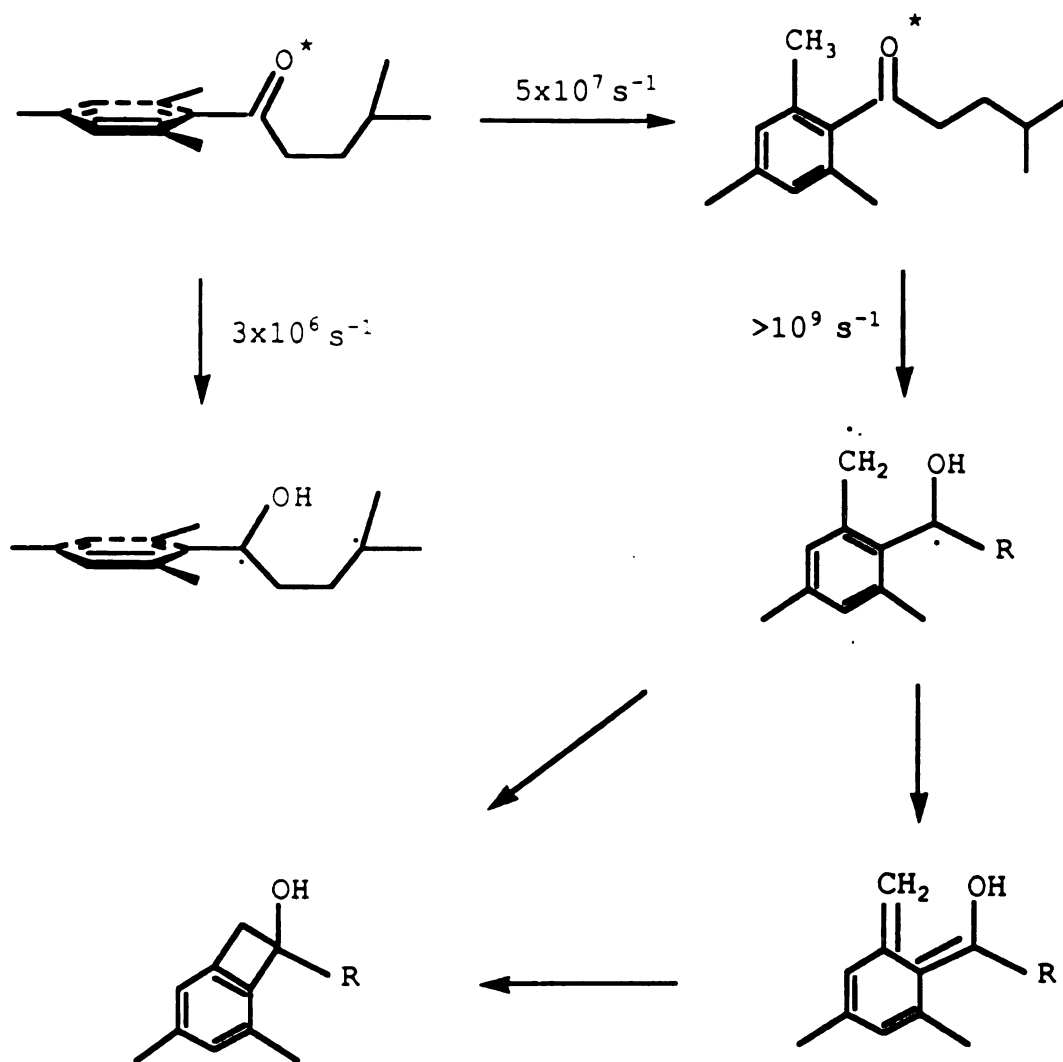


Scheme 13

Another closely related photochemical system involves the photochemistry of 2,4,6-trialkylphenyl ketones (Scheme 13). The introduction of additional alkyl groups to the phenyl ring causes dramatic changes in the photobehaviors of the ketones. In an extensive study of 2, 4,6-trialkylphenyl ketones, Matsuura<sup>45</sup> observed that cyclobutenol formation was the preferred course of the reaction. They also deduced that dienols were first formed and then underwent ring closure to give cyclobutenols.

Wagner<sup>43</sup> studied a group of 2,4,6-trimethylvalerophenone derivatives (Scheme 14). It was concluded that there are two kinetically distinct excited





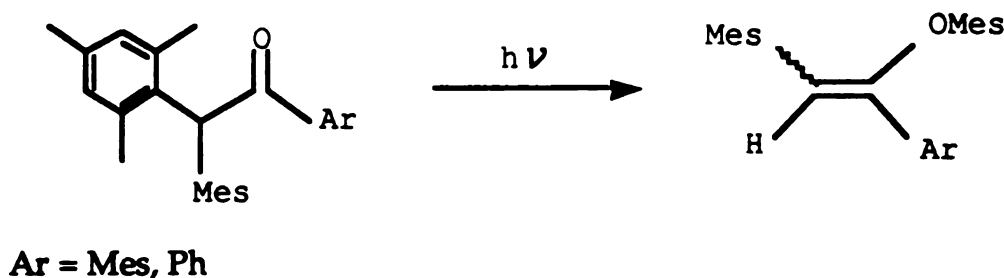
Scheme 14



triplets, one with a twisted form with respect to the carbonyl and aromatic ring, the other with a planar form. The more twisted triplet can undergo type II hydrogen abstraction or rotate with a rate constant of  $5 \times 10^7 \text{ s}^{-1}$  to the more planar form, which can readily abstract an ortho-benzylic hydrogen. The long-lived triplet decays with a rate of  $10^6$ - $10^7 \text{ s}^{-1}$  but does not produce benzocyclobutenol. The short-lived triplet forms benzocyclobutenol with a rate constant of  $\sim 10^9 \text{ s}^{-1}$ .

### Unusual 1,3-Aryl Migrations

Hart<sup>46-47</sup> has reported a novel 1,3-aryl migration reaction with 1,2,2-trimesitylethanone and 2,2-dimesityl-1-phenylethanone (Reaction 8). Irradiation of the ketones afforded the corresponding aryl vinyl ethers. There was only one precedent of the reaction in literature, reported by Heine in the case of 1,2,2,2-tetraphenylethanone.<sup>48</sup> No mechanistic detail was presented in these reports.



Reaction 8

The initial objective of our research started with the following question. There are at least three decay modes for excited 1,2,2-trimesitylethanone:



$\alpha$ -cleavage,<sup>24</sup>  $\delta$ -hydrogen abstraction to form the corresponding indanol,<sup>35</sup> and  $\gamma$ -hydrogen abstraction to give the cyclobutenol.<sup>43,45</sup> The last two reactions are known to have a rate constant of  $\sim 10^9 \text{ s}^{-1}$ . However, none of these reactions were observed. Instead the ketone underwent a 1,3-aryl migration. Why is it so? A similar question can also be applied to 2,2-dimesityl-1-phenylethanone.

We envisioned that conformational factors must be responsible, since it was noted that all the ketones which undergo the 1,3-aryl migration are sterically congested. In addition, the examples of conformational effects on photochemistry in literature have shown that photoreactions can be very sensitive to conformational factors in certain systems.

We investigated a series of  $\alpha$ -arylacetophenone derivatives with varying steric congestion. We found that these ketones represent a group of sterically rigid compounds. The bond rotations in the molecules are restricted. The molecules are locked into certain conformations on the time-scale of photoreactions. Only the reactions allowed by the conformation in which the molecules are set can occur. Therefore, the reactions have shown great individuality. The detail of the study will be discussed later.

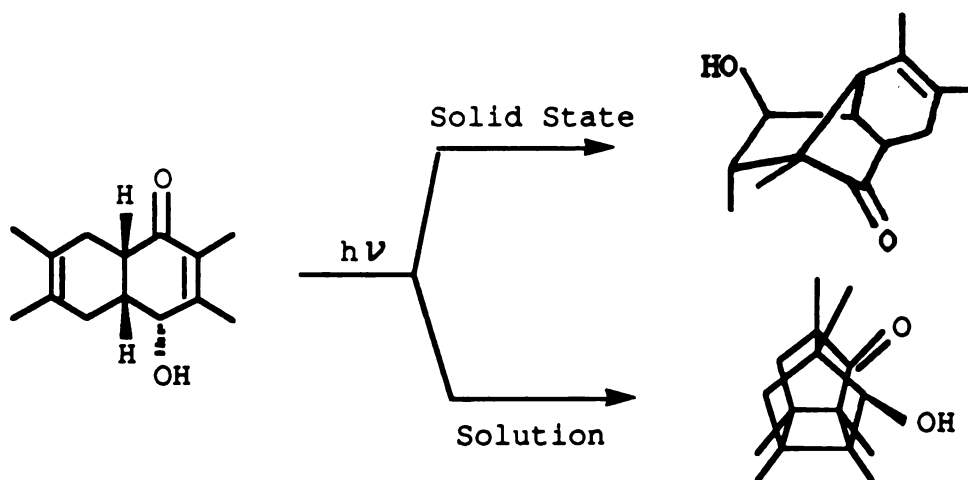
The results from  $\alpha$ -arylacetophenone system encouraged us to extend our studies further. We decided to extend our studies in two directions. First, we started to investigate microenvironmental effects on the photobehavior of the ketones. The photochemistry of organic molecules in organized assemblies are being studied with great interest in order to understand the features controlling the selectivity in the photoreactions brought by these media.<sup>49-52</sup> These studies have paved the way to an intriguing number of possibilities by which photoreactivities can be modified. Second, we increased the number of methylene groups between the carbonyl group and aryl



groups. We studied several  $\beta$ -arylpropiophenones to investigate the possibility of long-range  $\epsilon$ -hydrogen abstraction competing with a fast charge transfer quenching process of the excited ketones by the  $\beta$ -aryl groups.

### Photoreactions in Organized Assemblies such as Solid State and Cyclodextrin complexes.

Many unimolecular organic photorearrangements take place by mechanism requiring drastic conformational or configurational changes along the reaction coordinate. Equally obvious is the idea that physical restraints on a given set of atomic and molecular motions can prevent these motions and lead to alternative pathways. Crystal lattice provides an excellent physical restraint.

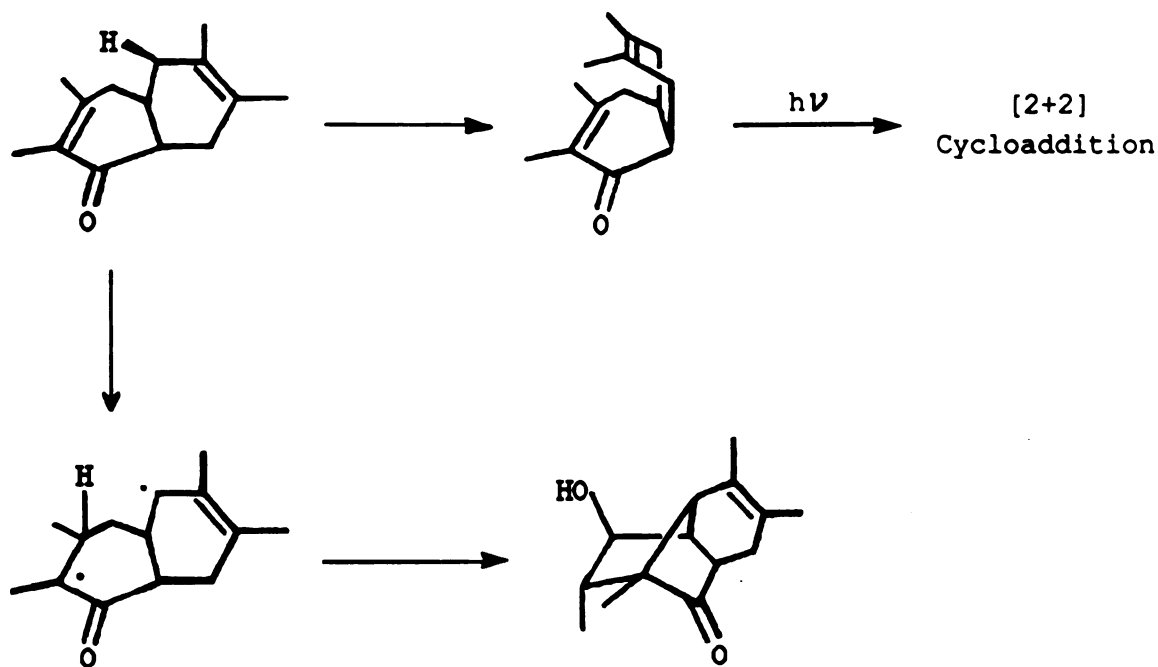


Reaction 9

Sheffer has reported a dramatic change of photoreactivity of 4a,5,8,8a-tetrahydro-6,7-dimethyl-1-naphthoquin-4-ol going from solution to



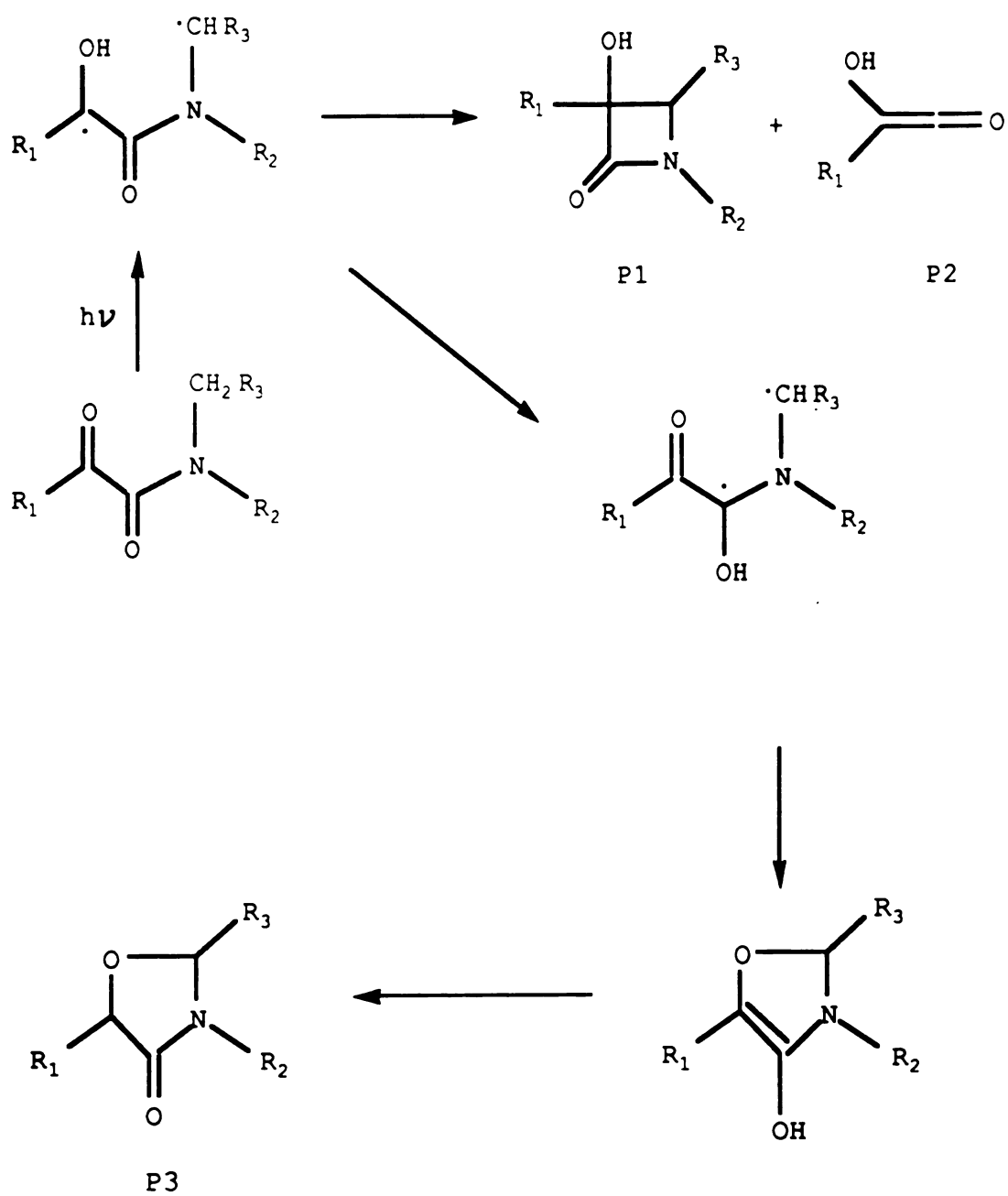
solid state. Direct or benzophenone sensitized irradiation of benzene solution of the tetrahydronaphthoquinol affords essentially quantitative yield of intramolecular [2+2] cycloaddition product.<sup>53</sup> In contrast, irradiation of the substrate in solid state gives no cage product. Irradiation of polycrystalline samples (powder) of the starting compound gives high yield of the keto alcohol (Reaction 9).<sup>54</sup> X-ray crystallography provided the conformation of the tetrahydronaphthoquinol in solid state, which can be described as consisting of a half-chair cyclohexene ring cis fused to a second half-chair-like cyclohexenone moiety. The immobility of the molecule in solid state prevents



Scheme 15

it from getting to the geometry for [2+2] cycloaddition, therefore no cage product is formed. On the other hand, the formation of the keto alcohol, a reaction requiring less molecular motions, can be achieved by a C-5 to C-3



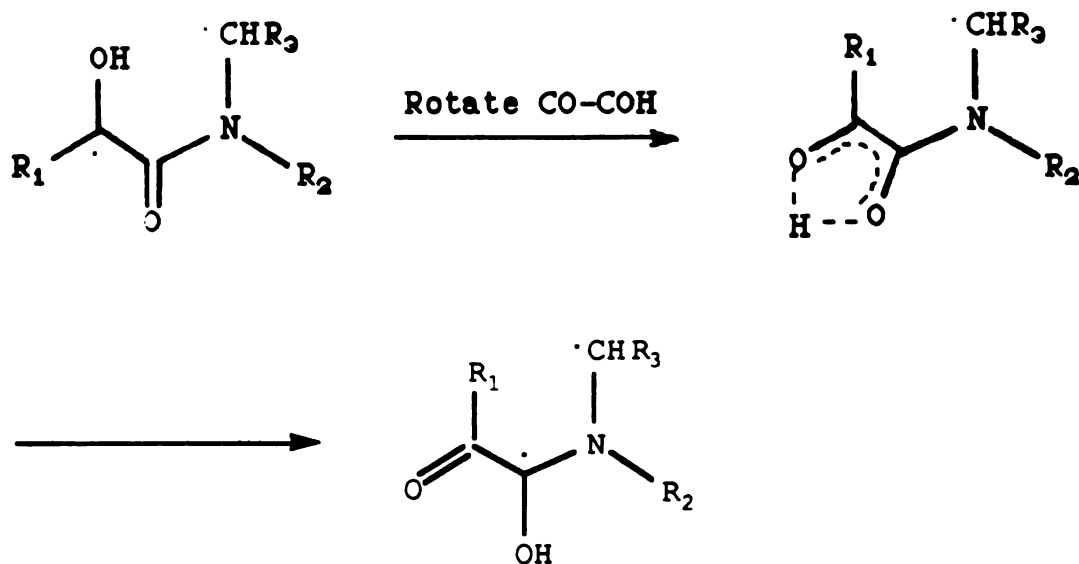


Scheme 16



allylic hydrogen transfer and subsequent C-2 to C-5 bonding in the intermediate so produced (Scheme 15).

Aoyama<sup>55-56</sup> reported a very interesting solid phase study of intramolecular type II hydrogen abstraction in the N,N-dialkyl- $\alpha$ -oxoamide system. The samples were irradiated in solutions and solid state respectively. Product P3 is the major product in solution, but the minor product in solid phase. Product P1 and P2 (type II products) are the minor products in solution, but the major products in solid state. The authors proposed that product P3 is formed through a 1,4-hydrogen shift in the initially formed



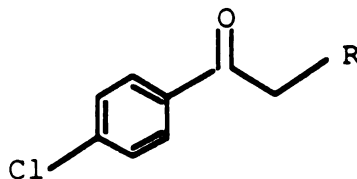
Scheme 17

1,4-biradical, followed by a cyclization and ketonization (Scheme 16). This process involves considerably more molecular motions of the 1,4-biradical intermediate than does formation of P1 and P2. The 1,4-hydrogen migration is constrained to a planar or nearly planar cisoid transition state (scheme 17),<sup>57</sup> which requires the rotation of the C(OH)-CO bond of the initially



formed 1,4-biradical since  $\gamma$ -hydrogen abstraction in the starting oxoamides leads to a transoid biradical. Such molecular motions are possible in solution but prevented by crystal lattice restraints in solid state.

Scheffer<sup>58</sup> has studied the solid photochemistry of a group of  $\alpha$ -cycloalkyl-p-chloroacetophenones (Figure 3). All of these compounds undergo smooth type II reaction in crystalline phase. Analyses of geometric parameters from X-ray crystallography and photochemical results lead to the following conclusions. 1) A chair-like six atom ground state geometry is not a necessary requirement for the type II reaction. 2) Abstraction can occur over distances substantially longer than the previously supposed limitations.<sup>59-60</sup> 3) There is no strict requirement that the hydrogen undergoing abstraction be in the plane of the carbonyl n-orbital.

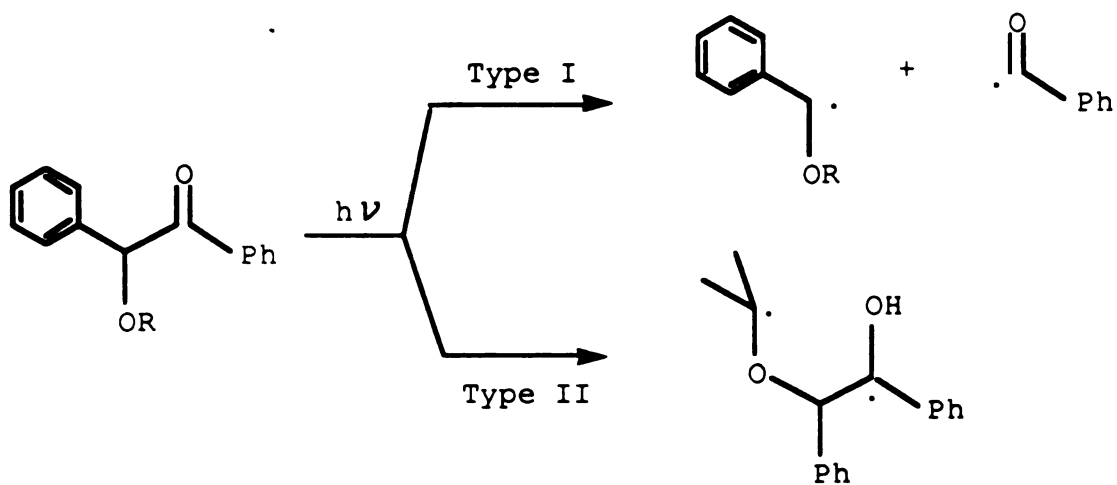


R = cyclobutyl, cyclopentyl, cyclohexyl, cycloheptyl,  
exo-2-norbonyl, 1-adamantyl

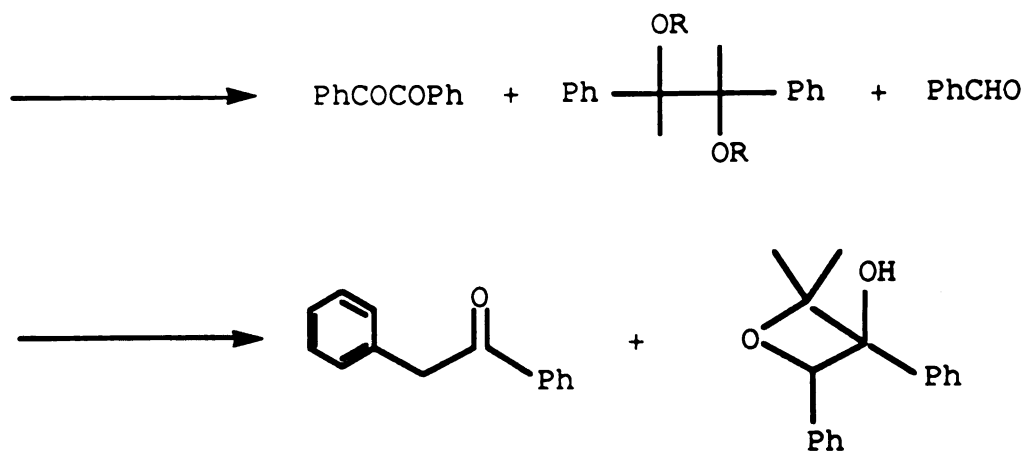
Figure 3

Another specific subarea of photochemistry in organized assemblies concerns reactivity of molecules incorporated in "host-guest" compounds.<sup>61</sup> Cyclodextrins, one of the most commonly used "host" systems, possess hydrophobic cavities that are able to include in aqueous solution a variety of





R = methyl, ethyl, isopropyl

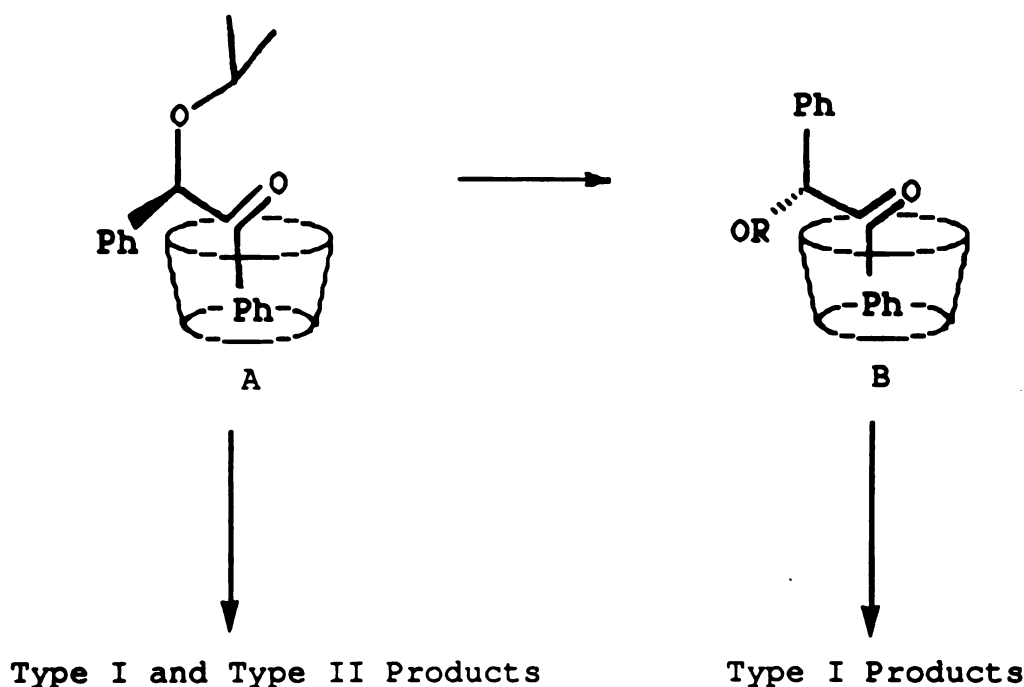


Scheme 18



organic compounds. Although the potential of cyclodextrins as "reaction vessels" for thermal reactions has been widely acknowledged, their use in photochemical reactions is yet to be fully explored.

One of the most dramatic alteration of photobehavior from solutions to cyclodextrin complexes has been reported by Ramamurthy.<sup>62</sup> The authors studied the photochemistry of several benzoin alkyl ethers. It was found that the type II process which is absent in benzene and methanol occurs in competition with the type I process in aqueous cyclodextrin complex solutions (Scheme 18). Most importantly, the photolysis of solid cyclodextrin complexes results in the type II products near quantitative yields.



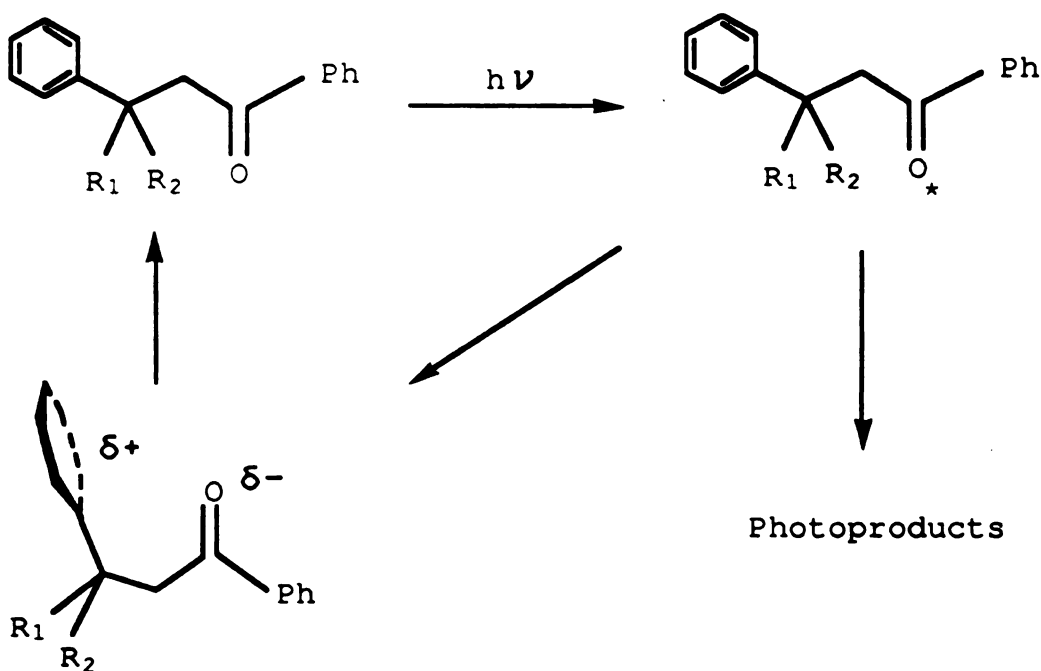
Scheme 19

Complexes A and B (Scheme 19) are two representative possible structures of the benzoin alkyl ethers in cyclodextrin. While complex A can



give both type I and type II reactions, complex B can undergo only type I reaction. The enhancement of type II products can be due to either the suppression of type I reaction by the increased cage effect in cyclodextrin complexes, which reduces the possibility of paired radicals to escape out of the cage and enhance the number of molecules to recombine to the ground state starting ketones,<sup>63-64</sup> or the increased possibility for conformation A in cyclodextrin complexes.

### Charge Transfer Quenching of Excited Ketones by Aromatic Compounds



Scheme 20

The ability of aromatic rings to deactivate  $n, \pi^*$  carbonyl triplet has been recognized for a number of years. Wagner<sup>65</sup> showed some years ago that even weak electron donors like alkylbenzenes reduce highly electron



deficient ketones by a charge transfer mechanism.

This charge transfer quenching process occurs most efficiently when it happens intramolecularly and the aromatic ring is two carbons away from the carbonyl group, such as in  $\beta$ -arylpropiophenones. In 1970, three independent reports by Wagner,<sup>66</sup> Stermitz,<sup>67</sup> and Whitten,<sup>68</sup> clearly illustrated the effect. It was found that  $\beta$ -phenylpropiophenone derivatives undergo type II reaction or photoreduction with significantly lower quantum yields and much shorter lifetimes than those for the analogous ketones without  $\beta$ -phenyl group. It was concluded that the  $n,\pi^*$  triplets undergo a very rapid irreversible intramolecular quenching process which specifically requires a  $\beta$ -phenyl ring. This process is now generally considered as a charge transfer quenching involving nonemitting exciplex intermediates (Scheme 20). Scaiano<sup>69</sup> recently published a detailed flash photolysis study of the photochemistry of  $\beta$ -arylpropiophenones. The results indicate that the triplet lifetimes of various ketones are rather insensitive to substituent effects on the  $\beta$ -aryl rings, all of the order of  $10^9 \text{ s}^{-1}$ . Scaiano suggested that the rate of the intramolecular quenching is mainly controlled by the ability of the substrate to achieve a critical conformation required for the interaction. Therefore, it does not vary with the electron donating ability of the  $\beta$ -rings. This process resembles a diffusion controlled intermolecular quenching process where the rate depends on how fast the molecules can get close to each other.

Since a great deal of the work presented in this thesis deals with conformational analysis of the sterically congested ketones. A introduction of two most frequently used tools is given briefly.

### Dynamic NMR Studies



Dynamic NMR (DNMR) studies the effects of chemical exchange processes on NMR spectra, and is used to provide information about changes in the environment of magnetic nuclei.

DNMR spectra may be interpreted to give information not only on structures of conformations but also on energy differences between conformers and on energy barriers.<sup>70</sup>

Conformational energy differences can be determined by measuring the relative populations of various conformers at a single temperature. Use of Boltzman equation then leads to the energy differences between the conformers.

Determination of barrier height requires comparison of NMR spectra at several temperatures. As the temperature changes, the rate of interconversion changes. At low temperature, the rate of rotation may be slow enough that signals of a proton in different environments can be separated in its NMR spectrum. At high temperature, interconversion may become so rapid that a single proton moves back and forth between different environments within the time required for the NMR measurements. The resulting spectrum often becomes simpler since the separate chemical shift peaks for a proton in different conformations merge into a single peak representative of the averaged environments

At intermediate exchange, two peaks merge into one peak and strong broadening is observed. If the nuclei are protons and the two sites are equally populated, the rotational rate can be derived with equation (2),<sup>71</sup> where  $\omega$  is the linewidth at the halfheight of the signal in Hz,  $\Delta\nu$  is the difference of chemical shifts in different environments in Hz.

$$k = \{\pi\Delta\nu[(\Delta\nu/\omega)^2 - (\omega/\Delta\nu)^2 + 2]^{1/2}\}/2 \quad (2)$$



## Molecular Mechanics Calculations

A system of analyzing the energy differences among various geometries of a particular molecule has been developed, based on some fundamental concept formalized by Westheimer.<sup>72</sup> The method is known as molecular mechanics, or force field method sometimes.<sup>73</sup>

In molecular mechanics, a molecule is considered as a collection of atoms held together by elastic or harmonic forces. The forces can be described by potential energy functions of structural features like bond lengths, bond angles, nonbonded interactions, and so on. The combination of these potential energy functions is the force field. The energy,  $E$ , of the molecule in the force field arises from deviations from ideal structural features, and can be approximated by a sum of energy contributions,

$$E = E_s + E_b + E_w + E_{nb} + \dots \quad (3)$$

$E$  is sometimes called the 'steric energy'. It is the difference in energy between the real molecule and a hypothetical molecule where all the structural features like bond lengths and bond angles are exactly at their ideal or natural values.  $E_s$  is the energy of stretching or compressing bonds from their natural bond length.  $E_b$  is the energy of bending bond angles from their natural values.  $E_w$  is the torsional energy due to twisting about bonds, and  $E_{nb}$  is the energy of non-bonding interactions. If there are other intramolecular mechanisms affecting the energy, such as hydrogen bonding etc., these too may be added to the force field. A mathematical process then is involved to minimize the steric energy by adjusting the structural features.

It is important to recognize that  $E$  is only a measure of intramolecular



strain relative to a hypothetical situation. By itself E has no physical meaning. However, the differences in E for different geometries of the same molecule are appropriate for comparison.

Finally, the author wishes to present briefly the general method used to measure the kinetic parameters of the photoreactions.

### Measurements of Quantum Yields and Excited State Lifetimes

Quantum yields of photoreactions are defined as the amount of products formed divided by the amount of light absorbed by the reactants. Therefore quantum yields can be obtained by measuring the product concentration and the light absorbed in unit volume during the course of the reaction through actinometers.

The quantum yield for any photochemical process can be expressed as a product of probabilities. Thus, for a given triplet photoreaction,

$$\Phi = \Phi_{isc} k_T \tau P \quad (4)$$

$$1/\tau = k_T + k_d \quad (5)$$

where  $\Phi_{isc}$  is the intersystem crossing quantum yield,  $k_T$  is the rate constant for the reaction,  $k_d$  is the rate constant for triplet decay other than the interested reaction,  $\tau$  is the triplet lifetime, and P is the probability that the intermediate will go on to the products. In the presence of an external quencher, (5) becomes

$$1/\tau = k_T + k_d + k_q[Q] \quad (6)$$



where  $k_q$  is the bimolecular quenching rate constant. A mathematical relationship, referred to as the Stern-Volmer equation, can be derived between the ratio of photoproduct in the absence and presence of quencher and the concentration of quencher used,

$$\Phi^0/\Phi = 1 + k_q\tau[Q] \quad (7)$$

Thus a plot of  $\Phi^0/\Phi$  versus  $[Q]$  should give a straight line with an intercept of 1.0 and a slope of  $k_q\tau$ . In most cases, the rate of energy transfer quenching by dienes or naphthalene is close to the rate of diffusion in a given solvent. For example,  $k_q$  is known to equal to  $5-6 \times 10^9 \text{M}^{-1}\text{s}^{-1}$  in benzene at room temperature.<sup>3c,89</sup> Therefore, the triplet lifetime can be calculated from the slope of the Stern-Volmer plot.

In this thesis, the photochemistry of  $\alpha$ -arylacetophenone derivatives will be presented, along with the preliminary results concerning the photoreactivities of these ketones in organized assemblies and the photochemistry of several  $\beta$ -arylpropiophenone derivatives.



## Results

### I. $\alpha$ -Arylacetophenone Derivatives

#### A. Photoreactions in Solutions

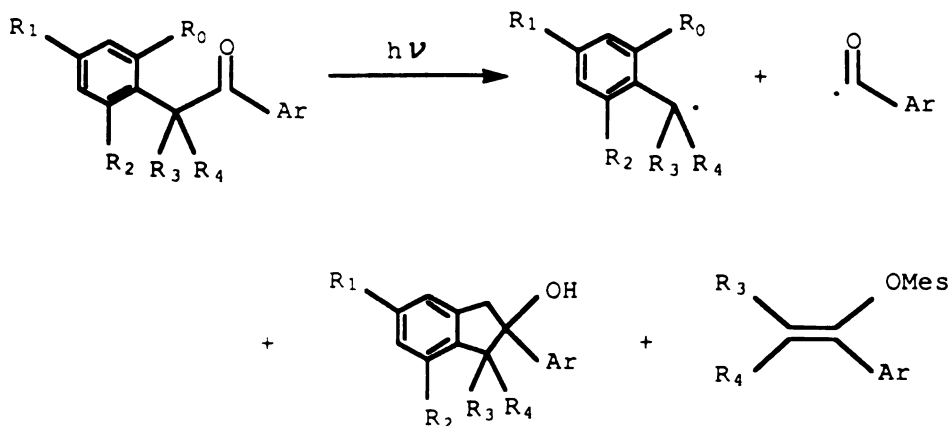
##### 1. General Preparations of the Ketones

$\alpha$ -(o-Tolyl)propiophenone,  $\alpha$ -(o-tolyl)valerophenone and  $\alpha$ -(o-tolyl)-isobutyrophenone were prepared by alkylation of  $\alpha$ -(o-tolyl)acetophenone with methyl iodide, or propyl bromide.  $\alpha$ -Mesitylpropiophenone,  $\alpha$ -mesitylvalerophenone,  $\alpha$ -mesitylisobutyrophenone, and  $\alpha$ -mesityl-o-methylacetophenone were prepared by the reaction of corresponding nitriles with aryl magnesium bromide.  $\alpha$ -Mesityl-2,4,6-trimethylacetophenone,  $\alpha$ -mesityl- $\alpha$ -phenyl-p-methoxyacetophenone,  $\alpha$ -mesityl- $\alpha$ -phenyl-2,4,6-trimethylacetophenone,  $\alpha$ -phenyl-2,4,6-trimethylacetophenone, and  $\alpha$ -(o-tolyl)-p-methoxyacetophenone were synthesized by Friedel-Crafts acylation with corresponding acetyl chloride and aromatic substrates.  $\alpha$ -Mesityl- $\alpha$ -phenylacetophenone and  $\alpha$ -mesityl- $\alpha$ -phenyl-p-cyanoacetophenone were prepared by Friedel-Crafts alkylation of mesitylene with  $\alpha$ -chloro- $\alpha$ -phenylacetophenone and  $\alpha$ -chloro- $\alpha$ -phenyl-p-cyanoacetophenone.

##### 2. Identification of Photoproducts

Irradiation of approximately 0.3 g of  $\alpha$ -arylacetophenone derivatives in 500 ml cyclohexane or benzene with a Pyrex filter afforded a mixture of





- 1  $R_0=CH_3, R_1=R_2=R_3=R_4=H, Ar=p\text{-MeOPh},$   
 $\alpha\text{-(o-Tolyl)-p-Methoxyacetophenone}$
- 2  $R_0=R_4=CH_3, R_1=R_2=R_3=H, Ar=Ph, \alpha\text{-(o-Tolyl)propiofenone}$
- 2-d  $R_0=R_4=CH_3, R_1=R_2=H, R_3=D, Ar=Ph, \alpha\text{-(o-Tolyl)propiofenone-d}_1$
- 3  $R_0=CH_3, R_1=R_2=R_3=H, R_4=(CH_2)_2CH_3, Ar=Ph,$   
 $\alpha\text{-(o-Tolyl)valerophenone}$
- 4  $R_0=R_3=R_4=CH_3, R_1=R_2=H, Ar=Ph, \alpha\text{-(o-Tolyl)isobutyrophenone}$
- 5  $R_0=R_1=R_2=R_3=CH_3, R_4=H, Ar=Ph, \alpha\text{-Mesitylpropiofenone}$
- 6  $R_0=R_1=R_2=CH_3, R_3=H, R_4=(CH_2)_2CH_3, Ar=Ph,$   
 $\alpha\text{-Mesitylvalerophenone}$
- 7  $R_0=R_1=R_2=R_3=CH_3, Ar=Ph, \alpha\text{-Mesitylisobutyrophenone}$
- 8  $R_0=R_1=R_2=CH_3, R_3=H, R_4=Ph, Ar=Ph,$   
 $\alpha\text{-Mesityl-}\alpha\text{-Phenylacetophenone}$
- 8-d  $R_0=R_1=R_2=CH_3, R_3=D, R_4=Ph, Ar=Ph,$   
 $\alpha\text{-Mesityl-}\alpha\text{-Phenylacetophenone-d}_1$
- 9  $R_0=R_1=R_2=CH_3, R_3=H, R_4=Ph, Ar=p\text{-CH}_3\text{OPh},$   
 $\alpha\text{-Mesityl-}\alpha\text{-Phenyl-p-Methoxyacetophenone}$



- 10  $R_0=R_1=R_2=CH_3$ ,  $R_3=H$ ,  $R_4=Ph$ ,  $Ar=p-CNPh$ ,  
 $\alpha$ -Mesityl- $\alpha$ -Phenyl-*p*-Cyanoacetophenone
- 11  $R_0=R_1=R_2=CH_3$ ,  $R_3=H$ ,  $R_4=Ph$ ,  $Ar=Mesityl$ ,  
 $\alpha$ -Mesityl- $\alpha$ -Phenyl-2,4,6-Trimethylacetophenone
- 12  $R_0=R_1=R_2=R_3=R_4=H$ ,  $Ar=Mesityl$ ,  
 $\alpha$ -Phenyl-2,4,6-Trimethylacetophenone
- 13  $R_0=R_1=R_2=CH_3$ ,  $R_3=R_4=H$ ,  $Ar=o-Tolyl$ ,  
 $\alpha$ -Mesityl-*o*-Methylacetophenone
- 14  $R_0=R_1=R_2=CH_3$ ,  $R_3=R_4=H$ ,  $Ar=Mesityl$ ,  
 $\alpha$ -Mesityl-2,4,6-Trimethylacetophenone
- 15  $R_0=CH_3$ ,  $R_1=R_2=R_3=R_4=H$ ,  $Ar=Ph$ ,  $\alpha$ -(*o*-Tolyl)acetophenone
- 16  $R_0=R_1=R_2=CH_3$ ,  $R_3=R_4=H$ ,  $Ar=Ph$ ,  $\alpha$ -Mesitylacetophenone
- 16-d  $R_0=R_1=R_2=CH_3$ ,  $R_3=R_4=D$ ,  $Ar=Ph$ ,  $\alpha$ -Mesitylacetophenone-d<sub>2</sub>
- 17  $R_0=R_1=R_2=CH(CH_3)_2$ ,  $R_3=R_4=H$ ,  $Ar=Ph$ ,  
 $\alpha$ -(2,4,6-Triisopropylphenyl)acetophenone
- 17-d  $R_0=R_1=R_2=CH(CH_3)_2$ ,  $R_3=R_4=D$ ,  $Ar=Ph$ ,  
 $\alpha$ -(2,4,6-Triisopropylphenyl)acetophenone-d<sub>2</sub>

## Reaction 10

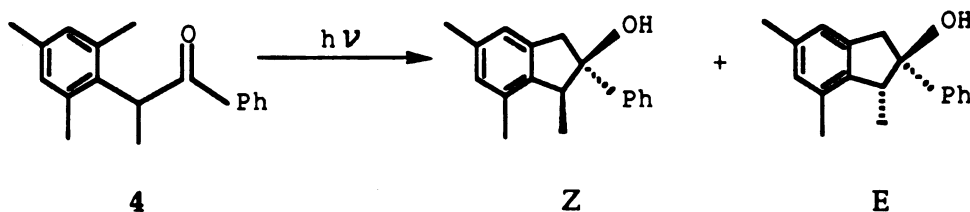


$\alpha$ -cleavage products, type II products, corresponding 2-phenyl-2-indanols, and aryl vinyl ethers in the cases of several  $\alpha$ -mesitylacetophenones (Reaction 10).

The products were normally isolated by GC. Preparative tlc plates were used for isolations of products from  $\alpha$ -mesityl- $\alpha$ -phenylacetophenone 8,  $\alpha$ -mesityl- $\alpha$ -phenyl-p-methoxyacetophenone 9, and  $\alpha$ -mesityl- $\alpha$ -phenyl-p-cyanoacetophenone 10, using a mixture of hexane and ethyl acetate as eluent.

The photoreactivities of the ketones showed an unusually sensitive substituent effect. Irradiation of ketone 5, 6, 8, 9 and 10 led to the formation of type I products, indanols, and aryl vinyl ethers, while type I reaction was the only reaction observed for ketones 4, 7, 12 and 14. Although type II products were the major products formed from 3, ketone 6 only gave trace amount of type II products.

Structural assignments of the photoproducts were based on spectral data ( $^1\text{H}$  and  $^{13}\text{C}$  NMR, IR, UV, and MS). The characteristic feature of the indanol derivatives is an AB quartet appearing between 3.0 ppm and 4.0 ppm in  $^1\text{H}$  NMR, which corresponds to the methylene portion of the five-member ring.



Reaction 11

$\alpha$ -Mesitylpropio-phenone 4 gave a mixture of stereoisomeric indanols, with a Z/E ratio of 5.1/1 in cyclohexane by GC (Reaction 11).  $^1\text{H}$  NMR was



used to assign the stereochemistry of the diastereomers.

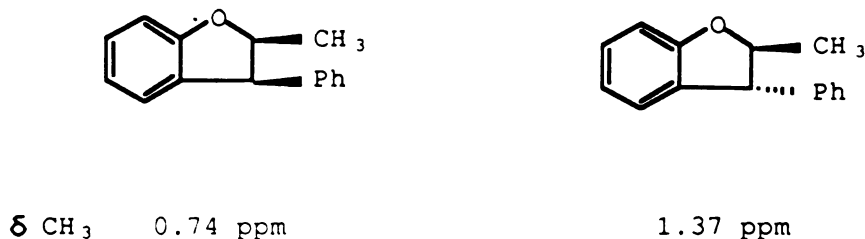


Figure 4

Pappas<sup>74</sup> has reported that the diastereomer of 2-methyl-3-phenyl-2,3-dihydrobenzofuran in which the phenyl and methyl substituents are cis to each other has a methyl signal at 0.74 ppm. The methyl group in the trans isomer appears at 1.37 ppm (Figure 4). Lewis<sup>75</sup> observed the same effect for the two diastereomers of 2-methyl-1-phenylcyclobutanols (Figure 5). Wagner<sup>76a</sup> has found that the same was true with the t-butyl groups of Z/E 2-t-butyl-1-phenylcyclobutanols



Figure 5

(Figure 6). The three methyl groups of the t-butyl group in the E isomer absorb 0.45 ppm more upfield than the ones of the Z isomer. Wagner and



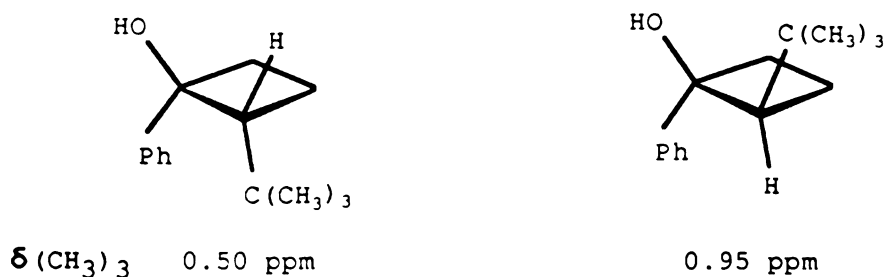


Figure 6

Meador<sup>76b</sup> reported that a similar effect was also observed with stereoisomeric 3-hydroxy-3-methyl-2-phenyl-2,3-dihydrobenzofurans. The methyl group of E-3-hydroxy-3-methyl-2-phenyl-2,3-dihydrobenzofuran absorbs upfield of the methyl group of the Z isomer (Figure 7). Thus the stereochemical assignments of the indanol products from  $\alpha$ -mesitylpropiophenone **5** were based upon these considerations.

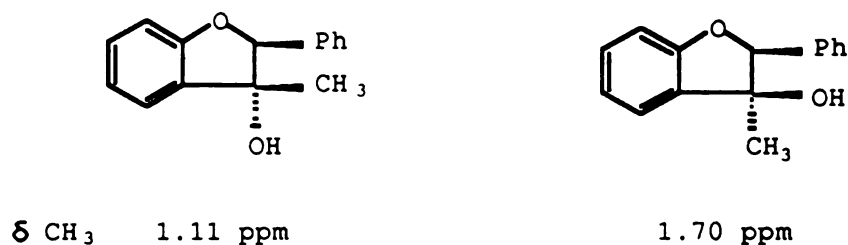


Figure 7

When the methyl group of 3,4,6-trimethyl-2-phenyl-2-indanol is cis to the phenyl group, it appears upfield of the methyl group in the trans form, because it is in the shielding cone of the benzene ring. Therefore, the isomer



with its methyl group at 1.32 ppm is assigned as the Z form; the one with the methyl group at 0.75 ppm as the E isomer (Figure 8).

$\alpha$ -(o-Tolyl)propiophenone 2,  $\alpha$ -mesitylvalerophenone 6, and  $\alpha$ -mesityl- $\alpha$ -phenylacetophenone 8 all afforded only one of the possible isomeric indanols. The structural assignment is made difficult by the fact that there is no comparison like what there is with two isomers. However there are indications that all of these indanols are the Z isomers, where the  $\alpha$ -substituent is cis to the hydroxyl group.

The methyl group of the indanol from  $\alpha$ -(o-tolyl)propiophenone 2 absorbs at 1.26 ppm, very close to the methyl group of Z-3,4,6-trimethyl-2-phenyl-2-indanol, indicating a Z structure.

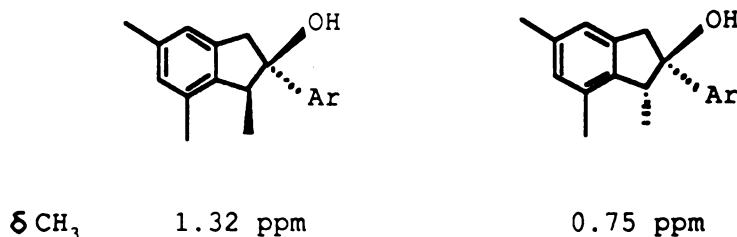


Figure 8

A Z structure is assigned to 4,6-dimethyl-2-phenyl-3-propyl-2-indanol from  $\alpha$ -mesitylvalerophenone 6, based upon the consideration that the chemical shifts of the diastereomeric methylene protons (1.64-1.98 ppm) are too downfield to be the one of the E form. The increment in ppm of a proton signal changing from a methyl group to a methylene group is approximately 0.25. The adjustment of the methyl signal of E-3,4,6-trimethyl-2-phenyl-2-indanol by 0.25 ppm gives a chemical shift of 1.0 ppm, while the same adjustment made for Z-3,4,6-trimethyl-2-phenyl-2-indanol gives a chemical



shift 1.57 ppm. The chemical shift of the  $\text{CH}_2$  protons of 4,6-dimethyl-2-phenyl-3-propyl-2-indanol appears in better agreement with a *Z* assignment (Figure 9).

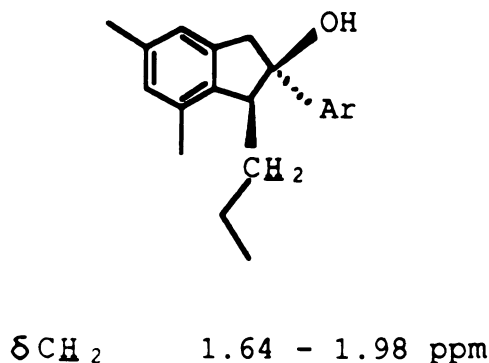


Figure 9

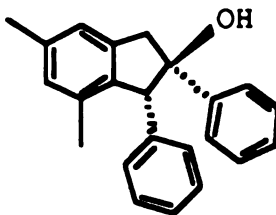


Figure 10

A simple inspection of a model shows that the steric congestion between the two phenyl groups in *cis*-4,6-dimethyl-2,3-diphenyl-2-indanol requires them to face each other (Figure 10). This will make the phenyl proton NMR signals appear relatively upfield. Farnia and Knorr<sup>77-78</sup> have shown that the aromatic signals of several 2,3-diphenylindans are as far upfield as 6.30 ppm when the phenyl groups are *cis* to each other. The fact that the two phenyl groups of 4,6-dimethyl-2,3-diphenyl-2-indanol have



signals ranging from 7.00 to 7.43 ppm suggests that the trans (E) isomer was formed.

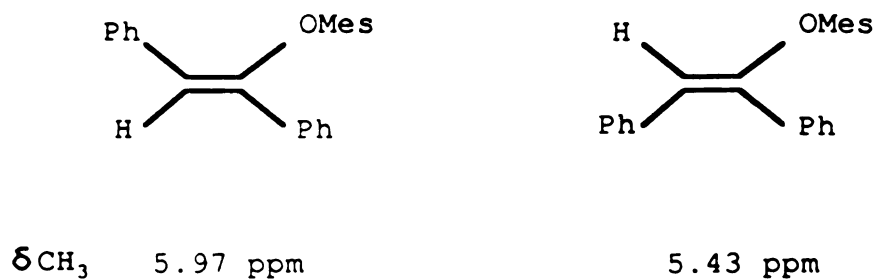
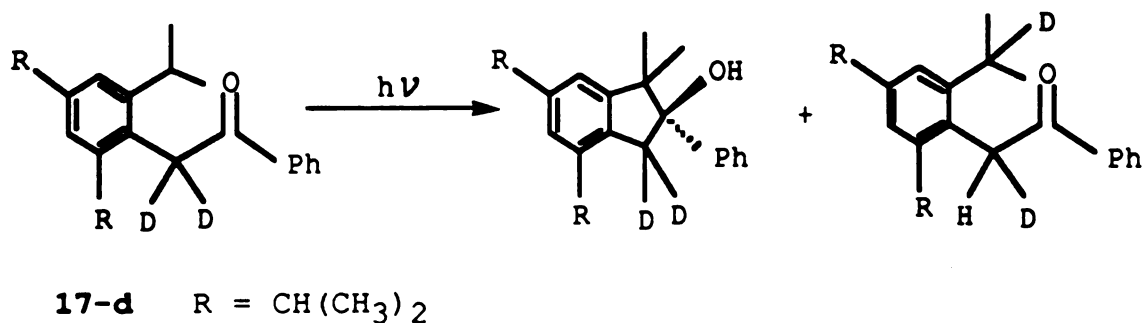


Figure 11

The vinyl protons of the enol ethers absorb between 5.0 ppm and 6.0 ppm in most of the cases. The Z and E form of the ethers are assigned, assuming that the vinyl proton of the Z form would shift downfield from the one of the E form due to the deshielding by the phenyl group.<sup>46</sup> For instance, the vinyl proton of 5.97 ppm is assigned to Z-1-mesitoxy-1,2-diphenylethylene, and the vinyl proton of 5.43 ppm is assigned to E-1-mesitoxy-1,2-diphenylethylene (Figure 11).



Reaction 12



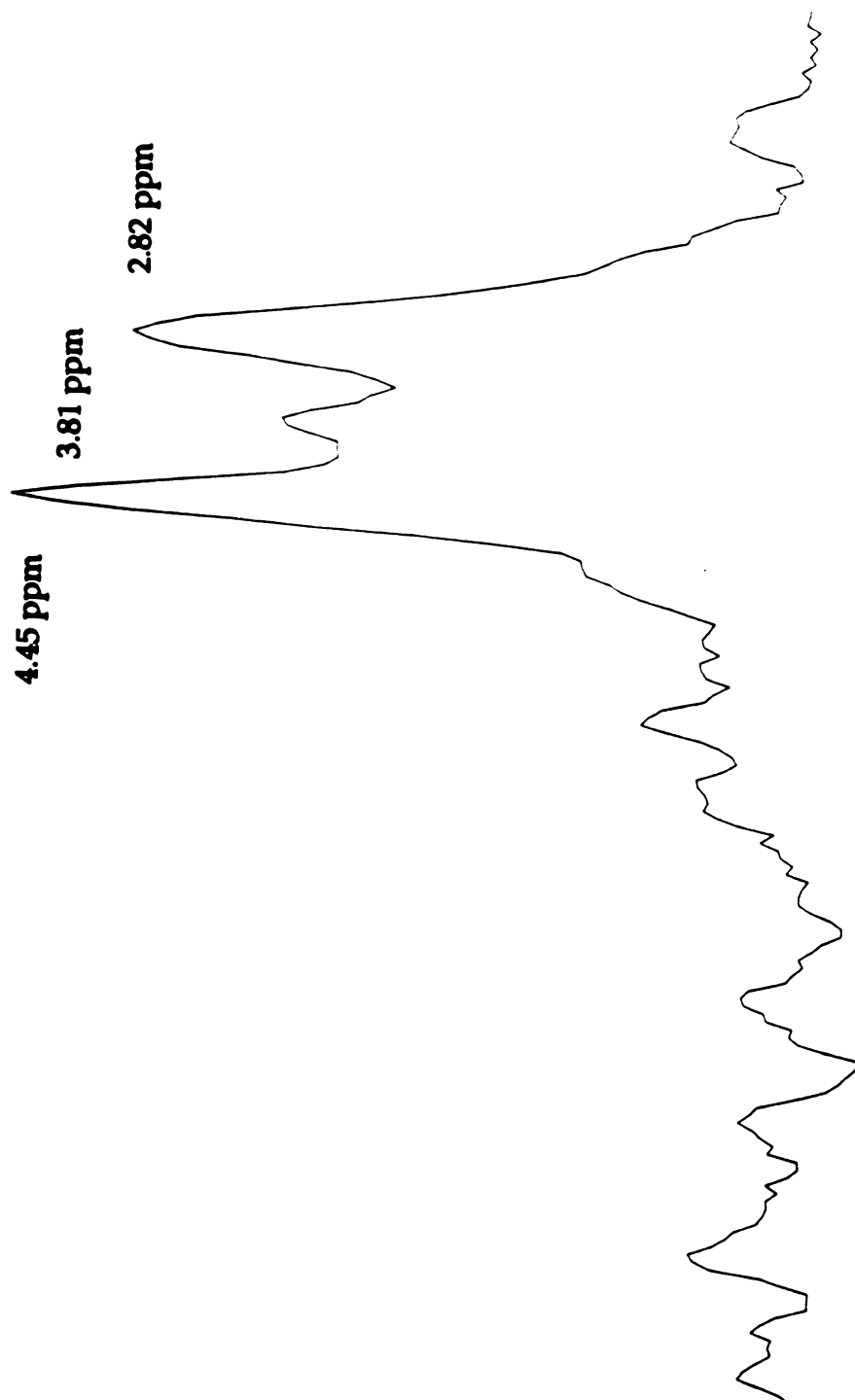


**Figure 12.** Deuterium NMR Spectrum of Reaction Mixture from  $\alpha$ -(2,4,6-Triisopropylphenyl)acetophenone- $d_2$



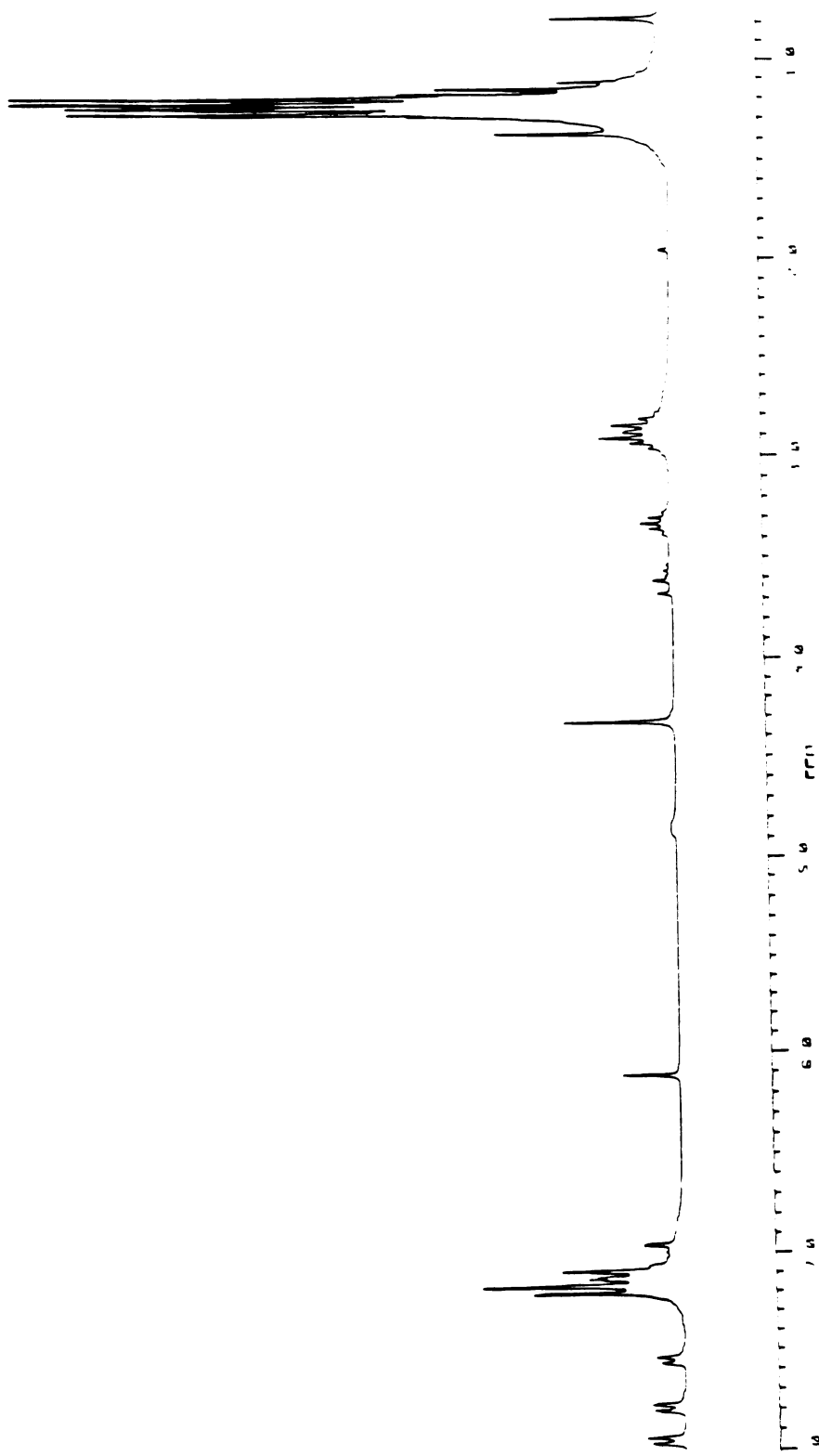


Figure 13.  $^1\text{H}$  NMR Spectrum of Reaction Mixture from  $\alpha$ -(2,4,6-Triisopropylphenyl)acetophenone



The following deuterium exchange experiments were conducted in order to confirm the mechanism proposed by Wagner<sup>79</sup> for the photoenolization of  $\alpha$ -(2,4,6-triisopropylphenyl)acetophenone and  $\alpha$ -mesitylacetophenone. All the samples were degassed by bubbling through Argon gas prior to irradiation.

$\alpha$ -(2,4,6-Triisopropylphenyl)acetophenone-d<sub>2</sub> 17-d was irradiated in carbon tetrachloride in a pyrex NMR tube at 365 nm until the relative amount of the indanol formed to the remained ketone was 35% (by the area ratio of one of methyl signals (0.78 ppm) at C<sub>1</sub> of the indanol to the ortho proton signal of the benzoyl group in the starting ketone in NMR). <sup>1</sup>H NMR of the irradiated sample showed the appearance of the  $\alpha$ -methylene protons at 4.46 ppm in the unreacted ketone. The relative area ratio of the  $\alpha$ -methylene peak to the benzoyl ortho proton peaks in the unreacted ketone was 0.11 by integration. This indicated that ~22% of the unreacted ketone underwent deuterium exchange. <sup>2</sup>H NMR of a separately irradiated sample showed deuterium migration from the  $\alpha$ -carbon to the benzylic carbon (Figure 12). The  $\alpha$ -methylene deuterium signal in the remained starting ketone was identified by its position away from CDCl<sub>3</sub> signal in a separate sample with added CDCl<sub>3</sub>. This peak was then zeroed at 4.45 ppm. Due to the similarity of the chemical shifts in <sup>1</sup>H and <sup>2</sup>H NMR, the deuterium absorptions at 3.81 ppm and 2.82 ppm thus correspond to the methylene deuteriums in the indanol and the benzylic deuteriums in the ketone respectively. The benzylic deuterium signal of the ketone at 2.82 ppm overlaps with one of the  $\alpha$ -methylene deuteriums which should be around 3.08 ppm.

Similar experiments were performed on  $\alpha$ -(o-tolyl)propiophenone-d<sub>1</sub> 2-d,  $\alpha$ -mesitylacetophenone-d<sub>2</sub> 16-d, and  $\alpha$ -mesityl- $\alpha$ -phenylaceto-



phenone-d<sub>1</sub> 8-d. The deuterated ketones dissolved in carbon tetrachloride or benzene-d<sub>6</sub> in a pyrex NMR tube were irradiated at 365 nm. The irradiation time was controlled so that the relative amount of the indanol formed to the remained ketone was 20% for  $\alpha$ -(o-tolyl)propiophenone-d<sub>1</sub> 2-d (by the area ratio of  $\alpha$ -methyl signal in the product and unreacted ketone), 35% for  $\alpha$ -mesitylacetophenone-d<sub>2</sub> 16-d (by the area ratio of mesityl methyl signal in the product and unreacted ketone), 25% for  $\alpha$ -mesityl- $\alpha$ -phenylacetophenone-d<sub>1</sub> 8-d (by the area ratio of mesityl methyl signal in the product and unreacted ketone). <sup>1</sup>H NMR showed no appearance of the  $\alpha$ -methylene proton signal at 4.30 ppm for  $\alpha$ -mesitylacetophenone, or the  $\alpha$ -methine proton signals at 4.26 ppm and 5.99 ppm for  $\alpha$ -(o-tolyl)propiophenone 2 and  $\alpha$ -mesityl- $\alpha$ -phenylacetophenone 8, respectively.

$\alpha$ -(2,4,6-Triisopropylphenyl)acetophenone 17 was irradiated in benzene-d<sub>6</sub> in a Pyrex NMR tube at 365 nm until the relative amount of the indanol formed to the remained ketone was 80% (by the area ratio of one of methyl signals (0.78 ppm) at C<sub>1</sub> of the indanol to the  $\alpha$ -methylene proton signal of the starting ketone in NMR). A peak was observed at 6.13 ppm in the <sup>1</sup>H NMR spectrum of the reaction mixture (Figure 13). It did not disappear after 20 hr. standing at room temperature. But with a drop of acetic acid, it slowly disappeared over a period of 3 days. It was found later that this peak disappeared over 3 days even without adding acetic acid. This signal is assigned to the vinyl proton of the Z enol of the ketone.<sup>79</sup> The signal for the E enol as reported by Wagner was not observed. The area ratio of the vinyl proton signal to the methyl signal (0.78 ppm) at C<sub>1</sub> of the indanol is 1/2.9, indicating a ratio of 1 for the enol and indanol.



### 3. Kinetic Data

The initial ketone concentrations for all the measurements were 0.025-0.06 M. The ketone conversion was normally controlled at 7%-12%. In the cases of  $\alpha$ -mesityl- $\alpha$ -phenylacetophenone 8,  $\alpha$ -mesityl- $\alpha$ -phenyl-p-methoxyacetophenone 9,  $\alpha$ -mesityl- $\alpha$ -phenyl-p-cyanoacetophenone 10, and  $\alpha$ -(2,4,6-triisopropyl)acetophenone, samples were analyzed with lower ketone conversion, i.e. 4%-7%. Benzaldehyde formation was quenched with naphthalene in benzene with ca. 0.07 M dodecanthiol at 365 nm for  $\alpha$ -(o-tolyl)propiophenone 2,  $\alpha$ -(o-tolyl)isobutyrophenone 4, and  $\alpha$ -mesityl-isobutyrophenone 7.  $\alpha$ -(o-Tolyl)acetophenone was quenched with 2,5-dimethyl-2,4-hexadiene in benzene at 313 nm for  $\alpha$ -(o-tolyl)valerophenone 3. Indanol formation was quenched with naphthalene in benzene at 365 nm for  $\alpha$ -mesitylpropiophenone 5,  $\alpha$ -mesitylvalerophenone 6, and  $\alpha$ -mesityl-o-methylacetophenone 13, with 2,5-dimethyl-2,4-hexadiene in benzene at 313 nm for  $\alpha$ -(o-tolyl)-p-methoxyacetophenone 1. Both indanol and enol ethers were quenched with 2,5-dimethyl-2,4-hexadiene in benzene at 365 nm for  $\alpha$ -mesityl- $\alpha$ -phenylacetophenone 8 and  $\alpha$ -mesityl- $\alpha$ -phenyl-p-methoxyacetophenone 9, with the exception that the enol ethers from  $\alpha$ -mesityl- $\alpha$ -phenylacetophenone 8 was quenched in hexane. Enol ethers were quenched with 2,5-dimethyl-2,4-hexadiene in benzene at 365 nm for  $\alpha$ -mesityl- $\alpha$ -phenyl-p-cyanoacetophenone 10. Mesitaldehyde was quenched with 2,5-dimethyl-2,4-hexadiene in benzene with ca. 0.07 M dodecanthiol at 313 nm for  $\alpha$ -mesityl-2,4,6-trimethylacetophenone 14,  $\alpha$ -mesityl- $\alpha$ -phenyl-2,4,6-trimethylacetophenone 11, and  $\alpha$ -phenyl-2,4,6-trimethylacetophenone 12.

The suspected type II cyclization products could not be separated from



Table 1. Lifetimes<sup>a</sup> of  $\alpha$ -Arylacetophenones

Ketones	$k_q\tau$	$\tau^{-1}\times 10^{-9}$
1	2900 <sup>b</sup>	0.0017
2	97.8 (10) <sup>f</sup>	0.051
3	27.7 (1.1) <sup>g</sup>	0.18
4	121 (16) <sup>f</sup>	0.041
5	17.2 (1.5) <sup>c</sup>	0.29
6	A curved Stern-Volmer plot was obtained	
7	7.28 (1.3) <sup>f</sup>	0.69
8	0.94 (0.04) <sup>c</sup> , 0.79 <sup>e</sup>	5.3
9	46.9 (1.0) <sup>c</sup> , 41.8 (1.7) <sup>d</sup>	0.11
10	1.18 <sup>d</sup>	3.2
11	0.62 (0.2) <sup>f</sup>	8.1
12	3.80 (0.7) <sup>f</sup>	1.38
13	1.87 (1.0) <sup>b</sup>	2.7
14	6.88 (0.8) <sup>f</sup>	0.73

a. Measured in benzene at 313 nm unless otherwise stated, with ketone conversions of 4-7% for 8, 9, 10 and 7-12% for the others.  $k_q = 5\times 10^9 \text{ s}^{-1}$  is used. Precisions of repeated measurements in parentheses. b. Quenching indanol. c. Quenching indanol at 365 nm. d. Quenching enol ethers at 365 nm. e. Quenching enol ethers in hexane at 365 nm. f. Quenching aldehyde formation in the presence of 0.007 M dodecanthiol. g. Quenching type II cleavage product.



Table 2. Quantum Yields of Photoproducts from  $\alpha$ -Arylacetophenones

Ketones	$\Phi(I)^a$	$\Phi(II)^b$	$\Phi(\delta)^c$		$\Phi(E)^d$	
			benzene	polar solvent	benzene	polar solvent
<u>1</u>			0.54			
				0.021, <sup>e</sup>		
<u>2</u>	0.28		0.048	0.018, <sup>f</sup> 0.015 <sup>g</sup>		
<u>2-d</u>			0.044			
		0.06 (0.02) <sup>m</sup>				
<u>3</u>	0.03	0.21 <sup>j</sup> (0.13) <sup>m</sup>	0.014 <sup>j</sup>			
<u>4</u>	0.38					
			0.55, <sup>h</sup>		0.010, <sup>h</sup>	
<u>5</u>	0.017		0.24	0.74, <sup>i</sup> 0.68 <sup>j</sup>	0.012	0.0077, <sup>i</sup> 0.012 <sup>j</sup>
			0.37, <sup>h</sup>		0.0051, <sup>h</sup>	
<u>6</u>	0.0063		0.12	0.70, <sup>i</sup> 0.78 <sup>j</sup>	0.0038	0.0047, <sup>i</sup> 0.0053 <sup>j</sup>
<u>7</u>	0.31					
			0.033, <sup>h</sup>		0.020 <sup>h</sup>	
<u>8</u>	0.0038		0.020	0.069, <sup>i</sup> 0.049 <sup>j</sup>	0.025	0.021, <sup>i</sup> 0.023 <sup>j</sup>
<u>8-d</u>			0.018		0.021	
<u>9</u>	0.0052		0.024	0.041 <sup>h</sup>	0.0084	0.0012 <sup>h</sup>
<u>10</u>	0.0058		0.0077	0.012 <sup>h</sup>	0.0046	0.0049 <sup>h</sup>
<u>11</u>	0.33					
<u>12</u>	0.016					
<u>13</u>	0.029		0.035	0.049, <sup>f</sup> 0.051 <sup>k</sup>		
<u>14</u>	0.35					
<u>16</u>			0.44	0.48, <sup>i</sup> 0.54 <sup>l</sup>		
<u>16-d</u>			0.43			



Table 2 (cont'd)

<b>17</b>	0.23	0.016 <sup>k</sup>
<b>17-d</b>	0.38	0.027 <sup>k</sup>

a. Aldehyde in 0.007 M dodecanthiol. b. Type II cleavage product. c. Indanol. d. Enol ethers. e. Acetonitrile with 2% H<sub>2</sub>O. f. t-Butyl alcohol. g. 0.5 M pyridine in benzene. h. 2 M dioxane in benzene. i. Acetonitrile. j. Methanol. k. Dioxane. l. 1 M pyridine in benzene. m. Quantum yields for a mixture of two suspected cyclobutanols in parentheses. n. Measured at 365 nm with ketone conversions of 4-7% for ketones 8, 9, 10, 15, 15-d and at 313 nm with ketone conversions of 7-12% for the others.



each other by GC. The  $^1\text{H}$  NMR of the mixture (possibly with other impurities) was too complex to be resolved. However the pattern of the spectrum and the solvent effect in the quantum yield indicate the identity of the cyclobutanols.

The triplet lifetimes and photoproduct quantum yields of the ketones were measured and are given in Table 1 and Table 2.

Flash photolysis of  $\alpha$ -mesityl- $\alpha$ -phenyl-p-methoxyacetophenone **9** indicated a triplet lifetime of 10.0 ns.<sup>80</sup> Our quenching study provided a  $k_q\tau$  value of 47. A  $k_q$  value of  $4.7 \times 10^9 \text{ M}^{-1}\text{s}^{-1}$  is thus derived for this ketone. This verifies that energy transfer quenching in our system is still diffusion-controlled within experimental error. Therefore, a  $k_q$  value of  $5.0 \times 10^9 \text{ M}^{-1}\text{s}^{-1}$  is used to obtain the lifetimes of the ketones studied.

A curved Stern-Volmer plot was obtained in the case of  $\alpha$ -mesitylvalerophenone **6** (Figure 14). This usually indicates the existence of more than one excited state of which the rate of interconversion is comparable to the rates of excited state decay.<sup>81</sup>

It has been known that the radicals generated by Norrish type I cleavage exist in a solvent cage as radical pairs. The radical pair can either recombine to the starting ketone or diffuse apart. The free radicals can be trapped by added hydrogen donors, such as thiols.<sup>20,24</sup> All the type I quantum yields in Table 1 were measured in the presence of approximately 0.07 M dodecanthiol or octadecanthiol. The dependence of the  $\alpha$ -cleavage efficiency on the concentration of dodecanthiol for  $\alpha$ -(o-tolyl)propiophenone **2** and  $\alpha$ -(o-tolyl)isobutyrophenone **4** was given in Figure 15 and Figure 16. The plateau indicates 100% trapping of the out-cage radicals.

The intersystem crossing quantum yield was measured for  $\alpha$ -mesityl- $\alpha$ -phenylacetophenone **8**, and found to be  $\sim 1.0$ . The measurement



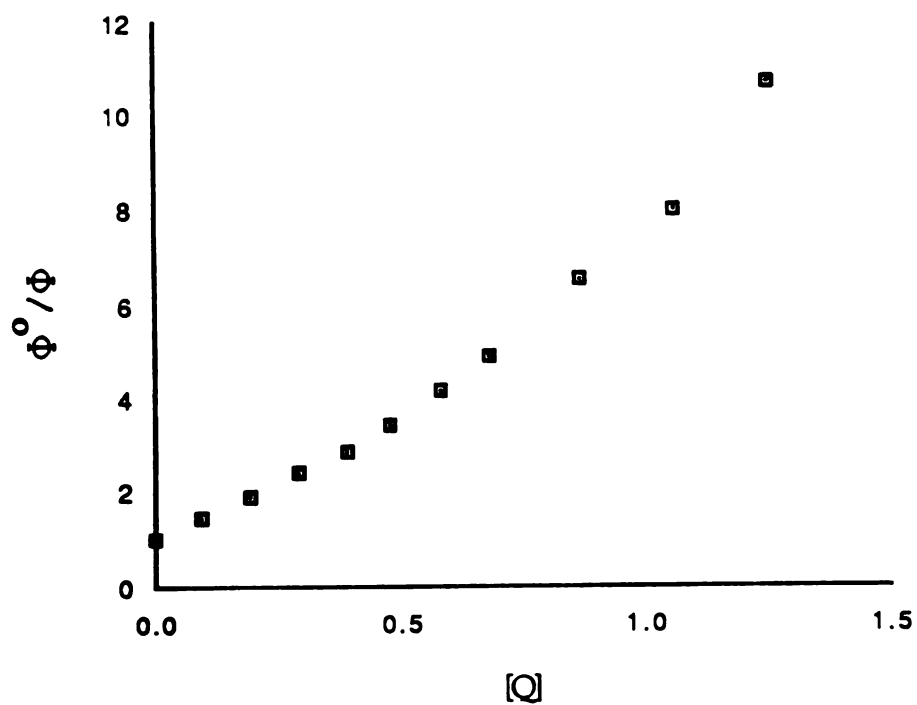
Table 14. Stern-Volmer Plot for  $\alpha$ -Mesitylvalerophenone



Table 15. Dependence of Benzaldehyde Formation from  $\alpha$ -(o-Tolyl)propiophenone on the Concentration of Dodecanthiol

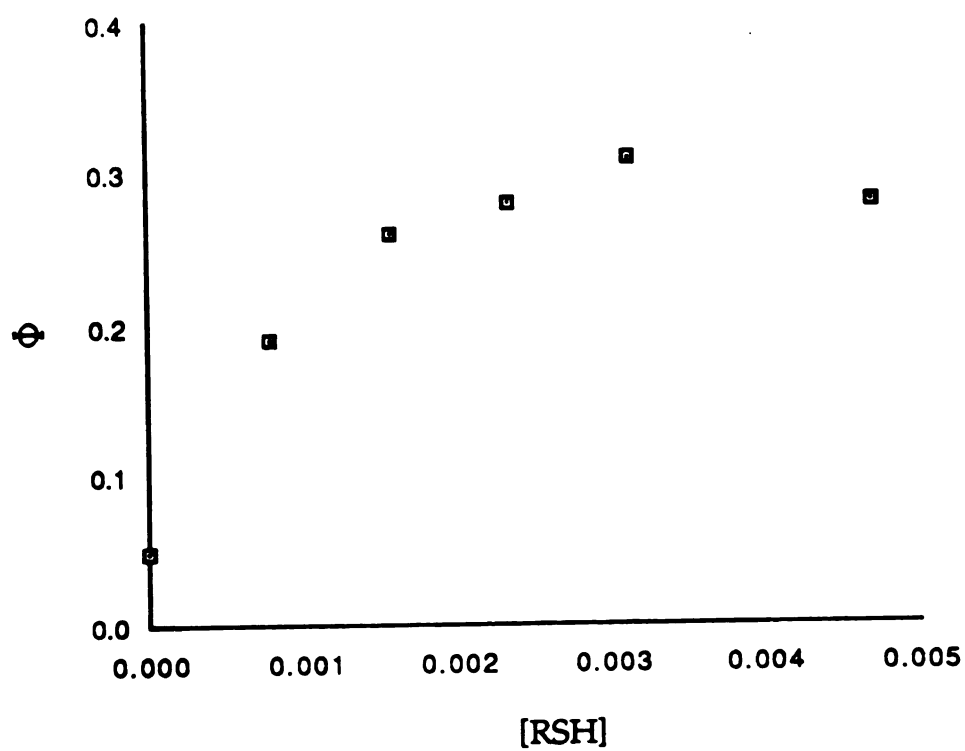
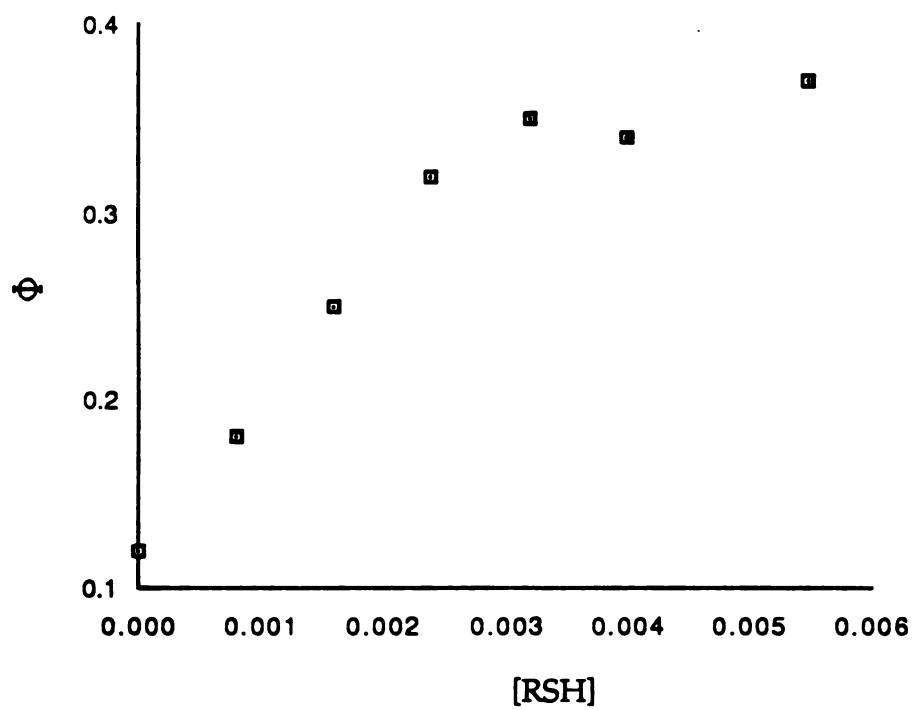




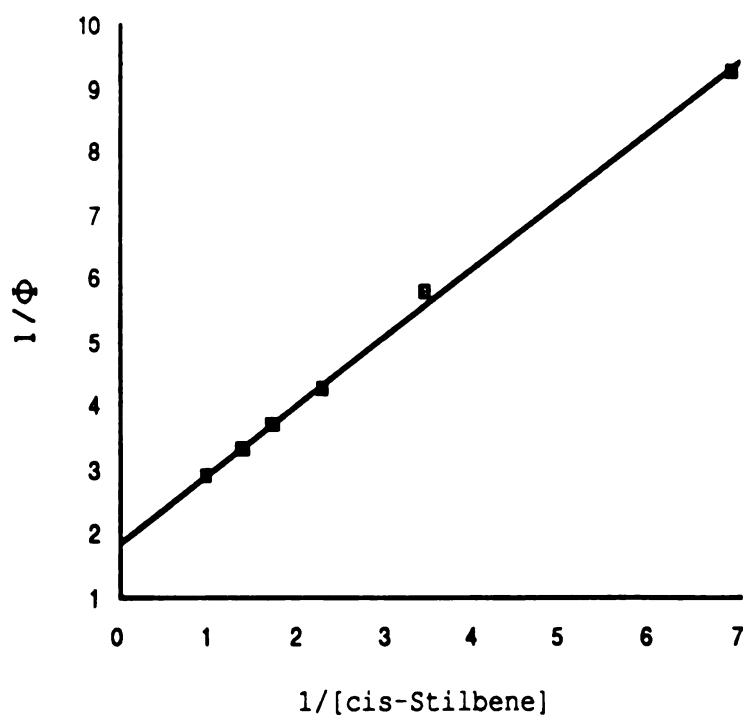
Table 16. Dependence of Benzaldehyde Formation from  $\alpha$ -(*o*-Tolyl)isobutyrophenone on the Concentration of Dodecanthiol





**Figure 17.** Plot of  $1/\Phi_{\text{isom}}$  versus  $1/[\text{cis-Stilbene}]$  in Sensitized  
Isomerization of cis-Stilbene by  $\alpha$ -Mesityl- $\alpha$ -Phenylacetophenone

8





was conducted by using the ketone to sensitize the isomerization of cis-stilbene.<sup>97c</sup> The quantum efficiency of cis to trans isomerization of stilbene,  $\Phi_{\text{isom}}$ , is given by equation (8),<sup>81</sup>

$$\Phi_{\text{isom}} = 2.5\Phi_{\text{isc}}k_{\text{q}}[\text{S}]/(k_{\text{q}}[\text{S}] + k_{\text{dt}}) \quad (8)$$

where  $\Phi_{\text{isc}}$  is the intersystem crossing quantum yield of the ketone,  $k_{\text{q}}$  is the quenching rate constant.  $k_{\text{dt}}$  is the rate constant for total triplet decay of the ketone, 0.41 is the percentage population of trans stilbene in the photostationary state with acetophenone as sensitizer.<sup>97c</sup> A plot of reciprocal  $\Phi_{\text{isom}}$  versus reciprocal cis-stilbene concentration gives a straight line, from which  $\Phi_{\text{isc}}$  can be derived from the intercept,

$$1/\Phi_{\text{isom}} = 2.5\Phi_{\text{isc}}(1 + k_{\text{dt}}/k_{\text{q}}[\text{S}]) \quad (9)$$

Benzene solutions of 0.04 M  $\alpha$ -mesityl- $\alpha$ -phenylacetophenone **8** with varying cis-stilbene concentrations were irradiated at 365 nm. The quantum yields of trans-stilbene formation were measured. Reciprocal  $\Phi_{\text{isom}}$  values were plotted versus reciprocal cis-stilbene concentrations (Figure 17). An intercept of 1.86 was obtained, which corresponds to a  $\Phi_{\text{isc}}$  of 1.31.

The Z/E ratios of the aryl vinyl ethers from  $\alpha$ -mesityl- $\alpha$ -phenylacetophenone **8**,  $\alpha$ -mesityl- $\alpha$ -phenyl-p-methoxyacetophenone **9** and  $\alpha$ -mesityl- $\alpha$ -phenyl-p-cyanoacetophenone **10** change with the ketone conversion. At high ketone conversion, the Z/E ratios equal the relative absorbances of the isomeric ethers at 365 nm, as expected for a photostationary state of the cis and trans photoisomerization. When the conversion is low, the Z/E ratios are close to 1.0. Table 3 shows how the Z/E ratios correspond to the



Table 3. Dependence of Z/E Ratios of Aryl Vinyl Ethers upon Their Relative Absorbances at 365 nm

Aryl Vinyl Ether <sup>a</sup>	Absorbance (365 nm)	Z/E Ratio at		Z/E Ratio at	
		Normal Conversion <sup>b</sup>	Low Conversion <sup>b</sup>	Equilibrium <sup>c</sup>	
8 AVE	Z	7	0.025M/8%	0.1M/0.16%	
	E	47	5.8/1.0	1.2/1.0	5.7/1.0
9 AVE	Z	12	0.036M/8%	0.1M/0.09%	
	E	63	6.2/1.0	1.6/1.0	6.0/1.0
10 AVE	Z	1100	0.015M/6%	0.1M/0.10%	
	E	620	1.0/1.8	1.0/1.0	1.0/1.8

a. # AVE--aryl vinyl ethers from ketone #. b. Top--initial ketone concentration with conversion, bottom--Z/E ratio. c. Prolonged irradiation of isolated aryl vinyl ethers.



absorbances of the aryl viny ethers at 365 nm.

#### 4. Dynamic NMR Studies

Dynamic proton NMR spectra (Figure 31-33) of  $\alpha$ -(o-tolyl)isobutyrophenone **4** showed broadening of the two  $\alpha$ -methyl group signals below 220 K, indicating that rotation is restrained along the  $C_\alpha$ -CO bond (Figure 18). They coalesced at around 180 K, and separated at 1.52 ppm and 1.78 ppm at 170 K.

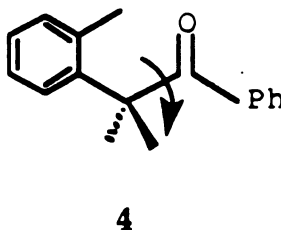
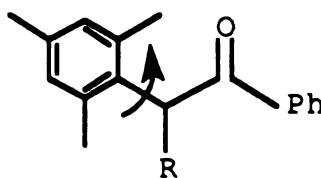


Figure 18



**5** R=CH<sub>3</sub>, **6** R=CH<sub>3</sub>(CH<sub>2</sub>)<sub>2</sub>, **8** R=Ph

Figure 19

Restricted rotations around the bond between  $\alpha$ -carbon and mesityl group were observed with  $\alpha$ -mesitylpropionophenone **5**,  $\alpha$ -mesitylvalero-



phenone **6**, and  $\alpha$ -mesityl- $\alpha$ -phenylacetophenone **8** (Figure 19). The two *o*-methyl groups coalesced at 240 K for **5**, 260 K for **6**, and 188

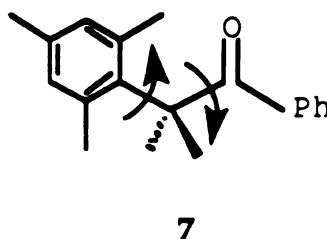


Figure 20

K for **8**. The same two methyl groups of **5** appeared at 1.90 ppm and 2.59 ppm at 200 K, the ones of **6** at 2.01 ppm and 2.59 ppm at 230 K, and the ones of **8** at 1.96 ppm and 2.44 ppm at 170 K (Figure 34-42).

$\alpha$ -Mesitylisobutyrophenone **7** showed restricted rotations along  $\alpha$ -carbon and mesityl bond as well as  $C_\alpha$ -CO bond (Figure 20). The coalescence temperatures of the two bond rotations are 200 K and 183 K respectively (Figure 43-46).

Linewidth analyses of the broadened NMR signals using equation (2) afforded the rotational rate constants at various temperatures. Based on equation (10) and (11), values of  $\ln k$  are plotted against  $1/T$ . The activation

$$k = A \times \text{Exp}(-E/RT) \quad (10)$$

$$\ln k = \ln A - E/RT \quad (11)$$

energy  $E$  and the  $A$  factor are calculated from the intercept and slope of the plots with equation (12) and (13). The rate constant at 300 K is calculated from



Table 4. Kinetic Parameters of C<sub>α</sub>-CO Bond Rotation for  
α-(o-Tolyl)isobutyrophenone 4

T(K)	185	190	195	200
k(s <sup>-1</sup> )	156	282	399	896
1/Tx10 <sup>3</sup>	5.41	5.26	5.13	5.00
lnk	5.05	5.64	5.99	6.63
E(Kcal/mole)=7.43x10 <sup>3</sup> A=9.53x10 <sup>10</sup> k(300K)=3.66x10 <sup>5</sup>				

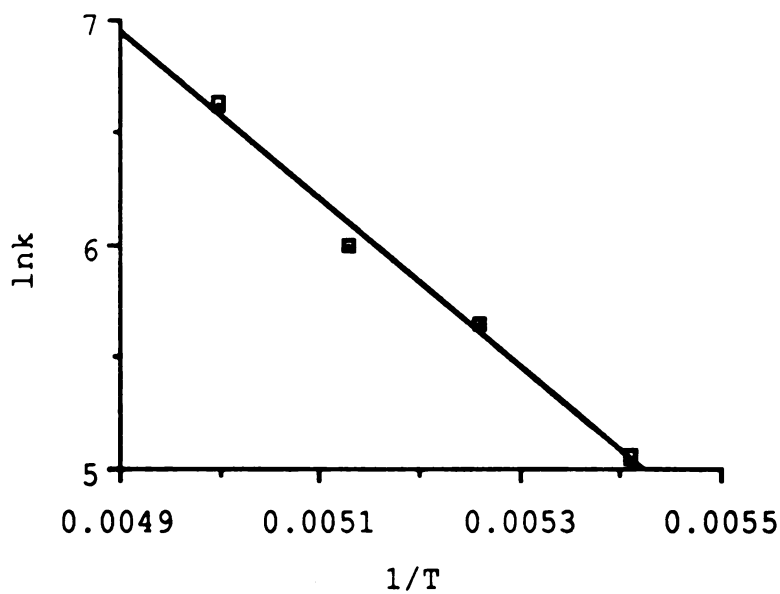


Figure 21. Plot of lnk vs. 1/T for C<sub>α</sub>-CO Bond Rotation in  
α-(o-Tolyl)isobutyrophenone 4



Table 5. Kinetic Parameters of C<sub>α</sub>-Mes Bond Rotation for  
α-Mesitylpropiophenone 5

T(K)	250	260	270	280	290
k(s <sup>-1</sup> )	723	1170	2117	3770	6260
1/Tx10 <sup>3</sup>	4.00	3.85	3.70	3.57	3.45
lnk	6.58	7.06	7.66	8.23	8.74
$E(\text{Kcal/mole})=7.89 \times 10^3$ $A=5.31 \times 10^9$ $k(300\text{K})=9.50 \times 10^3$					

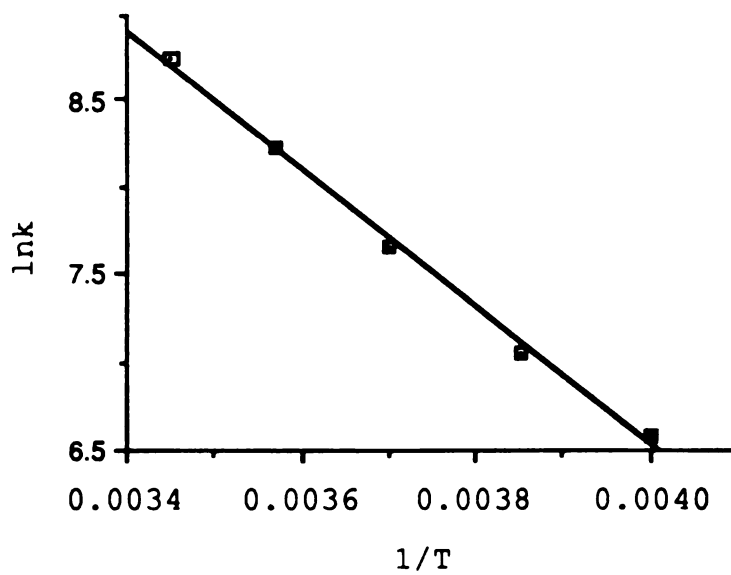


Figure 22. Plot of lnk vs. 1/T for C<sub>α</sub>-Mes Bond Rotation in  
α-Mesitylpropiophenone 5



Table 6. Kinetic Parameters of C<sub>α</sub>-Mes Bond Rotation for  
α-Mesitylvalerophenone 6

T(K)	280	290	300	310	320
k(s <sup>-1</sup> )	625	827	1400	2070	3090
1/Tx10 <sup>3</sup>	3.57	3.45	3.33	3.23	3.13
lnk	6.44	6.72	7.24	7.64	8.04
$E(\text{Kcal/mole})=7.42 \times 10^3$ $A=3.55 \times 10^8$ $k(300\text{K})=1.40 \times 10^3$					

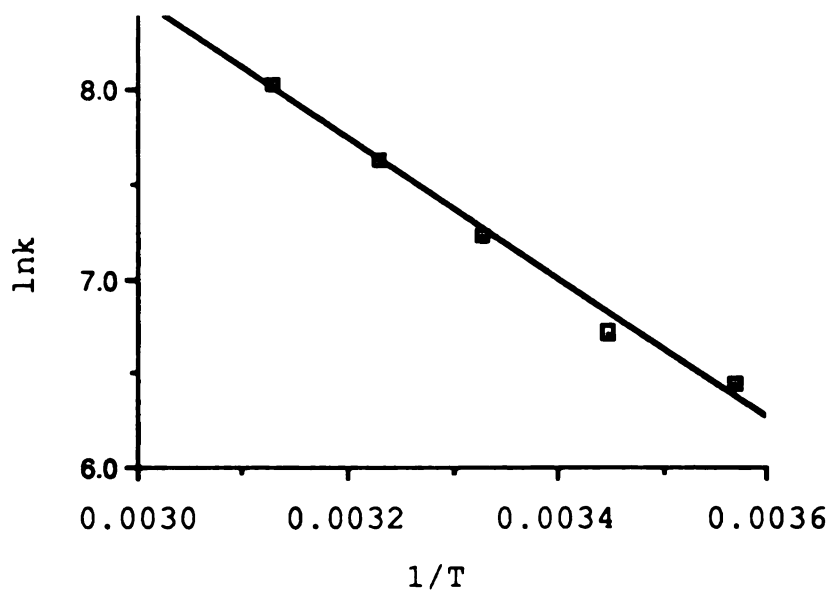


Figure 23. Plot of lnk vs. 1/T for C<sub>α</sub>-Mes Bond Rotation in  
α-Mesitylvalerophenone 6



Table 7. Kinetic Parameters of  $C_{\alpha}$ -CO Bond Rotation for  $\alpha$ -Mesitylisobutyrophenone 7

T(K)	185	190	200	210
k(s <sup>-1</sup> )	89	152	305	489
1/Tx10 <sup>3</sup>	5.41	5.26	5.00	4.76
lnk	4.49	5.02	5.72	6.19
<u>E(Kcal/mole)=5.16x10<sup>3</sup>      A=1.23x10<sup>8</sup>      k(300K)=2.14x10<sup>4</sup></u>				

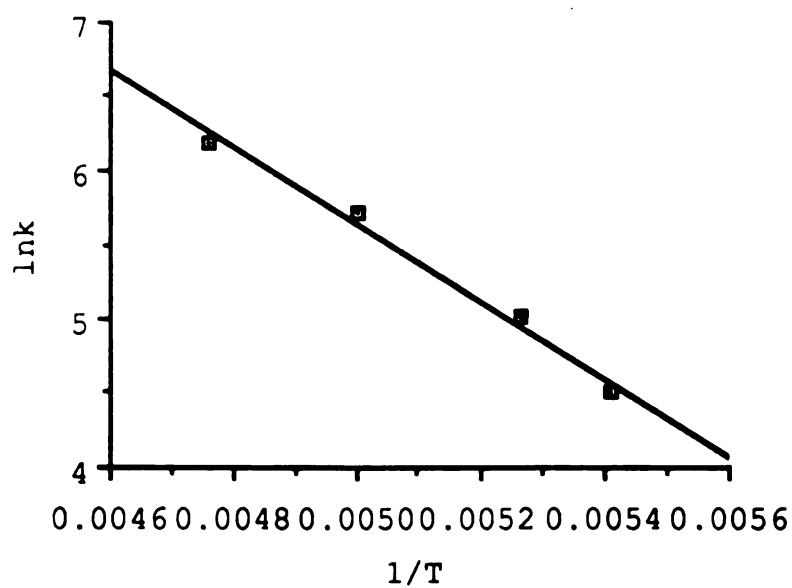


Figure 24. Plot of lnk vs. 1/T for  $C_{\alpha}$ -CO Bond Rotation in  $\alpha$ -Mesitylisobutyrophenone 7



Table 8. Kinetic Parameters of  $C_{\alpha}$ -Mes Bond Rotation for  $\alpha$ -Mesitylisobutyrophenone 7

T(K)	210	220	230	240
$k(s^{-1})$	1510	3410	6790	10200
$1/T \times 10^3$	5.41	5.26	5.13	5.00
$\ln k$	5.12	5.63	6.14	6.80
$E(Kcal/mole)=6.50 \times 10^3$ $A=9.32 \times 10^9$ $k(300K)=1.72 \times 10^5$				

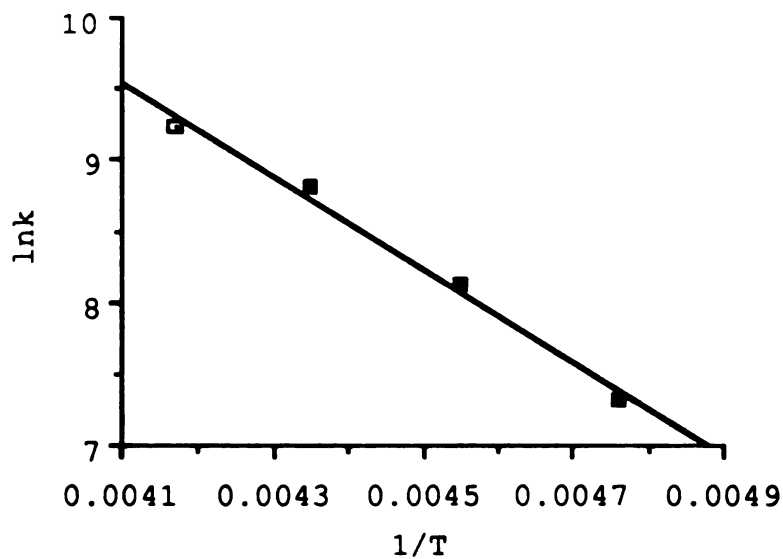


Figure 25. Plot of  $\ln k$  vs.  $1/T$  for  $C_{\alpha}$ -Mes Bond Rotation in  $\alpha$ -Mesitylisobutyrophenone 7



Table 9. Kinetic Parameters of  $C_{\alpha}$ -Mes Bond Rotation for  
 $\alpha$ -Mesityl- $\alpha$ -Phenylacetophenone 8

T(K)	180	185	190	210	230
k(s <sup>-1</sup> )	125	184	273	1314	2616
1/Tx10 <sup>3</sup>	5.56	5.41	5.26	4.76	4.35
lnk	4.83	5.21	5.61	7.18	7.87
$E(\text{Kcal/mole})=5.18 \times 10^3$ $A=2.58 \times 10^8$ $k(300\text{K})=4.35 \times 10^4$					

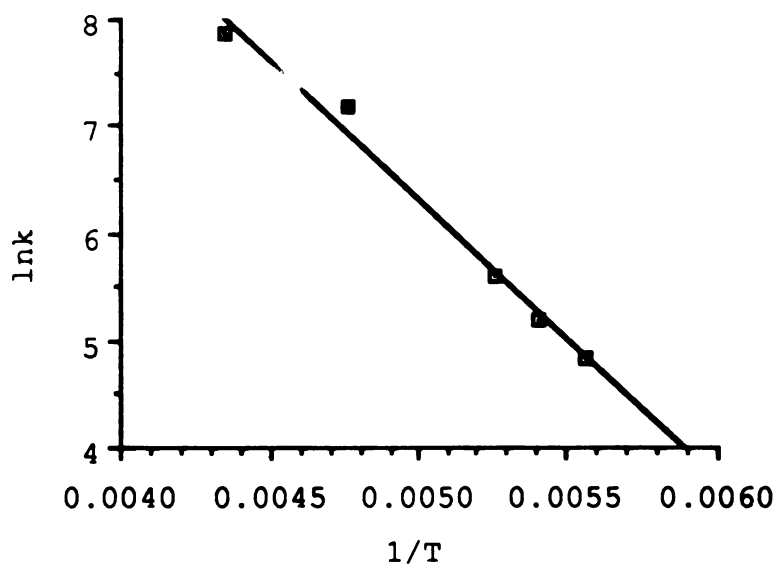


Figure 26. Plot of lnk vs. 1/T for  $C_{\alpha}$ -Mes Bond Rotation in  
 $\alpha$ -Mesityl- $\alpha$ -Phenylacetophenone 8



the activation energy,  $E$ , and the  $A$  factor following equation (10). All the parameters are listed in Table 4-9.

$$E = -R \times \text{Slope} \quad (12)$$

$$A = \text{Exp}(\text{Intercept}) \quad (13)$$

## 5. Molecular Mechanics Calculations

A molecular mechanics program, MMPMI distributed by Serena Software, Box 3076, Bloomington, IN 47402, was used in the effort to analyze the energy-minimized conformations of the ketones in ground state and their energetics. This program was adapted from the original MM program of N. L. Allinger by J. J. Gajewski and K. E. Gilbert. The term "energy-minimized conformation" refers to conformations with energetic minima on rotational energy surfaces. In cases where more than one conformation are found, the relative energies of different conformations are listed in Table 10. The values are all relative, and it makes sense only to compare between different conformations of the same molecules.

"Steric energy" in the table is defined as the energy arising from deviations from hypothetical ideal structures of the molecules, which can be expressed as the sum of bond stretching, bond bending, torsional, non-bonding interaction energies, and so on.

"Pi resonance energy" is the resonance stabilization energy of the Pi systems in the molecules.

"Total energy" for a conformation of a given molecule is arbitrarily defined as its steric energy from which a Pi system correction has been



Table 10. Relative Energies of different conformations of  $\alpha$ -Arylacetophenones

Ketone	Conformation	Steric Energy (Kcal/mole)	Pi Resonance Energy (Kcal/mole)	Total Energy (Kcal/mole)
	S	25.9	42.8	25.8
	G	26.8	42.7	26.8
<u>15</u>	S'	25.7	42.8	25.6
	S	27.1	42.9	26.3
<u>16</u>	G	27.6	42.1	27.6
	G	28.8	42.9	28.3
	G'	29.7	42.9	29.2
<u>2</u>	E	30.2	42.4	30.2
	G	31.0	42.6	30.7
<u>3</u>	E	33.4	42.3	33.3
	G	30.8	42.3	30.8
<u>5</u>	E	32.9	42.4	32.8
	G	32.8	42.6	32.8
<u>6</u>	E	36.2	42.6	36.2
	G	33.5	42.8	33.2
<u>4</u>	G'	37.5	42.5	37.5
	E	42.5	42.8	42.1
<u>8</u>	G	42.7	42.4	42.7
	E	29.6	42.5	29.6
<u>14</u>	G	28.7	42.7	28.5

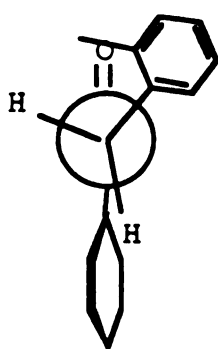


subtracted, i.e.

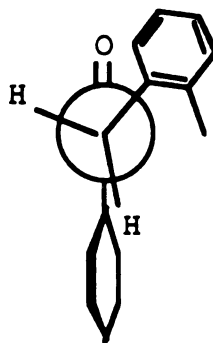
$$\text{Total Energy} = \text{Steric Energy} - \Delta\text{Pi} \quad (14)$$

$\Delta\text{Pi}$  is the difference in Pi resonance energies between this conformation and the conformation with the lowest Pi resonance energy for this given molecule. The purpose of the correction is to take the Pi conjugation into the consideration of the stability of conformations. There may be higher energy conformations with better p-conjugation, but the values for each ketone are relative.

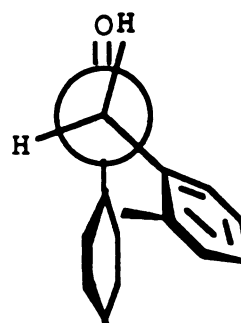
For the following conformations, letter E is used to designate the conformations with the  $\text{C}_\alpha$ -Ar bond eclipsing the carbonyl group, letter G the conformations with the  $\text{C}_\alpha$ -Ar bond  $120^\circ$  away from the carbonyl group, and letter S the conformations with the  $\text{C}_\alpha$ -Ar bond  $60^\circ$  away from the carbonyl group.



15S



15S'

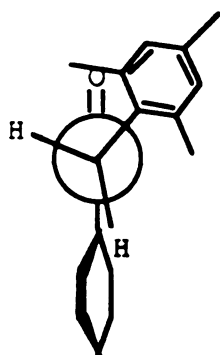


15G

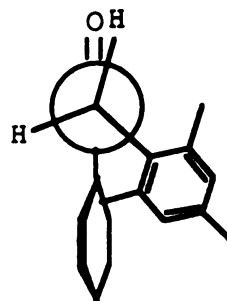
Attention should be given to two types of bond rotations in the molecules, rotations along  $\text{C}_\alpha$ -CO and  $\text{C}_\alpha$ -Ar bonds. The results of the calculations suggest that  $\alpha$ -(o-tolyl)acetophenone 15 adopts conformation 15S



as its most stable conformer, in which the aryl group is more or less  $60^\circ$  away from the carbonyl group. There is a less stable conformation of this ketone, 15G. Rotation of the tolyl group in conformation 15S leads to two alike conformations which differ only in the arrangement of the tolyl group. The arrangement can be such that the o-methyl group is next to the carbonyl group, 15S, or tilted away from it, 15S'. These two conformations are calculated to have comparable energies.

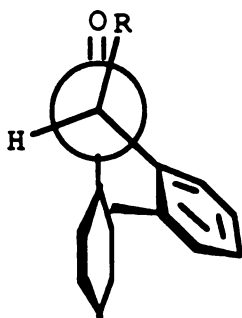


16S

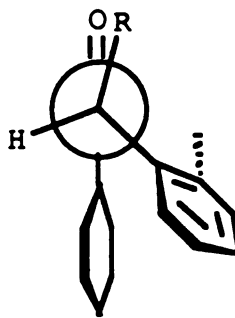


16G

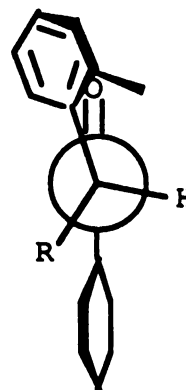
$\alpha$ -Mesitylacetophenone has two energy-minimized conformations, 16S and 16G, with 16S being 1.3 Kcal/mole more stable.



2G, 3G



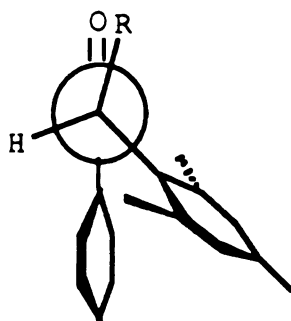
2G', 3G'



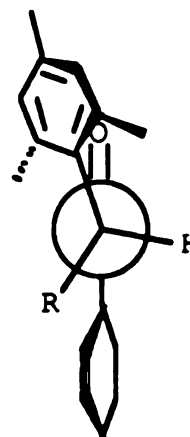
2E, 3E



The lowest energy conformation for  $\alpha$ -(o-tolyl)propiophenone **2** and  $\alpha$ -(o-tolyl)valerophenone **3** is the one with the  $\alpha$ -alkyl group more or less eclipsing with the carbonyl group, 2G and 3G. Again there is a second conformation regarding the orientation of the tolyl group, 2G' and 3G'. The third calculated conformation of these ketones is the one with the tolyl group eclipsing with the carbonyl group, 2E and 3E.

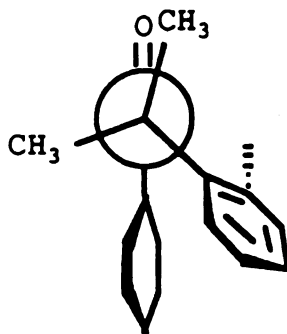


5G, 6G

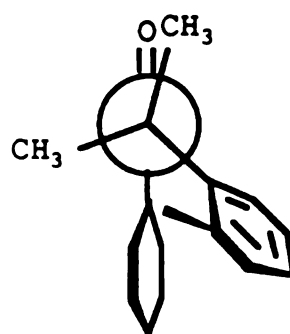


5E, 6E

$\alpha$ -Mesitylpropiophenone **5** and  $\alpha$ -mesitylvalerophenone **6** are calculated to have two conformations, 5G and 6G and 5E and 6E. Conformer



4G



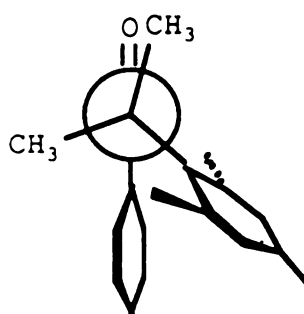
4G'



G is the more stable one of these two conformers.

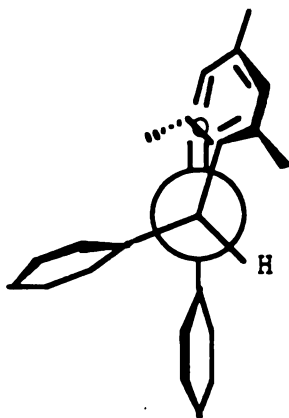
Conformation 4G is calculated to be the most stable conformation for  $\alpha$ -(o-tolyl)isobutyrophenone 4, in which one of the methyl group is eclipsing with the carbonyl group. A second conformation is suggested, 4G', which differs from 4G in the orientation of the tolyl group.

$\alpha$ -Mesitylisobutyrophenone 7 adopts conformation 7G as its stable conformation.

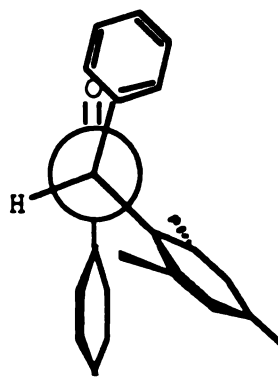


7G

For  $\alpha$ -mesityl- $\alpha$ -phenylacetophenone 8 the calculations suggest 8E as the most stable conformation along with 8G being slightly less stable.



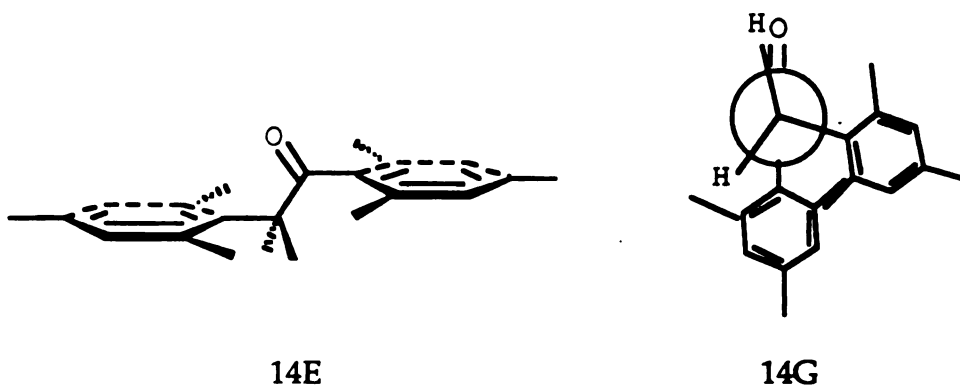
8E



8G



One of the calculated energy-minimized conformations of  $\alpha$ -mesityl-2,4,6-trimethylacetophenone **14**, **14E**, is most interesting due to the suggestion that the two mesityl groups are both perpendicular to the plane of the carbonyl group. The second calculated conformation for this ketone is **14G**, whose two mesityl groups are also oriented perpendicularly with respect to the carbonyl group as in **14E**. This latter conformation is calculated to be 1.1 Kcal/mole more stable than conformation **14E**.



## 6. Relative Conformation of Carbonyl Aryl and Carbonyl Group

Normally the phenyl and the carbonyl group in a phenyl ketone tend to be coplanar. However steric factors can affect the coplanarity, and thus the conjugation between the carbonyl aryl and the carbonyl group. The extent of the conjugation should be reflected in  $^{13}\text{C}$  chemical shift,<sup>82-84,95</sup> IR absorption of the latter,<sup>84,95</sup> and the  $\epsilon$  value of the K band in UV absorption spectra.<sup>85-86,95</sup>

Loss of conjugation will lead to a downfield shift of the carbonyl carbon signal in  $^{13}\text{C}$  NMR spectra, a blue shift of C=O stretching in IR, and a decreased  $\epsilon$  value of the K band in UV.



Table 11. Spectroscopic Data Related to Ar and C=O Conjugation

<b>Ketones</b>	<b>15</b>	<b>2</b>	<b>4</b>	<b>16</b>	<b>5</b>	<b>7</b>	<b>TMK<sup>a</sup></b>	<b>14</b>
$\lambda$ (nm)	238	239	240	237	239	240	250	no peak
$\epsilon$	14000	13000	10900	15200	12400	11600	11000	
$\delta(^{13}\text{C}=\text{O})$	197.4	200.4	203.9	197.1	202.3	204.0	204.05	206.7
$\nu_{\text{CO}}$	1690 to 1698							1710

a. TMK--1,1,2-trimesitylethanone.<sup>95</sup>

Table 11 lists the spectroscopic data, which show almost a complete loss of conjugation between the mesityl group and the carbonyl group in ketone 14.

## 7. X-Ray Crystallography

The resolved x-ray structure of 6, 8, and 14 are given in Figure 27-29 The samples were carefully recrystallized from ethanol. Detailed crystallographic parameters are given in the Appendix at the end of the thesis.

## 8. Spectroscopy

### a. Ultraviolet-Visible Absorption Spectra

The UV absorption spectra were recorded for all the ketones. The wavelengths of the absorption maxima and their corresponding extinction coefficients are reported in Table 12.



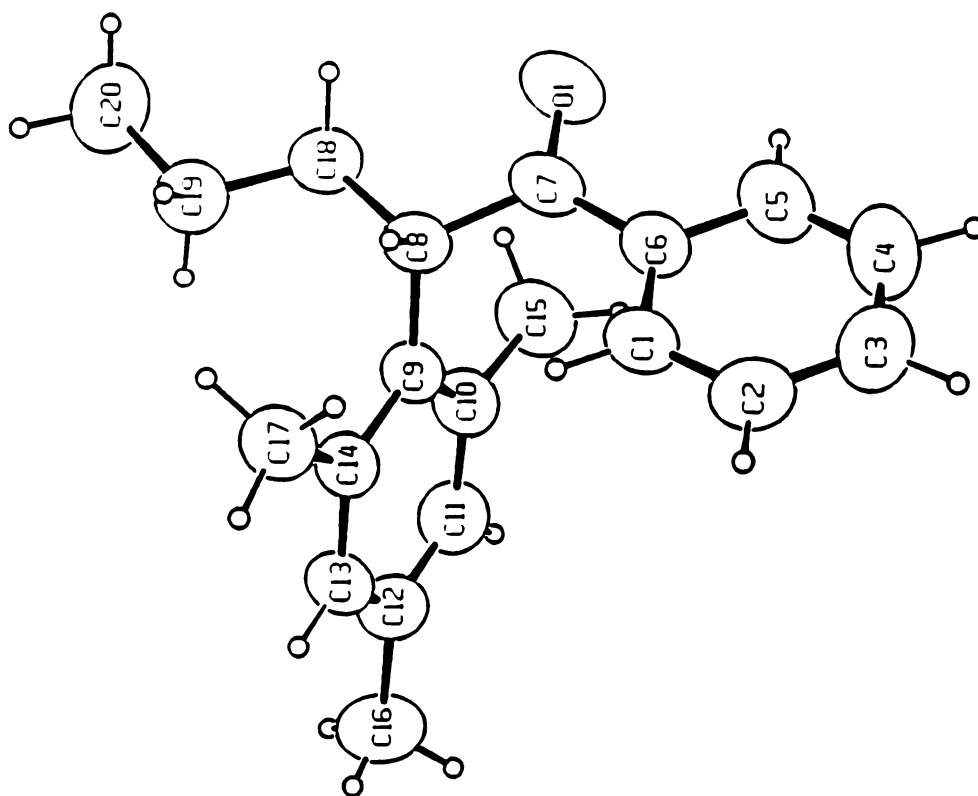
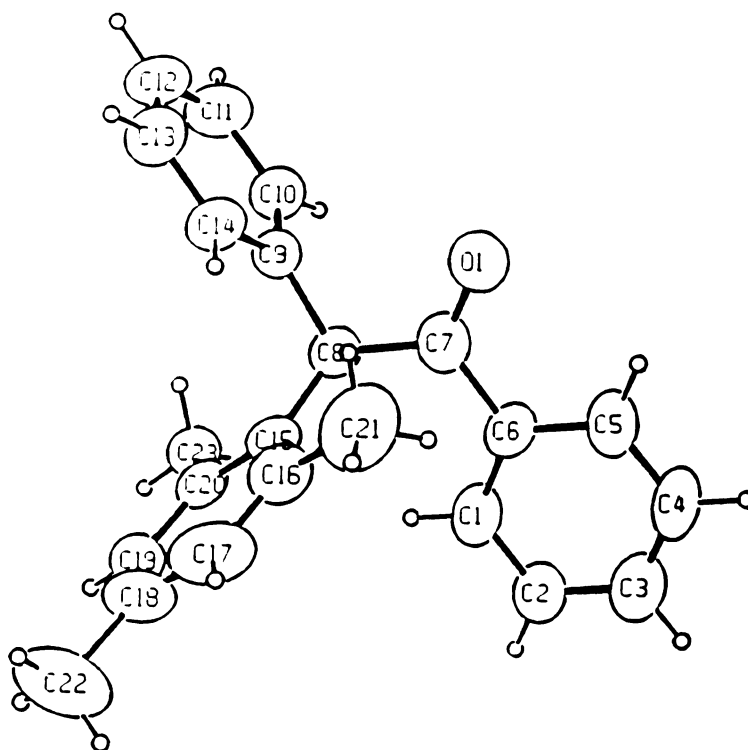


Figure 27. X-Ray Structure of  $\alpha$ -Mesitylvalerophenone 6





**Figure 28. X-Ray Structure of  $\alpha$ -Mesityl- $\alpha$ -Phenylacetophenone 8**



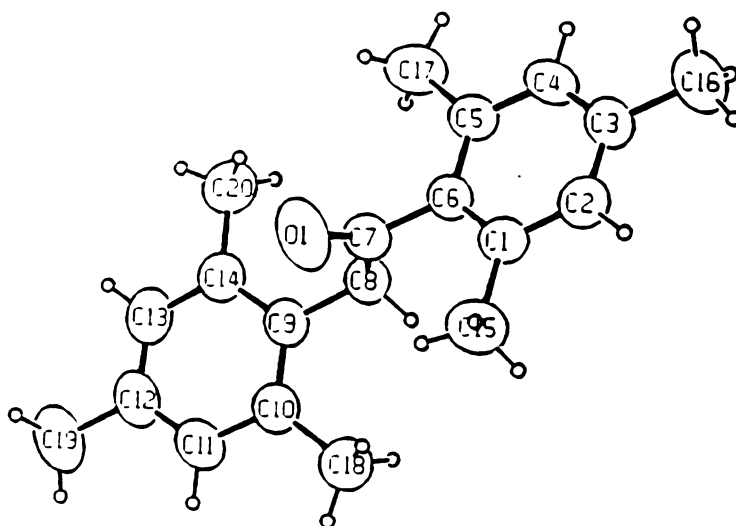


**Figure 29.** X-Ray Structure of  $\alpha$ -Mesityl-2,4,6-Trimethylacetophenone **14**



Table 12. UV Absorption Maxima and Extinction Coefficients of  $\alpha$ -Arylacetophenones

Ketones		Absorption Maxima in nm and Extinction Coefficients			
	$\lambda$	213		265	319
<b>1</b>	$\epsilon$	20000		1710	173
	$\lambda$	200	239	286	319
<b>2</b>	$\epsilon$	39500	13000	1230	115
	$\lambda$	201	240	288	325
<b>3</b>	$\epsilon$	65100	9100	607	141
	$\lambda$	200	240	274	324
<b>4</b>	$\epsilon$	46800	10900	1020	88
	$\lambda$	201	220	239	280
<b>5</b>	$\epsilon$	59200	13400	12100	1050
	$\lambda$		219	239	275
<b>6</b>	$\epsilon$		13700	12300	1470
	$\lambda$	203	221	240	274
<b>7</b>	$\epsilon$	60600	14000	12100	1430
	$\lambda$	200		238	
<b>8</b>	$\epsilon$	72100		13800	
	$\lambda$			270	310
<b>9</b>	$\epsilon$			16500	203
	$\lambda$		247	284	329
<b>10</b>	$\epsilon$		23765	3902	821
	$\lambda$	200	243		316
<b>11</b>	$\epsilon$	52800	8275		705
	$\lambda$	202	235	275	315
<b>13</b>	$\epsilon$	68600	12100	1370	101



Table 12 (cont'd)

$\lambda$	200	218	324
<b>14</b> $\epsilon$	63300	21700	400

---



## b. Phosphorescence Spectra

Table 13. Phosphorescence Maxima ( $\lambda_{0,0}$ ) and Triplet Energy of  $\alpha$ -Arylacetophenones

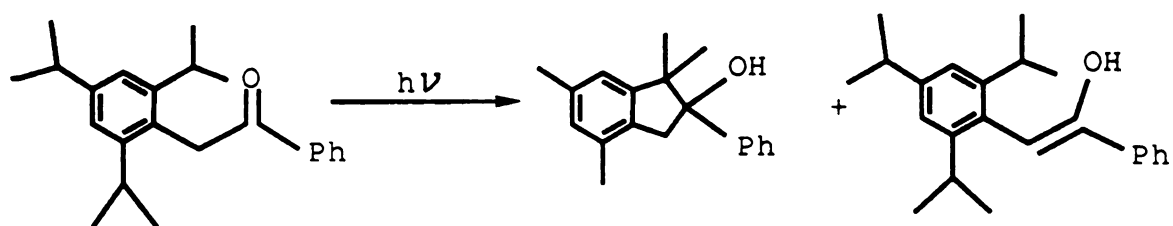
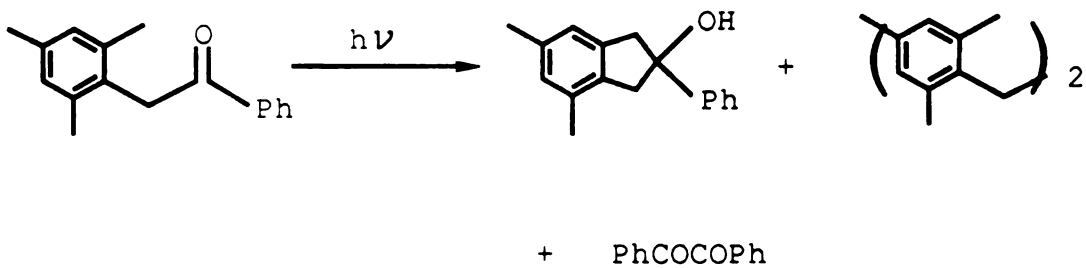
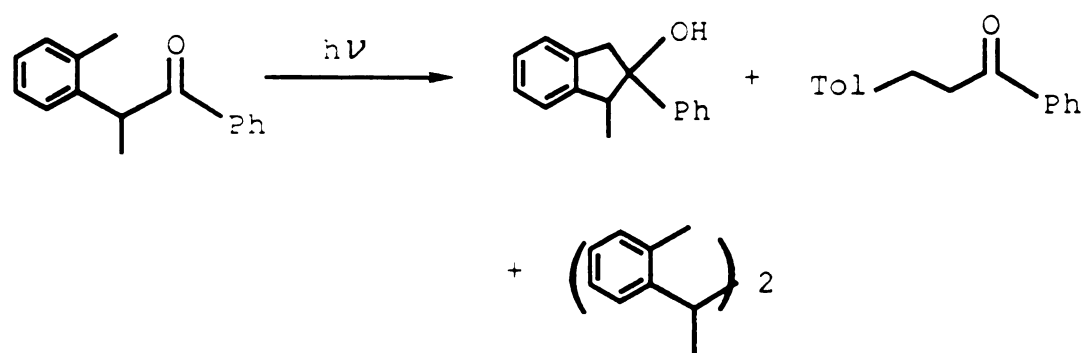
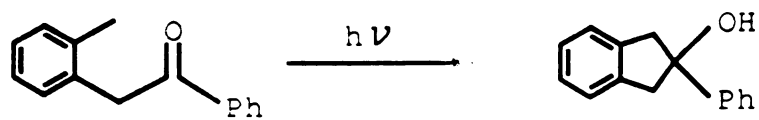
Ketones	1	2	3	4	5	6	7
$\lambda_{0,0}(\text{nm})$	406	393	394	395	391	392	394
$E_T(\text{Kcal/mol})$	70.4	72.8	72.6	72.4	73.1	72.9	72.6
Ketones	8	9	10	11	13	14	
$\lambda_{0,0}(\text{nm})$	392	407	420	393	388	392	
$E_T(\text{Kcal/mol})$	72.9	70.3	68.1	72.8	73.7	72.9	

Phosphorescence spectra were taken for all the ketones at 77 K in 2-methyltetrahydrofuran with ketone concentrations of ca. 0.03-0.04 M for most of the ketones. Samples of ca.  $10^{-4}$  M were used for  $\alpha$ -mesityl-o-methylacetophenone **13**,  $\alpha$ -mesityl-2,4,6-trimethylacetophenone **14**, and  $\alpha$ -mesityl- $\alpha$ -phenyl-2,4,6-trimethylacetophenone **11**. Representative phosphorescence spectra of some ketones are shown in Figure 47-53. The triplet energies of those ketones were calculated from the highest energy (0,0) band and are given in Table 13.

## B. Photoreactions in Solid State

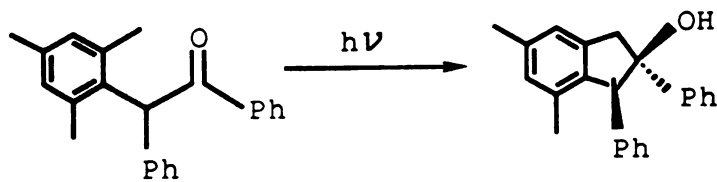
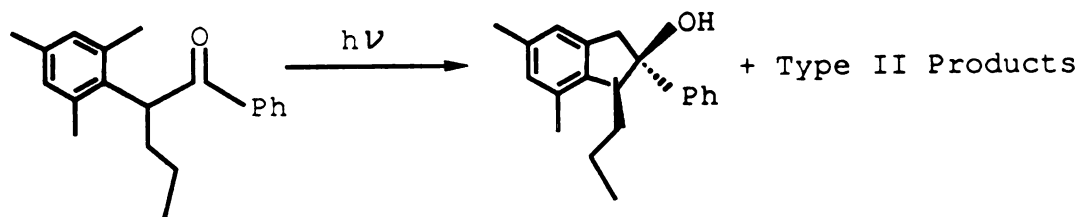
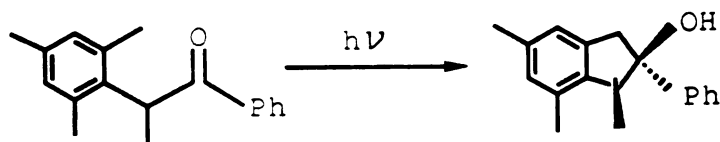
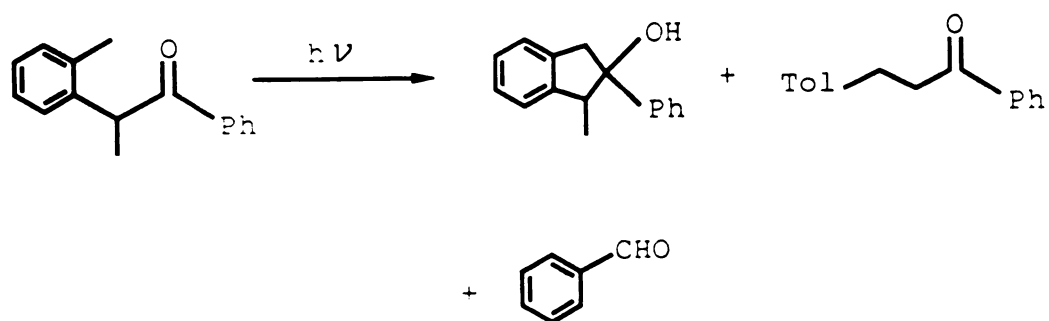
Two methods have been used to conduct the irradiation of the ketone samples in solid state. The ketones are irradiated either in powder or in crystal with a medium pressure mercury lamp filtered through an uranium sleeve for  $\alpha$ -(2,4,6-triisopropylphenyl)acetophenone **17**, and a Pyrex sleeve for the others. The powder form of the ketones was prepared by evaporating the





Reaction 14. Photolysis in Powder





Reaction 15. Photolysis in Crystal



solvent

plate.

were L

The pl

various

Table

H

1

—

—

—

a Ita

b. Ket

only

enol

the i

rearr

o-Me



solvent of methylene chloride solution of the ketones residing on a glass plate. The crystallized samples obtained in the purification of the ketones were used directly. The irradiation was carried out under Argon atmosphere. The photoreactions are shown in Reaction 14 and 15 and relative yields of various products are given in Table 14 and 15.

Table 14. Relative yields<sup>a</sup> of Photoproducts from Irradiation in Powder

Ketones <sup>b</sup>	Photoproducts			
	Indanol			
<b>15</b> (50%)	100%			
	Indanol	$\beta$ -TPP <sup>c</sup>	ArCHRCHRAr	Benzaldehyde
<b>2</b> (45%)	49.5%	11.5%	13.7%	25.3%
	Indanol	ArCHRCHRAr		PhCOCOPh
<b>16</b> (10%)	73.2%	24.4%		2.4%
	Indanol			Enol
<b>17</b> (27%)	9.9%			90.1%

a. Irradiated through an uranium sleeve for 17, a Pyrex sleeve for the others.

b. Ketone conversions in parentheses. c.  $\beta$ -(o-tolyl)propiophenone

In powder form,  $\alpha$ -(o-tolyl)acetophenone **15** gave the indanol as the only product, and  $\alpha$ -(2,4,6-triisopropylphenyl)acetophenone **17** produced the enol with small amount of the indanol.  $\alpha$ -(o-Tolyl)propiophenone **2** afforded the indanol and the products expected from  $\alpha$ -cleavage as well as a rearranged product,  $\beta$ -(o-tolyl)propiophenone in powder.  $\alpha$ -Mesitylacetophenone **16** gave some type I products besides the indanol.



phen

corre

$\alpha$ -m

dete

prod

in cr

T

—

—

—

—

—

—

a. L

Kete

46-

II. 1



The photoreactions of  $\alpha$ -mesitylpropiofenone **5** and  $\alpha$ -mesitylvalerophenone **6** are simpler in crystal than in solution. They both gave the corresponding indanols in high chemical yields. Irradiation of  $\alpha$ -mesityl- $\alpha$ -phenylacetophenone **8** in crystal afforded only the indanol in detectable amount by NMR.  $\alpha$ -(o-Tolyl)propiofenone **2** gave similar products in crystal as in podwer except for the absence of 2,3-di(o-tolyl)butane in crystal.

Table 15. Relative yields<sup>a</sup> of Photoproducts from Irradiation in Crystal

Ketones <sup>c</sup>	Photoproducts		
	Indanol	$\beta$ -TPP <sup>b</sup>	Benzaldehyde
<b>2</b> (7%)	66.7%	5.6%	27.7%
<b>5</b> (100%)	Indanol	Aryl Vinyl Ether	
	100%	0.0%	
<b>6</b> (23%)	Indanol	Aryl Vinyl Ether	Type II Products <sup>d</sup>
	94.2%	0.0%	5.8%
<b>8</b> (47%)	Indanol	Aryl Vinyl Ether	
	100%	0.0%	

a. Irradiated through a Pyrex sleeve. b.  $\beta$ -TPP-- $\beta$ -(o-tolyl)propiofenone. c. Ketone conversions in parentheses. d. Sum of  $\alpha$ -mesitylacetophenone and 4,6-dimethyl-2-phenyl-2-indanol.

## II. $\beta$ -Arylacetophenone Derivatives

### A. Identification of Photoproducts



18

19

20

20-d

21

21-d

deriv

the c

yield

$^1\text{H NMR}$

prese

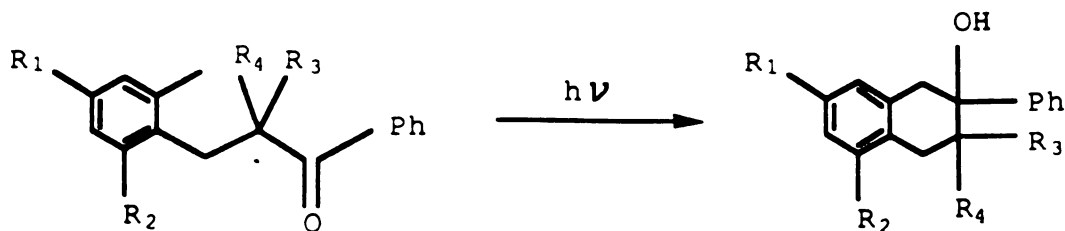
prod

meth

forma

even





- 18**  $R_1=R_2=R_3=R_4=H$ ,  $\beta$ -(*o*-tolyl)propionophenone  
**19**  $R_1=R_2=R_3=H$ ,  $R_4=CH_3$ ,  $\beta$ -(*o*-tolyl)isobutyrophenone  
**20**  $R_1=R_2=CH_3$ ,  $R_3=R_4=H$ ,  $\beta$ -mesitylpropionophenone  
**20-d**  $R_1=R_2=CH_3$ ,  $R_3=R_4=D$ ,  $\beta$ -mesitylpropionophenone- $d_2$   
**21**  $R_1=R_2=R_3=CH_3$ ,  $R_4=H$ ,  $\beta$ -mesitylisobutyrophenone  
**21-d**  $R_1=R_2=R_3=CH_3$ ,  $R_4=D$ ,  $\beta$ -mesitylisobutyrophenone- $d_1$

### Reaction 16

Irradiation of approximately 0.3 g of several  $\beta$ -arylpropionophenone derivatives in 500 ml cyclohexane or benzene through a Pyrex filter afforded the corresponding 1,2,3,4-tetrahydro-2-naphthols (Reaction 16). The chemical yields of the products range from 60% to 90%.

The structural identification of the photoproducts are based upon their  $^1H$  NMR,  $^{13}C$  NMR, MS, and IR spectra. The detailed spectral information is presented in the experimental section. A common feature of  $^1H$  NMR of the products is an AB quartet appearing at 2.90-3.50 ppm, which represents the methylene group at C-1.

Although the irradiation of  $\beta$ -(*o*-tolyl)propionophenone **18** did lead to the formation of photoproducts, as detected by GC, the conversion is too low, even after weeks' irradiation, for the products to be isolated and identified.

In the case of 1,2,3,4-tetrahydro-3-methyl-2-phenyl-2-naphthol and



1,2,3,

E is o

of Z-

becau

ppm

diffic

of the

meth

conc

$\alpha$ -me

presu

group

produ

I

pheno



1,2,3,4-tetrahydro-3,5,7-trimethyl-2-phenyl-2-naphthol, either a Z isomer or a E isomer can be formed. It has been reported that the methyl  $^1\text{H}$  NMR signal of Z-2-methyl-1-phenylcyclohexanol is upfield of the one of the E isomer, because it is shielded by the phenyl group, however the difference is only 0.10 ppm (Figure 30).<sup>87</sup>

The assignment of the stereochemistry of the naphthols is made difficult by lack of comparison because only one isomer was formed in both of the cases. On the other hand, the difference of the axial and equatorial methyl signal in 2-methyl-1-phenylcyclohexanol is too small to draw any conclusion upon. However, Lewis<sup>75</sup> has shown that  $\alpha$ -methylbutyrophenone gave only trans (Z) cyclobutanol upon irradiation, presumably, due to the less congested arrangement of the methyl and phenyl groups in the Z form. It therefore seems reasonable to assume that the products formed here are also the trans (Z) products.

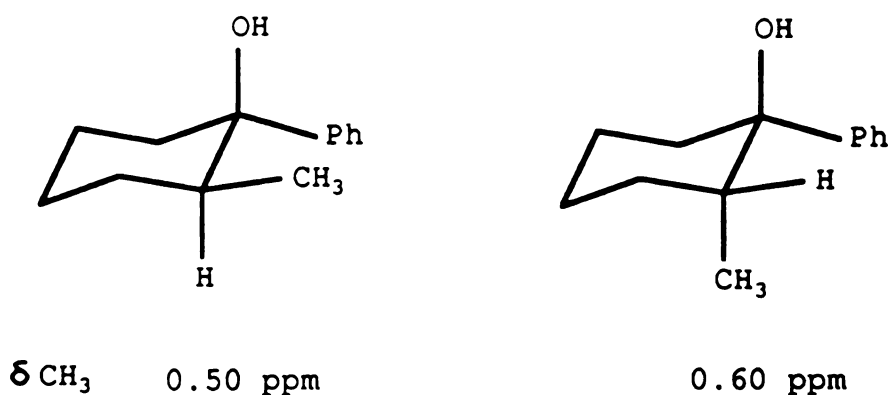


Figure 30

Irradiation of  $\beta$ -mesitylpropiophenone- $\text{d}_2$  20-d and  $\beta$ -mesitylisobutyrophenone- $\text{d}_1$  21-d was conducted to test the hypothesis that the enols of the



Table 16. Triplet lifetimes<sup>a</sup> of  $\beta$ -arylpropiophenones in Benzene

Ketones	$k_q\tau^b$	$\tau$ (ns)	$\tau^{-1}\times 10^{-8}(\text{sec}^{-1})$
<b>18</b>	6.8 <sup>c</sup>	1.4	7.1
<b>19</b>	8.0	1.6	6.3
<b>20</b>	4.8( 4.3 <sup>c</sup> )	0.96(0.86 <sup>c</sup> )	10.4(11.6 <sup>c</sup> )
<b>21</b>	5.5(0.5)	1.1	9.1

a. Measured at 313 nm.  $k_q=5\times 10^9 \text{ s}^{-1}$  is used. b. Precision of repeated measurements in parentheses. c. Measured by Scaiano<sup>69</sup> with flash photolysis.

ketones could have been formed from the intermediate biradical. The ketone samples (0.30 g) in benzene (500 ml) and dioxane (500 ml) were irradiated in a preparative photolysis apparatus with a Pyrex filter until ~20% conversion, <sup>1</sup>H NMR of the irradiated sample showed no appearance of the  $\alpha$ -protons of the ketones.

Table 17. Quantum Yields of Tetrahydronaphthols Formation in Various Solvents

Ketones	Benzene	Dioxane <sup>a</sup>	Acetonitrile	Methanol
<b>19</b>	0.00020	0.00017	0.00014	0.00032
<b>20</b>	0.00023	0.00028	0.00027	0.0012
<b>20-d<sub>2</sub></b>	0.00020	0.00025		
<b>21</b>	0.0022	0.0023	0.0015	0.012
<b>21-d</b>	0.0019	0.0019		

a. 2 M dioxane in benzene



## B. Kinetic Data

The formation of the tetrahydronaphthols is quenched by typical triplet quenchers such as 2,5-dimethyl-2,4-hexadiene. The triplet lifetimes were measured by Stern-Volmer quenching in benzene. The quantum yields of the photoproducts in various solvents were also measured. Both of the measurements were done at 313 nm. The results are listed in Table 16 and Table 17.

## C. MMPMI Calculations

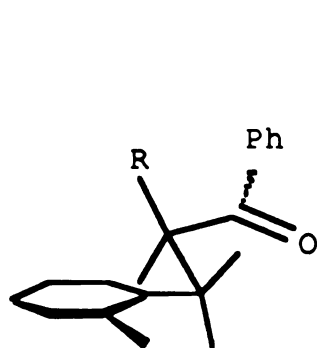
Table 18. Relative Energies of Different Conformations for  $\beta$ -Arylpropio-phenones

Ketone	Conformation	Steric Energy	Pi Resonance Energy	Total Energy
		(Kcal/mole)	(Kcal/mole)	(Kcal/mole)
<b>18</b>	G	27.4	42.8	27.4
	A	30.7	42.8	31.0
	A'	29.5	42.8	29.5
<b>19</b>	G	28.5	42.8	28.5
	A	30.9	42.9	31.3
	A'	29.3	42.8	29.3
<b>20</b>	G	28.3	42.9	28.2
	A	30.2	42.8	30.2
<b>21</b>	G	31.4	42.8	31.4
	A	31.9	42.8	31.9

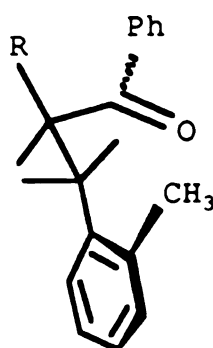


The relative energies of different conformations of those  $\beta$ -arylpropiophenone derivatives were calculated with MMPMI. The relative energies are given in Table 18. The definition of the terms used and the limitation on reliability of the values are the same as  $\alpha$ -arylacetophenone derivatives. Letter A is used to designate the conformations with the  $\beta$ -aryl group anti to the  $\alpha$ -alkyl group, and letter G with the conformations with the  $\beta$ -aryl group gauche to the  $\alpha$ -alkyl group.

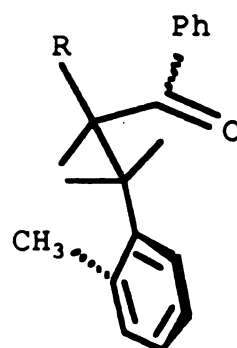
There are three interesting conformations by the calculations for  $\beta$ -(*o*-tolyl)propiophenone **18** and  $\beta$ -(*o*-tolyl)isobutyrophenone **19**, 18G and 19G, 18A and 19A, and 18A' and 19A'. For ketone **18**, conformation 18G is the most stable one of the three conformers. For ketone **19**, 19G is still more stable than the other two. But the energy gaps between 19G and 19A as well as 19A', in which the tolyl group is anti to the alkyl group, are significantly reduced. In both cases (ketone **18** and **19**), conformation A' is 1.5-2.0 Kcal/mole more stable than conformation A.



18G, 19G



18A, 19A

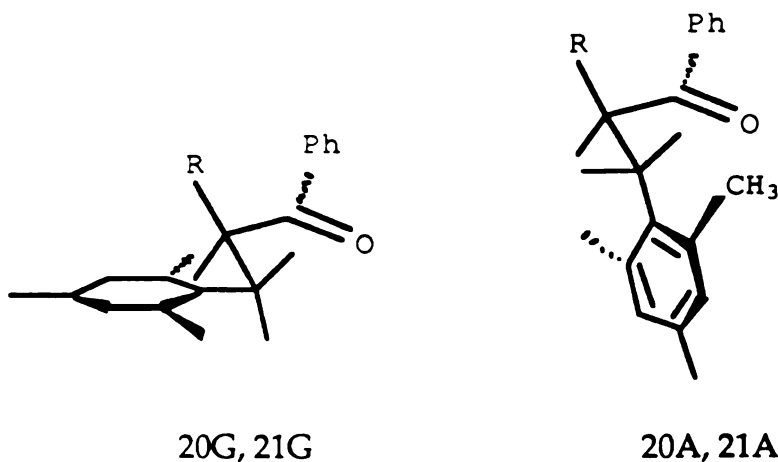


18A', 19A'

$\beta$ -Mesitylpropiophenone **20** and  $\beta$ -mesitylisobutyrophenone **21** can have two energy-minimized conformations, 20G and 21G, and 20A and 21A. Although 20G and 21G is the more stable conformation,  $\alpha$ -methylation does



lower the energy of 21A relative to the one of 21G by the calculations, since 21A has its mesityl group anti to the methyl group.



## D. Spectroscopy

### 1. Ultraviolet-Visible Absorption Spectra

Table 19. UV Absorption Maxima and Extinction Coefficients of  $\beta$ -Arylpropiophenones

Ketones						Absorption Maxima in nm and Extinction Coefficients							
		$\lambda$		239		272		323					
18		$\epsilon$		10400		967		60					
		$\lambda$		240		273		323					
19		$\epsilon$		12500		928		76					
		$\lambda$		201		219		238		269		326	
20		$\epsilon$		56300		11500		12100		840		64	
		$\lambda$		201		219		238		269		326	
21		$\epsilon$		51000		10500		10500		1130		79	



The UV absorption spectra were recorded for all the ketones. The wavelengths of the absorption maxima and their corresponding extinction coefficients are reported in Table 19.

## 2. Phosphorescence Spectra

Table 20. Phosphorescence Maxima ( $\lambda_{0,0}$ ) and Triplet Energy of  $\beta$ -Arylpropiophenones

Ketones	18	19	20	21
$\lambda_{0,0}(\text{nm})$	393	395	391	393
$E_T(\text{Kcal/mol})$	72.8	72.4	73.1	72.8

Phosphorescence spectra were taken for all the ketones at 77 K in 2-methyltetrahydrofuran with the ketone concentration of ca. 0.03-0.04 M. Representative phosphorescence spectra of some ketones are shown in Figure 47-53. The triplet energies of those ketones were calculated from the highest energy (0,0) band and are given in Table 20.

## III. Representative Low Temperature NMR and Phosphorescence Spectra







**Figure 32.**  $^1\text{H}$  NMR of  $\alpha$ -(*o*-Tolyl)isobutyrophenone **4** at 180 K



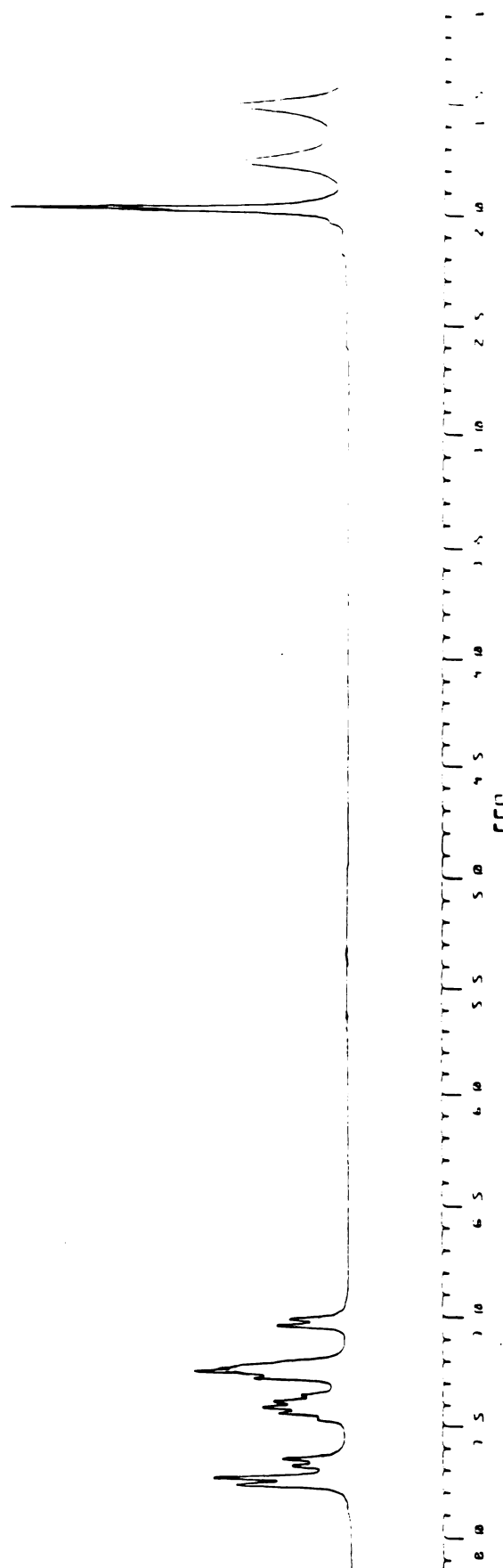
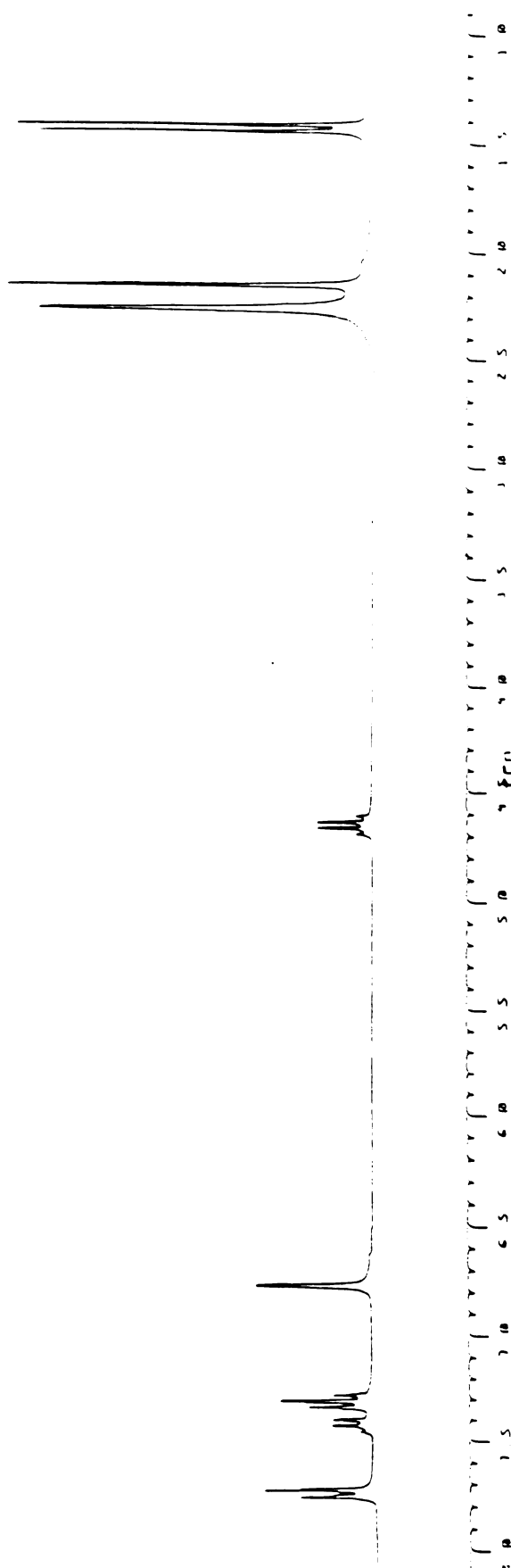


Figure 33.  $^1\text{H}$  NMR of  $\alpha$ -(o-Tolyl)isobutyrophenone **4** at 170 K





**Figure 34.  $^1\text{H}$  NMR of  $\alpha$ -Mesitylpropiphenone 5 at 300 K**



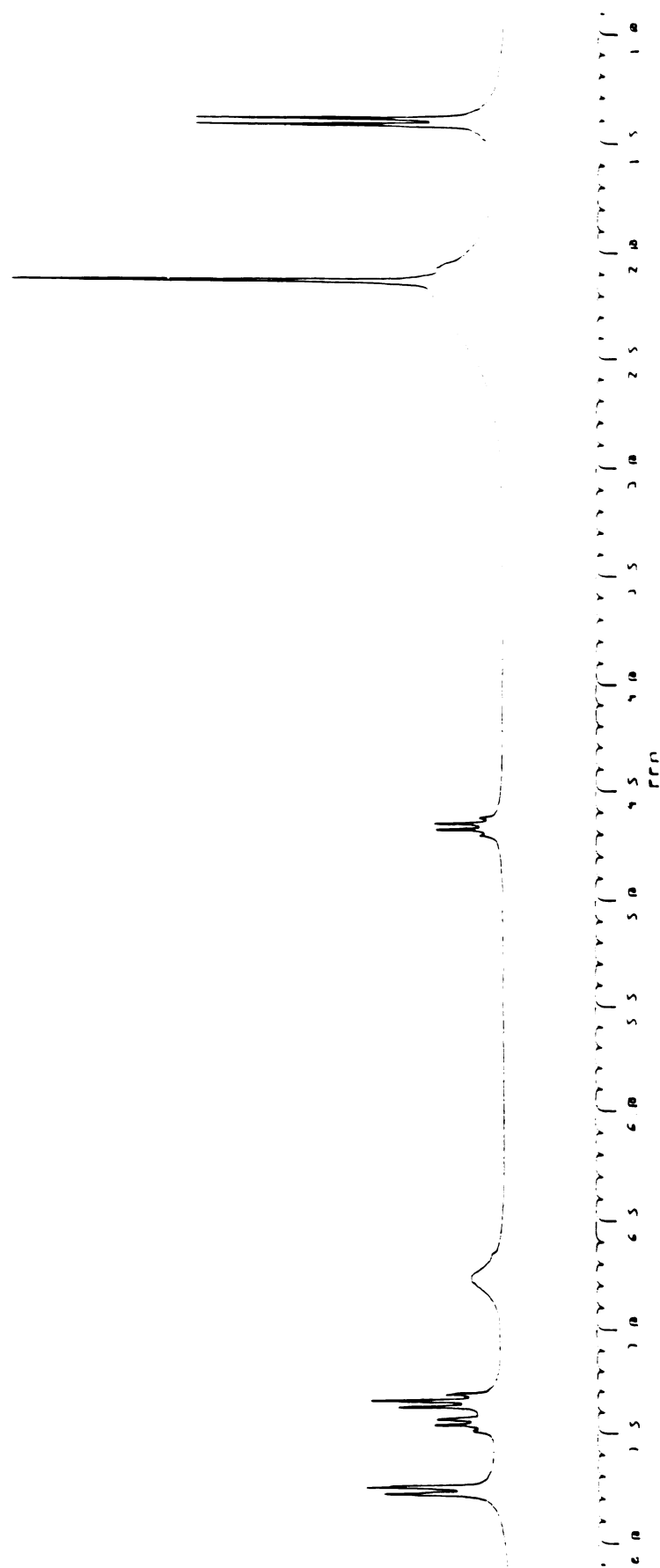


Figure 35.  $^1\text{H}$  NMR of  $\alpha$ -Mesitylpropiphenone 5 at 240 K



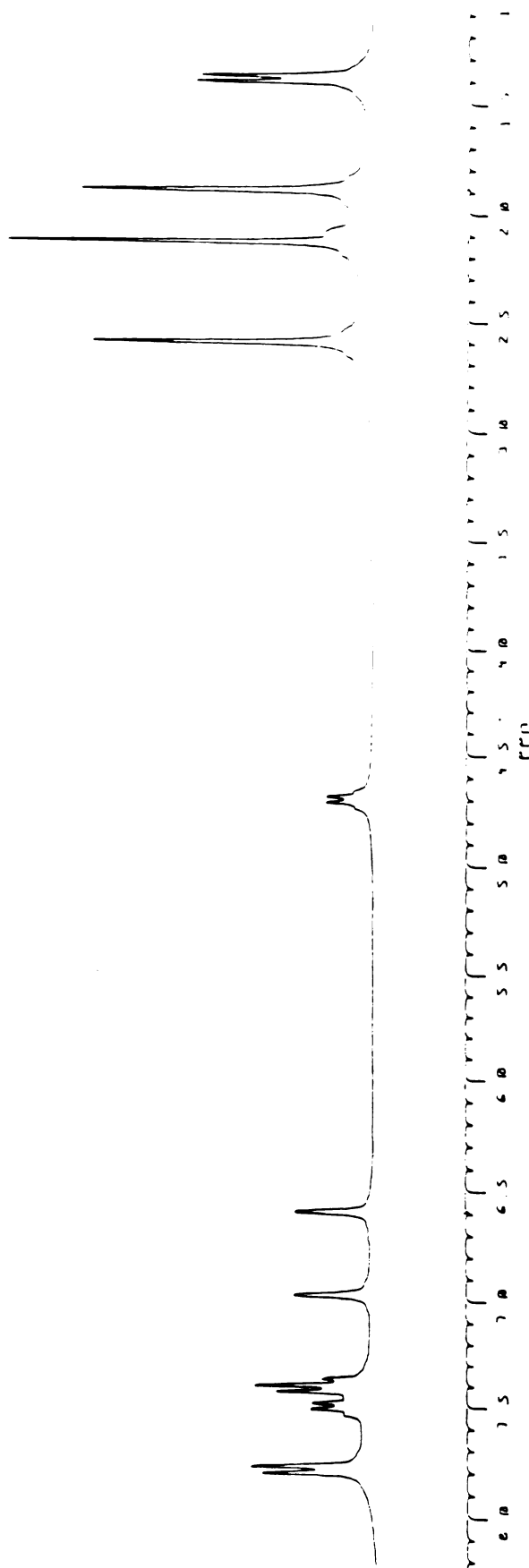


Figure 36.  $^1\text{H}$  NMR of  $\alpha$ -Mesitylpropiphenone **5** at 200 K



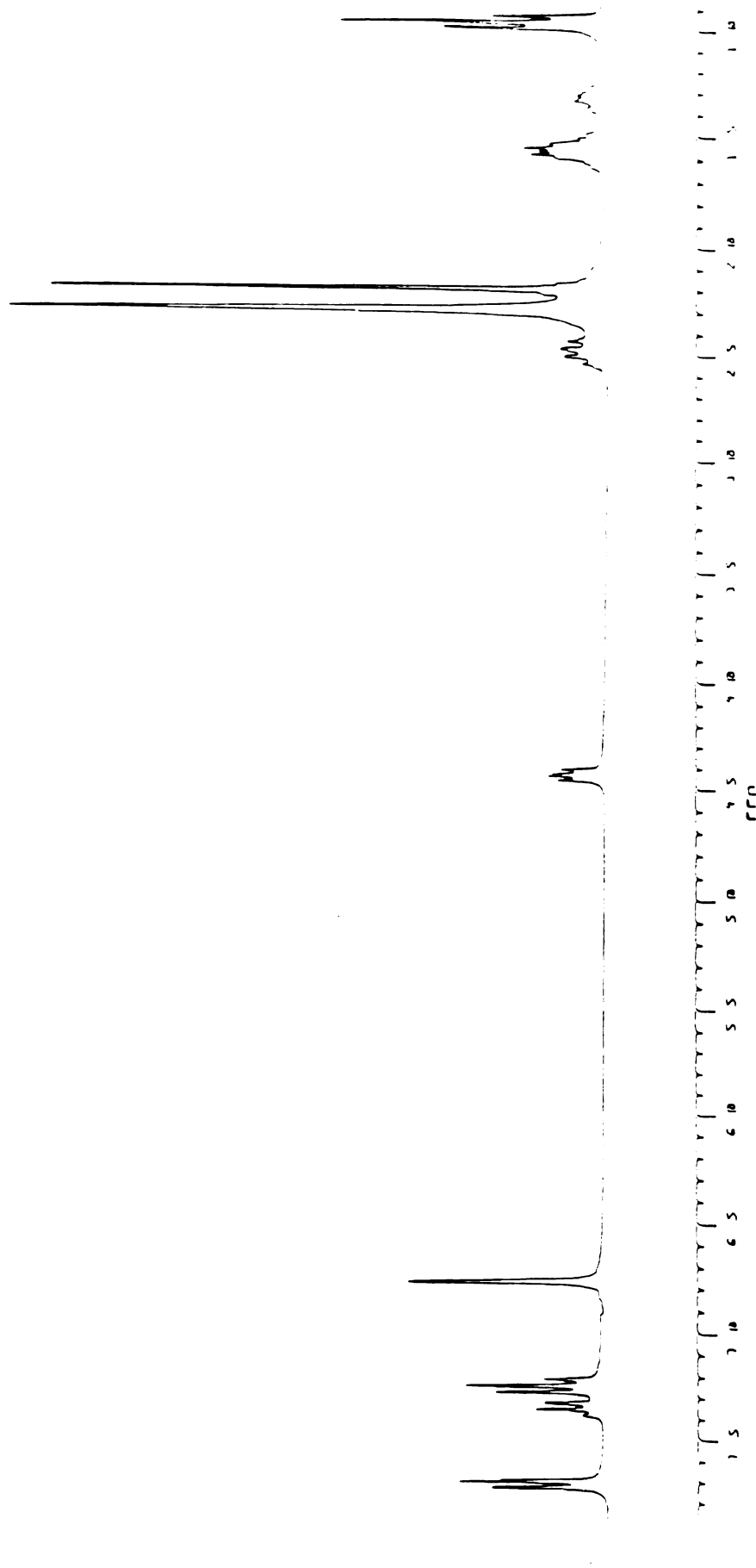


Figure 37.  $^1\text{H}$  NMR of  $\alpha$ -Mesitylvalerophenone **6** at 340 K



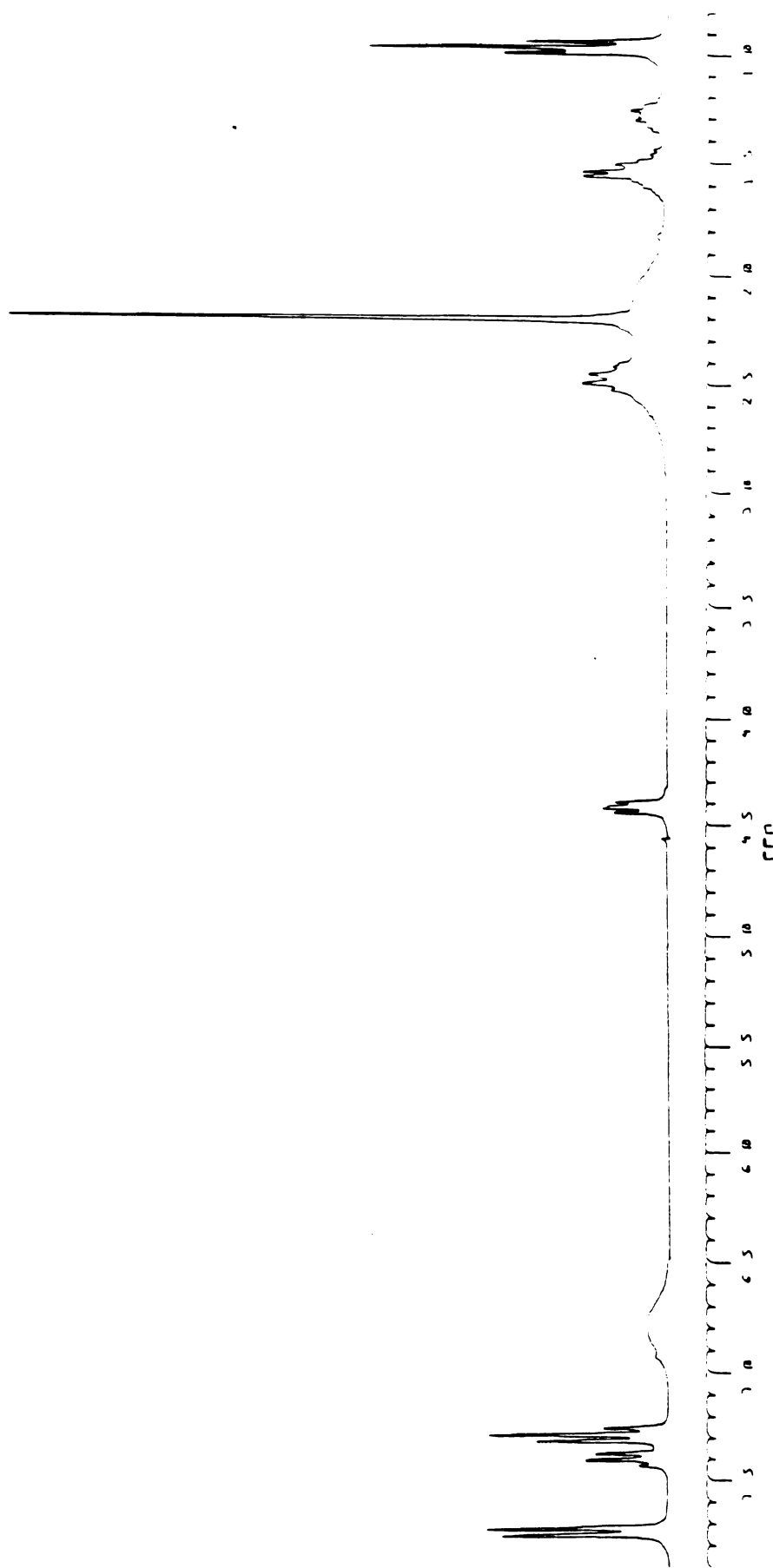


Figure 38.  $^1\text{H}$  NMR of  $\alpha$ -Mesitylvalerophenone 6 at 260 K



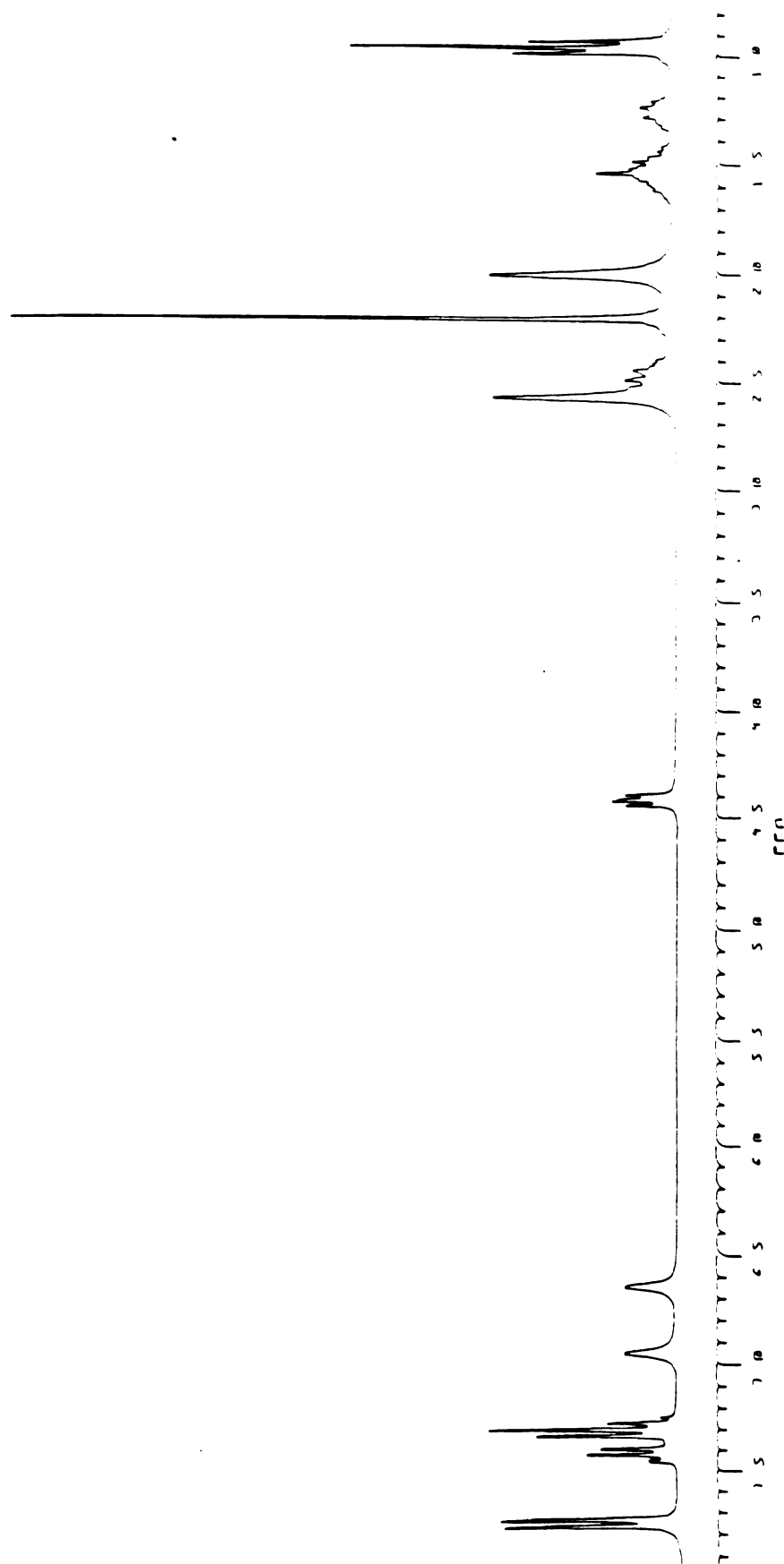
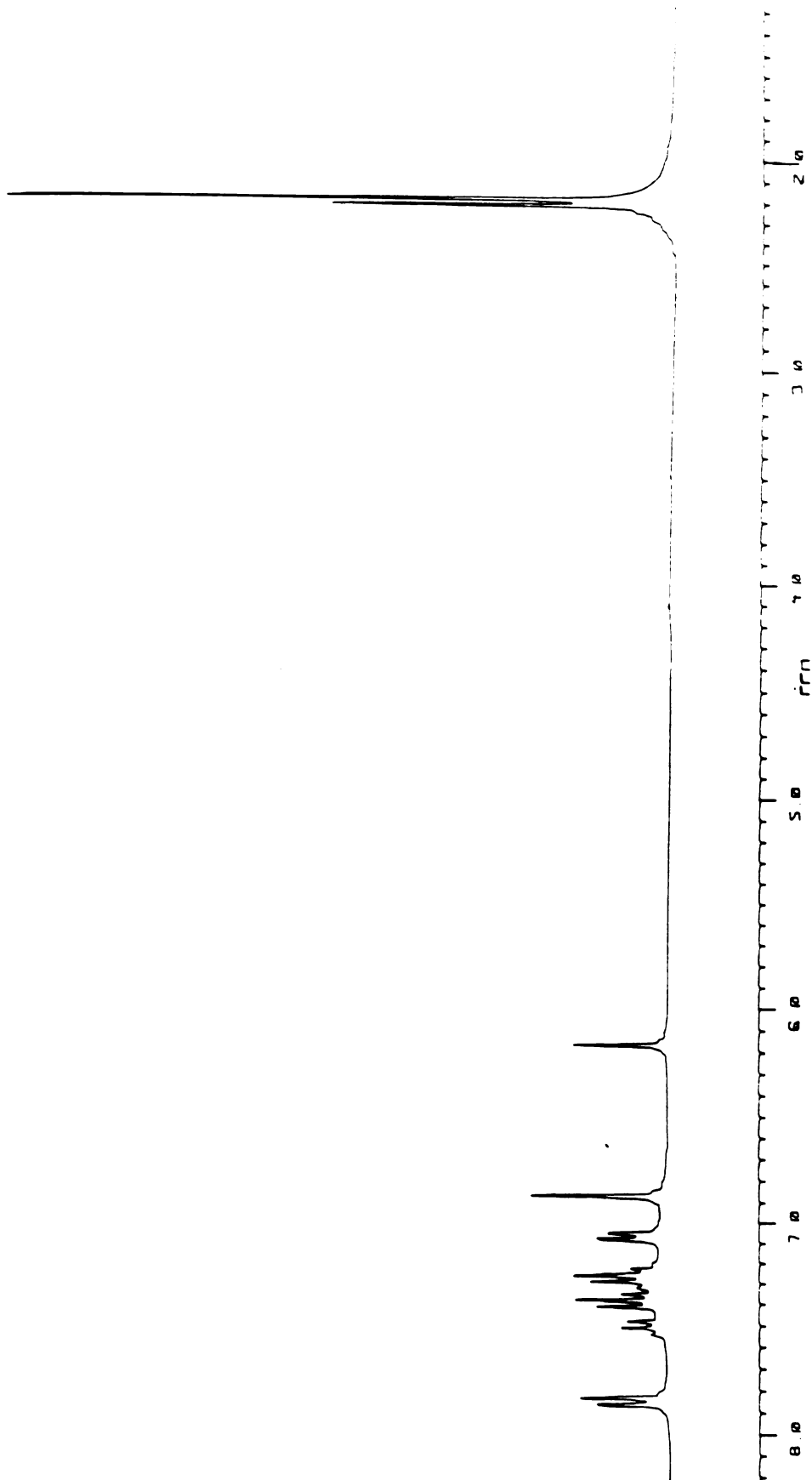


Figure 39.  $^1\text{H}$  NMR of  $\alpha$ -Mesitylvalerophenone **6** at 230 K





**Figure 40.  $^1\text{H}$  NMR of  $\alpha$ -Mesityl- $\alpha$ -Phenylacetophenone **8** at 300 K**



Figure 41.  $^1\text{H}$  NMR of  $\alpha$ -Mesityl- $\alpha$ -Phenylacetophenone **8** at 188 K



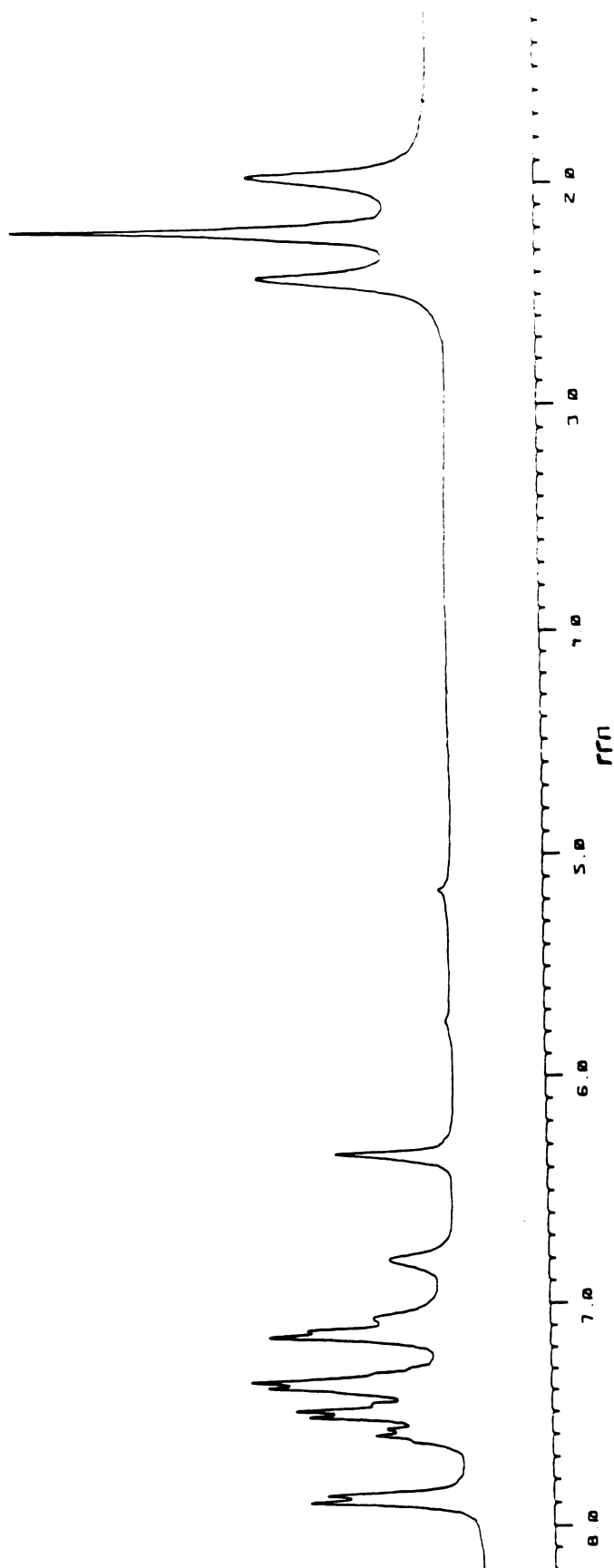


Figure 42.  $^1\text{H}$  NMR of  $\alpha$ -Mesityl- $\alpha$ -Phenylacetophenone **8** at 170 K



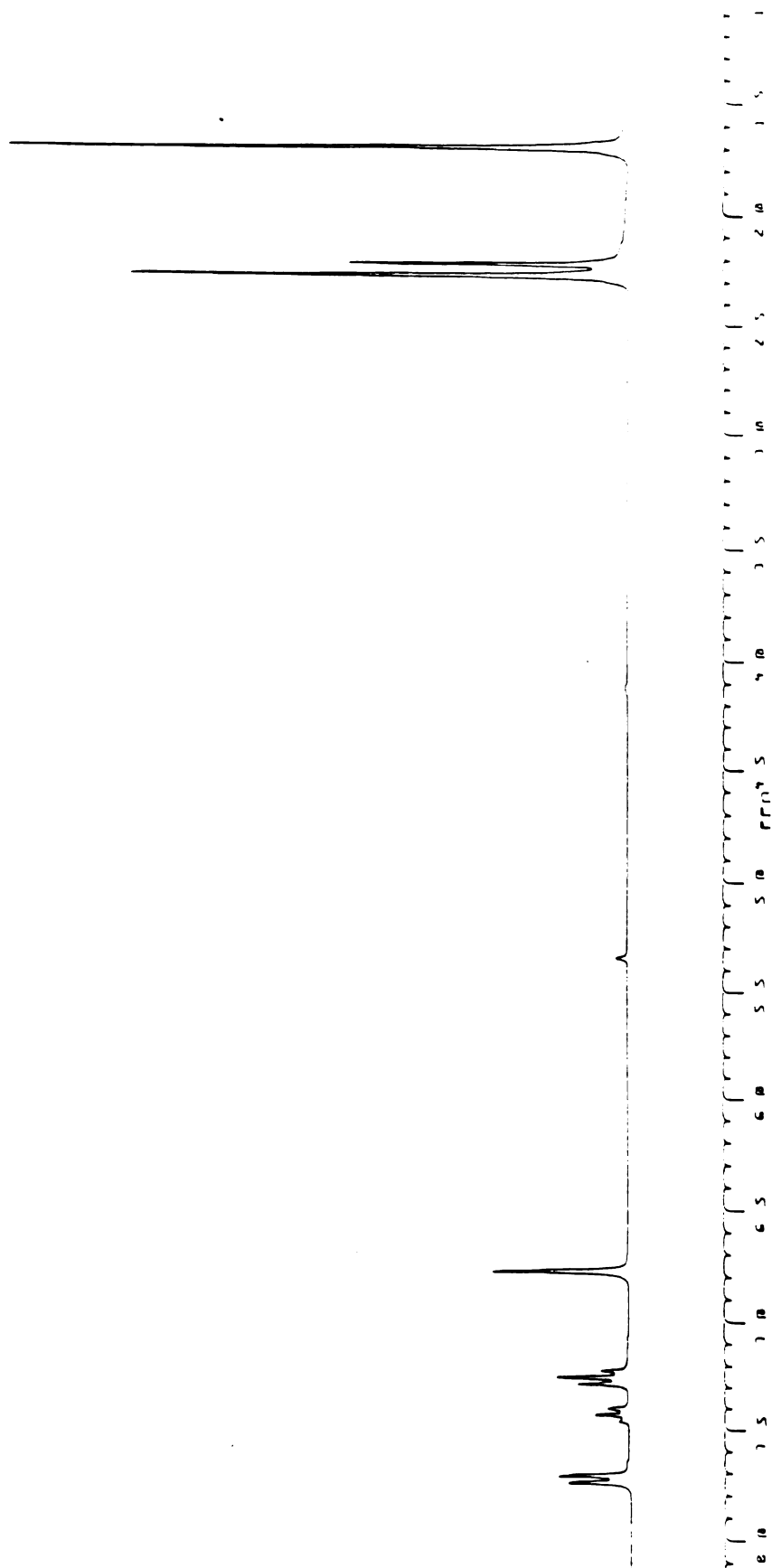


Figure 43.  $^1\text{H}$  NMR of  $\alpha$ -Mesitylisobutyrophenone 7 at 300 K



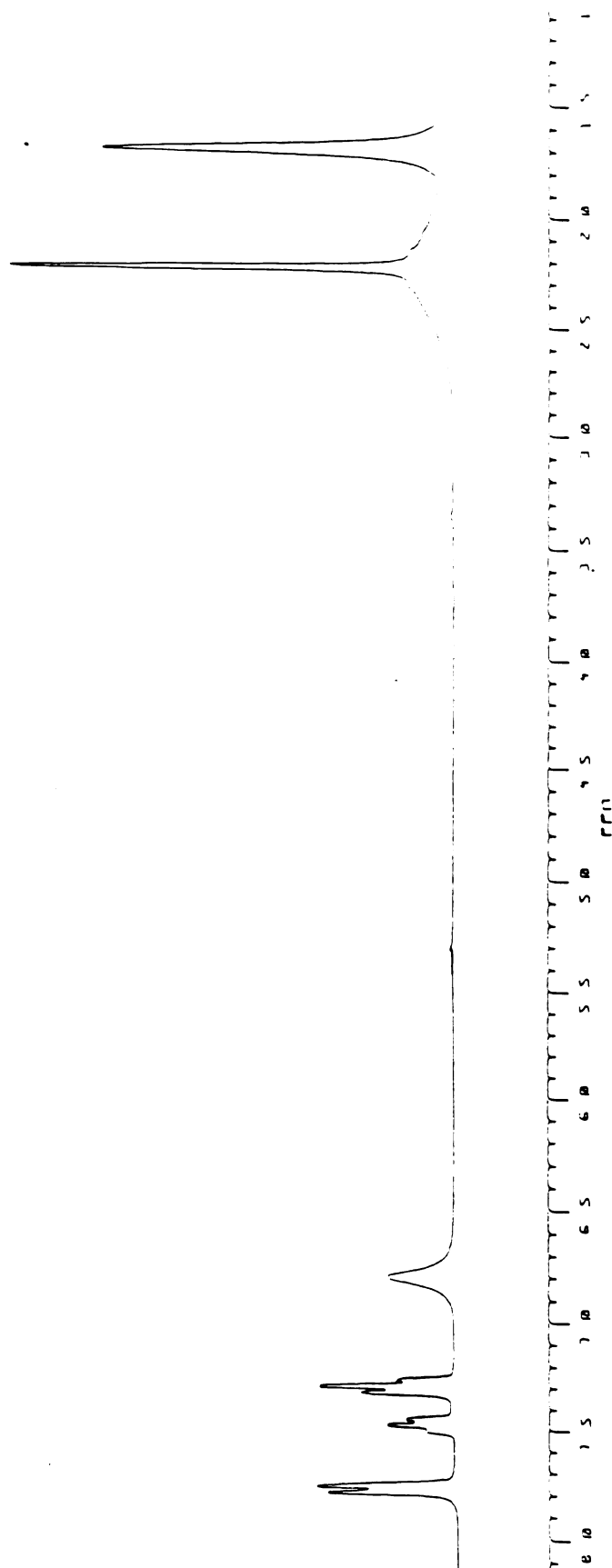


Figure 44.  $^1\text{H}$  NMR of  $\alpha$ -Mesitylisobutyrophenone 7 at 200 K



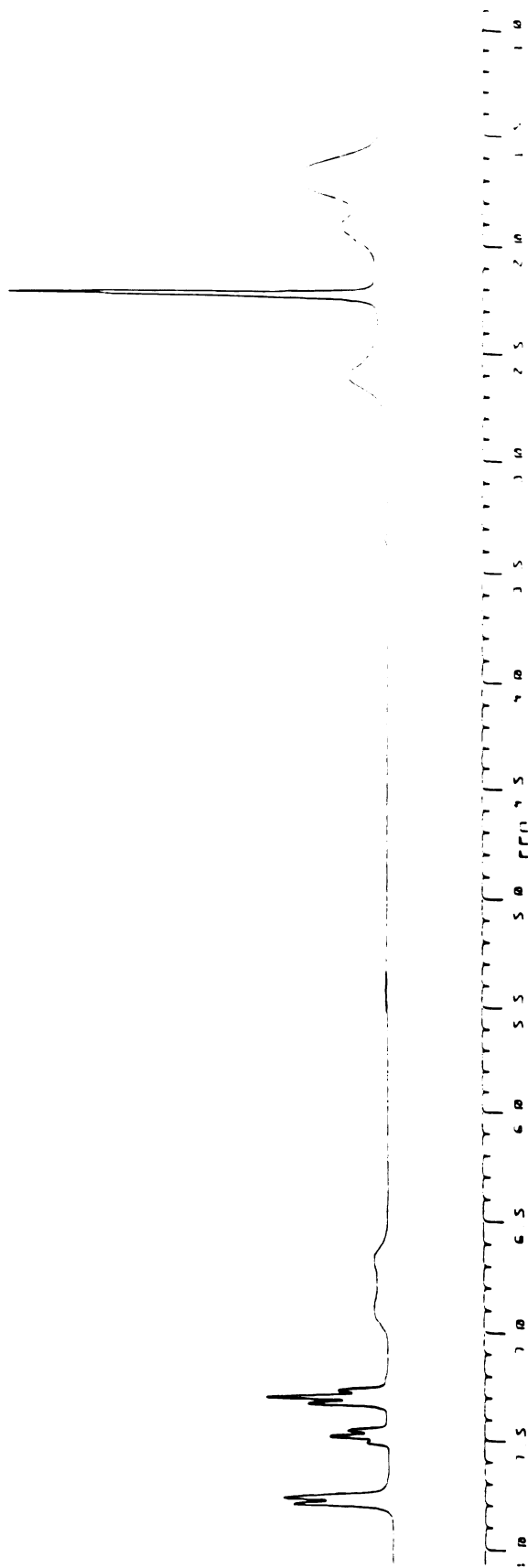


Figure 45.  $^1\text{H}$  NMR of  $\alpha$ -Mesitylisobutyrophenone 7 at 185 K



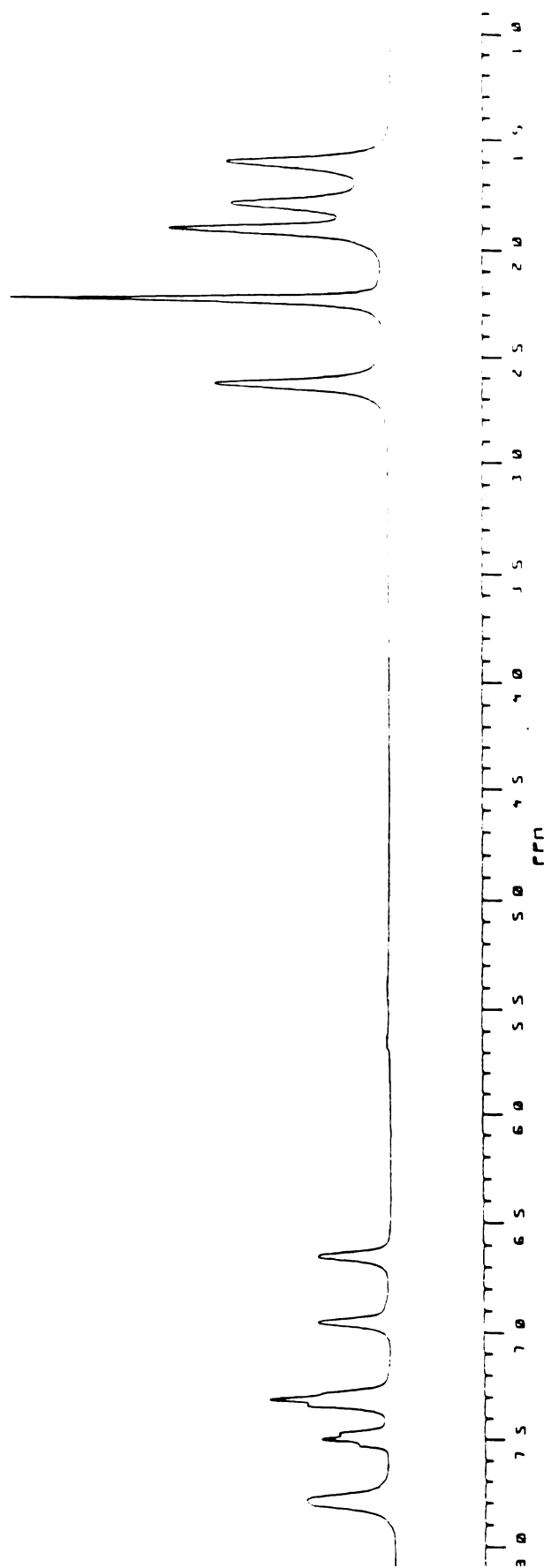


Figure 46.  $^1\text{H}$  NMR of  $\alpha$ -Mesitylisobutyrophenone 7 at 170 K



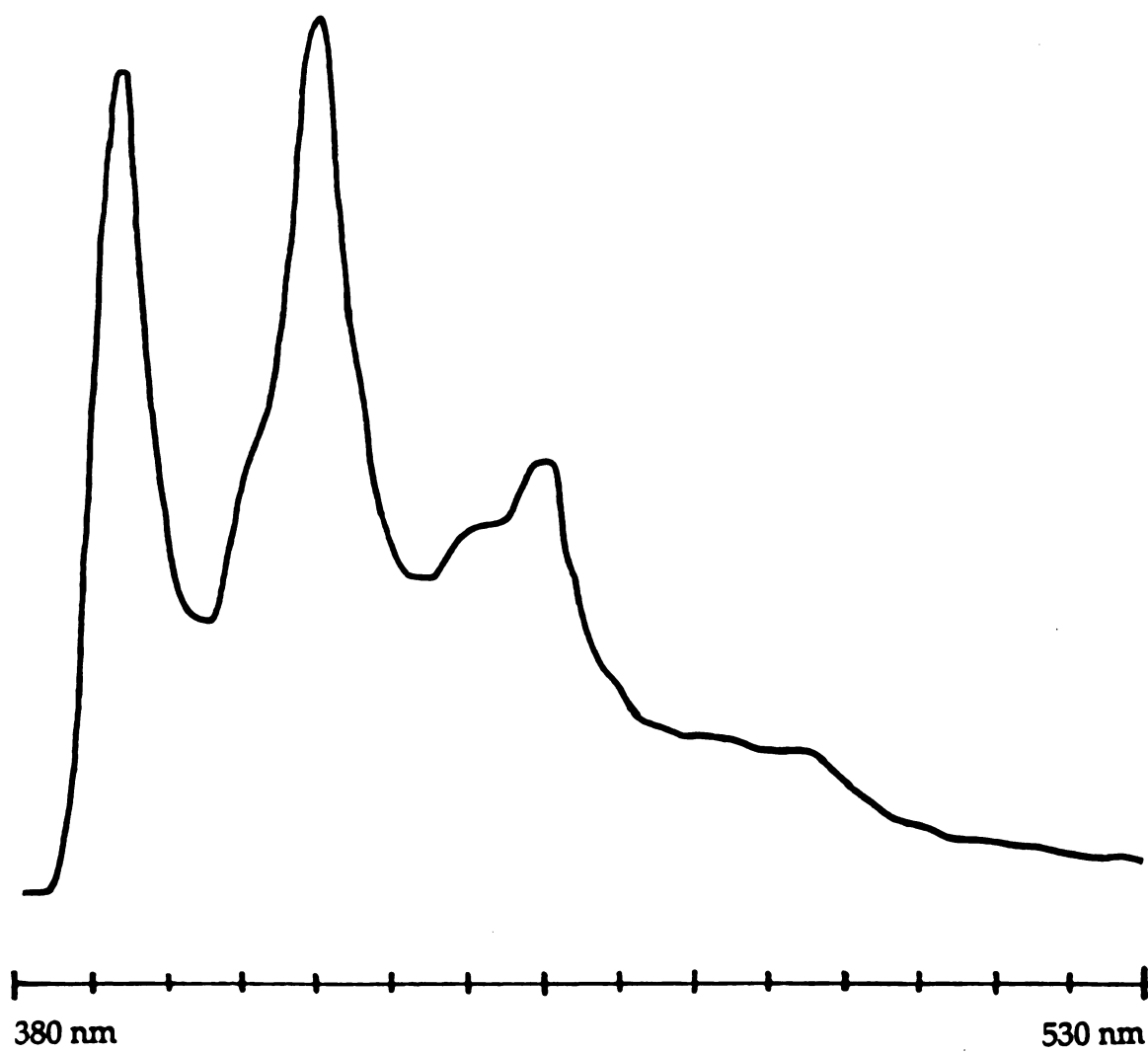


Figure 47. Phosphorescence Spectrum of  $\alpha$ -Mesitylpropiofenone 5 at 77 K



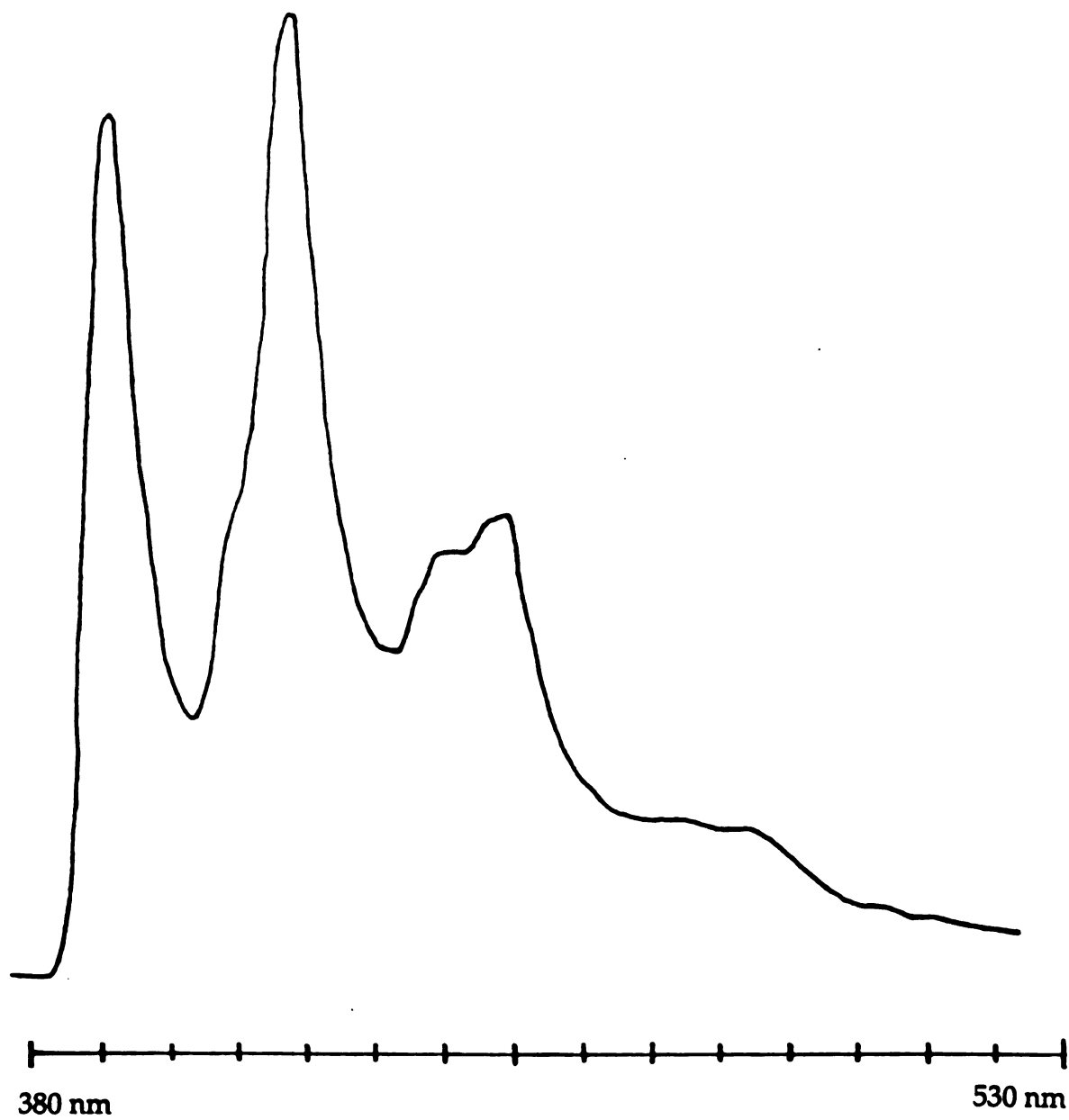


Figure 48. Phosphorescence Spectrum of  $\alpha$ -Mesitylvalerophenone **6** at 77 K



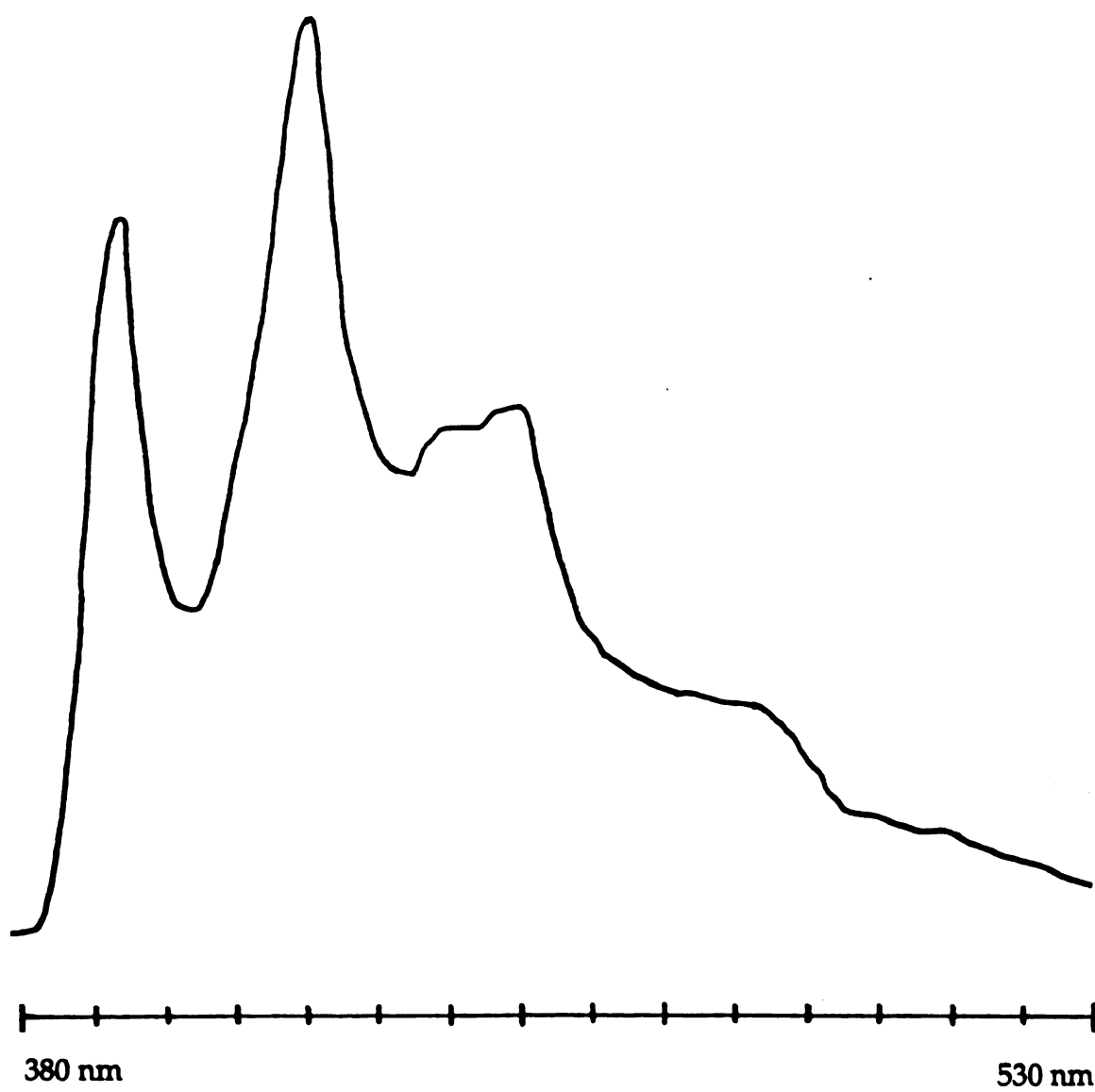


Figure 49. Phosphorescence Spectrum of  $\alpha$ -Mesitylisobutyrophenone 7 at 77K



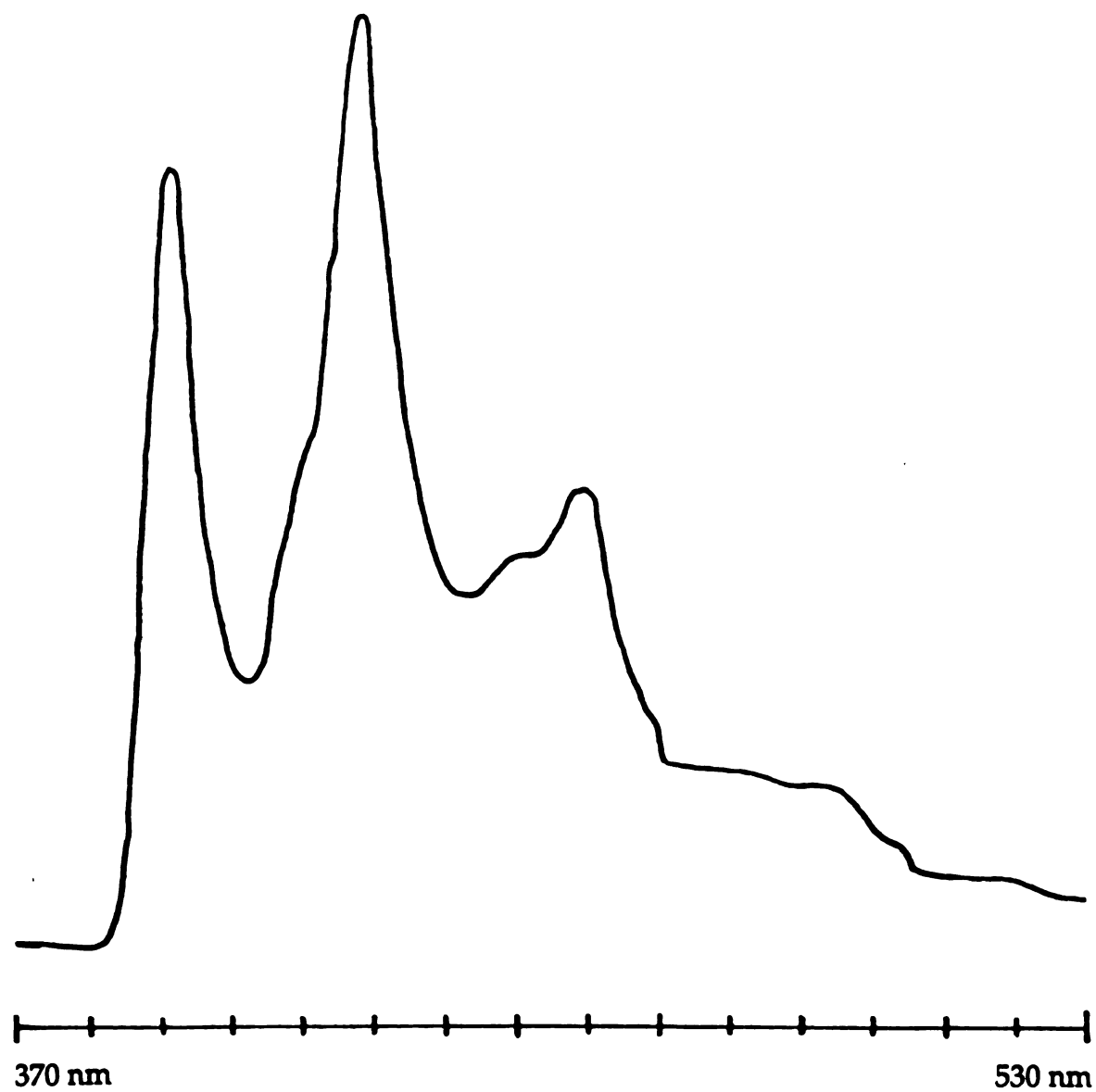


Figure 50. Phosphorescence Spectrum of  $\alpha$ -Mesityl- $\alpha$ -Phenylacetophenone 8 at 77 K



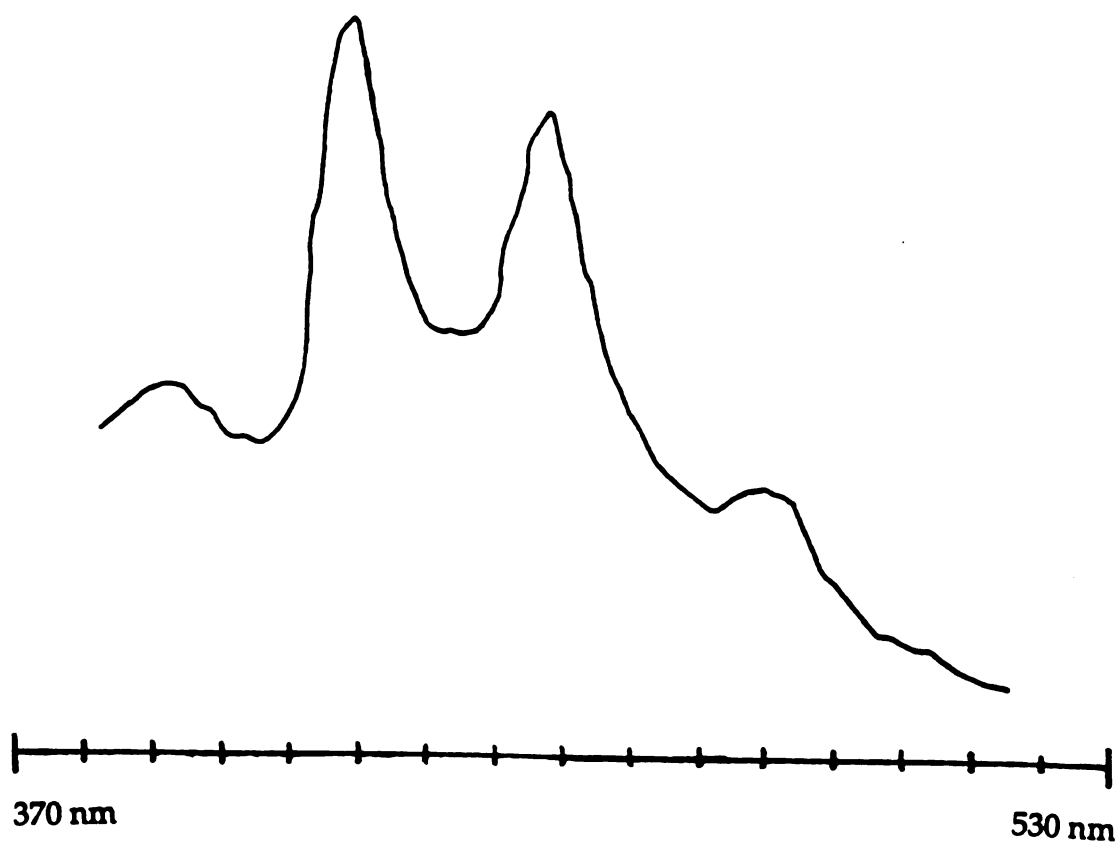


Figure 51. Phosphorescence Spectrum of  $\alpha$ -Mesityl- $\alpha$ -Phenyl-2,4,6-Trimethylacetophenone 11 at 77 K



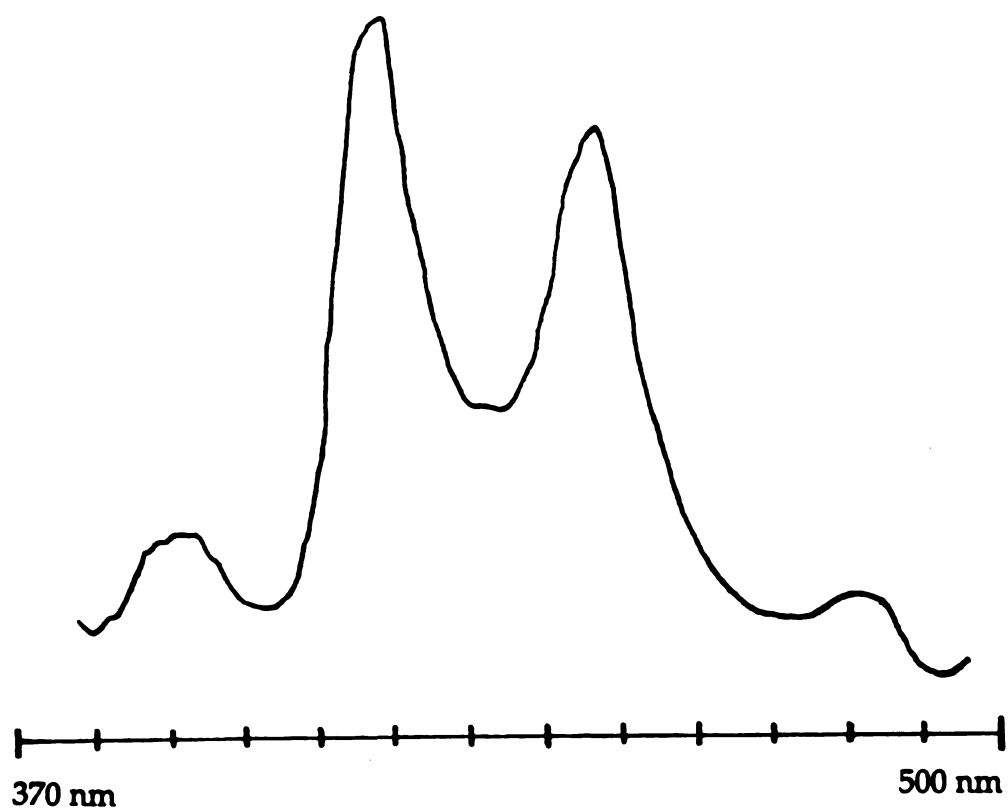


Figure 52. Phosphorescence Spectrum of  $\alpha$ -Mesityl-2,4,6-Trimethylacetophenone 14 at 77 K



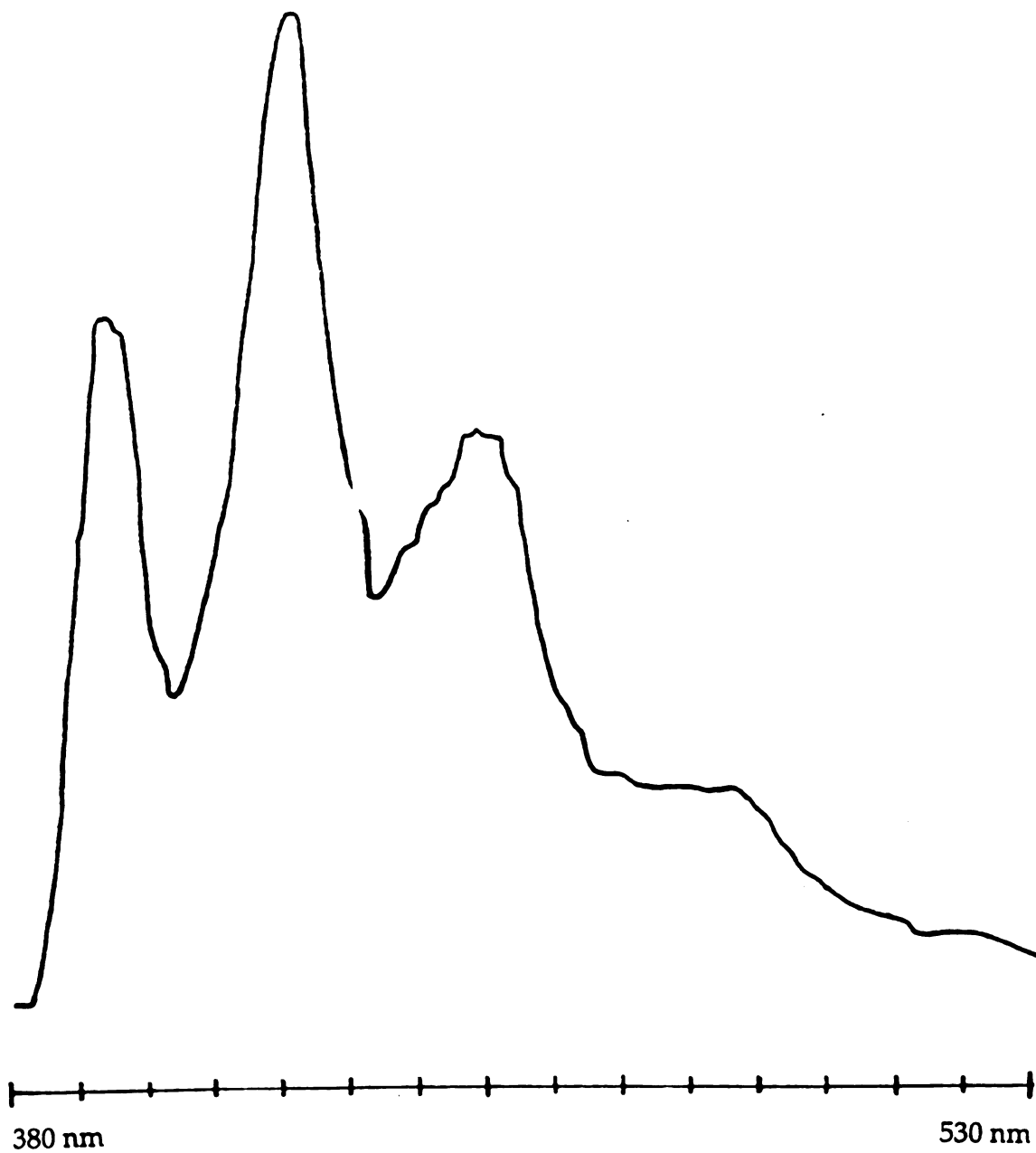


Figure 53 Phosphorescence Spectrum of  $\beta$ -Mesitylisobutyrophenone **21** at 77K



## Discussion

### I. $\alpha$ -Arylacetophenone Derivatives

#### A. Photochemistry in Solution

##### 1. Triplet Lifetimes and Reaction Rates

The Triplet lifetimes of the ketones can be calculated from the following equation:

$$\tau = \text{Slope}/k_q \quad (15)$$

However, a limitation of Stern-Volmer method is that it requires reliable  $k_q$  values. It is obvious that the chosen  $k_q$  values are of great importance in the accurate determination of triplet lifetimes from the above equation.

It is widely accepted that the rate constant for the quenching of triplets by energy transfer in benzene at 25°C is  $5.0\text{--}6.0 \times 10^9 \text{ M}^{-1}\text{s}^{-1}$ ,<sup>3</sup> about half of the diffusion-controlled limit. Scaiano<sup>89</sup> has undertaken a rather extensive study of the energy transfer quenching of various organic molecules with a number of triplet quenchers and has found this value to be accurate.

Although it is generally true that energy transfer quenching of organic molecules is diffusion-controlled, steric hindrance is expected to reduce the rate constant for energy transfer for some extremely congested molecules. Scaiano and Wagner<sup>89</sup> have measured the  $k_q$  values by nanosecond laser flash spectroscopy for a number of o-alkoxyphenyl ketones, having o-alkoxy



substituents of various sizes. The results demonstrate that the energy transfer quenching is sensitive to the degree of steric congestion ortho to the carbonyl group. The most sterically crowded ketone in this study, 2,2-dibenzoyloxybenzophenone, has a  $k_q$  value of  $8.4 \times 10^8 \text{ M}^{-1}\text{s}^{-1}$  in benzene. Since our study involves sterically congested ketones, we were concerned about the possibility that the  $k_q$  values for our compounds may be smaller than the ones under diffusion-controlled condition. A combination of Stern-Volmer quenching and flash photolysis studies of  $\alpha$ -mesityl- $\alpha$ -phenyl-p-methoxyacetophenone **9** provided a  $k_q$  value of  $4.7 \times 10^9 \text{ M}^{-1}\text{s}^{-1}$  in benzene. This justifies that a  $k_q$  value of  $5.0 \times 10^9 \text{ M}^{-1}\text{s}^{-1}$  can be used to obtain the lifetimes of the ketones studied.

Triplet lifetimes indicate how fast the excited triplet states can decay. Reciprocal triplet lifetimes are the sum of the rate constants of all the physical deactivations and chemical reactions that excited states undergo, i.e.

$$1/\tau = \sum k_r^i + \sum k_d^i \quad (16)$$

Hence, in the case that there are more than one process involved, it is desirable to estimate all the individual contributions of each process to the overall triplet lifetime.

Radiationless decay is a physical deactivation an excited molecule could undergo. Typical values for the rate constant,  $k_d$ , in phenyl ketones are on the order of  $10^5$ - $10^6 \text{ s}^{-1}$ .<sup>15, 24b, 90-91</sup> For instance, Lewis<sup>15</sup> measured the  $k_d$ 's for acetophenone, propiophenone, and isobutyrophenoene. and found them to be  $3.4 \times 10^5 \text{ s}^{-1}$ ,  $3.2 \times 10^5 \text{ s}^{-1}$ , and  $3.4 \times 10^5 \text{ s}^{-1}$  respectively. Lewis<sup>24b</sup> also reported that the  $k_d$  value for  $\alpha$ -phenylacetophenone is smaller than  $5 \times 10^5 \text{ s}^{-1}$ .



It seems unlikely that  $k_d$  values for the  $\alpha$ -arylacetophenone derivatives we studied would differ greatly from Lewis's values. There is no known reason why  $k_d$  values should be sensitive to the nature of the alkyl groups on the  $\alpha$ -ring. Thus, radiationless decay accounts for less than 1% of the overall triplet decay of the ketones. For practical consideration, the contribution of radiationless decay to the lifetimes can be ignored.

Radiative decay of triplet phenyl ketones (phosphorescence) normally takes place with a rate constant of  $\sim 10^3 \text{ s}^{-1}$ . It can by no means compete with the reactions of these ketones.

Three types of reactions were observed with the  $\alpha$ -arylacetophenone derivatives,  $\alpha$ -cleavage, formation of indanol, and 1,3-aryl migration. Which reaction predominates depends on the nature of the substituents. Generally,  $\alpha$ -dimethylation or 2,4,6-trimethylation of  $\alpha$ -arylacetophenones leads to exclusive  $\alpha$ -cleavage reactions.  $\alpha$ -Monosubstitution enhances the formation of 1,3-aryl shift products, and reduces the formation of indanols except for  $\alpha$ -mesitylpropiophenone 5 and  $\alpha$ -mesitylvalerophenone 6 in polar solvents. The quantum yields and rate constants for all the reactions are estimated and presented in Table 21. How these values are derived are described as follows for  $\alpha$ -cleavage and  $\delta$ -hydrogen abstraction. The evaluation of charge transfer rate constants will be discussed in the section for enol ethers formation.

It has been well established that  $\alpha$ -cleavage reactions involve the formation of caged radical pairs, which can then diffuse apart to give various products. The separated radicals can be trapped with radical scavengers such as thiols (Scheme 21). In Lewis's study of  $\alpha$ -cleavage from a series of  $\alpha$ -phenylacetophenone derivatives,<sup>24</sup> the quantum yields of benzaldehyde formation are greatly increased with the addition of low concentration of dodecanethiol and rise to a maximum of ca. 0.45 at  $2 \times 10^{-3} \text{ M}$  thiol



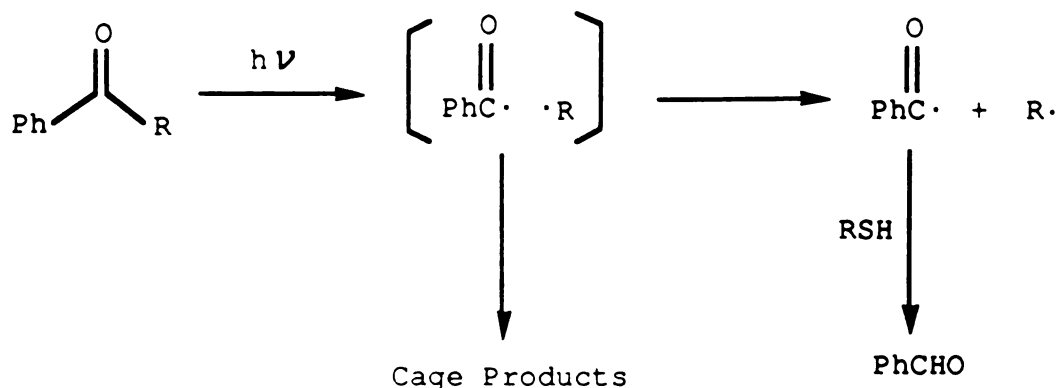
Table 21. Quantum Yields and Rate Constants of Reactions of  $\alpha$ -Arylacetophenones

Ketones	<sup>a</sup> $\Phi(\alpha)$	$\Phi(\delta)^b$	$k_\alpha \times 10^{-7} (S^{-1})^c$	$k_\delta \times 10^{-8} (S^{-1})^d$	$k_{ct} \times 10^{-8} (S^{-1})^e$
1		0.54		0.017	
2	0.7		3.6	<0.15	
3	0.08	0.013	1.5	0.023	
4	0.38 <sup>f</sup>		4.4		
5	0.04	0.55	1.2	1.6	1.2
6	0.015	0.37	A curved Stern-Volmer plot obtained		
7	0.31 <sup>f</sup>		69		
8	0.01	0.033	5.8	1.8	50.6
9	0.013	0.041	0.14	0.045	1.0
10	0.021	0.012	6.7	0.38	31.0
11	0.33 <sup>f</sup>		810		
12	0.040		5.5		
13	0.073		20		
14	0.35 <sup>f</sup>		73		
15		1.0		1.6	
16		0.54		6.8	5.8
TME8					>1.0 <sup>98</sup>

a. Quantum yield of  $\alpha$ -cleavage. b. Maximized quantum yields of indanol in the presence of Lewis bases. c. Rate constant of  $\alpha$ -cleavage. d. Rate constant of  $\delta$ -hydrogen abstraction. e. Rate constant of charge transfer. f. Maximized quantum yield of aldehyde formation. g. 1,2,3-trimesitylethanone.



concentration. This is the point where all the outcage benzoyl radicals have been trapped to form benzaldehyde.



Scheme 21

In our study, with the ketones which undergo  $\alpha$ -cleavage reactions, the quantum yields of benzaldehyde increase to a maximum value from 0.31 to 0.38 (Table 2) at more or less the same thiol concentration as in Lewis's study (Figure 15 and 16).

Since  $\alpha$ -cleavage is the only reaction that these ketones undergo, the maximized quantum yields of benzaldehyde formation in the presence of dodecanethiol can be taken as a measure for the cage-effect in the  $\alpha$ -cleavage reactions of these ketones. The quantum yields obtained in Lewis's and our studies average approximately 0.4.. This indicates that only 40% of the initially formed radicals are able to undergo reactions which give rise to products other than starting ketones. The other 60% of the radicals simply recombine in solvent cages to return to the starting ketones.

Keeping this in mind, we multiplied all the maximized quantum yields for benzaldehyde formation by 1/0.4 to give the estimated values of



$\alpha$ -cleavage quantum yields,  $\Phi(\alpha)$ . Since  $\alpha$ -cleavage quantum yield is related to the rate constant for  $\alpha$ -cleavage,  $k_\alpha$ , and the triplet lifetime,  $\tau$ , in the following way:

$$\Phi(\alpha) = k_\alpha \tau \quad (17)$$

$k_\alpha$  can then be estimated by equation (18), for the ketones which undergo  $\alpha$ -cleavage as well as other reactions:

$$k_\alpha = \Phi(\alpha)\tau^{-1} \quad (18)$$

The results so obtained are listed in Table 21.

Wagner<sup>31</sup> has deduced that the formation of indanols is from a  $\delta$ -hydrogen abstraction followed by the cyclization of the biradical produced. The identity of the biradical has been established by its transient UV absorption spectrum with flash photolysis technique.<sup>92</sup>

The estimation of rate constants for  $\delta$ -hydrogen abstraction can be accomplished in a similar way:

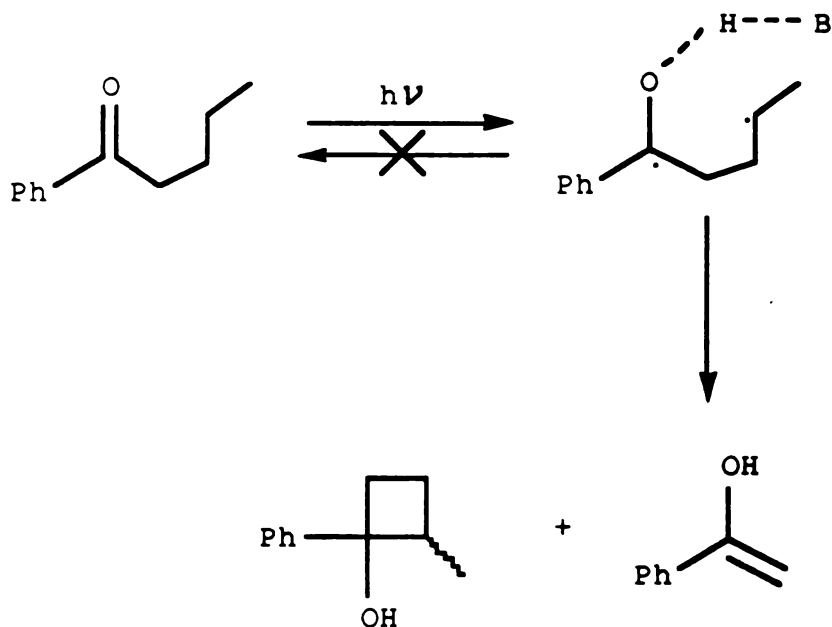
$$k_\delta = \Phi(\delta)\tau^{-1} \quad (19)$$

where  $k_\delta$  is the rate constant for  $\delta$ -hydrogen abstraction,  $\Phi(\delta)$  is the quantum yield for indanol formation,  $\tau$  is the triplet lifetime, However, in order for the equation to hold true, maximized quantum yields should be used. A maximized quantum yield is the quantum yield for product formation under the circumstance where all the biradicals react to give the indanol products.

It is now well known that any hydroxybiradical type of intermediate can



undergo reverse hydrogen transfer to generate ground state starting ketones, resulting in low quantum yields for product formation. Solvents that are reasonable Lewis bases can prevent the reversion by forming a hydrogen bond with the hydroxy group, therefore, making the hydroxy hydrogen not accessible (Scheme 22).<sup>93</sup> The quantum yields measured in the presence of a Lewis base can hence be used as the maximized quantum yields for indanol formations (Table 2).



Scheme 22

The quantum yields of indanol from  $\alpha$ -mesitylpropiophenone 5,  $\alpha$ -mesitylvalerophenone 6, and  $\alpha$ -mesityl- $\alpha$ -phenylacetophenone 8 in benzene with 2 M dioxane are used as the maximized quantum yields. Although the quantum yields in acetonitrile and methanol are higher, they are thought to be due to the increased formation of products from the charge transfer complexes involved in polar solvents. This will be discussed later.



forma

The u

subst

corres

know

differ

the fo

come

2. WI

keton

altera

such a

trimer

of the

contro

is that

6-hyd

$\alpha$ -clea

follow



For  $\alpha$ -(o-tolyl)propiophenone **2**, the quantum yield of indanol formation decreases in the presence of Lewis bases for an unknown reason. The upper limit of  $\delta$ -hydrogen abstraction rate is thus estimated by subtraction of  $k_\alpha$  from  $\tau^{-1}$  of the ketone.

The estimated  $k_\delta$  values are given Table 21.

It is noted that for the  $\alpha$ -mesityl ketones, the sum of  $k_\delta$  and  $k_\alpha$  corresponds to only a portion of the total decay rate. Since there is no other known excited state decay process for these ketones, it is believed that the difference represents the rates of the charge transfer reactions which lead to the formation of 1,3-aryl migration products in several ketones. We will come back to this point in the discussion of the migration reaction.

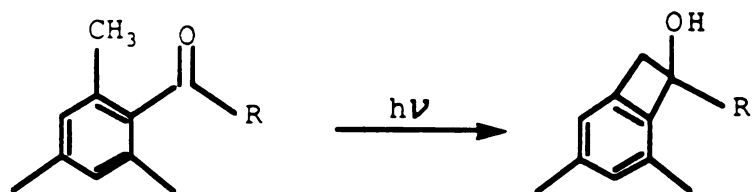
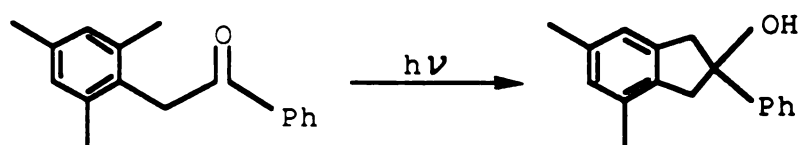
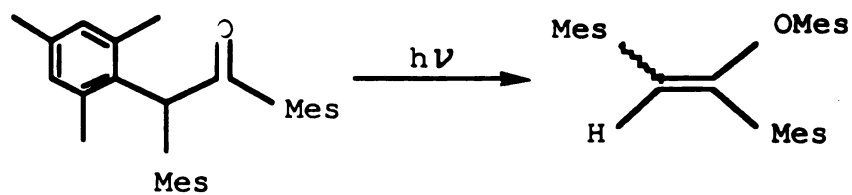
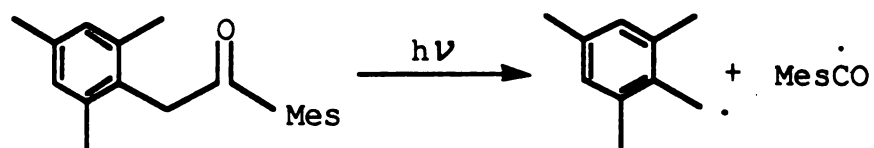
## 2. What Determines the Excited State Decay Modes?

As mentioned above, the photochemistry of these sterically congested ketones has shown such a sensitive substituent effect that only a minor alteration of structural features leads to completely different photoreactions, such as in Reactions 16-19.

$\alpha$ -Mesitylacetophenone, 1,2,2-trimesitylethanone,  $\alpha$ -mesityl-2,4,6-trimethylacetophenone **14** are all structurally capable of undergoing all three of the above reactions, however, only one reaction occurs in each case. What controls the photoreactivity?

It has been noticed that a general trend in the change of photoreactivity is that  $\alpha$ -substitution reduces the reactivity of the triplet ketones towards  $\delta$ -hydrogen abstraction, and causes the emergence of other products, such as  $\alpha$ -cleavage and 1,3-aryl migration products. The discussion will be presented following this logic line.



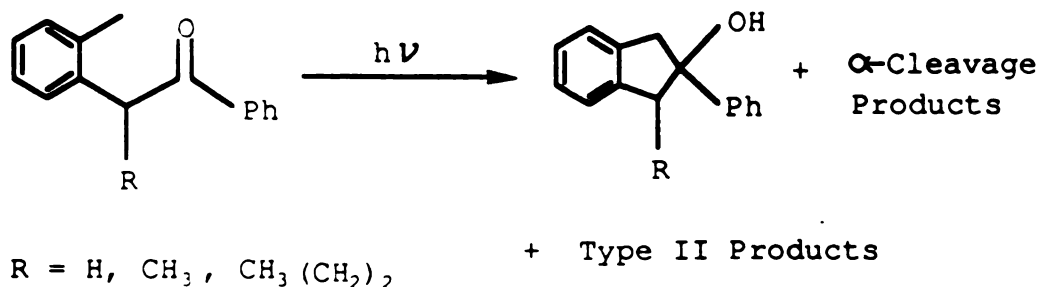
Reaction 16<sup>45</sup>Reaction 17<sup>35</sup>Reaction 18<sup>47</sup>

Reaction 19

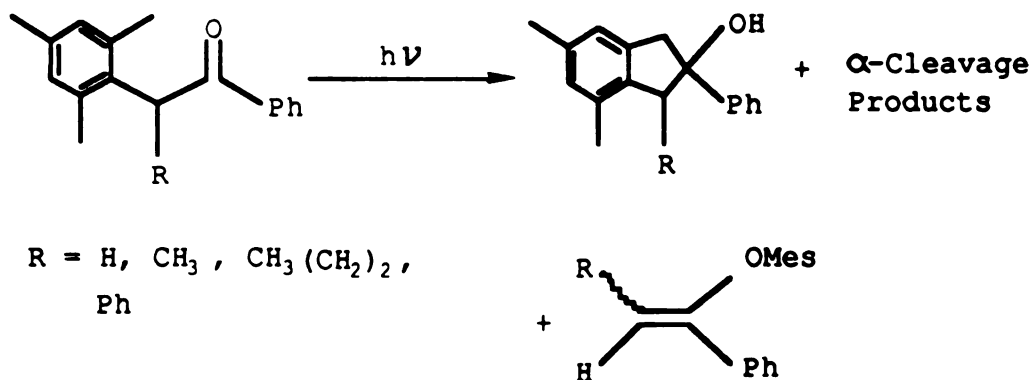


### 3. $\alpha$ -Substituent Effect on $\delta$ -Hydrogen Abstraction

Indanol formation is observed with the ketones shown in Reaction 20-21. The estimates of the rate constants are given in Table 21 which indicates a decrease of reactivity with  $\alpha$ -substitution.



Reaction 20



Reaction 21

For a hydrogen abstraction reaction, five parameters characterize the geometric relationship between the abstracting oxygen atom and the hydrogen atom being abstracted. These are  $d$ , the oxygen to hydrogen



distance;  $\eta$ , the angle defined by the oxygen...hydrogen vector and its projection on the nodal plane of the carbonyl group;  $\Delta$ , the angle between the carbonyl carbon, the carbonyl oxygen, and the target hydrogen atom;  $\theta$ , the angle between the carbonyl oxygen, the hydrogen atom, and the carbon to which the hydrogen atom is attached;  $\rho$ , the angle defined by the vector between the hydrogen atom and the carbon to which the hydrogen atom is attached and its projection on the nodal plane of the carbonyl group (Figure 54).<sup>58,88a</sup> The structure on the right is viewed from oxygen along the C=O bond.

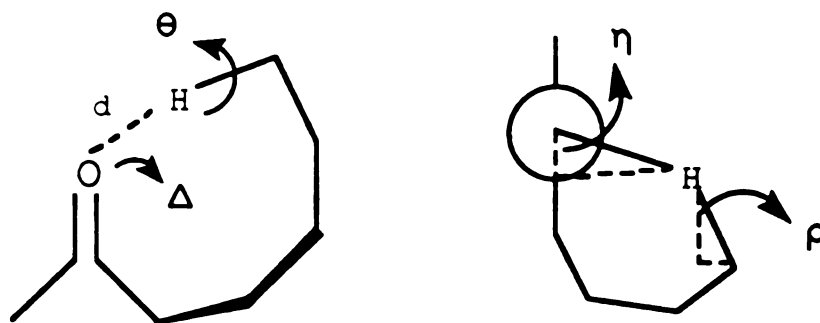


Figure 54

Scheffer<sup>58,88a</sup> has pointed out that the generally recognized ideal values for  $\eta$ ,  $\Delta$ ,  $\theta$ , and  $\rho$  are  $0^\circ$ ,  $90^\circ$ ,  $180^\circ$ , and  $0^\circ$  respectively. This is not a surprising conclusion if we realize that it is the half-filled  $n$  orbital of the oxygen which is responsible for the reaction.

The conformation in Figure 55 is thus the best geometry possible for  $\delta$ -hydrogen abstraction from  $\alpha$ -arylacetophenone derivatives on the basis of above consideration. This conformation may or may not be a conformation with a minimized energy of the molecule. It is the ideal transition state geometry for the reaction.



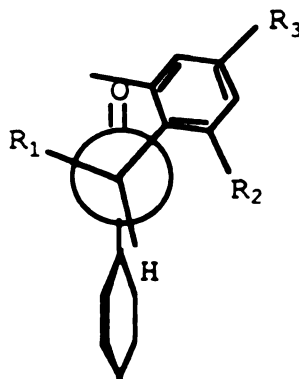


Figure 55

Any structural features destabilizing the ideal geometry for  $\delta$ -hydrogen abstraction relative to the most stable conformations of the molecules will reduce the reaction rate. The discussion how  $\alpha$ -substituents will affect  $\delta$ -hydrogen abstraction rate is classified by the types of ketones.

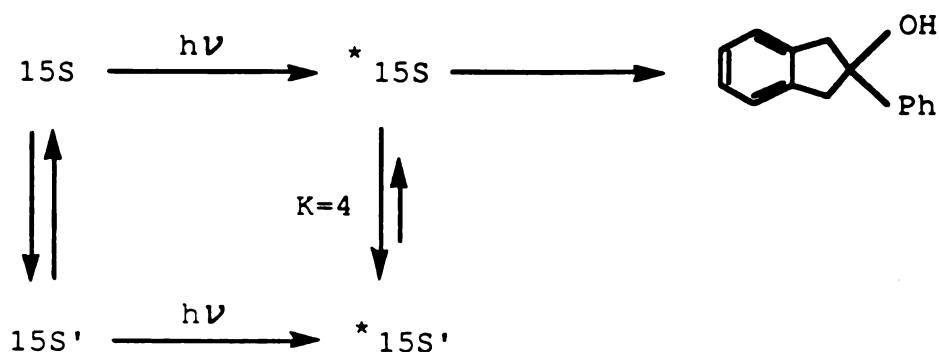
### $\alpha$ -Arylacetophenones

Molecular mechanics calculations show that  $\alpha$ -(*o*-tolyl)acetophenone **15** has two stable conformations of comparable energies, conformation **15S** and conformation **15S'**. The difference between these conformations is the orientation of the tolyl group. The methyl group can either point toward or away from the carbonyl group.  $\delta$ -Hydrogen abstraction can only occur from conformation **\*15S**, which happens to be the ideal geometry for the reaction. In order for conformation **\*15S'** to react, the tolyl group has to rotate  $180^\circ$  to achieve conformation **\*15S**.

For a ketone with a 2,6-symmetrically methylated  $\alpha$ -ring, such as  $\alpha$ -mesitylacetophenone **16**, molecular mechanics calculations reveal that conformation **16S** is the most stable conformation. The impossibility for



$\alpha$ -mesitylacetophenone **16** to have a nonreactive conformation like 15S' accounts for the rate increase from **15** to **16**.



Scheme 2

This argument was originally made by Wagner and Meador,<sup>35</sup> although conformations proposed there are slightly different from the ones obtained from molecular mechanics calculations. An excited state equilibration between 15S and 15S' was assumed, and an equilibrium constant of 4 was estimated for the excited state interconversion between 15S and 15S' in favor of 15S' (Scheme 23).

The above argument was reinforced by our results, however an equilibrium constant of 4 is now believed to be inaccurate, because it is realized that the hydrogen abstraction rate from  $\alpha$ -mesitylacetophenone **16** is only  $6.8 \times 10^8 \text{ s}^{-1}$  (Table 21) and that a charge transfer quenching of the ketone is responsible for the rest of the excited state decay. A revised procedure following the same logic, assuming that  $\alpha$ -mesitylacetophenone **16** reacts by  $\delta$ -hydrogen abstraction only 4 times as fast as  $\alpha$ -(*o*-tolyl)acetophenone **15** (Table 21), gives an equilibrium constant of 1 between excited 15S and 15S'. It agrees very well with the results from molecular mechanics calculations.



The most stable or one of the most stable conformations of the  $\alpha$ -arylacetophenone happens to be the conformation ideal for  $\delta$ -hydrogen abstraction. Therefore, fast hydrogen abstraction is observed with these ketones, compared to their  $\alpha$ -monosubstituted derivatives.

**$\alpha$ -Arylpropiophenones,  $\alpha$ -Arylvalerophenone and  $\alpha$ -Mesityl- $\alpha$ -Phenylacetophenone**

When a alkyl group is added to the  $\alpha$ -carbon of the acetophenones, dynamic NMR studies indicate that there is a significant restriction on the rotation of the mesityl group in  $\alpha$ -mesitylpropiophenone 5,  $\alpha$ -mesitylvalerophenone 6 and  $\alpha$ -mesityl- $\alpha$ -phenylacetophenone 8 (Figure 56). The two o-methyl groups differentiate themselves at low temperatures (Figure 34-42).

Analyses of linebroadening give rate constants of  $9.5 \times 10^3 \text{ s}^{-1}$ ,  $1.4 \times 10^3 \text{ s}^{-1}$  and  $4.4 \times 10^4 \text{ s}^{-1}$  for the mesityl rotation in  $\alpha$ -mesitylpropiophenone 5,  $\alpha$ -mesitylvalerophenone 6 and  $\alpha$ -mesityl- $\alpha$ -phenylacetophenone 8 respectively (Table 5, 6 and 9).

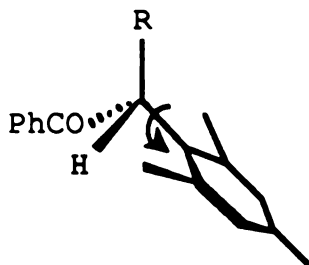


Figure 56



These results imply that a strong steric interaction will arise if the mesityl o-methyl groups are close to the  $\alpha$ -alkyl group in the molecules (Figure 57).

Molecular mechanics calculations also reveal an unfavorable interaction between the aryl o-methyl groups and the  $\alpha$ -substituents in the  $\alpha$ -arylpropiophenones,  $\alpha$ -arylvalerophenones and  $\alpha$ -mesityl- $\alpha$ -phenylacetophenone 8, when they are near each other. All the energy-minimized conformations of the molecules have these two groups as far apart as possible. A conformation in which they are close together can't become an energy-minimized conformation of the molecules. It is noted that the ideal conformation for  $\delta$ -hydrogen abstraction is such a destabilized conformation (Figure 58).

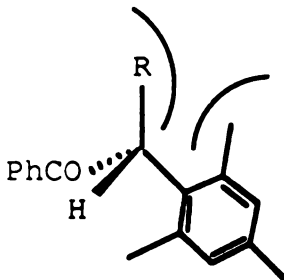


Figure 57

Based upon these results, it is reasonable to conclude that the conformation required for  $\delta$ -hydrogen abstraction is destabilized due to the steric repulsion between the aryl o-methyl groups and the  $\alpha$ -alkyl group. It is an unstable (non-minimized) conformation of the molecule.

The energy-minimized conformations of these molecules have been calculated for the ketones. They are 2G/3G, 2G'/3G', and 2E/3E for



$\alpha$ -(o-tolyl)propiophenone **2** and  $\alpha$ -(o-tolyl)valerophenone **3**, 5G/6G and 5E/6E for  $\alpha$ -mesitylpropiophenone **5** and  $\alpha$ -mesitylvalerophenone **6**, and 8E and 8G for  $\alpha$ -mesityl- $\alpha$ -phenylacetophenone **8**, with 2G/3G and 5G/6G being the most stable ones for the corresponding ketones and 8E and 8G having comparable energies.

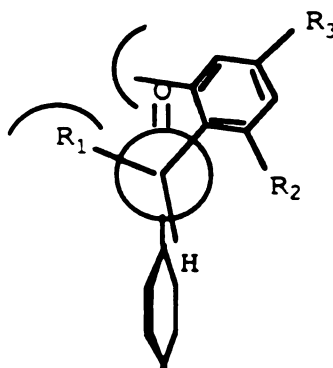


Figure 58

The X-ray structures of  $\alpha$ -mesitylvalerophenone **6** and  $\alpha$ -mesityl- $\alpha$ -phenylacetophenone **8** have shown that these two ketones adopt a conformation similar to 6G and 8G in solid state (Figure 27 and 28). If it is assumed that these molecules do crystallize in their most stable conformations, the crystallographic results suggest that 6G and 8G are the most stable conformations of the molecules in solution. This conclusion does not contradict the results from molecular mechanics calculations, although calculations have shown that  $\alpha$ -mesityl- $\alpha$ -phenylacetophenone **8** has conformation 8E besides 8G. This seems to suggest the possible coexistence of the two conformations in solution.

From the results presented so far, it is clear that the substituent at the  $\alpha$ -carbon of  $\alpha$ -arylacetophenones has two conformational effects:



- a. it changes the structures of the most stable conformations for the ketones.
- b. it makes the geometry ideal for  $\delta$ -hydrogen abstraction an unstable (non-minimized) conformation.

How will the conformational changes affect the photoreactivities of the ketones

Let's assume that an excited state equilibrium between different conformations is established prior to the  $\delta$ -hydrogen abstraction for all the ketones which undergo the reaction except for  $\alpha$ -mesitylvalerophenone 6. The interconversion between the conformations of the ketones requires a  $C_\alpha$ -CO bond rotation. Although  $\alpha$ -arylisobutyrophenones have restricted rotations along their  $C_\alpha$ -CO bonds, we believe that the additional methyl group at the  $\alpha$ -carbon plays an important role. With three large substituents at the  $\alpha$ -carbon, any rotation larger than  $60^\circ$  will suffer from a disfavored interaction between the phenyl group attached to the C=O group and one of the  $\alpha$ -substituents. The interconversion between the energy-minimized conformations of the  $\alpha$ -arylpropiophenones,  $\alpha$ -tolylvalerophenone 3 and  $\alpha$ -mesityl- $\alpha$ -phenylacetophenone 8 however can be achieved without creating such steric interaction in the molecules. In addition, the more rigid orientation of the  $\alpha$ -aryl ring imposed by the two  $\alpha$ -methyl groups in  $\alpha$ -arylisobutyrophenones can cause more resistance towards the rotation. The  $\alpha$ -aryl groups are oriented in such a way (4G and 7G) that they will interfere strongly with the carbonyl phenyl group during rotation. On the other hand, the more flexible orientation of the  $\alpha$ -aryl ring in ketones 2, 3, 5, and 8 makes it easier to avoid such interference.

As it has been pointed out, the ideal geometry for  $\delta$ -hydrogen



abstraction is destabilized by  $\alpha$ -substitution.  $\alpha$ -Mesitylpropiophenone 5 and  $\alpha$ -mesitylvalerophenone 6 have an activation energy as high as ca. 8 Kcal/mole regarding the mesityl rotation in the molecules (Table 5 and 6). Although the energy barrier of the conformational change from the most stable conformations to the ideal geometry for  $\delta$ -hydrogen abstraction in these molecules is not quite the same as that of mesityl rotation in 5 and 6, it is obvious that such conformational change has to be an up-hill process of substantial magnitude in terms of energetics, because the ideal geometry suffers from a similar disfavored steric interaction between the o-methyl groups of the mesityl group and the  $\alpha$ -substituent as in the transition state of the mesityl rotation (Figure 57 and 58). So it is reasonable to conclude that the  $\delta$ -hydrogen abstraction of these ketones can not occur from the ideal geometry with these  $\alpha$ -substituted  $\alpha$ -arylacetophenones.

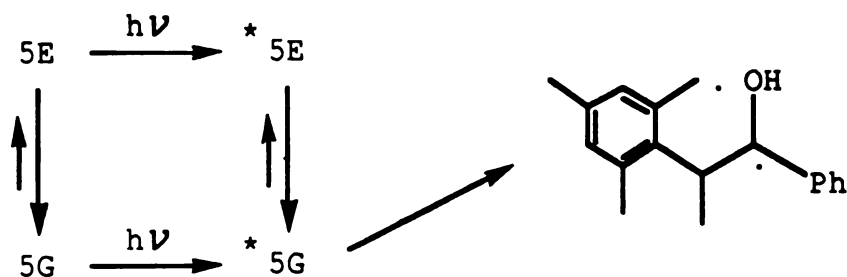
It is generally accepted that when the geometric parameters of hydrogen abstraction deviate from their ideal values, the reaction rate will be reduced. But no experimental results have been reported so far in literature to demonstrate to what extent the rate will be decreased.

Scheffer<sup>58</sup> has reported that there is no strict geometric requirement for hydrogen abstraction to occur in a group of  $\alpha$ -cycloalkyl-p-chloro-acetophenone in solid state. This result suggests that hydrogen abstraction can indeed occur from a non-ideal geometry, although probably with a slower rate.

The stable conformations by molecular mechanics for the  $\alpha$ -substituted  $\alpha$ -arylacetophenones can be classified into two types, the conformations with the C $\alpha$ -Ar bond eclipsing with the carbonyl group (the E type), and the conformations with C $\alpha$ -Ar bond rotated ca. 120° away from the carbonyl group (the G type). In the cases of  $\alpha$ -tolyl ketones, the tolyl group may be



oriented differently with regard to the placement of the tolyl o-methyl group. Since it has been concluded that it is impossible for the ketones to rotate to the ideal geometry and react from there, we believe that the reaction proceeds from some of these stable conformations which are not ideal but still possible for the hydrogen abstraction to occur. Conformations 2G/3G, and 2E/3E can be ruled out immediately due to the obviously unfavorable arrangements of the tolyl o-methyl group for the reaction. Careful examination of models suggests a  $\Delta$  of 70-80°,  $\eta$  of 60-70°,  $\theta$  of 160-170° and  $\rho$  of 60-70° for 2G'/3G', 5G/6G, and 8G; and a  $\Delta$  of 80-90°,  $\eta$  of ca. 90°,  $\theta$  of 170-180° and  $\rho$  of 30-40° for 5E/6E, and 8E between the carbonyl oxygen and the o-methyl group of the  $\alpha$ -aryl group near the carbonyl group in these conformations. Although the E type conformations of ketones 5, 6, and 8 have very attractive  $\Delta$ ,  $\theta$  and  $\rho$  values, a  $\eta$  of ca. 90° indicates an almost perpendicular orientation of the hydrogen...oxygen vector to the n-orbital of the carbonyl oxygen. Such arrangement does not seem to be possible for the hydrogen to be abstracted at a reasonable rate. So we conclude that the  $\delta$ -hydrogen abstraction occurs from the G type conformations (2G'/3G', 5G/6G, and 8G) of these  $\alpha$ -substituted  $\alpha$ -arylacetophenones.



Scheme 24



In support of the above proposal is the fact that  $\alpha$ -mesitylvalerophenone **6** and  $\alpha$ -mesityl- $\alpha$ -phenylacetophenone **8** undergo  $\delta$ -hydrogen abstraction to give the indanols with high chemical yields in solid state, and X-ray crystallographic results show that the ketones adopt conformations similar to conformation 6G and 8G in solid state.

A mechanistic scheme is thus provided (Scheme 24), using  $\alpha$ -mesitylpropiophenone as an example. The molecules are excited in their stable conformations 5G and 5E, between which an excited state equilibrium is established. The hydrogen abstraction then occurs from 5G. The rate constant has the following expression,

$$k_{\text{obs}} = k_{\delta}^{\text{r}} X(r) \quad (20)$$

where  $k_{\text{obs}}$  is the observed rate constant,  $k_{\delta}^{\text{r}}$  is intrinsic rate constant from the reacting conformation,  $X(r)$  is the percentage population of the reacting conformer of the ketone in the excited state equilibrium.

Scheme 24 can be applied to all the other  $\alpha$ -substituted  $\alpha$ -arylacetophenones except for  $\alpha$ -mesitylvalerophenone **6**, which shows two non-equilibrated excited states, and will be discussed later.

The decrease of  $\delta$ -hydrogen abstraction rate in the  $\alpha$ -substituted ketones can be due to two factors, a decrease in the intrinsic rate of the reacting conformation caused by non-ideal geometric arrangement, or a decrease in the percentage population of the reacting conformer.

Since conformation 5G is the most stable conformation of  $\alpha$ -mesitylpropiophenone **5**, like 16S being the one of  $\alpha$ -mesityacetophenone **16**, majority of the excited molecules will be in this conformation. Therefore, a 4 fold decrease of the reaction rate from ketone **16** to ketone **5** can't be



explained by the reduced population of the reacting conformation. The only alternative explanation is then that the reaction occurs from 5G of ketone 5 with a rate of 4 times slower than that from 16S of ketone 16.

A rate decrease of at least 10 times from  $\alpha$ -(o-tolyl)acetophenone 15 to  $\alpha$ -(o-tolyl)propiophenone 2 is due to a combination of a reduced population as well as a reduced intrinsic rate constant of the reacting conformer 2G'. If the same reduction (4 fold) in rate constant is assumed from conformation 15S of ketone 15 to conformation 2G' of ketone 2 as from  $\alpha$ -mesitylacetophenone 16 to  $\alpha$ -mesitylpropiophenone 5, then at least 2.5 fold reduction has to be attributed to the decreased number of reacting conformer 2G' for ketone 2, compared to the population of 15S for  $\alpha$ -(o-tolyl)acetophenone 15. It is noted that ketone 2 has conformation 2G, which is more stable than 2G', as the most stable conformation of the molecules by calculations.

Similarly  $\alpha$ -mesityl- $\alpha$ -phenylacetophenone 8 is also affected by both of the factors, a decreased population and a decreased intrinsic rate of the reacting conformer. Because an  $\alpha$ -phenyl and  $\alpha$ -methyl group may impose different steric congestions around  $\alpha$ -mesityl group, it does not seem justified to assume that conformation 8G of  $\alpha$ -mesityl- $\alpha$ -phenylacetophenone 8 has the same intrinsic rate as conformation 5G of  $\alpha$ -mesitylpropiophenone 5. Such difference is indicated by the different activation energies of mesityl rotation for ketone 5 and 8, with the phenyl group having a weaker steric resistance towards the rotation (Table 5 and 9). A less sterically congested mesityl group may be able to undergo a faster reaction. If it is assumed that ketone 8 has an excited state equilibrium constant of ca. 1 between 8G and 8E, as indicated by molecular mechanics calculations, 2 fold out of the overall 4 fold decrease of the reaction rate from  $\alpha$ -mesitylacetophenone 16 to



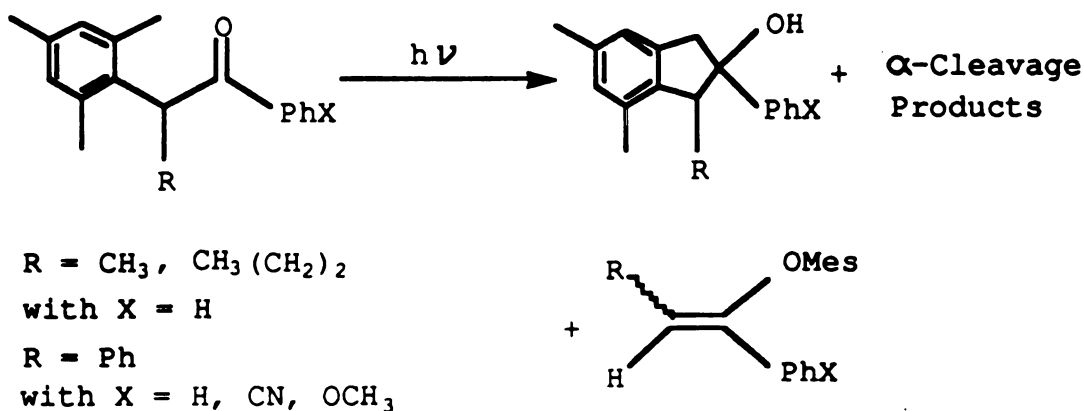
$\alpha$ -mesityl- $\alpha$ -phenylacetophenone **8** is then caused by the reduced population of reacting conformer **8G**, and another 2 fold reduction is due to the bad geometric parameters for the reaction for  $\alpha$ -mesityl- $\alpha$ -phenylacetophenone **8**.

$\alpha$ -(*o*-Tolyl)valerophenone **3** can be described qualitatively in the same way, although lack of data makes it impossible to do any quantitative analyses.

#### 4. Formations of Aryl Vinyl Ethers

1,3-Aryl shift has been observed with the several ketones (Reaction 22).

Table 22 shows that the quantum yields generally increase with the increasing bulk of the ketones. The least congested  $\alpha$ -mesitylacetophenone gives no aryl vinyl ethers. On the other hand, the most crowded 1,2,2-trimesitylethanone forms the ethers with a quantum yield of 0.4. The ketones with varying steric congestions in between the two ketones give the ethers with quantum yields between the extreme values.



Reaction 22



The ether formations is quenched with typical triplet quenchers such as 2,5-dimethyl-2,4-hexadiene and naphthalene. The lifetimes obtained from quenching the ethers and indanols with  $\alpha$ -mesityl- $\alpha$ -phenylacetophenone **8** and  $\alpha$ -mesityl- $\alpha$ -phenyl-p-methoxyacetophenone **9** are identical within experimental error. This implies that the two different photoproducts have the same triplet precursor.

Table 22. Quantum Yields of Aryl Vinyl Ether Formations in Benzene

Ketones	16	5	6	8	9	10	TME <sup>a</sup>	DMAP <sup>a</sup>
$\Phi(E)$	0.0	0.012	0.0038	0.025	0.0084	0.0046	0.4	low

a.  $\alpha$ -DMAP-- $\alpha$ , $\alpha$ -dimesitylacetophenone,<sup>46</sup> TME--1,2,2-trimesitylethanone<sup>47</sup>

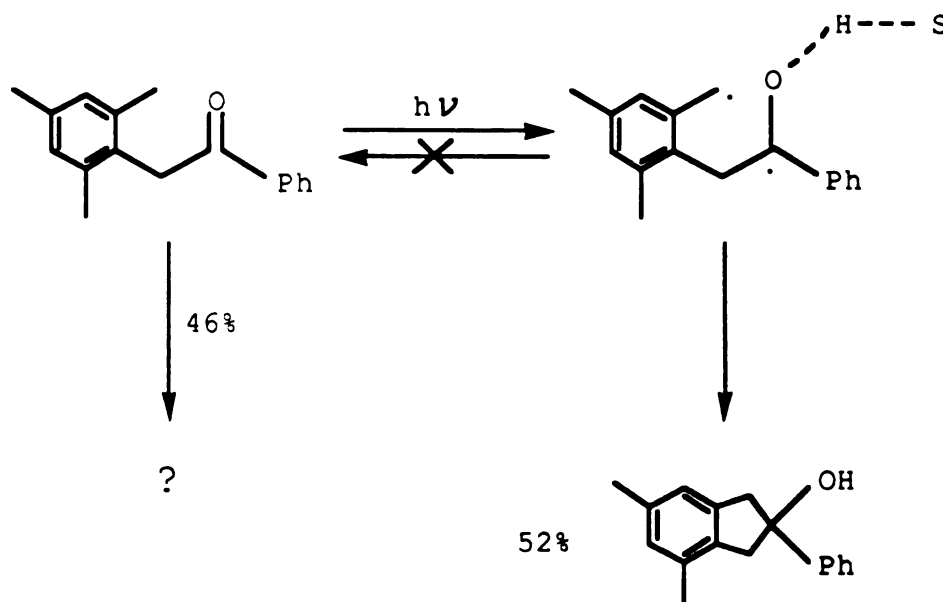
It has been well documented that p-methoxy phenyl ketones have a  $\pi,\pi^*$  triplet as their lowest triplet state. Such a ketone shows a dramatic decrease in the rate constants for any  $n,\pi^*$  reactions, which reflects the reduced population of the reactive  $n,\pi^*$  triplets in a  $n,\pi^*$  and  $\pi,\pi^*$  equilibrium.<sup>5a,9-11</sup> A nearest example of this effect is provided by  $\alpha$ -(o-tolyl)-p-methoxyacetophenone **1**. This ketone undergoes  $\delta$ -hydrogen abstraction with a rate ca. 100 times slower than that of  $\alpha$ -(o-tolyl)acetophenone **15**.

This conclusion can be used vice versa. If a reaction displays a reduced reactivity with the introduction of a methoxy group, it is probably a  $n,\pi^*$  reaction. The observation that  $\alpha$ -mesityl- $\alpha$ -phenyl-p-methoxyacetophenone **9** has a lifetime 40 times longer than the one of  $\alpha$ -mesityl- $\alpha$ -phenylacetophenone **8** clearly suggests that the aryl vinyl ether



formation is a reaction from  $n, \pi^*$  triplets.

Before the discussion of possible mechanisms for the 1,3-mesityl migration, let's first look into an unanswered puzzle in the photochemistry of  $\alpha$ -mesitylacetophenone 16.

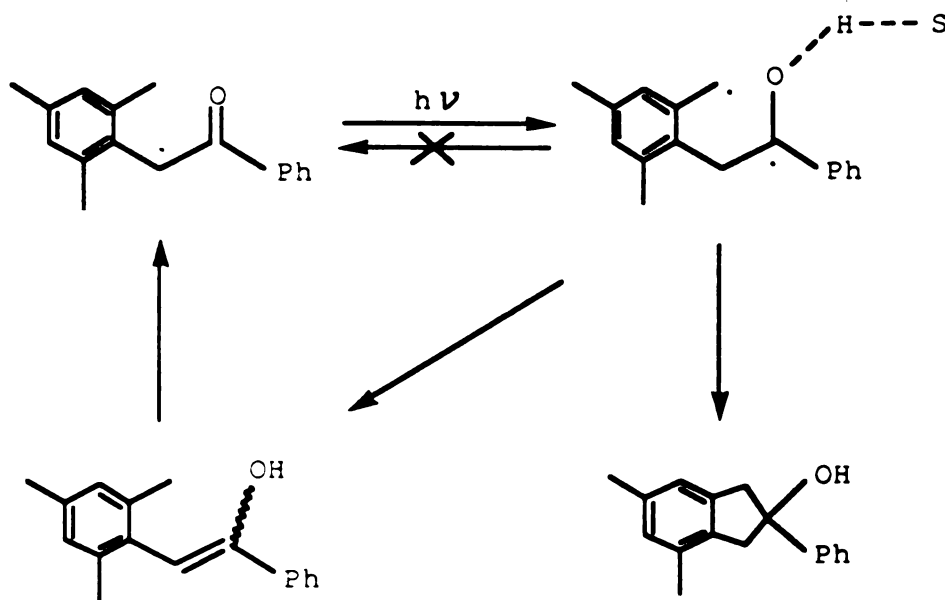


Scheme 25

Irradiation of  $\alpha$ -mesitylacetophenone 16 affords 5,7-dimethyl-2-phenyl-2-indanol as the only product. But the quantum yield of the product reaches only 0.54 in the presence of Lewis bases.<sup>31</sup> This brings up a question: where do the other 46% of the excited ketones go (Scheme 25)?

An explanation is that the formation of the corresponding enols of the ketone through the 1,5-biradical generated in the  $\delta$ -hydrogen abstraction (Scheme 26). This is a sound possibility, since Wagner<sup>79</sup> has reported that  $\alpha$ -(2,4,6-triisopropylphenyl)acetophenone forms the indanol product as well as its enols upon irradiation.





Scheme 26

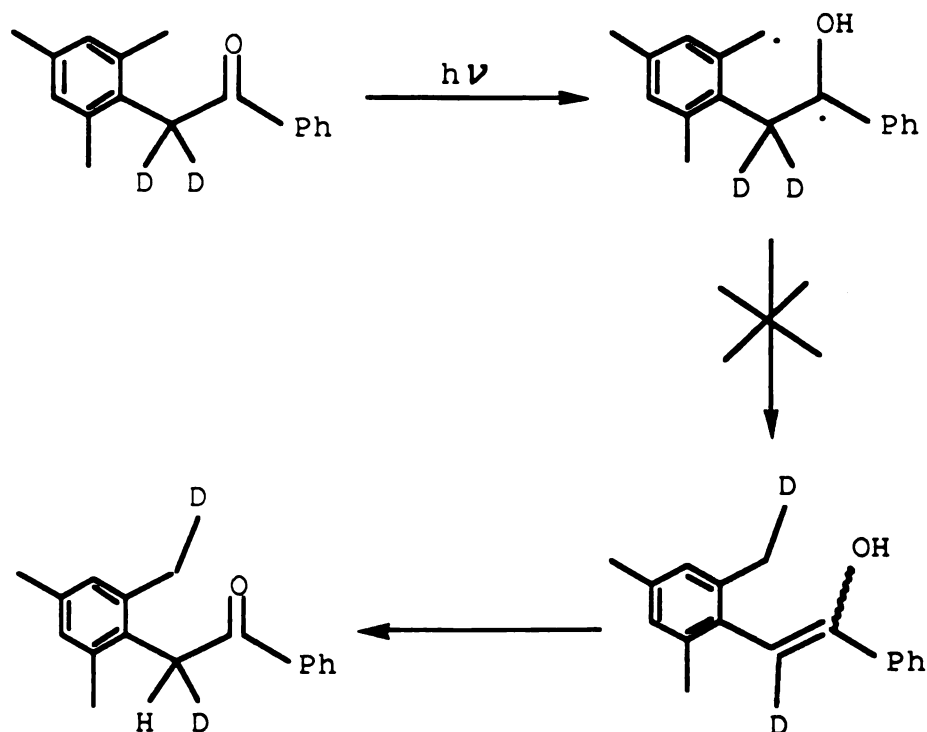
If the enol formation is indeed involved, irradiation of  $\alpha$ -mesitylacetophenone- $d_2$  16-d is expected to lead to a deuterium exchange in the starting ketone and an isotope effect in the indanol formation, with  $\alpha$ -mesitylacetophenone- $d_2$  16-d showing a higher quantum efficiency for the product formation (Scheme 27).<sup>94</sup>

However, the negative results of the isotope labelling experiments rule out possible enol formation.

As we have noticed before, the same type of quantum inefficiency exists with the other  $\alpha$ -mesityl ketones. The sum of the rates of the known reactions for the ketones corresponds to only a portion of the total triplet decay rate. This therefore leaves us a task of finding a mechanism which requires participation of the excited ketones, but produces no products. It is recalled that  $\beta$ -arylpropiophenones undergo a fast intramolecular charge transfer quenching of  $n, \pi^*$  states by the  $\beta$ -rings.<sup>66-69</sup> It is possible that such



quenching process can also occur with  $\alpha$ -mesitylacetophenone **16** and its several derivatives.



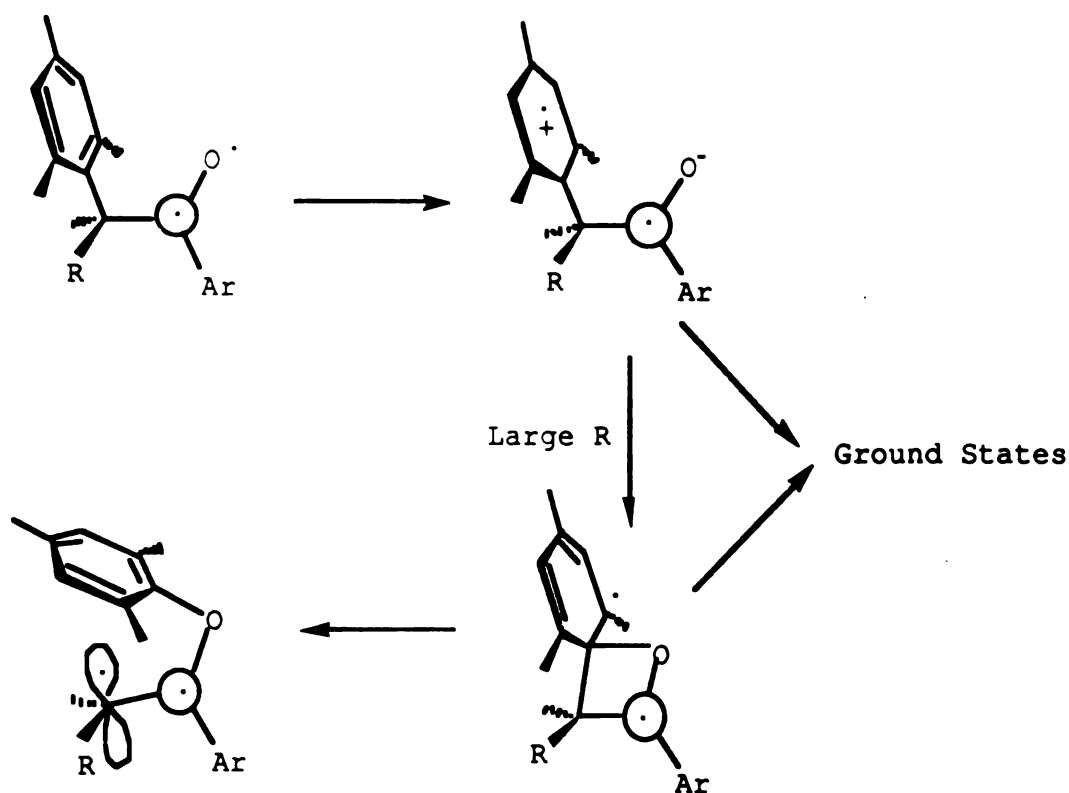
Scheme 27

The mesityl group is known to be a good electron donor.<sup>88b</sup> It is not far beyond imagination that a charge transfer complex can be formed between an electron deficient oxygen and an electron rich mesityl group in these ketones.

The charge transfer complex can decay to the ground state starting ketones, which will account for the quantum inefficiency in the formations of the photoproducts from these ketones. The complex may also rearrange to form an intermediate with a four-member ring, which is a precursor for the aryl vinyl ethers. Opening-up of the ring will afford the ethers (Scheme 28).



As it has been pointed, the least crowded  $\alpha$ -mesitylacetophenone 16 does not form the corresponding aryl vinyl ether. Only the more crowded ketones can undergo such a reaction. The formation of the intermediate with a four-member ring is expected to be an up-hill process in terms of energetics, due to the strain of the structure. So its formation is limited to sterically congested ketones. The release of the steric congestion in the ketones can be a driving force for the transformation.



Scheme 28

In Rapport's extensive study of ketone-enol interconversion of simple ketones,<sup>95</sup> it has been found that the steric congestion in the ketones makes the ketones less stable than their enol forms which are sterically favorable.



For instance, the enol of 1,2,2-trimesitylethanone is so much more stable than the ketone itself, no successful synthesis of the ketone was reported until recently by Rapport. The spectroscopic data of the ketone indicates severe distortions in the molecule, which can be released by forming the corresponding enols.

The breaking-up of the four-member ring intermediate then leaves a twisted C=C bond. This structure pictures the geometry of an excited aryl vinyl ether. Since it is well known that an excited stilbene decays to its ground state with a Z:E ratio of roughly 1:1,<sup>96-97</sup> the fact that Z:E ratios of the ethers are indeed close to 1:1 in all the cases where they can be experimentally measured strongly suggest the idea of forming an excited aryl vinyl ether.

The strained structure of the four-member ring intermediate implies that such a process may be accessible energetically. The initially formed excited C=C then decays to the ground state with a Z:E ratio of 1:1. The intermediate may also return to the starting ketones. This will provide an additional pathway responsible for the low quantum efficiency of enol ether formation.

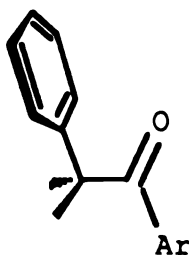


Figure 59

The rate constant of charge transfer can be derived by subtracting  $k_{\alpha}$



and  $k_g$  from the reciprocal lifetime for each ketone,

$$k_{ct} = 1/\tau - k_\alpha - k_g \quad (21)$$

The results are listed in Table 21.

The charge transfer process seems to require a geometry more or less with the aryl- $C_\alpha$  bond eclipsing with the carbonyl group and the aryl ring perpendicular to the plane of the carbonyl group (Figure 59).

This geometry is not an energy-minimized conformation of  $\alpha$ -mesitylacetophenone 16. The ketone therefore has to rotate to this geometry to react. The reaction can occur from all the conformations. The charge transfer rate has an expression including the contributions from all the conformers in an excited state equilibrium,

$$k_{ct} = \sum X(i)k_{ct}^i \quad (22)$$

If the conformations other than the most stable conformation can be neglected, then

$$k_{ct} = k_{ct}^m \quad (23)$$

where  $k_{ct}^m$  is the rate constant of the most stable conformer.

The most stable conformation of  $\alpha$ -mesitylacetophenone 16 is in the neighbourhood of the geometry in Figure 59. As a result, a decent rate constant is observed with this ketone.

One of the energy-minimized conformations of  $\alpha$ -mesitylpropio-phenone 5 and  $\alpha$ -mesityl- $\alpha$ -phenylacetophenone 8, i.e. 5E/6E and 8E by



molecular mechanics, happens to have a similar structure to the ideal geometry indicated in Figure 59. The charge transfer occurs from this conformer in an excited state equilibrium. The reaction rate equals the intrinsic rate from the reacting conformer multiplied by its percentage population in the equilibrium,

$$k_{\text{ct}} = X(r)k_{\text{ct}}^{\text{r}} \quad (24)$$

where  $X(r)$  is the percentage population of the reacting conformer,  $k_{\text{ct}}^{\text{r}}$  is the rate constant of the reacting conformer. Any changes in  $X(r)$  will affect the overall  $k_{\text{ct}}$ . Molecular mechanics calculations have suggested the steric energy of the reacting conformer is lowered significantly from  $\alpha$ -mesitylpropiophenone 5 to  $\alpha$ -mesityl- $\alpha$ -phenylacetophenone 8. This corresponds to a bigger  $X(r)$ , and thus a larger  $k_{\text{ct}}$  for  $\alpha$ -mesityl- $\alpha$ -phenylacetophenone 8.

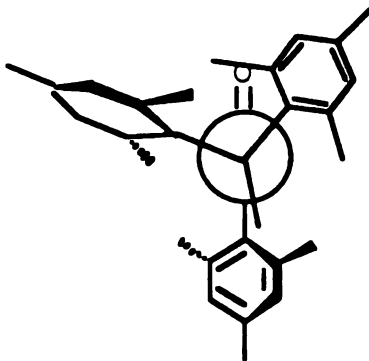


Figure 60

Rappoport<sup>95</sup> has reported that 1,2,2-trimesitylethanone has a conformation as given in Figure 60. Both  $\delta$ -hydrogen abstraction and charge



transfer are easily accessible from this conformation. However, it has been concluded that  $\delta$ -hydrogen abstraction occurs with a rate constant of  $\sim 5 \times 10^8 \text{ s}^{-1}$  even when the ketone has the right conformation, such as in the case of  $\alpha$ -mesitylacetophenone 16. On the other hand, the charge transfer can have a rate constant as fast as  $\sim 5 \times 10^9 \text{ s}^{-1}$  with  $\alpha$ -mesityl- $\alpha$ -phenylacetophenone 8, implying that such process could be significantly faster than  $\delta$ -hydrogen abstraction in 1,2,2-trimesitylethanone too. The carbonyl mesityl group of 1,2,2-trimesitylethanone is twisted by  $\sim 50^\circ$ . This could very well reduce the rate of  $\gamma$ -hydrogen abstraction in the ketone. So a mechanistic picture for 1,2,2-trimesitylethanone would be that a fast charge transfer, dominating over the other two hydrogen abstraction processes, leads to the formation of the complex upon irradiation, which is then forced to form the enol ethers by the steric congestion in the ketone.

## 5. $\alpha$ -Cleavage Reactions

$\alpha$ -(*o*-Tolyl)isobutyrophenone 4,  $\alpha$ -mesitylisobutyrophenone 7,  $\alpha$ -mesityl-2,4,6-trimethylacetophenone 14, and  $\alpha$ -mesityl- $\alpha$ -phenyl-2,4,6-trimethylacetophenone 11 undergo exclusive  $\alpha$ -cleavage reactions. The lifetimes of these ketones and the quantum yields of the aldehydes formed as the trapping products of the benzoyl radicals generated in the cleavages by dodecanethiol are listed in Table 1 and 2. The reciprocal triplet lifetimes are taken as the cleavage rates.

There are two interesting aspects of the reactions.

First, although all these ketones can undergo reactions such as the formation of indanols or aryl vinyl ethers in terms of structural possibilities, none of the reactions are observed, except for  $\alpha$ -cleavage.



Second, these ketones have triplet lifetimes much shorter than the ones of their less congested analogues, which also undergo only  $\alpha$ -cleavage, e.g.  $\alpha$ -phenylacetophenone, and  $\alpha$ -phenylisobutyrophenone.<sup>24</sup>

Since the individual ketones all have different structure-reactivity relationships, we will pursue the discussions by the types of the ketones.

### $\alpha$ -Arylisobutyrophenones

Low temperature  $^1\text{H}$  NMR studies of  $\alpha$ -(*o*-tolyl)isobutyrophenone **4** and  $\alpha$ -mesitylisobutyrophenone **7** show restricted rotations of the  $\text{C}_\alpha\text{-CO}$  bond in the molecules (Figure 61). The rate constants are estimated to be on the order of  $10^4\text{-}10^5\text{ s}^{-1}$  at  $25^\circ\text{C}$  (table 4 and 7).

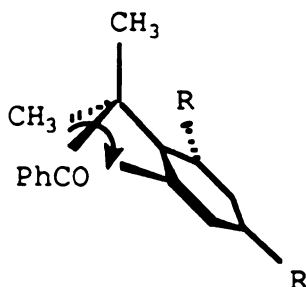


Figure 61

The two methyl groups are differentiated at low temperatures (Figure 31-33, 43-46). The different chemical shifts of the two methyl groups indicate an asymmetric arrangement of the methyl groups with respect to the molecular plane (the plane which contains the carbonyl group). So it is suggested that the conformation in Figure 62 is the most stable conformation of the molecules, in which one of the methyl groups is more or less eclipsing



the carbonyl group, and the other  $120^\circ$  away from it. Molecular mechanics calculations agree very well with this notion.

The mesityl rotation in  $\alpha$ -mesitylisobutyrophenone **7** also suffers from restriction. The rotational rate constant is  $1.7 \times 10^5 \text{ s}^{-1}$  at  $25^\circ\text{C}$  (Table 8). The conformation in Figure 62 complies with the requirement that the o-methyl groups of the methyl groups be as far away from the  $\alpha$ -methyl groups as possible. The separated o-methyl signal at 1.90 ppm in low temperature NMR spectra is thought to be the one of the methyl group near the carbonyl group, because it is somewhat in the shielding zone of the  $\text{C}=\text{O}$  bond. The methyl group at 2.63 ppm is the methyl group away from the carbonyl group (Figure 43-46).

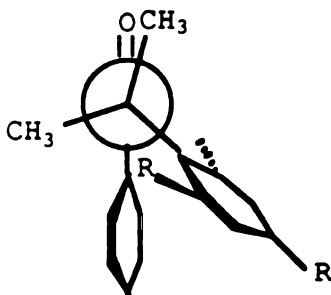


Figure 62

The steric interaction between the o-methyl group away from the carbonyl group and the two  $\alpha$ -methyl group in Figure 62 raises the energy of this conformation relative to the one of the conformation in Figure 63 for  $\alpha$ -mesitylisobutyrophenone **7**, which is the energetic peak along the  $\text{C}_\alpha$ -mesityl bond rotation. Thus  $\alpha$ -mesitylisobutyrophenone **7** has a mesityl rotational rate constant greater than  $\alpha$ -mesitylpropiophenone **5** (Table 5 and 8).



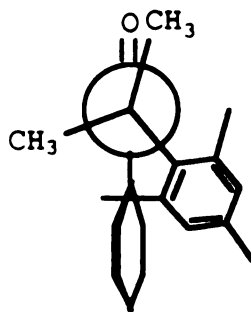


Figure 63

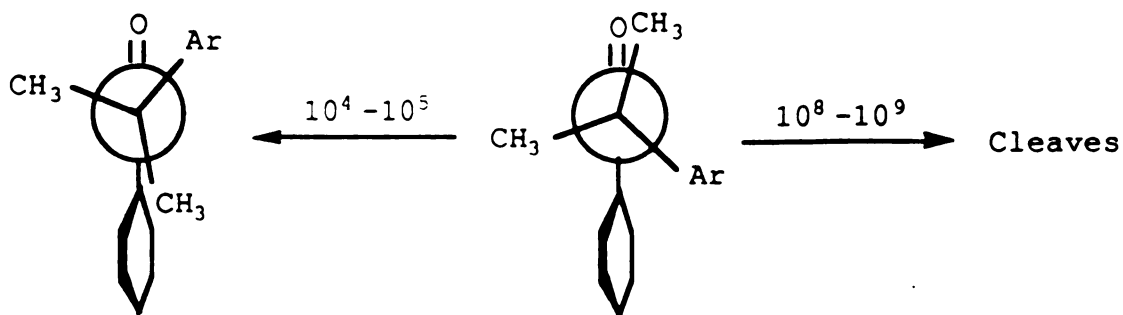
The tolyl methyl group in  $\alpha$ -(*o*-tolyl)isobutyrophenone **4** has a methyl signal at 1.98 ppm, implying that the methyl group is near the shielding zone of the C=O bond, such as in conformation 4G. Molecular mechanics calculations also suggest that conformation 4G is the most stable conformation for this ketone, in which the unfavorable interaction between the tolyl methyl group and the two  $\alpha$ -methyl groups can be avoided.

The photoreactivities of the  $\alpha$ -arylisobutyrophenones are completely governed by their ground state conformations. Irradiation of the ketones generates the excited molecules in their ground state conformations. Since the rotations of the molecules to obtain the conformations required either for the  $\delta$ -hydrogen abstraction or for the charge transfer quenching are as slow as  $10^4$ - $10^5$  s<sup>-1</sup> per mole (table 4 and 7), and the  $\alpha$ -cleavage rates range from ca.  $10^8$ - $10^9$  s<sup>-1</sup> per mole (table 1), it is not surprising that  $\alpha$ -cleavage reactions are the only reactions observed for these ketones (Scheme 29).

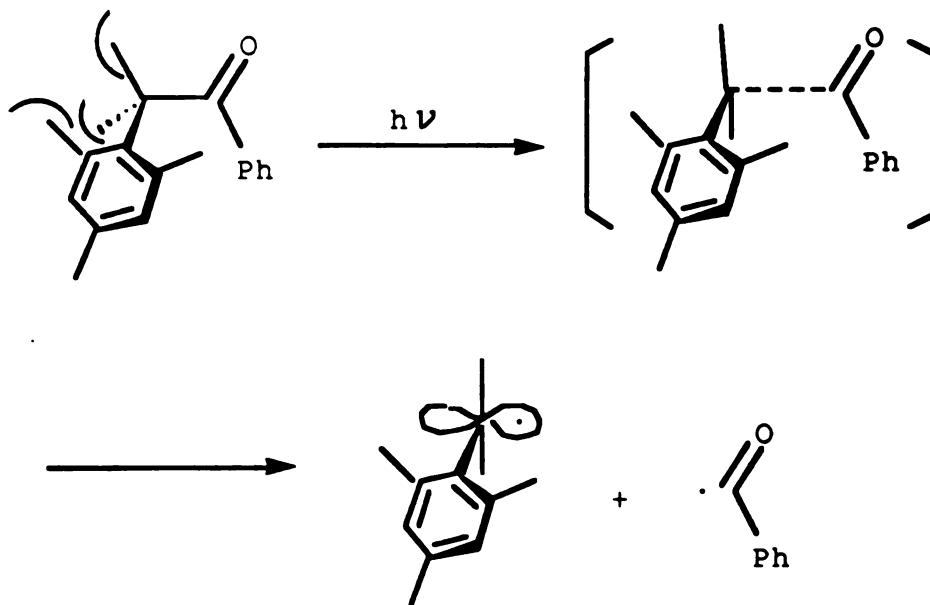
Although it has been concluded that ketones **2**, **3**, **5**, **6**, and **8** undergo  $\delta$ -hydrogen abstraction from the nonideal conformations in which they are set,  $\alpha$ -arylisobutyrophenones **4** and **7** have their aryl rings oriented differently in their ground state conformations from these



$\alpha$ -monosubstituted ketones. The aryl rings in ketones **4** and **7** have to parallel with the  $C_{\alpha}$ -CO bond of the ketones due to the presence of the two  $\alpha$ -methyl groups, which makes the benzylic methyl group of the aryl groups more distant from the carbonyl oxygen than in the monosubstituted ketones.



Scheme 29



Scheme 30



Furthermore, the more rigid orientation of the aryl groups imposed by the two methyl groups prohibits slight movement of the rings to reach a reasonable transition state geometry.

Lewis<sup>24</sup> has measured the rate of  $\alpha$ -cleavage with  $\alpha$ -phenylisobutyrophenone, and found that the rate constant is  $1.2 \times 10^8 \text{ s}^{-1}$ . The cleavage rate constant for  $\alpha$ -mesitylisobutyrophenone **7** is  $7.3 \times 10^8 \text{ s}^{-1}$ . The significant enhancement in the rates reflects the extent of release of the indicated steric congestion in  $\alpha$ -mesitylisobutyrophenone **7** on going to the transition state (Scheme 30).

#### **$\alpha$ -Mesityl-2,4,6-trimethylacetophenone**

X-ray crystallography shows that  $\alpha$ -mesityl-2,4,6-trimethylacetophenone **14** has a conformation as given in Figure 29 in solid state. Let's assume that this ketone has the same conformation in solution as in solid state. This assumption is supported by molecular mechanics calculations (Conformation 14E) and other spectroscopic data.

Phenyl ketones absorb strongly around 240 nm due to an allowed transition (K band) which may be represented by  $\text{PhC=O} \rightarrow {}^+\text{Ph}=\text{C-O}^-$ . The K band absorbance ( $\epsilon$ ) of the ketones depends on the extent of conjugation between the phenyl and carbonyl group, therefore on the coplanarity of the phenyl and carbonyl group. nonplanarity caused by o-methylation on the phenyl ring reduces the extent of the conjugation. Loss of conjugation will in turn lead to a decrease in  $\epsilon$ .<sup>86</sup>

IR absorption of C=O bond is another measure for the Ph-CO conjugation. The resonance structure  ${}^+\text{Ph}=\text{C-O}^-$  as a result of conjugation weakens the C=O bond and causes a bathochromic shift in the absorption



frequency. A reduced conjugation will, on the other hand, produce a hypsochromic shift.<sup>85</sup>

$^{13}\text{C}$  NMR absorption of the carbonyl carbon in a phenyl ketone is also affected by the extent of conjugation between the phenyl and carbonyl group. Acetone absorbs at 203.8 ppm. Replacement of the methyl group of acetone by a phenyl group causes an upfield shift of the  $\text{C}=\text{O}$  absorption to 195.7 ppm. Presumably, charge delocalization by the benzene ring makes the carbonyl carbon less electron deficient. If the conjugation is restricted by any means, the  $\text{C}=\text{O}$  absorption is expected to experience an downfield shift.<sup>84</sup>

The spectroscopic data of several ketones are given in Table 11.

The disappearance of the K band in UV, the hypsochromic shift of the  $\text{C}=\text{O}$  absorption in IR, and the downfield shift in  $^{13}\text{C}$  NMR of  $\alpha$ -mesityl-2,4,6-trimethylacetophenone 14 support the structure with the carbonyl group orthogonal to the mesityl groups (14E). Such a structure simply makes the hydrogens not available for either the  $\delta$ -hydrogen abstraction to give the indanol, or the  $\gamma$ -hydrogen abstraction to give the cyclobutenol.

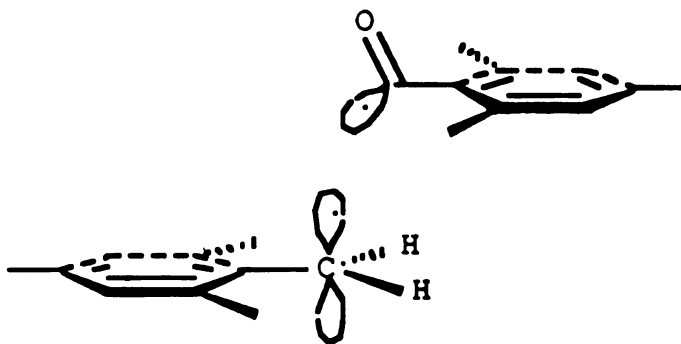


Figure 64



Lewis<sup>24</sup> has reported that  $\alpha$ -phenylacetophenone cleaves with a rate constant of  $2.4 \times 10^6 \text{ s}^{-1}$ . The  $\alpha$ -cleavage rate constant for  $\alpha$ -mesityl-2,4,6-trimethylacetophenone is on the order of  $10^8$ - $10^9 \text{ s}^{-1}$  (Table 1). The dramatic increase of the rate is due to the perfect geometry of the molecule for the cleavage. The two mesityl groups are properly oriented to stabilize the radical centers produced by the cleavage (Figure 64).

#### $\alpha$ -Mesityl- $\alpha$ -Phenyl-2,4,6-trimethylacetophenone

Rappoport<sup>95</sup> has reported the X-ray structure of  $\alpha$ -Mesityl- $\alpha$ -Phenyl-2,4,6-trimethylacetophenone **11** in solid state as described in Figure 65. Spectroscopic studies of the ketone in solution suggest a similar structure for the ketone. The mesityl group attached to the carbonyl group is twisted ca.  $70^\circ$  with respect to the plane of the carbonyl group.

$\alpha$ -Mesityl- $\alpha$ -phenyl-2,4,6-trimethylacetophenone **11** undergoes  $\alpha$ -cleavage at a rate of  $8.1 \times 10^9 \text{ s}^{-1}$  per mole (Table 1). Two factors may be responsible for the fast cleavage.

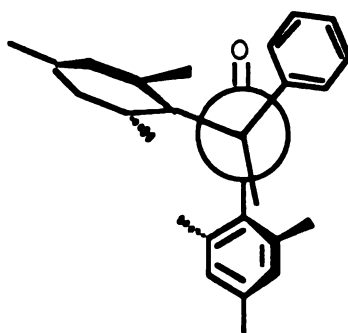


Figure 65



First, the nearly orthogonal arrangement of the phenyl group and the mesityl group attached to the carbonyl group with respect to the carbonyl group favors the cleavage due to the stabilization of the radicals by the aromatic  $\pi$  system.

Second, the release of steric strain in the molecule accompanying the cleavage may serve as an additional driving force for the reaction.

Neither the hydrogen abstractions ( $\gamma$  and  $\delta$ ) nor the 1,3-aryl shift can occur with the conformation of the ketone at a rate comparable to the one for cleavage, since the mesityl groups are badly oriented for these reactions. Furthermore,  $\delta$ -hydrogen abstraction can't compete with the cleavage even if the mesityl group has the right geometry, if we recall that  $\alpha$ -mesitylacetophenone undergoes the hydrogen abstraction only with a rate constant of  $5.8 \times 10^8 \text{ s}^{-1}$ .

## 6. Kinetic Rotational Control in $\alpha$ -Mesitylvalerophenone

An interesting observation with  $\alpha$ -mesitylvalerophenone **6** is that this ketone shows a substantially lower quenching efficiency than  $\alpha$ -mesitylpropiofenone **5**. In another word, the excited state of  $\alpha$ -mesitylvalerophenone **6** decays faster than the one of  $\alpha$ -mesitylpropiofenone **5** (Figure 14).

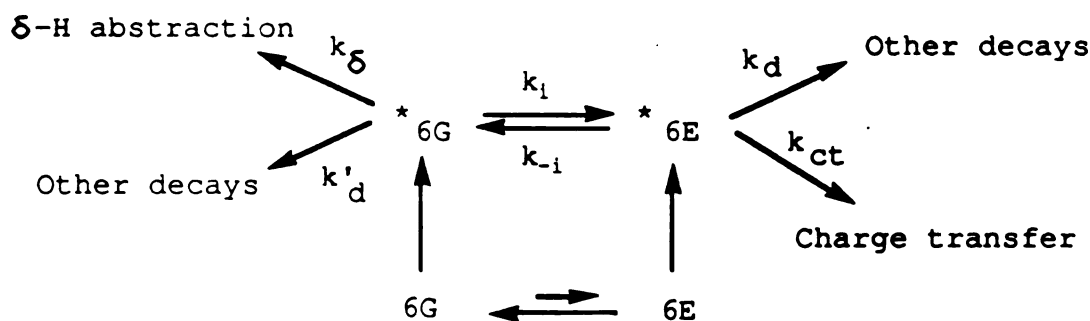
$\alpha$ -Mesitylvalerophenone **6** can undergo the same types of reactions as  $\alpha$ -mesitylpropiofenone **5** except that type II reaction could occur with  $\alpha$ -mesitylvalerophenone **6**, but not with  $\alpha$ -mesitylpropiofenone **5**. The observation that  $\alpha$ -mesitylvalerophenone **6** gives only trace amount of type II products even in the presence of a lewis base eliminates the possibility that type II reaction is responsible for the faster decay of  $\alpha$ -mesitylvalerophenone



6 triplets, although the molecule seems to have the right conformation for the reaction. So the faster decay of  $\alpha$ -mesitylvalerophenone can't be explained with what we have known about this ketone.

In addition, Stern-Volmer quenching of  $\alpha$ -mesitylvalerophenone 6 gives rise to a curved plot, which indicates the existence of two excited states interconverting at a rate comparable with the rates of photoreactions.

Molecular mechanics calculations reveal that  $\alpha$ -mesitylvalerophenone 6 has two conformations with minimized energies. One is the most stable conformation, 6G. The other with the mesityl group more or less eclipsing with the carbonyl group can be depicted as conformation 6E.



Scheme 31

$\alpha$ -Cleavage can occur from both conformation 6G and 6E. On the other hand, 1,3-aryl migration is limited to 6E, and  $\delta$ -hydrogen abstraction as well as type II reaction to 6G. It can be assumed that only conformation 6G is populated in ground state, since a 3-4 Kcal/mole energy gap is suggested by molecular mechanics calculations between the two conformations. It corresponds to an equilibrium constant of  $>153$  in favor of conformation 6G. Irradiation generates the excited molecules in conformation 6G, which then



can convert to conformation 6E, or undergo the reactions possible for conformation 6G. Conformation 6E can either return to 6G, or react. A general scheme, which includes the population of 6E in ground state, illustrates all the possible decay pathways (Scheme 31).

A stern-volmer equation concerning the quenching of the indanol is derived based on the scheme (Equation 26),

$$\Phi^0/\Phi = (1 + A[Q] + B[Q]^2)/(1 + C[Q]) \quad (25)$$

$$A = k_q L/M, \quad B = k_q^2/M, \quad C = k_q(k_\delta - X(6E)k_\delta)/N$$

$$L = k_\delta + k_d' + k_{-i} + k_{ct} + k_d + k_i$$

$$M = k_{-i}k_\delta + k_{ct}k_\delta + k_dk_\delta + k_{-i}k_d + k_{ct}k_d' + k_dk_d' + k_ik_{ct} + k_ik_d$$

$$N = k_{-i}k_\delta + k_{ct}k_\delta + k_dk_\delta - X(6E)k_{ct}k_\delta - X(6E)k_dk_\delta$$

where  $X(6E)$  is the percentage population of conformation 6E in ground state.

If  $X(6E) = 0$ , then,

$$N = k_{-i}k_\delta + k_{ct}k_\delta + k_dk_\delta$$

$$C = k_qk_\delta/N$$

The detail of the derivation of the equation is given at the end of the chapter.

A curve fitting of the experimental data displayed in Figure 14 by



KINFIT affords the estimated values for the individual parameters in the equation,

$$A = 3.6 \quad B = 3.9 \quad C = 0.10$$

The ratio of A and B equals approximately 1. Thus we can obtain the following equation,

$$A/B = L/k_q = 1 \quad (26)$$

This leads to an estimate of  $5 \times 10^9$  ( $k_q$ ) for L, which is a sum of several rate constants. The rotational rate from 6G to 6E,  $k_i$ , is expected to be slow because 6G is more stable than 6E. The  $\delta$ -hydrogen abstraction rate constant from conformation 6G,  $k_\delta$ , should be substantially smaller than the one for  $\alpha$ -mesitylacetophenone 16,  $6.8 \times 10^8$ . So  $k_i$  and  $k_\delta$  can both be neglected along with  $k_d'$  and  $k_d$  in equation (26). Then equation (26) becomes,

$$L = k_{-i} + k_{ct} = 5 \times 10^9 \quad (27)$$

This gives an upper limit of  $5 \times 10^9 \text{ s}^{-1}$  for either  $k_{-i}$  or  $k_{ct}$ .

Therefore, the fast triplet decay of  $\alpha$ -mesitylvalerophenone 6 can be attributed to the fast decay of conformation 6E by the charge transfer mechanism, and the rapid interconversion between 6G and 6E.

The inefficiency of type II reaction from  $\alpha$ -mesitylvalerophenone 6 can be due to the two facts. First, the type II reaction from conformation 6G has to compete with the conformational change from 6G to 6E, followed by a fast decay of 6E. This will reduce the efficiency of the type II reaction from



conformation 6G.

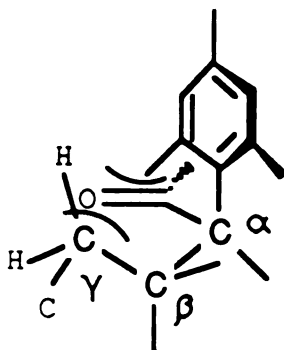


Figure 66

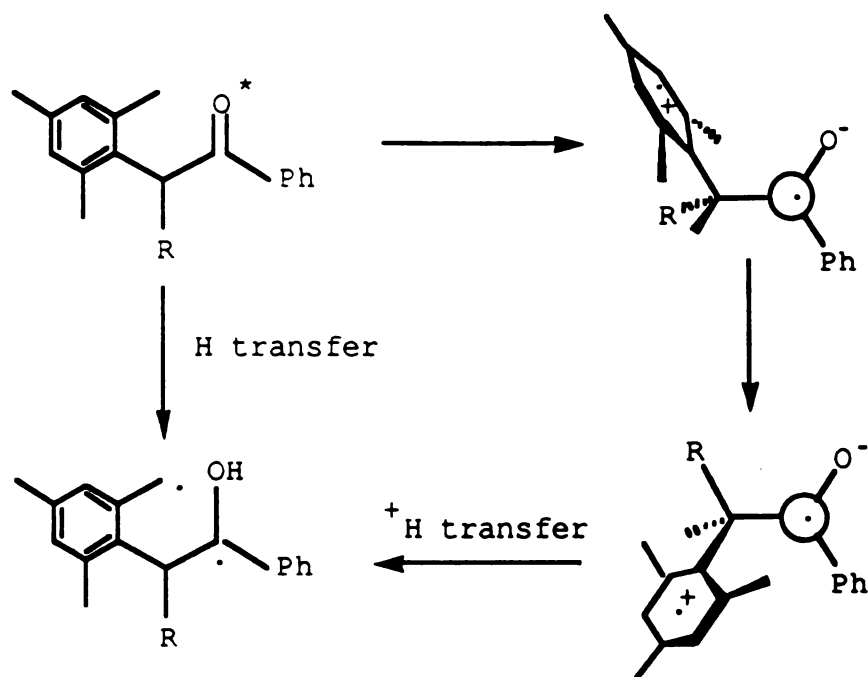
Second, the type II reaction from conformation 6G may very well be limited by the structure of  $\alpha$ -mesitylvalerophenone **6** itself. Careful inspection of a molecular model shows that a pseudo chair transition state for type II reaction with the  $C_{\alpha}$ - $C_{\beta}$  bond eclipsing with the carbonyl group will suffer from a steric interaction between one of mesityl methyl groups and the methylene group at  $C_{\gamma}$  (Figure 66) This interaction will decrease the rate for type II reaction.

## 7. Possible Formation of the 1,5-Biradical via a Proton Transfer from a Charge Transfer Complex

The indanol formation quantum yields of  $\alpha$ -mesitylpropiophenone **5**,  $\alpha$ -mesitylvalerophenone **6**, and  $\alpha$ -mesityl- $\alpha$ -phenylacetophenone **8** change with the nature of the solvents used. They are increased in benzene with 2M dioxane, acetonitrile, and methanol (Table 2). The enhancement in the presence of dioxane is thought to be due to the ability of the added dioxane to



form a hydrogen bond with the hydroxy group in the biradical, and retard the reverse hydrogen transfer to give the starting ketones. More increase of the quantum yields in acetonitrile than in 2 M dioxane is most amazing, since acetonitrile is known to be a less efficient Lewis base to stop the reverse hydrogen transfer.



Scheme 32

One important aspect of well studied ketone photoreduction reaction is the fact that hydrogen atom abstraction can occur directly or via a charge transfer followed by a proton transfer to give the same radicals as the direct hydrogen abstraction will. The charge transfer path was first evident with amine donors, which are orders of magnitude more reactive than they would be as simple hydrogen atom sources.<sup>99-100</sup> Wagner<sup>65</sup> has pointed out the possibility that the photoreduction of triplet ketones by alkylbenzenes might occur under certain conditions by a combination of competing charge transfer



and direct hydrogen atom abstraction. A recent publication by Wagner<sup>101</sup> reported the extent to which such direct abstraction competes with the charge transfer mechanism:

The ketones we studied may represent an intramolecular case of such competition. The geometry of the charge transfer complex is believed to have the C<sub>α</sub>-Ar bond eclipsing with the carbonyl group and the mesityl group perpendicular to the nodal plane of carbonyl group. This conformation is not suitable for the proton transfer. In order for it to occur, the mesityl group in the complex has to rotate to a geometry which has the right geometry and is energetically accessible as well. The conformational change will inevitably create a charge separation in the complex. Such charge separation has to be compensated by either solvation in polar solvents, or a favorable steric energy gain during the conformational change. The G type conformations of α-mesitylpropiophenone 5, α-mesitylvalerophenone 6 satisfy all the above requirements. They are more stable than their E type conformations. The conformational change from the charge transfer complex to a charge-separated intermediate with the G type conformation is a down-hill process in terms of steric energy. The proton transfer from the G type conformations is expected to have a reasonable rate, since even the more geometry-requiring hydrogen atom transfer can occur from them (Scheme 32). The charge separation can be furthermore compensated by solvation in polar solvents. Acetonitrile and methanol can both serve as polar solvents to stabilize the charge separation through dipole-dipole interaction with the charges in the complex. This alternative pathway for forming the 1,5-biradical from the charge transfer complex will increase the quantum yields of the indanols from the ketones in polar solvents.

Although the quantum yield of indanol from α-mesityl-α-phenylaceto-



phenone **8** is doubled in acetonitrile as in 2 M dioxane in benzene, the absolute amount is only a few percent. This is not surprising if we realize that conformation **8G** has comparable steric energy as conformation **8E**, which happens to be the geometry of the charge transfer complex. These two conformations are the most stable conformations of the ketone by calculations. The lack of a drive from the steric energy difference during the conformational change from **8E** to **8G** or any other possible conformations is responsible for the reluctant proton transfer in the complex of ketone **8**.

Similar result was observed with  $\alpha$ -mesitylacetophenone **16**. The quantum yield for indanol formation from **16** in acetonitrile is essentially the same as in benzene, implying that the proton transfer in the charge transfer complex does not occur in significant amount with this ketone. We believe that this is due to the same reason as in the case of  $\alpha$ -mesityl- $\alpha$ -phenylacetophenone **8**. The conformation adopted by the charge transfer complex from ketone **16** is calculated to be only 0.5 Kcal/mole less stable than the most stable conformation of the ketone, **16S**, and more stable than **16G**. The charge transfer complex therefore can't find a conformation which will allow the proton transfer and provide a steric energy compensation.

#### **8. Photoenolization of $\alpha$ -(2,4,6-Triisopropylphenyl)acetophenone**

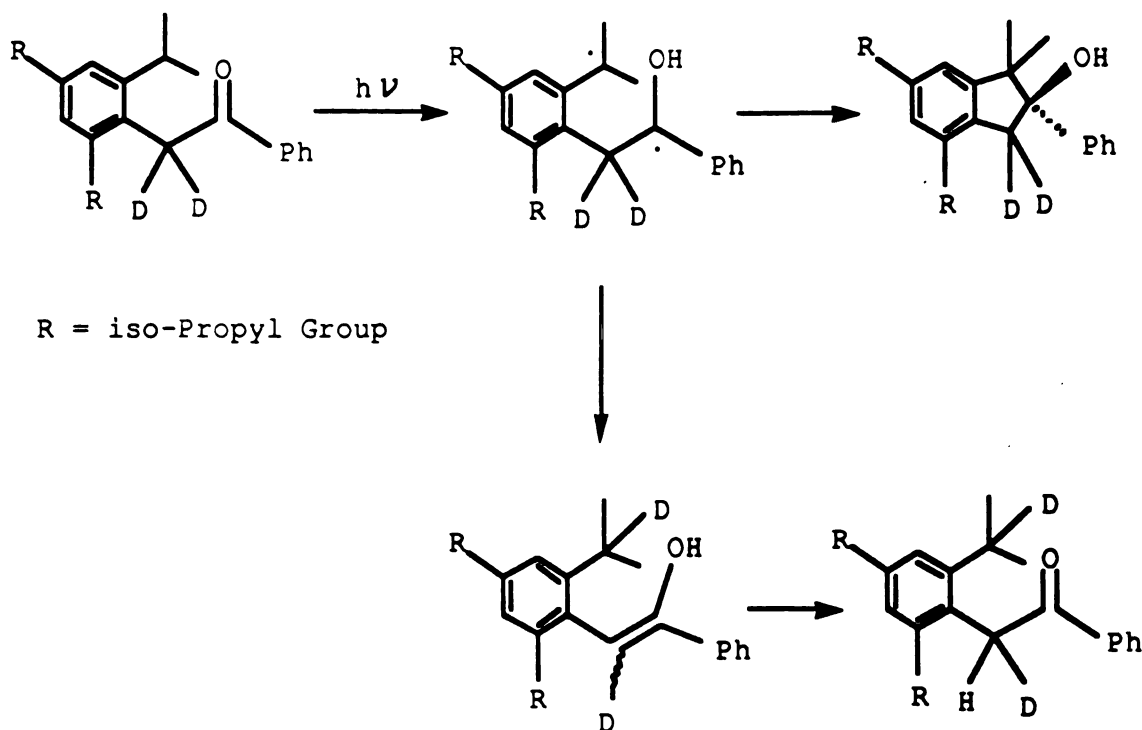
Wagner<sup>79</sup> has reported that  $\alpha$ -(2,4,6-triisopropylphenylacetophenone) forms 4,6-diisopropyl-1-dimethyl-2-phenyl-indanol as well as the enols of the ketone. It has been postulated that the enols are formed from the 1,5-biradical involved in the  $\delta$ -hydrogen abstraction. However, this postulation needs experimental proof, since a photochemically allowed 1,3-hydrogen shift could



also lead to the formation of the same products.

For this purpose, deuteriated  $\alpha$ -(2,4,6-triisopropylphenyl)acetophenone) was studied.  $^1\text{H}$  and  $^2\text{H}$  NMR studies revealed the deuterium exchange which can only be explained by the involvement of the biradical (Scheme 33).

Furthermore, an isotope effect in the indanol formation was observed. The quantum yield of the indanol is approximately doubled with  $\alpha$ -(2,4,6-triisopropylphenyl)acetophenone- $\text{d}_2$  16 (Table 2), because  $\alpha$ -deuteration disfavors the formation of the enols by the primary isotope effect.



Scheme 3

The quantum yield of indanol formation is decreased more than ten times for both  $\alpha$ -(2,4,6-triisopropylphenyl)acetophenone and



$\alpha$ -(2,4,6-triisopropylphenyl)acetophenone-d<sub>2</sub> **16** in dioxane. The hydrogen bonding of the hydroxy group in the 1,5-biradical by the solvent increases the steric crowding around the hydroxy group, and hence slows down the cyclization of the biradical due to the reluctance for the two congested radical centers to get close. As a result, the enol formation is enhanced as an alternative decay pathway for the biradical.<sup>79</sup>

Since Wagner<sup>79</sup> has observed a ratio of 15/1 for the enols and indanol in dioxane, while the ratio is found to be 1/1 in benzene, the quantum yields of the enols in dioxane and benzene are estimated to be 0.24 and 0.23 respectively.

## B. Photochemistry in Solid State

The photochemical studies of the ketones in organized assemblies are just initiated, especially in the area concerning cyclodextrin complexes. However, the preliminary results will be discussed here.

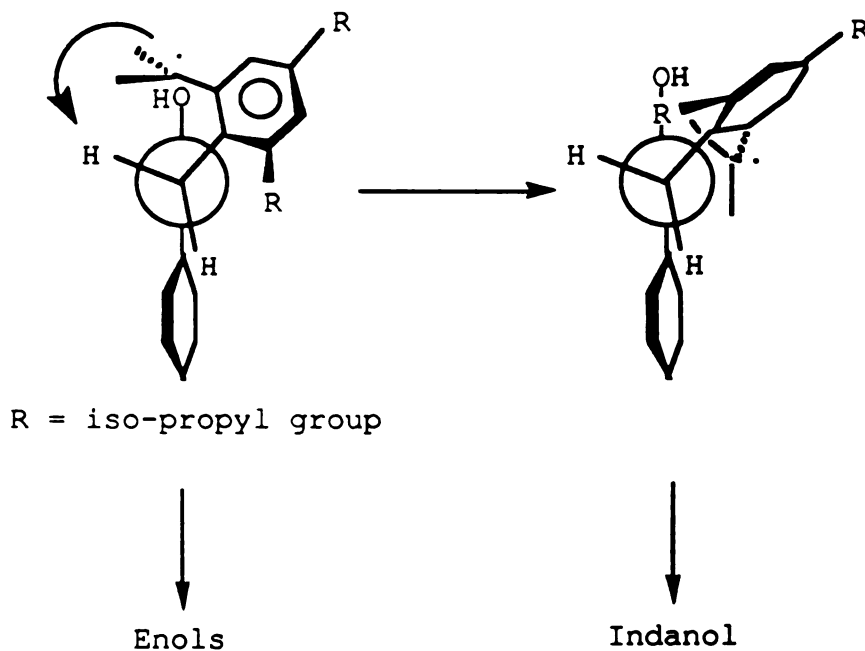
### $\alpha$ -(2,4,6-Triisopropylphenyl)acetophenone

The irradiation of  $\alpha$ -(2,4,6-triisopropylphenyl)acetophenone in solution is known to give the corresponding indanol and the enols of the ketone. The indanol formation is as efficient as the enol formation in benzene. We have just established that the enols are formed from the biradical produced in the  $\delta$ -hydrogen abstraction. In solid state, the ketone gives the enol as the major product, with a product composition of 91.1%, and the indanol as the minor product, with a product composition of 9.9%.

The confinement imposed by crystal lattices makes it difficult for the



biradical to rotate ca.  $90^\circ$  to achieve the critical conformation for the indanol formation. While the enol formation requires almost no rotation of the 2,4,6-triisopropylphenyl group. The indanol formation is thus retarded by the difficulty in the rotation of the aryl ring in solid state (Scheme 34).



Scheme 34

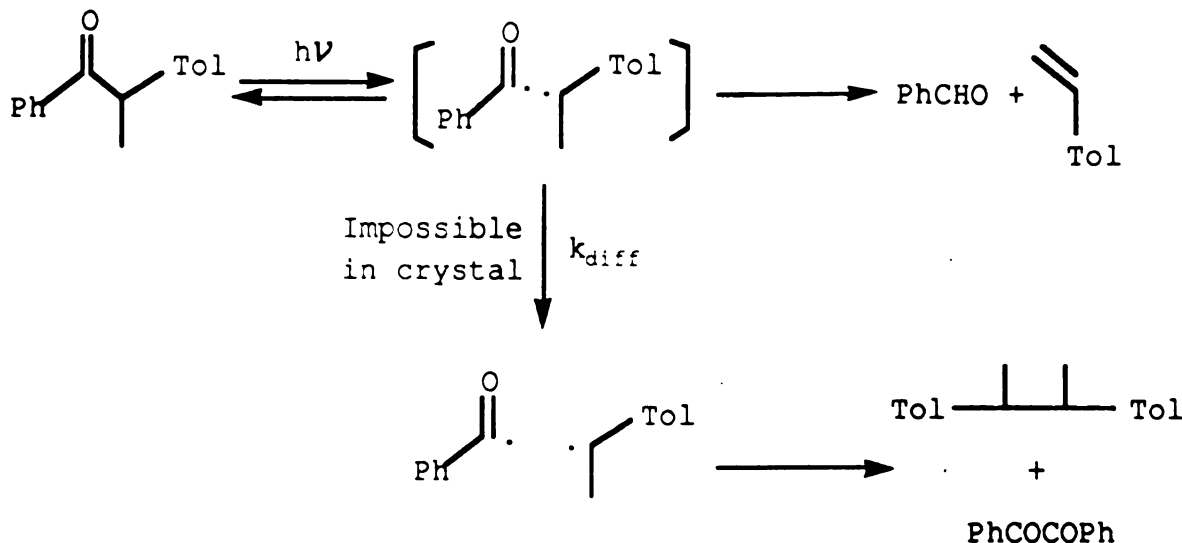
Although dioxane does increase the enol formation in solution, it is due to a different reason.

### $\alpha$ -(o-Tolyl)propiophenone

$\alpha$ -(o-Tolyl)propiophenone 2 forms 2,3-di(o-tolyl)butane as the major  $\alpha$ -cleavage product and 3-methyl-2-phenyl-2-indanol in solution. The irradiation of this ketone in crystal eliminates the formation of the coupling



product 2,3-di(o-tolyl)butane, and in the meantime, the  $\alpha$ -cleavage reaction takes the course of forming benzaldehyde by disproportionation between the initially formed radicals. An unusual rearranged product,  $\beta$ -(o-tolyl)propiophenone, is produced upon the irradiation in crystal or powder, along with the indanol.



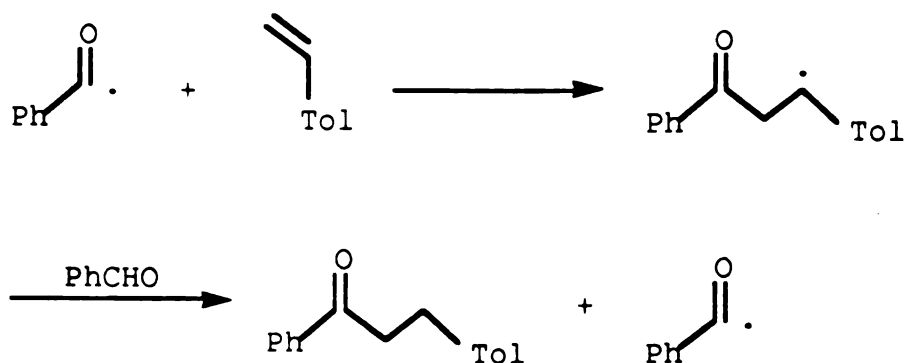
Scheme 35

The failure of forming 2,3-di(o-tolyl)butane in crystal is caused by the impossibility of the benzyl radicals to move around coupling with each other. Instead the benzoyl and benzyl radicals disproportionate to give the benzaldehyde and tolylethylene (Scheme 35). Turro has reported that  $\alpha$ -phenylisobutyrophenone gives disproportionation products as the major cleavage products in micelle, presumably due to the increased cage-effect in the medium.<sup>63d</sup>

The rearrangement of  $\alpha$ -(o-tolyl)propiophenone 2 to  $\beta$ -(o-tolyl)propiophenone is believed to be a result of a secondary reaction of the



$\alpha$ -cleavage products (Scheme 36). In solution, such a rearrangement requires that benzoyl radicals escape the solvent cage, and then react with  $\alpha$ -(o-tolyl)ethylene molecules. Since disproportionation is not the major



Scheme 36

mode of the reactions that benzoyl and benzyl radicals undergo in solution, the concentration of  $\alpha$ -(o-tolyl)ethylene is limited. Benzoyl radicals will also have to face the competitions from some other fast reactions in solution, such as coupling between the radicals. Thus the rearrangement is not favored in solution. In solid state,  $\alpha$ -(o-tolyl)ethylene and benzaldehyde molecules exist in a fairly high concentration, because the disproportionation now is the major mode of the radical reactions and solid state is a very condensed phase. There is a good statistic chance that a benzoyl radical is produced nearby  $\alpha$ -(o-tolyl)ethylene and benzaldehyde molecule. The inability of the radicals to undergo other reactions in solid adds another plus factor for the rearrangement.

**$\alpha$ -Mesitylpropiophenone,  $\alpha$ -Mesitylvalerophenone, and  $\alpha$ -Mesityl- $\alpha$ -Phenyl-acetophenone**



Irradiations of  $\alpha$ -mesitylpropiophenone 5,  $\alpha$ -mesitylvalerophenone 6, and  $\alpha$ -mesityl- $\alpha$ -phenylacetophenone 8 in solid state afford nearly quantitatively the corresponding indanols. The X-ray crystallography of  $\alpha$ -mesitylvalerophenone 6 and  $\alpha$ -mesityl- $\alpha$ -phenylacetophenone 8 has provided the conformations of the ketones in solid state (Figure 27 and 28), which deviate substantially from the ideal conformation for  $\delta$ -hydrogen abstraction (Figure 55). However careful examinations of the structures reveal that the geometric factors concerning hydrogen abstractions of these ketones in solid state are ca.  $60^\circ$ - $70^\circ$  for  $\eta$ ,  $70^\circ$ - $80^\circ$  for  $\Delta$ ,  $160$ - $170^\circ$  for  $\theta$ , and  $60$ - $70^\circ$  for  $\rho$ . They are by no means the ideal values. But they do not stop the reaction in solid state. Scheffer<sup>58</sup> has reported a similar observation that in the solid state photochemistry of several  $\alpha$ -cycloalkyl-p-chloroacetophenone derivatives, there is no strict requirement for the hydrogen being abstracted to be in the plane of the carbonyl oxygen n orbital, and  $\eta$  and  $\Delta$ , particularly the former, can vary quite considerably from its optimum values of  $0^\circ$  and  $90^\circ$ . These results indicate that the deviation of the geometric factors from the ideal values may reduce the hydrogen abstraction rate, but only to a certain extent.

The disappearance of 1,3-aryl shift products for these ketones in solid state supports the suggestion that the charge transfer quenching requires a geometry as mentioned before for a maximum orbital overlap of the aryl group and oxygen. The solid state conformations of the ketones are such that the interaction between the aryl  $\pi$  electrons and the oxygen n orbital is unlikely.

Interestingly,  $\alpha$ -mesitylpropiophenone 5 forms only one of the isomeric indanols, the Z isomer. The Z:E ratio in cyclohexane is 5.1:1. Apparently, the biradical formed in solid state is too restrained to rotate to give the E isomer.



## II. $\beta$ -Arylpropiophenone Derivatives

It has been known for a number of years that aromatic rings can deactivate  $n,\pi^*$  carbonyl triplets by a charge transfer mechanism. The process can be very efficient when it takes place intramolecularly as illustrated in the case of  $\beta$ -phenylpropiophenones.<sup>68</sup> Detailed time-resolved studies of the

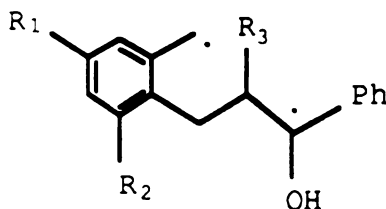


Figure 67

transient photoprocess in the photochemistry of various ring substituted  $\beta$ -phenylpropiophenones have been published recently.<sup>69</sup> However, in all of those studies, no formation of photoproducts has been reported. We have for the first time found out the formation of substituted 1,2,3,4-tetrahydro-2-naphthols from several  $\beta$ -arylpropiophenones 18-21 upon irradiation (Reaction 16).

The product formation is quenched by typical triplet quencher such as 2,5-dimethyl-2,4-hexadiene. The triplet lifetimes and the quantum yields of product formation in various solvents are listed in Table 16 and 17 respectively. The reaction is believed to be via a 1,6-biradical generated from long range  $\epsilon$ -hydrogen abstraction of the triplet ketones (Figure 67).

Based upon the consideration of the geometric parameters defined before, the conformation in Figure 68 is believed to be the best conformation



for the  $\epsilon$ -hydrogen abstraction. This conformation happens to be one of the energy-minimized conformations of the  $\beta$ -arylpropiophenones, the A type copnformations.

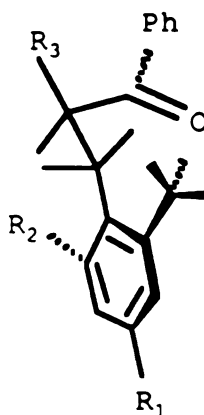


Figure 68

The triplet lifetimes of the ketones are rather insensitive to  $\alpha$ -methylation, or the methylation of the  $\beta$ -ring. Scaiano<sup>69</sup> has shown that the rate of intramolecular charge transfer quenching is mainly controlled by the molecular motion to achieve the critical geometry. It is like a intermolecular quenching process which is controlled by the diffusion rate in a given solvent. Introduction of a  $\alpha$ -methyl group or a methyl group on the  $\beta$ -ring does not alter the rate of molecular motion substantially, which is in turn reflected by the similar triplet lifetimes for these ketones.

Although the triplet lifetimes of the ketones are not affected by the  $\alpha$ -methylation, the quantum yield of the product formation is increased about 10 times by the addition of a methyl group at the  $\alpha$ -carbon, or by changing from an o-tolyl group to a mesityl group at the  $\beta$ -carbon. The quantum yield is directly associated with the population of the molecules in



the conformation accessible for the hydrogen abstraction in terms of the reaction rate constant. The rate constant for the reaction equals the intrinsic rate constant multiplied by the percentage population of the suitable conformation. So the hydrogen abstraction rate is expected to be sensitive to any conformational change. If an excited state equilibrium is assumed between different conformers of the ketones, the quantum yield can be expressed as follows,

$$\Phi = k\tau = X(r)k_r\tau \quad (28)$$

where  $X(r)$  is the percentage population of the reacting conformer,  $k_r$  is the intrinsic rate of the reacting conformer,  $k$  is the observed rate constant,  $\tau$  is the triplet lifetime. An increase in  $X(r)$  will raise the quantum yield for the product formation.

The observed rate constant can then be calculated from the measured quantum yields and lifetimes,

$$k = k_r X(r) = \Phi \tau^{-1} \quad (29)$$

Table 23. Rate Constants for  $\epsilon$ -Hydrogen Abstraction in Several Ketones

Ketones	17 <sup>a</sup>	18	19	20
$k \times 10^5 (s^{-1})$	<0.1	1.1	3.2	20.0

a. Estimated from reaction time and amount of unidentified peaks on GC

Table 23 lists the  $k$  values so obtained, using the quantum yields in



benzene with 2M dioxane as maximized quantum yields.

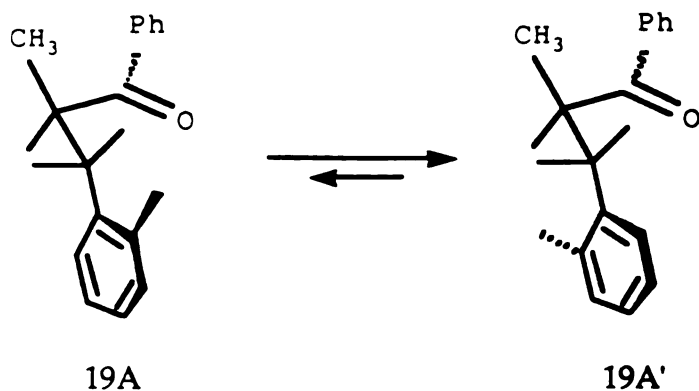


Figure 69

Our molecular mechanics calculations suggest that the  $\alpha$ -methylation lowers the energy of the A type conformations relative to other calculated conformations. This result is understandable in the following sense. The aryl groups in the A type conformations are anti to the  $\alpha$ -substituent, and they are gauche to the  $\alpha$ -substituent in the G type conformations. For ketone 19 and 21 with a  $\alpha$ -methyl group, the aryl groups prefer the anti arrangement more than for ketone 18 and 20 having no  $\alpha$ -substituent. Since A type conformations are responsible to the  $\epsilon$ -hydrogen abstraction, the  $k$  of  $\epsilon$ -hydrogen abstraction and the quantum yield of the product formation are enhanced dramatically by the  $\alpha$ -substitution.

It is noticed that there is an approximately ten fold increase of quantum yield from  $\beta$ -(*o*-tolyl)isobutyrophenone 18 to  $\beta$ -mesitylisobutyrophenone 20 in benzene or benzene with 2M dioxane. This corresponds to a eighteen fold increase in the  $k$  value (Table 23). The same type of conformational arguments as used by Wagner<sup>35</sup> can be used to account for the observation.



As Wagner has pointed out, the enhancement of  $\delta$ -hydrogen abstraction rate from  $\alpha$ -(*o*-tolyl)acetophenone 15 to  $\alpha$ -mesitylacetophenone 16 is in part due to the fact that  $\alpha$ -mesitylacetophenone 16 does not have an unreactive conformation with regard to the orientation of the  $\alpha$ -aryl group like  $\alpha$ -(*o*-tolyl)acetophenone 15. It is believed that we have a similar case here with these  $\beta$ -arylpropiophenones. There are two factors affecting the  $k$  of the reaction. An increase in the biradical stability will speed up the reaction by making a larger  $k_T$ . A factor of 2 can thus be attributed to the inductive stabilization of the benzyl radical by the additional two methyl group<sup>65,102</sup> on the  $\beta$ -ring in the 1,6-biradical. The remaining factor of nine is due to the conformational effect, i.e. changes of  $X(r)$ . Molecular mechanics calculations indicate that  $\beta$ -(*o*-tolyl)isobutyrophenone 19 has two conformations with different orientations of the tolyl group, 19A and 19A' (Figure 69). Conformation 19A can undergo the  $\epsilon$ -hydrogen abstraction directly, but conformation 19A' has to rotate to 19A in order to react. The calculations also suggest that conformation 19A' is the more stable one of the two conformations, which are in an excited state equilibrium prior to the reaction. The reaction rate is proportional to the population of 19A. With  $\beta$ -mesitylisobutyrophenone 21, there is only one possible arrangement concerning the orientation of the mesityl group, 21A, which makes the reacting conformation for the ketone. The population of the reacting conformer is thus enhanced, and so are the  $k$  and quantum yield of product formation. If it is assumed that the replacement of a *o*-tolyl group by a mesityl group does not alter the relative population of other unconcerned conformers, the following equations can be used to estimate the relative concentration of conformation 19A and 19A', where  $K$  is the equilibrium constant between the two conformations,



$$[19A] + [19A'] = [21A] \quad (30)$$

$$[21A] = 9x[19A] \quad (31)$$

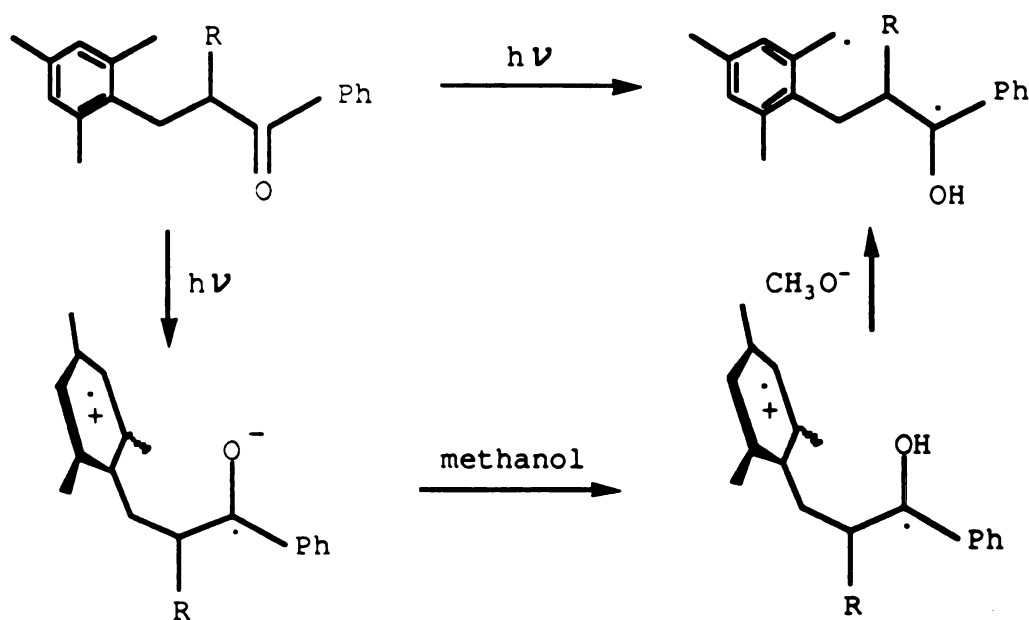
$$\text{so, } [19A'] = 8x[19A] \text{ or } K = [19A']/[19A] = 8 \quad (32)$$

The quantum yields for the product formation increase ca. 5 times in protic solvents such as methanol. Wagner<sup>27c</sup> has reported a solvent specific photoreaction from  $\beta$ -naphthyl  $\gamma$ -dimethylaminopropyl ketone. The most significant aspect of the photochemistry of this ketone is that methanol allows the lowest triplet to react with a moderate efficiency. In all the solvents, a charge transfer complex is formed immediately upon irradiation, but only in methanol, the complex rearranges to the 1,4-biradical. The biradical is formed with the help of an external protonation of the partially negative oxygen from methanol.

Our studies of  $\beta$ -arylpropiophenones reveal similar acid-catalysis in the reaction. The fact that dioxane does not enhance the quantum yields eliminates the possibility that methanol makes the reaction more efficient by preventing the reverse hydrogen transfer from occurring, because dioxane is known to have the same capability. The enhancement of product formation in methanol therefore has to arise from a different mechanism. The most likely alternative is that a proton transfer in the charge transfer complex can occur in methanol to generate the same biradical as what is given by a direct hydrogen atom transfer from a ketone triplet.<sup>65,101</sup> However, since acetonitrile does not affect the quantum yields, it can not be a simple proton transfer through a charge-separated geometry or a solvated radical-ion pair dissociated from the complex, which can be stabilized by methanol. Instead,



protonation of the negative oxygen in the complex by methanol must be responsible. So it is concluded that direct  $\epsilon$ -hydrogen abstraction competes with the charge transfer quenching of the triplet excited ketones in all the solvents, and in methanol, a good portion of the biradical is formed from the charge transfer complex via an external protonation of the oxygen in the complex by methanol (Scheme 37).



Scheme 37

### III. Derivation of Equation (25)



### Derivation of Stern-Volmer Equation for $\alpha$ -Mesitylvalerophenone 6

Let  $A=[6G]$ ,  $B=[6E]$ ,

$$\Phi^0 = k_{\delta} A / (k_d' A + k_{\delta} A + k_d B + k_{ct} B)$$

From steady state assumption,

$$k_i A + X(6E)I = k_{-i} B + k_d B + k_{ct} B$$

$$I = k_d' A + k_{\delta} A + k_d B + k_{ct} B, \quad I = \text{amount of light absorbed}$$

$$\text{So, } k_i A + X(6E)(k_d' A + k_{\delta} A + k_d B + k_{ct} B) = k_{-i} B + k_d B + k_{ct} B$$

$$A = [k_{-i} B + (1 - X(6E))(k_d B + k_{ct} B)] / [k_i + X(6E)(k_d' + k_{\delta})]$$

$$\begin{aligned} \Phi^0 &= \{k_{\delta} [k_{-i} + (1 - X(6E))(k_d + k_{ct})] / [k_i + X(6E)(k_d' + k_{\delta})]\} \\ &\quad / \{(k_d' + k_{\delta}) [k_{-i} + (1 - X(6E))(k_d + k_{ct})] / [k_i + X(6E)(k_d' + k_{\delta}) + k_d + k_{ct}]\} \\ &= k_{\delta} [k_{-i} + (1 - X(6E))(k_d + k_{ct})] \\ &\quad / \{(k_d' + k_{\delta}) [k_{-i} + (1 - X(6E))(k_d + k_{ct})] + (k_d + k_{ct}) [k_i + X(6E)(k_d' + k_{\delta})]\} \end{aligned}$$

Let  $Q=[Q]$ ,

$$\Phi = k_{\delta} A / (k_d' A + k_{\delta} A + k_q Q A + k_d B + k_{ct} B + k_q Q B)$$

From steady state assumption,

$$k_i A + X(6E)I = k_{-i} B + k_d B + k_{ct} B + k_q Q B$$

$$I = k_d' A + k_{\delta} A + k_q Q A + k_d B + k_{ct} B + k_q Q B$$

$$k_i A + X(6E)(k_d' A + k_{\delta} A + k_q Q A + k_d B + k_{ct} B + k_q Q B)$$

$$= k_{-i} B + k_d B + k_{ct} B + k_q Q B$$

$$A = [k_{-i} B + (1 - X(6E))(k_d B + k_{ct} B) + (1 - X(6E))k_q Q B] / [k_i + X(6E)(k_d' + k_{\delta} + k_q Q)]$$

$$\begin{aligned} \Phi &= \{k_{\delta} [k_{-i} + (1 - X(6E))(k_d + k_{ct}) + (1 - X(6E))k_q Q] / [k_i + X(6E)(k_d' + k_{\delta} + k_q Q)]\} \\ &\quad / \{(k_d' + k_{\delta} + k_q Q) [k_{-i} + (1 - X(6E))(k_d + k_{ct}) + (1 - X(6E))k_q Q] / [k_i + X(6E)(k_d' + k_{\delta} + k_q Q)] \\ &\quad + k_d + k_{ct} + k_q\} \end{aligned}$$

Simplify the expression for  $\Phi$



$$\Phi = \{k_{\delta}[k_{-i} + (1 - X(6E))(k_d + k_{ct})] + (k_{\delta} - X(6E)k_{\delta})k_q Q\} / \{(k_d' + k_{\delta})[k_{-i} + (1 - X(6E))(k_d + k_{ct})] + (k_d + k_{ct})[k_i + X(6E)(k_d' + k_{\delta})] + (k_d' + k_{\delta} + k_i + k_{ct} + k_d + k_{-i})k_q Q + k_q^2 Q^2\}$$

Divide  $\Phi^0$  by  $\Phi$ , and simplify the equation obtained,

$$\Phi^0 / \Phi = (1 + A[Q] + B[Q]^2) / (1 + C[Q])$$

$$A = k_q L / M, \quad B = k_q^2 / M, \quad C = k_q (k_{\delta} - X(6E)k_{\delta}) / N$$

$$L = k_d' + k_{\delta} + k_{-i} + k_d + k_{ct} + k_i$$

$$M = k_{-i}k_{\delta} + k_{ct}k_{\delta} + k_dk_{\delta} + k_{-i}k_d' + k_{ct}k_d' + k_dk_d' + k_i k_c + k_i k_d$$

$$N = k_{-i}k_{\delta} + k_c k_{\delta} + k_d k_{\delta} - X(6E)k_c k_{\delta} - X(6E)k_d k_{\delta} + k_i k_d$$



## Experimental

### I. Purification of Chemicals

#### A. Solvents and Additives

**Benzene**<sup>103</sup> - One gallon of reagent grade benzene was repeatedly stirred with 200 ml portions of sulfuric acid for 12-24 hr periods until the sulfuric acid remained water white. The benzene and the sulfuric acid were separated and the benzene was washed with distilled water and then saturated aqueous sodium bicarbonate solution. The benzene was separated, dried over sodium sulfate and filtered into a 5 l round bottom flask. Phosphorus pentoxide (100 g) was added and the solution was refluxed overnight. After refluxing, the benzene was distilled through a one meter column packed with stainless steel helices. The first and last 10% were discarded.

**t-Butyl Alcohol**<sup>104</sup> - Reagent grade t-butyl alcohol (Baker) was refluxed over sodium for 12 hr and distilled through a half meter column packed with glass helices.

**Dioxane**<sup>105</sup> - AR grade 1,4-dioxane (Mallinkrodt) was refluxed over lithium aluminum hydride and distilled through a half meter column packed with glass helices.

**Acetonitrile**<sup>106</sup> - Reagent grade acetonitrile (EM Science) was purified by keepyung Nahm.

**Hexane** - Reagent grade hexane (Baker) was purified the same way as benzene.

**Methanol**<sup>107</sup> - Reagent grade absolute methanol (Baker) was refluxed over magnesium turning for 2 hr and distilled through a half meter column



packed with glass helices. The first and last 10% was discarded.

**Cyclohexane** - Spectral grade cyclohexane (Mallinkrodt) was used as received.

**Pyridine**<sup>43a</sup> - Pyridine (EM Science) was refluxed over barium oxide for 12 hr and distilled through a half meter column packed with glass helices. The first and last 10% was discarded.

## **B. Internal Standards**

**Pentadecane** - Pentadecane (Columbia Organics) was washed with sulfuric acid and distilled by Dr. Peter J. Wagner.

**Hexadecane** - Hexadecane (Aldrich) was purified by washing with sulfuric acid, followed by distillation, by Dr. Peter J. Wagner.

**Heptadecane** - Heptadecane (Chemical Samples Company) was purified by washing with sulfuric acid, then distilled by Dr. Peter J. Wagner.

**Nonadecane** - Nonadecane (Chemical Samples Company) was recrystallized from ethanol.

**Eicosane** - Eicosane (Aldrich) was purified by recrystallization from ethanol

## **C. Quenchers**

**2,5-Dimethyl-2,4-hexadiene** - 2,5-Dimethyl-2,4-hexadiene (Aldrich) was allowed to sublime in the refrigerator.

**cis-Stilbene** - cis-Stilbene (Aldrich) was used as received.

**Naphthalene** - Naphthalene (Matheson Coleman & Bell) was recrystallized from methanol.



red

II.

gls

wa

wa

so:

hr

for

ov

py

ap

dr

**B.**

m.

vo

Int



**1,3-Pentadiene** - 1,3-Pentadiene (Aldrich) was used as received.

**n-Dodecylmercaptan** - n-Dodecylmercaptan (Aldrich) was distilled at reduced pressure.

## **II. Equipment and Procedures**

### **A. Photochemical Glassware**

All volumetric glassware (pipettes and volumetric flasks) used were glsee A type. This glassware was rinsed with acetone, then with distilled water, and boiled in a solution of Alconox laboratory detergent in distilled water for 12 hr. The glassware was carefully rinsed with distilled water, and soaked in distilled water for two days, with the water being changed every 12 hr. This procedure was also used to clean the syringes and the pyrex test tubes for irradiations. After final distilled water rinse, the glassware was dried in an oven at 140°C.

Ampoules used for irradiations were made by heating 13 x 100 mm pyrex test tubes (previously cleaned by the procedure described above) approximately 2 cm from the top with an oxygen-natural gas torch and drawing them out to a uniform 15 cm length.

### **B. Sample Preparations**

All solutions were prepared either by directly weighing the desired material into volumetric flasks or by dilution of a stock solution. Equal volumes (2.8 ml) of sample were placed via syringes into each ampoule. Internal standards used for GC and HPLC analyses were weighed directly into



the ketone starting material.

### C. Degassing Procedure

Filled irradiation tubes were attached to a vacuum line with a diffusion pump. These tubes were arranged on a circular manifold equipped with twelve vacuum stopcocks each fitted with size 00 one-hole rubber stoppers. The sample tubes were frozen to liquid nitrogen temperature and evacuated for 5-10 min. The vacuum was removed and the tubes were allowed to thaw at room temperature. This freeze-pump-thaw cycle was repeated three times. The tubes were then sealed with an oxygen-natural gas torch while still under vacuum.

### D. Irradiation Procedure

All samples for kinetic measurements were irradiated in parallel with actinometer solutions in a Merry-Go-Round apparatus immersed in a water bath at approximately 25°C. A water cooled Hanovia medium pressure mercury lamp was used as the irradiation source. An alkaline potassium chromate solution (0.002 M  $K_2CrO_4$  in 1% aqueous potassium carbonate) was used to isolate the 313 nm emission band. A Corning CS 7-37 Filter was used for 365 nm emission band.

Preparative scale photolyses were performed using a Hanovia 450-watt medium pressure lamp filtered through a pyrex tube. Ketones were dissolved with the chosen solvent in a 500 ml photochemical reaction vessel. A quartz cooling jacket was inserted. The sample was irradiated at room temperature under a steady stream of argon.



Irradiation in solid state has been conducted in powder form or crystal. The detailed description of the methods was given later along with the product identification in solid state.

#### **E. Analysis Procedures**

All gas chromatographic analyses were performed on a Varian Aerograph 1400, or 3400 Gas Chromatogram equipped with a flame ionization detector. Model 1400 Gas chromatograms were connected to either a Hewlett-Packard 3393A, or 3392A Integrating Recorder.

Four types of columns have been used for gas chromatograms.

Column # 1 - 5% SE-30 on Chromsorb G, 3 meter in length

Column # 2 - Magabore DB1, 15 meter in length

Column # 3 - Magabore DB210, 15 meter in length

Column # 4 - Magabore DBWAX, 30 meter in length

Analyses by HPLC were performed on a Beckman 332 Gradient Liquid Chromatograph System equipped with a Perkin-Elmer LC-75 Ultraviolet-Visible Detector and a DuPont 860 Column Compartment. An Altex Ultrasphere Si Absorption Phase column was used. The HPLC system was connected to a Hewlett-Packard 6080 Integrating Recorder.

#### **F. Calculation of Quantum Yields**

Quantum yields were calculated with the following equation,



$$\Phi = [P]/I \quad (33)$$

where [P] is the concentration of products and I is the intensity of light absorbed by samples.

The intensity of light was determined by valerophenone or o-methylvalerophenone actinometry. Thus a degassed 0.10 M valerophenone or o-methylvalerophenone solution was irradiated in parallel with the samples to be analysed. Upon completion of the irradiation the valerophenone or o-methylvalerophenone sample was analysed for acetophenone or o-methylacetophenone, using the following equations,

$$[AP] = R_f[Std]A_{AP}/A_{Std} \quad (34)$$

$$\text{or } [MAP] = R_f'[Std]A_{MAP}/A_{Std} \quad (35)$$

where [AP] is the concentration of acetophenone,  $R_f$  is the instrument response factor for acetophenone,  $A_{AP}$  is the integrated area for acetophenone, [MAP] is the concentration of o-methylacetophenone,  $R_f'$  is the instrument response factor for o-methylacetophenone,  $A_{MAP}$  is the integrated area for o-methylacetophenone, [Std] is the concentration of the added internal standard, and  $A_{Std}$  is the integrated area for the internal standard.

The intensity of light absorbed by each sample, in ein l<sup>-1</sup>, can be calculated from the acetophenone or o-methylacetophenone concentration knowing that  $\Phi$  is 0.33<sup>108</sup> for acetophenone, and 0.016<sup>43a</sup> for o-methylacetophenone,



$$I = [AP]/0.33 \quad (36)$$

$$\text{or } I = [MAP]/0.016 \quad (37)$$

The response factors for each photoproduct on GC or HPLC were obtained by the following equation,

$$R_f = (\text{Moles}_{\text{Photo}}/\text{Moles}_{\text{Std}})(A_{\text{Std}}/A_{\text{Photo}}) \quad (38)$$

These response factors are presented in Appendix.

#### **G. Methods Used for Product Isolation**

All the photoproducts were isolated either with a Varian Aerograph 900 Gas Chromatogram equipped with a 20% SE-30 column and a thermal conductivity detector or a ANALTECH preparative thin layer silica gel plate.

#### **H. Spectroscopic Measurements**

$^1\text{H}$  NMR spectra were recorded on either a Varian T-60 or a Bruker WM-250 Fourier Transform Spectrometer.  $^{13}\text{C}$  NMR spectra were recorded on the Bruker WM-250 instrument. Infrared spectra were recorded on a Perkin-Elmer 599 IR Spectrometer. Ultraviolet-visible spectra were recorded on either a Varian Carey 219 or a Shimadzu UV-160 Spectrometer. Mass spectra were recorded on a Finnigan 4000 GC/MS. Phosphorescence spectra were recorded on a Perkin-Elmer MPF-44A Fluorescence Spectrometer.



### III. Preparation of Starting Ketones

**$\alpha$ -(o-Tolyl)-p-Methoxyacetophenone<sup>108</sup>** -  $\alpha$ -(o-Tolyl)acetic acid (Aldrich, 12.0 g, 0.080 mole) in phosphorus trichloride (MC/B, 11.4 g, 0.083 mole) was heated at 70-80°C for 2 hr. The mixture was cooled and mixed with anisole (60 ml). The resulting solution was added to anhydrous aluminium chloride (MCB, 11.4 g, 0.085 mole) in anisole (30 ml) at 0°C. The mixture was stirred at r.t. for 15 min until all the aluminium chloride had dissolved and then heated at 75°C for 2 hr. After cooling, it was poured into iced aqueous hydrochloric acid (38%). The aqueous phase was separated and extracted with a mixture of benzene and ether (1:1, 2x150 ml). The extracts were washed with saturated sodium bicarbonate solution and distilled water, and dried over sodium sulfate. The solvent was evaporated. The crude product was recrystallized from ethanol to give the pure product as colorless crystal (10.8 g, 56.3% yield). m.p. 76.0-77.2°C

<sup>1</sup>H NMR (250 MHz, CDCl<sub>3</sub>) 2.27 (s, 3H, ArCH<sub>3</sub>), 3.87 (s, 3H, OCH<sub>3</sub>), 4.26 (s, 2H, ArCH<sub>2</sub>), 6.84-8.07 (m, 8H, ArH)

<sup>13</sup>C NMR (250 MHz, CDCl<sub>3</sub>) 19.69, 43.02, 55.34, 113.70, 125.96, 126.98, 129.85, 130.12, 130.20, 130.53, 133.78, 136.87, 163.43, 195.95

MS 240 (M<sup>+</sup>), 135 (base), 105, 91, 77

IR (CCl<sub>4</sub>) 3080-2860, 1685 (C=O), 1605, 1512, 1465, 1262, 1170

**$\alpha$ -(o-Tolyl)propiophenone<sup>109</sup>** - A solution of  $\alpha$ -(o-tolyl)acetophenone (10.0 g, 0.048 mole) in dry toluene (40ml) was added to a suspension of sodium hydride (Aldrich, 80% dispersion in mineral oil, 1.4 g, 0.047 mole) in dry toluene (120 ml), and the mixture was refluxed for 1 hr. The solution was cooled, and methyl iodide (Baker, 20.0 g, 0.142 mole) was introduced at 25°C.



The mixture was refluxed for 12 hr, then cooled and filtered. The filtrate was diluted with ether (150 ml), then washed with distilled water, and dried over sodium sulfate. The solvent was evaporated. Distillation of the residue gave the ketone, which was then recrystallized from ethanol as colorless crystal (6.2 g, 58.1% yield). m.p. 46.5-47.5°C.

$^1\text{H}$  NMR (250 MHz,  $\text{CDCl}_3$ ) 1.48 (d,  $J=7.3$  Hz, 3H,  $\text{ArCHCH}_3$ ), 2.50 (s, 3H,  $\text{ArCH}_3$ ), 4.76 (q,  $J=7.3$  Hz, 1H,  $\text{ArCHCH}_3$ ), 7.05-7.85 (m, 9H, ArH)

$^{13}\text{C}$  NMR (250 MHz,  $\text{CDCl}_3$ ) 17.72, 19.22, 44.21, 126.44, 126.57, 128.14, 128.20, 130.68, 132.29, 134.21, 136.25, 136.61, 139.87, 200.42

MS 224 ( $\text{M}^+$ ), 119, 105 (base), 91, 77

IR ( $\text{CCl}_4$ ) 3080-2860, 1693 ( $\text{C}=\text{O}$ ), 1603, 1498, 1453, 1335, 1230

$\alpha$ -(*o*-Tolyl)valerophenone -  $\alpha$ -(*o*-Tolyl)acetophenone (7.0 g, 0.033 mole) in dry toluene (30 ml) was added to a suspension of sodium hydride (Aldrich, 80% dispersion in mineral oil, 1.0 g, 0.033 mole) in dry toluene (80 ml), and the mixture was refluxed for 1 hr. The solution was cooled, and propyl bromide (Baker, 8.1 g, 0.066 mole) was introduced at 25°C. The mixture was refluxed for 24 hr, then cooled and filtered. The filtrate was diluted with ether (150 ml), then washed with distilled water, and dried over sodium sulfate. The solvent was evaporated. The crude product was purified by column chromatography with 40% benzene in hexane as eluent. The same purification procedure was repeated two more times to obtain the product as colorless liquid (4.0 g, 48.1% yield).

$^1\text{H}$  NMR (250 MHz,  $\text{CDCl}_3$ ) 0.94 (t,  $J=7.7$  Hz, 3H,  $(\text{CH}_2)_2\text{CH}_3$ ), 1.23-2.09 (m, 4H,  $(\text{CH}_2)_2\text{CH}_3$ ), 2.01 (s, 3H,  $\text{ArCH}_3$ ), 4.42 (dd,  $J^1=7.8$  Hz,  $J^2=5.7$  Hz, 1H,  $\text{ArCHPr}$ ), 7.07-7.86 (m, 9H, ArH)

$^{13}\text{C}$  NMR (250 MHz,  $\text{CDCl}_3$ ) 14.02, 19.60, 20.95, 35.65, 49.25, 126.37, 126.57,



126.96, 128.05, 128.22, 130.69, 132.36, 134.70, 137.12, 138.37, 200.17

MS 252 ( $M^+$ ), 210, 147, 131, 117, 105 (base), 91, 77

IR 3065-2875, 1690 (C=O), 1603, 1495, 1455, 1252, 1230

**$\alpha$ -(o-Tolyl)isobutyrophenone** - Potassium (6.0 g, 0.154 mole) was dissolved in dry t-butyl alcohol (Baker, 150 ml).  $\alpha$ -(o-Tolyl)acetophenone (7.0 g, 0.033 ml) was added as solid. The mixture was refluxed for 4 hr. Methyl iodide (Baker, 6.8 g, 0.048 mole) was added at r.t.. The content was refluxed for 8 hr. Second portion of methyl iodide (6.8 g, 0.048 mole) was introduced after cooling, and it was refluxed for another 4 hr. The mixture was filtered at r.t., and the filtrate was diluted with ether (150 ml), washed with distilled water, and dried over sodium sulfate. After evaporation of solvent, the mixture of product and starting material was treated with sodium hydride (Aldrich, 80% dispersion in mineral oil, 1.0 g, 0.033 mole) and methyl iodide (6.8 g, 0.048 mole) in toluene (140 ml) using the procedure described for the preparation of  $\alpha$ -(o-tolyl)propiophenone. The crude product was first distilled under vacuum, and then the portion collected at 106°/1 torr was purified several times by column chromatography with 20% benzene in hexane to afford the pure product as colorless liquid (1.5 g, 19% yield).

$^1\text{H}$  NMR (250 MHz,  $\text{CDCl}_3$ ) 1.67 (s, 6H,  $\text{ArC}(\text{CH}_3)_2$ ), 2.07 (s, 3H,  $\text{ArCH}_3$ ), 7.03-7.67 (m, 9H, ArH)

$^{13}\text{C}$  NMR (250 MHz,  $\text{CDCl}_3$ ) 20.33, 27.51, 51.44, 124.45, 126.59, 126.76, 127.79, 129.09, 132.01, 132.12, 135.46, 135.90, 143.85, 203.90

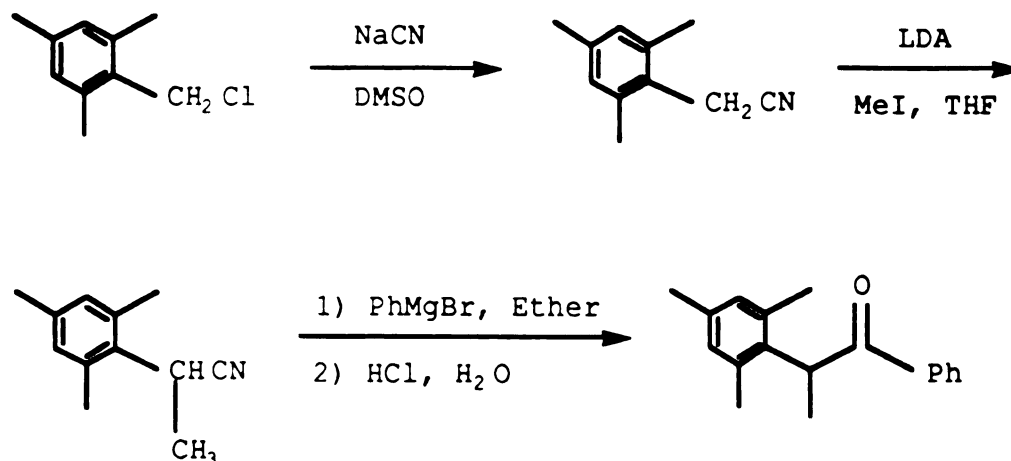
MS 238 ( $M^+$ ), 223, 133, 115, 105 (base), 91, 77

IR 3080-2885, 1692 (C=O), 1605, 1475, 1458, 1250, 1175

**$\alpha$ -Mesitylpropiophenone**



$\alpha$ -Mesitylpropionophenone was prepared by the reaction of phenyl magnesium bromide with  $\alpha$ -mesitylpropionitrile following the route given below.



$\alpha$ -Mesitylacetonitrile - A mixture of sodium cyanide (Fisher, 8.7 g, 0.189 mole) and dimethyl sulfoxide (100 ml) was heated at 80°C until all of the sodium cyanide had dissolved. 2,4,6-Trimethylbenzyl chloride (Aldrich, 20.0 g, 0.119 mole) was added to this solution. The mixture was stirred at this temperature overnight. It was then cooled to r.t. and poured into distilled water (300 ml). The resulting solution was extracted with ether (2x150 ml). The ether layers were combined, washed with distilled water, and dried over sodium sulfate. The solvent was removed to afford  $\alpha$ -mesitylacetonitrile as a brown solid (17.4 g, 92% yield). The crude product was used without further purification.

<sup>1</sup>H NMR (60 MHz, CDCl<sub>3</sub>) 2.30 (s, 3H), 2.38 (s, 6H), 3.60 (s, 2H), 6.92 (s, 2H)

$\alpha$ -Mesitylpropionitrile - Diisopropylamine (Aldrich, 10.8 g, 0.107 mole) in dry THF (70 ml) was added to n-butyl lithium (Aldrich, 2.5 M in hexane, 45



ml, 0.115 mole) at 0°C. The mixture was stirred for 15 min, and then cooled to -78°C with a dry-ice/acetone bath.<sup>110</sup>  $\alpha$ -Mesitylacetonitrile (17.4 g, 0.109 mole) in dry THF (140 ml) was added. The content was warmed to r.t., and stirred for 2 hr. Methyl iodide (baker, 16.9 g, 0.119 mole) was added. The mixture was stirred at r.t. for another 2 hr, and then refluxed overnight. The solution was cooled and the solvent was removed. Ether (150 ml) and distilled water (150 ml) was added to the residue, and then separated. The aqueous phase was extracted with ether (2x150 ml). The combined ether layers were washed with distilled water, dried over sodium sulfate. Evaporation of the solvent gave the product as a brown liquid (18.2 g, 97% yield), which was used without further purification.

<sup>1</sup>H NMR (60 MHz, CDCl<sub>3</sub>) 1.55 (d, 3H), 2.25 (s, 3H), 2.42 (s, 6H), 4.23 (q, 1H), 6.83 (s, 2H)

$\alpha$ -Mesitylpropiophenone - Bromobenzene (Fisher, 17.3 g, 0.110 mole) in anhydrous ether (100 ml) was added to magnesium shavings (MC/B, 10.0 g, 0.411 mole) in anhydrous ether (50 ml) activated with small amount of 1,2-dibromoethane under nitrogen atmosphere at r.t.. The mixture was refluxed for 3 hr.  $\alpha$ -Mesitylpropionitrile (18.2 g, 0.105 mole) in anhydrous ether (150 ml) was added. The mixture was refluxed overnight, and then cooled. The solid was collected by filtration, to which aqueous hydrochloric acid (19%) was added. The solution was refluxed for 10 hr. After cooling, it was extracted with ether (2x200 ml). The ether extracts were combined, washed with saturated aqueous sodium bicarbonate solution and dried over sodium sulfate. The ether was removed to give a dark brown solid. The crude product was chromatographed on silica gel using 40% benzene in hexane as the eluent, and then recrystallized from ethanol (10.2 g, 39% yield). m.p. 76.5-77.5°C.



**$^1\text{H}$  NMR (250 MHz,  $\text{CDCl}_3$ )** 1.48 (d,  $J=7.3$  Hz, 3H,  $\text{ArCHCH}_3$ ), 2.11 (s, 3H, p-Mes- $\text{CH}_3$ ), 2.16 (s, 6H, o-Mes- $\text{CH}_3$ ), 4.50 (q,  $J=7.3$  Hz, 1H,  $\text{ArCHCH}_3$ ), 6.78-7.73 (m, 7H, ArH)

**$^{13}\text{C}$  NMR (250 MHz,  $\text{CDCl}_3$ )** 14.96, 20.36, 20.63, 45.74, 128.14, 130.23, 132.34, 135.32, 136.00, 136.79, 202.30

**MS** 252 ( $\text{M}^+$ ), 147 (base), 105, 91, 77

**IR ( $\text{CCl}_4$ )** 3100-2890, 1693 ( $\text{C}=\text{O}$ ), 1602, 1488, 1455, 1325, 1230, 1187

### **$\alpha$ -Mesitylvalerophenone**

$\alpha$ -Mesitylvalerophenone was prepared by the reaction of phenyl magnesium bromide with  $\alpha$ -Mesitylvaleronitrile.

**$\alpha$ -Mesitylvaleronitrile** -  $\alpha$ -Mesitylvaleronitrile was synthesized by alkylation of  $\alpha$ -mesitylacetonitrile with propyl bromide (Aldrich) following the same procedure described for  $\alpha$ -mesitylpropionitrile. The crude product (90% yield) was used for the next reaction without further purification.

**$^1\text{H}$  NMR (60 MHz,  $\text{CDCl}_3$ )** 1.02 (t, 3H), 1.37-2.14 (m, 4H), 2.26 (s, 3H), 2.42 (s, 6H), 4.14 (dd, 1H), 6.87 (s, 2H)

**$\alpha$ -Mesitylvalerophenone** - This ketone was prepared by the reaction of phenyl magnesium bromide with  $\alpha$ -mesitylvaleronitrile following the same procedure described for  $\alpha$ -mesitylpropiophenone. The crude product was purified by chromatography with 30% benzene in hexane, and then recrystallized from ethanol as white crystal (45% yield). m.p. 61.8-63.0°C.

**$^1\text{H}$  NMR (250 MHz,  $\text{CDCl}_3$ )** 0.97 (t,  $J=7.3$  Hz, 3H,  $(\text{CH}_2)_2\text{CH}_3$ ), 1.25-2.54 (m, 4H,  $(\text{CH}_2)_2\text{CH}_3$ ), 2.19 (s, 3H, p-Mes- $\text{CH}_3$ ), 2.28 (s, 6H, o-Mes- $\text{CH}_3$ ), 4.42 (dd,  $J^1=7.3$  Hz,  $J^2=4.7$  Hz, 1H,  $\text{ArCHPr}$ ), 6.78-7.76 (m, 7H, ArH)

**$^{13}\text{C}$  NMR (250 MHz,  $\text{CDCl}_3$ )** 14.40, 20.61, 20.79, 21.45, 32.66, 50.97, 128.04,



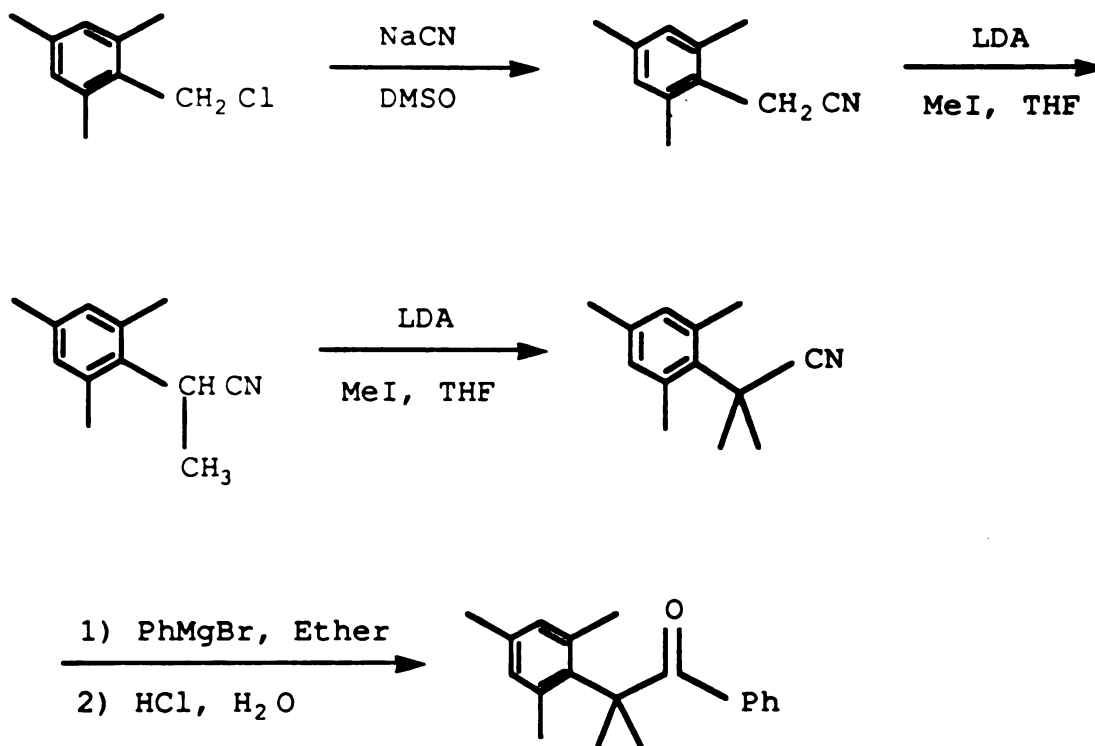
128.14, 130.27, 130.32, 132.20, 135.84, 135.89, 137.56, 201.58

MS 280 ( $M^+$ ), 175, 133 (base), 105, 91, 77

IR ( $CCl_4$ ) 3060-2875, 1689 (C=O), 1602, 1485, 1453, 1253, 1215

### $\alpha$ -Mesitylisobutyrophenone

$\alpha$ -Mesitylisobutyrophenone was prepared by the reaction of phenyl magnesium bromide with  $\alpha$ -mesitylisobutyronitrile following the route given below.



$\alpha$ -Mesitylisobutyronitrile - Diisopropylamine (Aldrich, 12.3 g, 0.122 mole) in dry THF (80 ml) was added to n-butyl lithium (Aldrich, 2.5 M in hexane, 47 ml, 0.118 mole) at 0°C. The mixture was stirred for 15 min.  $\alpha$ -Mesitylpropionitrile (20.0 g, 0.115 mole) in dry THF (160 ml) was added



after it was cooled to  $-78^{\circ}\text{C}$  with a dry-ice/acetone bath. The content was warmed to r.t., and stirred for 2 hr. Methyl iodide (Baker, 16.5 g, 0.116 mole) was added and the mixture was stirred at r.t. for another 2 hr, and then refluxed overnight. The solution was cooled and the solvent was removed. Ether (150 ml) and distilled water (150 ml) was added to the residue, and then separated. The aqueous phase was extracted with ether (2x150 ml). The combined ether layers were washed with distilled water, dried over sodium sulfate. Evaporation of the solvent gave the product as a dark brown liquid (21.0 g, 90.5% yield), which was used without further purification.

$^1\text{H}$  NMR (60 MHz,  $\text{CDCl}_3$ ) 1.94 (s, 6H), 2.28 (s, 3H), 2.56 (s, 6H), 6.86 (s, 2H)

$\alpha$ -Mesitylisobutyrophenone -  $\alpha$ -Mesitylisobutyrophenone was prepared by the reaction of phenyl magnesium bromide made in ether with  $\alpha$ -mesitylisobutyronitrile in benzene following the same procedure described for  $\alpha$ -mesitylpropiophenone. Hydrolysis with aqueous hydrochloric acid (19%) for 80 hr and normal work-up afforded the crude product, which was then purified by chromatography with 40% benzene in hexane and recrystallization from ethanol to give the pure ketone as white crystal (41.2% yield). m.p.  $64.5\text{--}66.0^{\circ}\text{C}$ .

$^1\text{H}$  NMR (250 MHz,  $\text{CDCl}_3$ ) 1.72 (s, 6H,  $\text{ArC}(\text{CH}_3)_2$ ), 2.23 (s, 3H, p-Mes- $\text{CH}_3$ ), 2.30 (s, 6H, o-Mes- $\text{CH}_3$ ), 6.77-7.74 (m, 7H, ArH)

$^{13}\text{C}$  NMR (250 MHz,  $\text{CDCl}_3$ ) 20.30, 23.60, 28.29, 53.28, 127.87, 129.38, 132.07, 132.12, 135.38, 135.55, 135.95, 139.37, 203.95

MS 266( $\text{M}^+$ ), 251, 236, 161 (base), 133, 121, 105, 91, 77

IR ( $\text{CCl}_4$ ) 3070-2870, 1686 ( $\text{C}=\text{O}$ ), 1600, 1480, 1455, 1245, 1166

$\alpha$ -Mesityl- $\alpha$ -Phenylacetophenone<sup>111</sup> - Desyl chloride (Aldrich, 10.0 g, 0.043 mole) in mesitylene (Aldrich, 30 ml) was added to anhydrous



aluminum chloride (MCB, 9.0 g, 0.067 mole) in mesitylene (10 ml). The mixture was heated at 45-50°C for 4 hr, and then poured into iced aqueous hydrochloric acid (38%) after being cooled. The aqueous phase was extracted with ether. The extracts were washed with saturated sodium bicarbonate solution and dried over sodium sulfate. After evaporation of the solvent, the crude product was recrystallized from ethanol to give pure colorless crystal (7.3 g, 53.4% yield). m.p. 112.5-113.5°C.

<sup>1</sup>H NMR (250 MHz, CDCl<sub>3</sub>) 2.19 (s, 6H, o-Mes-CH<sub>3</sub>), 2.28 (s, 3H, p-Mes-CH<sub>3</sub>), 5.99 (s, 1H, ArHPh), 6.89-7.93 (m, 12H, ArH)

<sup>13</sup>C NMR (250 MHz, CDCl<sub>3</sub>) 20.63, 21.05, 56.62, 126.55, 127.99, 128.19, 128.57, 129.30, 130.20, 132.54, 133.22, 136.66, 136.84, 137.00, 137.08, 199.63

MS 314(M<sup>+</sup>), 209 (base), 105, 91, 77

IR (CCl<sub>4</sub>) 3090-2860, 1697 (C=O), 1603, 1500, 1452, 1210

### **α-Mesityl-α-Phenyl-p-Cyanoacetophenone**

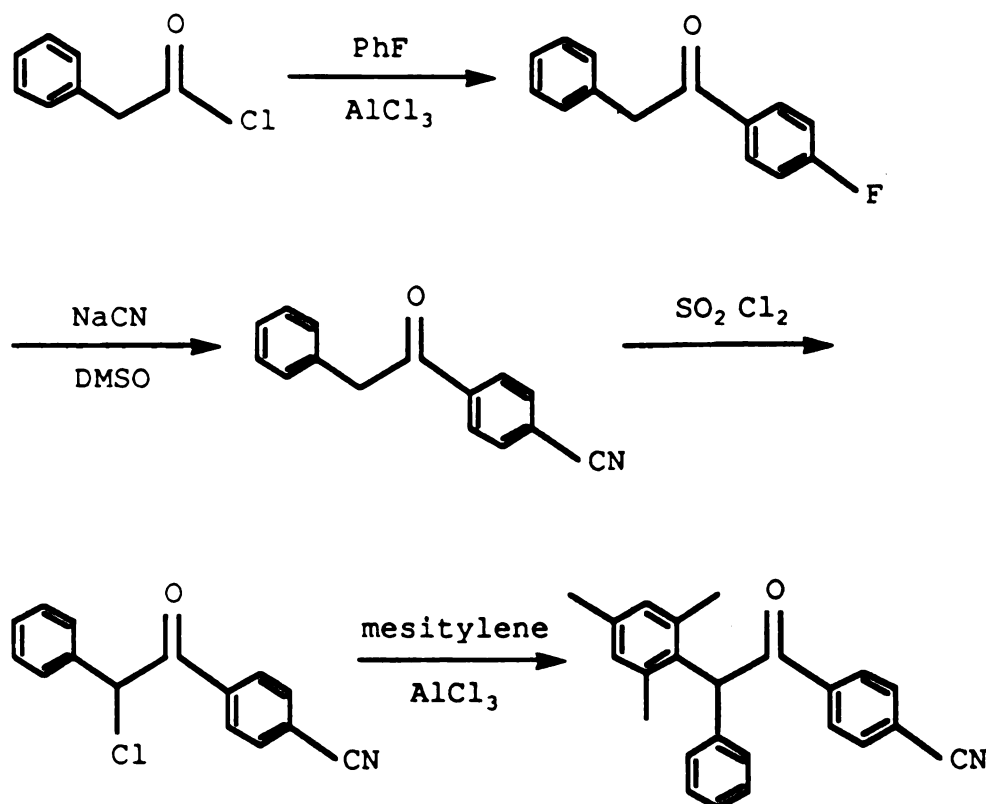
α-Mesityl-α-phenyl-p-cyanoacetophenone was prepared by the reaction of α-chloro-α-phenyl-p-cyanoacetophenone with mesitylene following the route given below.

α-Phenyl-p-Fluoroacetophenone - α-Phenylacetic acid (Aldrich, 25.0 g, 0.184 mole) in phosphorus trichloride (MC/B, 40.0 g, 0.291 mole) was heated at 70-80°C for 3 hr. Excess phosphorus trichloride was distilled. The residue was mixed with fluorobenzene (Aldrich, 80 ml), and was added to aluminium chloride in (MCB, 33.0 g, 0.246 mole) in fluorobenzene (80 ml). The mixture was stirred for 2 hr at r.t. and then heated at 50-60°C for 3 hr. The reaction mixture was poured over ice after cooling. The aqueous phase was extracted with ether (2x200 ml). The extracts were washed with saturated



sodium bicarbonate solution and dried over sodium sulfate. The solvent were evaporated. The crude product was used for the next reaction without further reaction (23 g, 58.4% yield).

$^1\text{H}$  NMR (60 MHz,  $\text{CDCl}_3$ ) 4.24 (s, 2H), 7.07-8.06 (m, 9H)



$\alpha$ -Phenyl-p-Cyanoacetophenone - Sodium cyanide (Fisher, 6.0 g, 0.122 mole) and dimethyl sulfoxide (100 ml) was heated at  $80^\circ\text{C}$  until all of the sodium cyanide had dissolved.  $\alpha$ -Phenyl-p-fluoroacetophenone (23 g, 0.107 mole) was added. The mixture was heated at  $120^\circ\text{C}$  overnight. After cooling, it was poured into distilled water (300 ml) The aqueous phase was extracted with ether (2x150 ml). The extracts were washed with distilled water, and dried over sodium sulfate. After the solvent was evaporated, the residue was distilled at reduced pressure to afford the product (7.0 g, 29.6% yield) as



yellowish solid.

$^1\text{H}$  NMR (60 MHz,  $\text{CDCl}_3$ ) 4.31 (s, 2H), 7.20-8.06 (m, 9H)

$\alpha$ -Chloro- $\alpha$ -Phenyl-*p*-Cyanoacetophenone<sup>112</sup> - Sulfuryl chloride (MC/B, 4.2 g, 0.031 mole) was added to well grounded  $\alpha$ -phenyl-*p*-cyanoacetophenone (6.0 g, 0.027 mole) at r.t.. The addition was slow enough not to warm up the mixture. The mixture was stirred at r.t. for 5 hr with a mechanic stirrer, and then dissolved in benzene (100 ml). The organic phase was washed with distilled water, and dried over sodium sulfate. The solvent was evaporated. The crude product, which contained 15% dichlorinated product, was used for the next reaction without further purification (7.0 g).

$^1\text{H}$  NMR (60 MHz,  $\text{CDCl}_3$ ) 6.25 (s, 1H), 7.35-8.06 (m, 9H)

$\alpha$ -Mesityl- $\alpha$ -Phenyl-*p*-Cyanoacetophenone -  $\alpha$ -Chloro- $\alpha$ -phenyl-*p*-cyanoacetophenone (7.0 g, crude) in mesitylene (Aldrich, 20 ml) was added to anhydrous aluminium chloride (MCB, 5.6 g, 0.042 mole) in mesitylene (8.0 ml). The mixture was heated at 50-60°C for 7 hr, and then poured into iced aqueous hydrochloric acid (38%) after being cooled. The aqueous phase was extracted with methylene chloride (2x100 ml). The extracts were washed with saturated sodium bicarbonate solution and dried over sodium sulfate. Evaporation of the solvent afforded a dark colored solid, which washed with hexane and ethanol. The crude product was recrystallized from a mixture of ethanol and chloroform to give the pure product (2.2 g). m.p. 159.0-160.0°C.

$^1\text{H}$  NMR (250 MHz,  $\text{CDCl}_3$ ) 2.17 (s, 6H, *o*-Mes- $\text{CH}_3$ ), 2.28 (s, 3H, *p*-Mes- $\text{CH}_3$ ), 5.90 (s, 1H, ArHPh), 6.88-7.90 (m, 11H, ArH)

$^{13}\text{C}$  NMR (250 MHz,  $\text{CDCl}_3$ ) 20.70, 21.00, 56.97, 115.74, 117.79, 126.97, 128.17, 128.58, 129.28, 130.46, 132.13, 135.82, 136.75, 137.34, 140.09, 198.60

MS 339 ( $\text{M}^+$ ), 209 (base), 130, 102, 91, 77

IR ( $\text{CCl}_4$ ) 3095-2870, 1700 (C=O), 2230 (CN), 1614, 1502, 1456, 1298, 1210



**$\alpha$ -Mesityl- $\alpha$ -Phenyl-p-Methoxyacetophenone**

$\alpha$ -Mesityl- $\alpha$ -phenyl-p-methoxyacetophenone was prepared from  $\alpha$ -mesityl- $\alpha$ -Phenylacetic acid and benzene.

$\alpha$ -Mesityl- $\alpha$ -Phenylacetic acid - Stannic chloride (Alfa, 68.5 g, 0.263 mole) was added slowly to a solution of mandelic acid (20.0 g, 0.131 mole) in mesitylene (Aldrich, 100 ml) at 65-70°C. The resulting solution was stirred for 6 hr at this temperature, and it was decomposed with ice water after cooling. The mixture was extracted with ether (3x300 ml). The extracts were washed with distilled water and dried over sodium sulfate. Evaporation of solvent afforded the crude product, which was then recrystallized from a mixture of hexane and chloroform (36.7 g, 54.9% yield).

<sup>1</sup>H NMR (60 MHz, CDCl<sub>3</sub>) 2.09 (s, 6H), 2.25 (s, 3H), 5.45 (s, 1H), 6.92-7.25 (m, ArH), 10.25 (s, 1H)

$\alpha$ -Mesityl- $\alpha$ -Phenyl-p-Methoxyacetophenone -  $\alpha$ -mesityl- $\alpha$ -Phenylacetic acid (5.0 g, 0.020 mole) in phosphorus trichloride (MC/B, 6.3 g, 0.046 mole) was heated at 70-80°C for 2 hr. The mixture was cooled and mixed with anisole (20 ml). The resulting solution was added to anhydrous aluminium chloride (MCB, 3.0 g, 0.022 mole) in anisole (5.0 ml) at 0°C. The mixture was heated at 75°C for 3 hr. After cooling, it was poured into iced aqueous hydrochloric acid (38%). The aqueous phase was separated and extracted with a mixture of benzene and ether (1:1, 2x150 ml). The extracts were washed with saturated sodium bicarbonate solution and distilled water, and dried over sodium sulfate. The solvent was evaporated. The crude product was purified by column chromatography with 7.5% ethyl acetate in hexane and recrystallization from ethanol (3.0 g, 47.8% yield). m.p. 96.4-98.5°C.

<sup>1</sup>H NMR (250 MHz, CDCl<sub>3</sub>) 2.18 (s, 6H, o-Mes-CH<sub>3</sub>), 2.27 (s, 3H, p-Mes-CH<sub>3</sub>),



3.80 (s, 3H, OCH<sub>3</sub>), 5.92 (s, 1H, ArCHPh), 6.80-7.84 (m, 11H, ArH)

**<sup>13</sup>C NMR (250 MHz, CDCl<sub>3</sub>)** 20.69, 21.12, 55.14, 56.44, 113.42, 126.49, 127.99, 129.35, 130.07, 130.20, 130.50, 133.67, 136.60, 136.91, 137.37, 162.97, 198.25

**MS** 344 (M<sup>+</sup>), 209, 135 (Base), 107, 91, 77

**IR (CCl<sub>4</sub>)** 3090-2840, 1690 (C=O), 1600, 1514, 1460, 1313, 1265, 1216, 1175

**α-Mesityl-α-Phenyl-2,4,6-Trimethylacetophenone** - α-Mesityl-α-phenylacetic acid (10.0 g, 0.037 mole) in phosphorus trichloride (MC/B, 15.7 g, 0.114 mole) was heated at 70-80°C for 3 hr. The mixture was cooled and mixed with mesitylene (Aldrich, 8 ml). The resulted solution was added to anhydrous aluminium chloride (MCB, 6.0 g, 0.045 mole) in a mixture of mesitylene (8.0 ml) and carbon disulfide (Mallinckrodt, 16 ml) at 0°C. The mixture was refluxed for 2 hr. After cooling, it was poured into iced aqueous hydrochloric acid (38%). The aqueous phase was separated and extracted with a mixture of benzene and ether (1:1, 2x150 ml). The extracts were washed with saturated sodium bicarbonate solution and distilled water, and dried over sodium sulfate. Evaporation of solvent, purification by column chromatography with 30% benzene in hexane, and recrystallization from ethanol and chloroform afforded the product as white crystal (5.7 g, 43.3% yield).

**m.p.** 161.0-162.0 °C

**<sup>1</sup>H NMR (250 MHz, CDCl<sub>3</sub>)** 1.93 (s, 12H, o-Mes-CH<sub>3</sub>), 2.27 (s, 6H, p-Mes-CH<sub>3</sub>), 5.98 (s, 1H, ArCHPh), 6.73 (s, 2H, ArH), 6.81 (s, 2H, ArH), 7.24-7.37 (m, 5H, ArH)

**<sup>13</sup>C NMR (250 MHz, CDCl<sub>3</sub>)** 18.42, 20.67, 20.93, 57.51, 126.14, 127.64, 128.22, 128.37, 129.26, 130.22, 133.70, 137.16, 138.22, 138.54, 139.45, 204.48

**MS** 356 (M<sup>+</sup>), 209, 147 (base), 119, 103, 91, 77



IR (CCl<sub>4</sub>) 3090-2860, 1705 (C=O), 1615, 1506, 1458, 1235, 1161

### **$\alpha$ -Mesityl-2,4,6-Trimethylacetophenone**

$\alpha$ -Mesityl-2,4,6-trimethylacetophenone was synthesized from  $\alpha$ -mesitylacetic acid and mesitylene.

$\alpha$ -Mesitylacetic acid<sup>113</sup> - A mixture of  $\alpha$ -mesitylacetonitrile (37.0 g, 0.172 mole) and potassium hydroxide (Baker, 27.0 g, 0.481 mole) in ethylene glycol (Baker, 340 ml) was heated at 155°C for 6 hr. After cooling, the solution was acidified with aqueous hydrochloric acid (38%). The solid was filtered, washed with distilled water, and recrystallized from acetone to afford the acid (23.6 g, 96.6% yield).

<sup>1</sup>H NMR (60 MHz, CDCl<sub>3</sub>) 2.22 (s, 3H), 2.28 (s, 6H), 3.64 (s, 2H), 6.82 (s, 2H)

$\alpha$ -Mesityl-2,4,6-Trimethylacetophenone<sup>114</sup> -  $\alpha$ -Mesitylacetic acid (10.0 g, 0.056 mole) in phosphorus trichloride (MC/B, 31.0 g, 0.226 mole) was heated at 70-80°C for 3 hr. The mixture was cooled and mixed with mesitylene (Aldrich, 5 ml). The resulting solution was added to anhydrous aluminium chloride (MCB, 12.5 g, 0.094 mole) in a mixture of mesitylene (15.0 ml) and carbon disulfide (Mallinckrodt, 20 ml) at 0°C. The mixture was refluxed for 15 hr. After cooling, it was poured into iced aqueous hydrochloric acid (38%). The aqueous phase was separated and extracted with a mixture of benzene and ether (1:1, 2x150 ml). The extracts were washed with saturated sodium bicarbonate solution and distilled water, and dried over sodium sulfate. Evaporation of solvent and recrystallization from methanol afforded the product as white crystal (8.5 g, 54.2% yield). m.p. 91.0-92.5°C.

<sup>1</sup>H NMR (250 MHz, CDCl<sub>3</sub>) 2.16 (s, 6H, o-Mes-CH<sub>3</sub>), 2.20 (s, 6H, o-Mes-CH<sub>3</sub>), 2.25 (s, 3H, p-Mes-CH<sub>3</sub>), 2.27 (s, 3H, p-Mes-CH<sub>3</sub>), 4.07 (s, 2H, ArCH<sub>2</sub>), 6.81 (s,



2H, ArH), 6.86 (s, 2H, ArH)

$^{13}\text{C}$  NMR (250 MHz,  $\text{CDCl}_3$ ) 19.11, 20.39, 20.76, 20.89, 45.89, 127.43, 128.44, 128.99, 132.67, 136.42, 137.22, 138.16, 139.40, 206.08

MS 280 ( $\text{M}^+$ ), 147 (base), 133, 119, 91, 77

IR ( $\text{CCl}_4$ ) 3010-2870, 1710 ( $\text{C}=\text{O}$ ), 1620, 1490, 1455, 1262

**$\alpha$ -Mesityl-o-Methylacetophenone** - o-Bromotoluene (Aldrich, 12.0 g, 0.070 mole) in anhydrous ether (100 ml) was added to magnesium shavings (MC/B, 6.8 g, 0.280 mole) in anhydrous ether (50 ml) activated with small amount of 1,2-dibromoethane under nitrogen atmosphere at r.t.. The mixture was refluxed for 3 hr.  $\alpha$ -Mesitylacetonitrile (11.0 g, 0.069 mole) in anhydrous ether (100 ml) was added. The mixture was refluxed overnight, and then cooled. The solid was collected by filtration, to which aqueous hydrochloric acid (19%) was added. The solution was refluxed for 10 hr. After cooling, it was extracted with ether (2x200 ml). The ether extracts were combined, washed with saturated aqueous sodium bicarbonate solution and dried over sodium sulfate. The ether was removed to give a dark brown solid. The crude product was chromatographed on silica gel using 30% benzene in hexane as the eluent, and then recrystallized from ethanol (6.5 g, 37.4% yield). m.p. 33.6-35°C.

$^1\text{H}$  NMR (250 MHz,  $\text{CDCl}_3$ ) 2.20 (s, 6H, o-Mes- $\text{CH}_3$ ), 2.28 (s, 3H,  $\text{ArCH}_3$ ), 2.47 (s, 3H,  $\text{ArCH}_3$ ), 4.26 (s, 2H,  $\text{ArCH}_2$ ), 6.92-7.80 (m, 6H, ArH)

$^{13}\text{C}$  NMR (250 MHz,  $\text{CDCl}_3$ ) 20.12, 20.79, 20.92, 42.23, 125.55, 127.82, 128.71, 129.15, 131.02, 131.78, 136.11, 136.58, 137.67, 138.27, 201.11

MS 252 ( $\text{M}^+$ ), 133, 119 (base), 105, 91, 77

IR ( $\text{CCl}_4$ ) 3100-2865, 1692 ( $\text{C}=\text{O}$ ), 1615, 1485, 1458, 1320, 1218



**$\alpha$ -Phenyl-2,4,6-Trimethylacetophenone -  $\alpha$ -Phenylacetic acid** (Aldrich, 10.0 g, 0.073 mole) in phosphorus trichloride (MC/B, 15.7 g, 0.114 mole) was heated at 70-80°C for 4 hr. The cooled mixture was mixed with mesitylene (Aldrich, 6 ml), and added to anhydrous aluminium chloride (MCB, 16.0 g, 0.120 mole) in a mixture of mesitylene (16.0 ml) and carbon disulfide (Mallinckrodt, 26 ml) at 0°C. The mixture was refluxed for 5 hr. After cooled, it was poured into iced aqueous hydrochloric acid (38%). The aqueous phase was separated and extracted with a mixture of benzene and ether (1:1, 2x150 ml). The extracts were washed with saturated sodium bicarbonate solution and distilled water, and dried over sodium sulfate. The solvent were evaporated. The crude product was purified by column chromatography with 30.0% benzene in hexane and recrystallization from methanol at -30°C (7.0 g, 40.2% yield).

<sup>1</sup>H NMR (250 MHz, CDCl<sub>3</sub>) 2.12 (s, 6H, o-Mes-CH<sub>3</sub>), 2.29 (s, 3H, p-Mes-CH<sub>3</sub>), 4.00 (s, 2H, ArCH<sub>2</sub>), 6.83-7.35 (m, 7H, ArH).

<sup>13</sup>C NMR (250 MHz, CDCl<sub>3</sub>) 18.98, 20.86, 51.57, 126.87, 128.32, 129.69, 132.55, 133.15, 138.27, 139.00, 207.21

MS 238 (M<sup>+</sup>), 147 (base), 119, 103, 91, 77

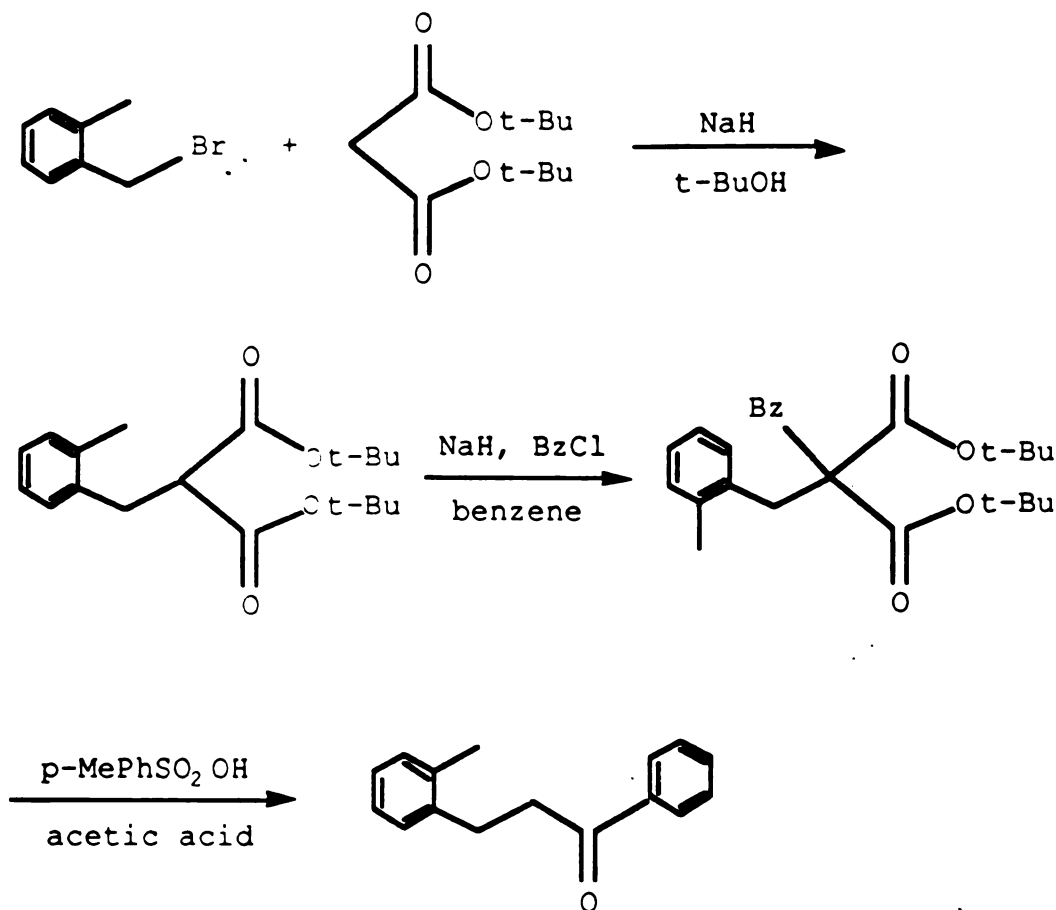
IR 3085-2820, 1704 (C=O), 1615, 1500, 1460, 1210, 1038

### **$\beta$ -(o-Tolyl)propiophenone**

$\beta$ -(o-tolyl)propiophenone was prepared by alkylation and acylation of t-butyl malonate with  $\alpha$ -bromo-o-xylene and benzoyl chloride following the route given below.<sup>115</sup>

t-Butyl (o-Tolylmethyl)malonate - Sodium hydride (Aldrich, 80% dispersion in mineral oil, 2.5 g, 0.083 mole) was added to t-butyl malonate<sup>116</sup>





(18.0 g, 0.083 mole) in t-butyl alcohol (Baker, 110 ml), and stirred at r.t. for 3 hr.  $\alpha$ -Bromo-o-xylene (15 g, 0.081 mole) in t-butyl alcohol (40 ml) was added and stirred at 65°C for 2 hr. The mixture was cooled and diluted with distilled water. The organic phase was separated. The aqueous phase was extracted with ether (2x150 ml). The extracts were washed with distilled water and dried over sodium sulfate with small amount of potassium carbonate. After evaporation of the solvent, the crude product was used without further purification (24.0 g, 100% yield).

<sup>1</sup>H NMR (60 MHz, CDCl<sub>3</sub>) 1.42 (s, 18H), 2.43 (s, 3H), 3.18 (d, 2H), 3.49 (t, 3H), 7.12 (s, 4H)

$\beta$ -(o-Tolyl)propiophenone - Sodium hydride (Aldrich, 80% dispersion in mineral oil, 3.3 g, 0.110 mole) was added to t-butyl (o-tolyl)-



methyl)malonate (22.0 g, 0.075 mole) in benzene (450 ml), and stirred at 80°C for 4 hr. Benzoyl chloride (Fisher, 10.9 g, 0.078 mole) in benzene (150 ml) was added. The mixture was stirred for another 4 hr. It was then cooled and the excess sodium hydride was decomposed by addition of p-toluenesulfonic acid monohydrate (Aldrich, 3.6 g). The salt was removed by filtration. After evaporation of solvent, the residue was refluxed with p-toluenesulfonic acid monohydrate (2.0 g) in glacial acetic acid (Mallinckrodt, 450 ml) containing acetic anhydride (Baker, 9 ml). The solution was cooled, poured over ice, and neutralized with 10% aqueous potassium hydroxide solution. The aqueous phase was extracted with ether (2x300 ml). The extracts were washed with distilled water, and dried over sodium sulfate. The solvent were evaporated. The crude product was purified by vacuum distillation and recrystallization from ethanol to give the pure ketone as colorless crystal (5.0 g, 29.8%). m.p. 46.5-47.5°C.

<sup>1</sup>H NMR (250 MHz, CDCl<sub>3</sub>) 2.35 (s, 3H, ArCH<sub>3</sub>), 3.07, 3.24 (A<sub>2</sub>B<sub>2</sub>, J=8.5 Hz, Ar(CH<sub>2</sub>)<sub>2</sub>), 7.11-7.99 (m, 9H, ArH)

<sup>13</sup>C NMR (250 MHz, CDCl<sub>3</sub>) 19.18, 27.32, 38.89, 126.03, 126.17, 127.88, 128.46, 128.58, 130.19, 132.90, 135.79, 136.70, 139.23, 199.06

MS 224(M<sup>+</sup>), 206, 119, 105 (base), 91, 77

IR 3100-2900, 1697 (C=O), 1606, 1500, 1455, 1210

**β-(o-Tolyl)isobutyrophenone** - Diisopropylamine (Aldrich, 15.2 g, 0.150 mole) in dry THF (100 ml) was added to n-butyl lithium (Aldrich, 2.5 M in hexane, 60 ml, 0.150 mole) at 0°C. The mixture was stirred for 10 min, and then cooled to -78°C with a dry-ice/acetone bath. Propiophenone (Mallinckrodt, 19.0 g, 0.142 mole) was added. The content was stirred for 30 min, and α-chloro-o-xylene (Aldrich, 20.0 g, 0.142 mole) in dry THF (100 ml)



was added. The mixture was warmed to r.t., stirred for 2 hr, and then refluxed for 4 hr. The solution was cooled and the THF was removed. Ether (150 ml) and distilled water (150 ml) was added to the residue, and then separated. The aqueous phase was extracted with ether (2x150 ml). The combined ether layers were washed with distilled water, dried over sodium sulfate. The solvent was evaporated and the residue was distilled under reduced pressure to afford a colorless liquid (15 g, 47.2% yield).

$^1\text{H}$  NMR (250 MHz,  $\text{CDCl}_3$ ) 1.21 (d,  $J=6.9$  Hz, 3H,  $\text{CHCH}_3$ ), 2.34 (s, 3H,  $\text{ArCH}_3$ ), 2.74 (A), 3.14 (B), 3.78 (X) (ABX,  $J_{AB}=14.9$  Hz,  $J_{BX}=7.7$  Hz, 3H,  $\text{ArCH}_2\text{CHCH}_3$ ), 7.06-7.92 (m, 9H, ArH)

$^{13}\text{C}$  NMR (250 MHz,  $\text{CDCl}_3$ ) 17.42, 19.42, 36.17, 41.03, 125.67, 126.10, 127.99, 128.38, 129.50, 130.11, 132.66, 135.89, 136.33, 137.86, 203.65

MS 238 ( $\text{M}^+$ ), 220, 133, 117, 105 (base), 91, 77

IR 3060-2875, 1695 ( $\text{C}=\text{O}$ ), 1600, 1492, 1450, 1230

**$\beta$ -Mesitylpropiophenone** -  $\beta$ -Mesitylpropiophenone was synthesized by alkylation and acylation of t-butyl malonate with 2,4,6-trimethylbenzyl chloride and benzoyl chloride, using the procedure described for  $\beta$ -(o-tolyl)propiophenone. m.p. 81.0-82.0°C.

$^1\text{H}$  NMR (250 MHz,  $\text{CDCl}_3$ ) 2.27 (s, 3H, p-Mes- $\text{CH}_3$ ), 2.32 (s, 6H, o-Mes- $\text{CH}_3$ ) 3.08, 3.24 (m, 4H,  $\text{Ar}(\text{CH}_2)_2$ ), 6.78-7.79 (m, 7H, ArH)

$^{13}\text{C}$  NMR (250 MHz,  $\text{CDCl}_3$ ) 19.66, 20.72, 23.63, 37.82, 127.93, 128.55, 128.99, 132.99, 134.72, 135.37, 135.96, 136.72, 199.45

MS 252 ( $\text{M}^+$ ), 234, 219, 147, 132, 117, 105, 91, 77 (base)

IR 3090-2860, 1695 ( $\text{C}=\text{O}$ ), 1602, 1490, 1452, 1290, 1208

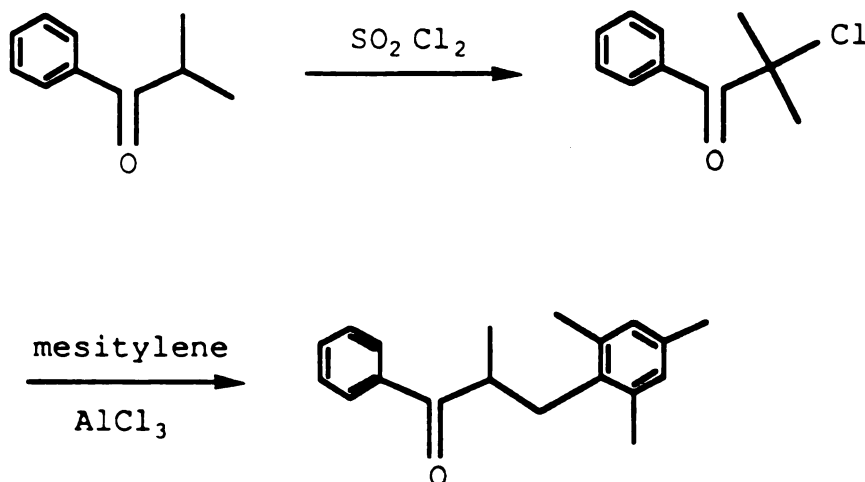
**$\beta$ -Mesitylisobutyrophenone**



$\beta$ -Mesitylisobutyrophenone was prepared by the reaction of  $\alpha$ -chloroisobutyrophenone with mesitylene following the route given below.

$\alpha$ -Chloroisobutyrophenone - Sulfuryl chloride (MC/B, 27.6 g, 0.204 mole) was slowly added to isobutyrophenone (OR, 30.0 g, 0.203 mole) at r.t.. After the addition was complete, the mixture was stirred for 3 hr. Benzene (200 ml) was added. The organic phase was washed with distilled water, and dried over sodium sulfate. After evaporation of the solvent, the residue was distilled at reduced pressure to afford the product (25.0 g, 67.5% yield).

$^1\text{H NMR}$  (60 MHz,  $\text{CDCl}_3$ ) 1.90 (s, 6H), 7.34-8.16 (m, 5H, ArH)



$\beta$ -Mesitylisobutyrophenone -  $\alpha$ -Chloroisobutyrophenone (15.0 g, 0.082 mole) in mesitylene (Aldrich, 45 ml) was added to anhydrous aluminum chloride (MCB, 13.5 g, 0.101 mole) in mesitylene (15 ml). The mixture was heated at 50–60°C overnight, and then poured into iced aqueous hydrochloric acid (38%) after being cooled. The aqueous phase was extracted with ether (3x150 ml). The extracts were washed with saturated sodium bicarbonate solution and dried over sodium sulfate. After evaporation of the solvent, the



crude product was purified by column chromatography with 30% benzene in hexane and recrystallization from ethanol to give pure colorless crystal (10.6 g, 48.6% yield). m.p. 53.0-54.0°C.

**$^1\text{H}$  NMR (250 MHz,  $\text{CDCl}_3$ )** 1.19 (d,  $J=7.3$  Hz, 3H  $\text{CHCH}_3$ ), 2.22 (s, 3H, p-Mes- $\text{CH}_3$ ), 2.32 (s, 6H, o-Mes- $\text{CH}_3$ ), 2.96 (m, 2H,  $\text{ArCH}_2$ ), 3.76 (m, 1H,  $\text{CH}_2\text{CHCH}_3$ ), 6.82-7.86 (m, 7H, ArH)

**$^{13}\text{C}$  NMR (250 MHz,  $\text{CDCl}_3$ )** 17.27, 20.29, 20.62, 32.33, 40.67, 128.02, 128.39, 129.01, 132.69, 133.56, 135.22, 136.42, 136.59, 204.62

**MS** 266 ( $\text{M}^+$ ), 248, 233, 161, 145, 133 (base), 105, 91, 77

**IR** 3090-2870, 1693 ( $\text{C=O}$ ), 1600, 1482, 1450, 1225

### Preparation of $\alpha$ -Deuteriated Ketones

The percentage of deuteriation was checked with MS. The  $\text{M}^+-1$  or  $\text{M}^+-2$  (for di-deuteriated ketones only) peak of deuteriated ketones can be from two sources, the undeuteriated impurity or the loss of one or two protons from the molecular ions of the ketones. The corrections for the loss of protons were made by comparing with the mass spectra of the undeuteriated ketones taken under the same condition. The values obtained from multiplying the intensities of the  $\text{M}^+-1$  or  $\text{M}^+-2$  peaks of the deuteriated ketones by the ratios of the same peaks to the  $\text{M}^+$  peak for the undeuteriated ketones were subtracted from the intensities of these peaks of the deuteriated ketones. The remained intensities were considered to be from the undeuteriated ketones. The percentages of deuteriation were given with each ketones. For a better evaluation, the much stronger  $\text{M}^+-105$  (benzoyl group) peak was used in the case of  $\alpha$ -mesitylacetophenone  $\alpha$ -(o-tolyl)propiophenone,  $\alpha$ -(2,4,6-triisopropylphenyl)acetophenone, and



$\alpha$ -mesityl- $\alpha$ -phenylacetophenone.

$\alpha$ -Mesitylacetophenone was  $\alpha$ -deuteriated by the following procedure.<sup>117</sup>

The ketone (0.020 mole) in dioxane (Mallinckrodt, 200 ml) was added to sodium carbonate (Mallinckrodt, 40 g, 0.378 mole) in D<sub>2</sub>O (Baker, 170 ml). The solution was refluxed overnight. The organic phase was separated. The aqueous phase was extracted with ether (2x250 ml). The extracts were combined, and dried over sodium sulfate. After evaporation of solvent, the crude product was recrystallized from hexane or ethanol-d<sub>1</sub>.

$\alpha$ -(*o*-Tolyl)propiophenone,  $\alpha$ -(2,4,6-triisopropylphenyl)acetophenone,  $\alpha$ -mesityl- $\alpha$ -phenylacetophenone were  $\alpha$ -deuteriated by the same procedure, but the reaction scale was reduced 50%.

**$\alpha$ -(*o*-Tolyl)propiophenone-d<sub>1</sub>**

<sup>1</sup>H NMR (250 MHz, CDCl<sub>3</sub>) 1.48 (s, 3H, ArCHCH<sub>3</sub>), 2.50 (s, 3H, ArCH<sub>3</sub>), 7.05-7.85 (m, 9H, ArH)

MS 225 (M<sup>+</sup>), 120, 105 (base), 91, 77

Relative intensity of the relevant peaks:

ketone 2 224 (2.71), 223 (0.0), 119 (19.00), 118 (1.52)

ketone 2-d 225 (4.41), 224 (0.0), 120 (16.58), 119(2.46)

Percentage of undeuteriated ketone 6.0%

**$\alpha$ -Mesitylacetophenone-d<sub>2</sub>**

<sup>1</sup>H NMR (250 MHz, CDCl<sub>3</sub>) 2.21 (s, 6H, *o*-Mes-CH<sub>3</sub>), 2.32 (s, 3H, *p*-Mes-CH<sub>3</sub>), 6.92-8.12 (s, 7H, ArH)

MS 240 (M<sup>+</sup>), 135, 119, 105, 91, 77

Relative intensity of the relevant peaks:



ketone 16      238 (6.07), 237 (0.0), 236 (0.0), 133 (39.23), 132 (1.18), 131 (0.87)

ketone 16-d<sub>2</sub>   240 (6.56), 239 (0.0), 238 (0.0), 135 (41.86), 134 (2.27), 133 (0.92)

Percentage of undeuteriated ketone 0.0%, percentage of mono-deuteriated ketone 2.4%

**$\alpha$ -(2,4,6-Triisopropylphenyl)acetophenone-d<sub>2</sub>**

<sup>1</sup>H NMR (250 MHz, CDCl<sub>3</sub>) 1.23 (overlapping d's, 18H, CH(CH<sub>3</sub>)<sub>2</sub>), 2.86 (m, 3H, CH(CH<sub>3</sub>)<sub>2</sub>), 7.05-8.10 (m, 7H, ArH)

MS 324 (M<sup>+</sup>), 219, 203, 105, 95, 91, 77

Relative intensity of the relevant peaks:

ketone 17      322 (2.51), 321 (0.0), 320 (0.0), 217 (42.18), 216 (0.0), 215 (0.97)

ketone 17-d<sub>2</sub>   324 (2.53), 323 (0.0), 322 (0.0), 219 (42.22), 218 (1.62), 217 (0.67)

Percentage of undeuteriated ketone 0.0%, percentage of mono-deuteriated ketone 3.7%

**$\alpha$ -Mesityl- $\alpha$ -phenylacetophenone-d**

<sup>1</sup>H NMR (250 MHz, CDCl<sub>3</sub>) 2.19 (s, 6H, o-Mes-CH<sub>3</sub>), 2.28 (s, 3H, p-Mes-CH<sub>3</sub>), 6.89-7.93 (m, 12H, ArH)

MS 315 (M<sup>+</sup>), 210 (base), 193, 179, 105, 91, 77

Relative intensity of the relevant peaks:

ketone 8      314 (5.61), 313 (0.0), 209 (82.14), 208 (0.0)

ketone 8-d   315 (4.89), 314 (0.50), 210 (80.79), 209(3.62)

Percentage of undeuteriated ketone 4.3%

$\beta$ -Mesitylpropiophenone,  $\beta$ -mesitylisobutyrophenone were  $\alpha$ -deuteriated by the following procedure.<sup>117</sup>

The ketone (0.010 mole) in dioxane (Mallinckrodt, 100 ml) was added to



sodium hydroxide (Mallinckrodt, 6.0 g, 0.150 mole) in D<sub>2</sub>O (Baker, 100 ml). The solution was refluxed overnight. The organic phase was separated. The aqueous phase was extracted with ether (2x250 ml). The extracts were combined, and dried over sodium sulfate. After evaporation of solvent, the crude product was recrystallized from hexane.

**$\beta$ -Mesitylpropiophenone-d<sub>2</sub>**

**<sup>1</sup>H NMR (250 MHz, CDCl<sub>3</sub>)** 2.27 (s, 3H, p-Mes-CH<sub>3</sub>), 2.32 (s, 6H, o-Mes-CH<sub>3</sub>) 3.08 (s, 2H, ArCH<sub>2</sub>CD<sub>2</sub>), 6.78-7.79 (m, 7H, ArH)

**MS** 254 (M<sup>+</sup>), 236, 149, 132, 117, 105, 91, 77 (base)

Relative intensity of the relevant peaks:

ketone 20      252 (2.11), 251 (0.0), 250 (0.0)

ketone 20-d<sub>2</sub>   254 (4.08), 253 (0.28), 252 (0.0)

Percentage of mono-deuteriated ketone 6.4%, percentage of undeuteriated ketone 0.0%

**$\beta$ -Mesitylisobutyrophenone-d**

**<sup>1</sup>H NMR (250 MHz, CDCl<sub>3</sub>)** 1.19 (s, 3H, CDCH<sub>3</sub>), 2.22 (s, 3H, p-Mes-CH<sub>3</sub>), 2.32 (s, 6H, o-Mes-CH<sub>3</sub>), 2.86, 3.03 (AB quartet, J=14.9 Hz, 2H, ArCH<sub>2</sub>), 6.82-7.86 (m, 7H, ArH)

**MS** 267 (M<sup>+</sup>), 249, 162, 145, 133 (base), 117, 105, 91, 77

Relative intensity of the relevant peaks:

ketone 21      266 (2.63), 265 (0.08)

ketone 21-d    267 (1.64), 266 (0.0)

Percentage of undeuteriated ketone 0.0%



#### IV. Isolation and Identification of Photoproducts

All the GC separations were performed on a VA 900 Gas Chromatogram with a SE-30 column. The carrier gas flow was adjusted at 55 ml/min. The injector and detector temperatures were maintained at 250°C and 270°C respectively. The separated components were collected with a s-shaped glass tube at the outlet of the GC. A dry-ice/acetone bath was used for cooling when low-boiling components were being collected. The sample was collected starting from the peak height which equals 20-30% of the overall peak height to avoid overlapping contaminations. The tlc separations were done with a mixture of hexane and ethyl acetate as eluent. The separated components were collected along with silica gel, and then extracted with chloroform, and filtered. The solvent was removed.

#### Products from $\alpha$ -(o-Tolyl)-p-Methoxyacetophenone

$\alpha$ -(o-tolyl)-p-methoxyacetophenone (0.30 g) in cyclohexane (500 ml) was irradiated until 100% ketone conversion by HPLC. The solvent was removed, and the crude product was analyzed by HPLC to contain one major component (>98%). The product was recrystallized and identified by its spectroscopic data as 2-(p-methoxyphenyl)-2-indanol.

#### 2-(p-Methoxyphenyl)-2-Indanol

m.p. 206-208°C

<sup>1</sup>H NMR (250 MHz, CDCl<sub>3</sub>) 1.96 (s, 1H, OH), 3.29, 3.51 (AB quartet, J=16.6 Hz, 4H, ArCH<sub>2</sub>), 3.82 (s, 3H, OCH<sub>3</sub>), 6.83-7.56 (m, 4H, ArH)

<sup>13</sup>C NMR (250 MHz, CDCl<sub>3</sub>)

MS 240 (M<sup>+</sup>), 222 (M<sup>+</sup>-18), 207, 135 (base), 105, 91, 77







IR (CCl<sub>4</sub>) 3600, 3080-2840, 1612, 1515, 1250, 1180, 1042

### Products from $\alpha$ -(o-Tolyl)propiophenone

$\alpha$ -(o-Tolyl)propiophenone (0.30 g) in cyclohexane (500 ml) was irradiated until 100% ketone conversion by GC. Three major components were isolated by GC at 240°C and identified by their spectroscopic data. The isomeric 2,3-di(o-tolyl)butanes were partially separated by the GC. Collections starting from half height of the peaks were able to isolate the two isomers with ca. 85-90% purity. The formation of benzaldehyde was verified by irradiation of the ketone in the presence of 0.007 M dodecanthiol in benzene and coinjections with authentic sample on HPLC and GC.

#### Z-1-Methyl-2-Phenyl-2-Indanol

<sup>1</sup>H NMR (250 MHz, CDCl<sub>3</sub>) 1.25 (d, J=7.3 Hz, 3H, CHCH<sub>3</sub>), 1.94 (s, 1H, OH), 3.17, 3.52 (AB quartet, J=16.6 Hz, 2H, ArCH<sub>2</sub>), 3.58 (q, J=7.3 Hz, 1H, CHCH<sub>3</sub>), 7.25-7.65 (m, 9H, ArH)

<sup>13</sup>C NMR (250 MHz, CDCl<sub>3</sub>) 10.9, 49.27, 50.38, 85.39, 123.66, 124.84, 125.35, 126.91, 127.01, 128.13, 128.60, 140.09, 144.17, 145.11

MS 224 (M<sup>+</sup>), 206 (M<sup>+</sup>-18), 191, 165, 119, 105 (base), 91, 77

IR (CDCl<sub>3</sub>) 3500, 3095-2860, 1608, 1480, 1455, 1183, 1080, 1020

#### 2,3-Di(o-tolyl)butane (Two Diastereomers)

##### Diastereomer (1)

<sup>1</sup>H NMR (250 MHz, CDCl<sub>3</sub>) 0.98 (d, J=7.7 Hz, 6H, CHCH<sub>3</sub>), 2.38 (s, 6H, ArCH<sub>3</sub>), 3.25 (m, 2H, CHCH<sub>3</sub>), 6.93-7.32 (m, 8H, ArH)

MS 238 (M<sup>+</sup>), 202, 119 (Base), 105, 91, 77

##### Diastereomer (2)

<sup>1</sup>H NMR (250 MHz, CDCl<sub>3</sub>) 1.32 (d, J=7.7 Hz, 6H, CHCH<sub>3</sub>), 2.15 (s, 6H,



ArCH<sub>3</sub>), 3.28 (m, 2H, CHCH<sub>3</sub>), 6.92-7.30 (m, 8H, ArH)

MS 238 (M<sup>+</sup>), 202, 119 (Base), 105, 91, 77

### **Products from $\alpha$ -(o-Tolyl)valerophenone**

$\alpha$ -(o-Tolyl)valerophenone (0.30 g) in cyclohexane (500 ml) was irradiated until 100% ketone conversion by GC. The products were isolated by GC at 250°C. The major product was 2-phenyl-2-indanol. A very minor product was identified as 2-phenyl-3-propyl-2-indanol by <sup>1</sup>H NMR. Isolation of photoproducts at approximately 40% ketone conversion gave  $\alpha$ -(o-tolyl)acetophenone as well as the above products.  $\alpha$ -(o-Tolyl)-acetophenone was characterized by its identical spectra with the ones of authentic sample. The formation of small amount of benzaldehyde was verified by irradiation of the ketone in the presence of 0.007 M dodecanthiol in benzene and coinjections with authentic sample on HPLC and GC.

#### **2-Phenyl-2-Indanol**

2-Phenyl-2-indanol was verified by its identical spectra with the ones of authentic sample.

#### **Z-2-Phenyl-3-Propyl-2-Indanol**

<sup>1</sup>H NMR (250 MHz, CDCl<sub>3</sub>) 0.84 (d, J=7.3 Hz, 3H, (CH<sub>2</sub>)<sub>2</sub>CH<sub>3</sub>), 1.25-1.82 (m, 4H, (CH<sub>2</sub>)<sub>2</sub>CH<sub>3</sub>), 2.01 (s, 1H, OH), 3.17, 3.44 (AB quartet, J=16.6 Hz, 2H, ArCH<sub>2</sub>), 3.58 (t, J=5.5 Hz, 1H, CHPr), 7.24-7.63 (m, 9H, ArH)

### **Products from $\alpha$ -(o-Tolyl)isobutyrophenone**

The ketone (0.30 g) in benzene (500 ml) with 0.007 M dodecanthiol was irradiated to 100% ketone conversion by GC. Two major products were



isolated by GC at 180°C and identified as benzaldehyde and o-cymene. The formation of benzaldehyde was verified by irradiation of the ketone in the presence of 0.007 M dodecanthiol in benzene and coinjections with authentic sample on HPLC and GC.

#### Benzaldehyde

<sup>1</sup>H NMR (250 MHz, CDCl<sub>3</sub>) 7.52-7.93 (m, 5H, ArH), 10.11 (s, 1H, CHO)

#### o-Cymene

<sup>1</sup>H NMR (250 MHz, CDCl<sub>3</sub>) 1.23 (d, J=7.3 Hz, 6H, CH(CH<sub>3</sub>)<sub>2</sub>), 2.34 (s, 3H, ArCH<sub>3</sub>), 3.14 (sep, J=7.3 Hz, 1H, CH(CH<sub>3</sub>)<sub>2</sub>), 7.12-7.18 (m, 4H, ArH)

#### **Products from α-Mesitylpropiophenone**

The ketone (0.30 g) in cyclohexane (500 ml) was irradiated to 100% ketone conversion by GC. The products were isolated by GC at 260°C and identified by their spectroscopic data. The formation of small amount of benzaldehyde was verified by irradiation of the ketone in the presence of 0.007 M dodecanthiol in benzene and coinjections with authentic sample on HPLC and GC.

#### Z-1,5,7-Trimethyl-2-Phenyl-2-Indanol

<sup>1</sup>H NMR (250 MHz, CDCl<sub>3</sub>) 1.25 (d, J=8.5 Hz, 3H, CHCH<sub>3</sub>), 2.02 (s, 1H, OH), 2.30 (s, 3H, ArCH<sub>3</sub>), 2.32 (s, 3H, ArH<sub>3</sub>), 3.28, 3.36 (AB quartet, J=18.6 Hz, 2H, ArCH<sub>2</sub>), 3.51 (q, J=8.5 Hz, 1H, CHCH<sub>3</sub>), 6.87-7.51 (m, 7H, ArH)

<sup>13</sup>C NMR (250 MHz, CDCl<sub>3</sub>) 13.51, 19.08, 21.12, 47.80, 49.85, 83.90, 122.82, 125.80, 126.81, 128.10, 129.73, 133.87, 136.62, 140.08, 141.02, 146.91

MS 252(M<sup>+</sup>), 234 (M<sup>+</sup>-18), 219, 147, 105 (base), 91 77

IR (CCl<sub>4</sub>) 3600, 3095-2878, 1610, 1480, 1450, 1176, 1072

#### E-1,5,7-Trimethyl-2-Phenyl-2-Indanol



The sample of E-1,5,7-trimethyl-2-phenyl-2-indanol can not be freed of the Z isomer. Its  $^1\text{H}$  NMR is derived from the spectrum of the mixture.

$^1\text{H}$  NMR (250 MHz,  $\text{CDCl}_3$ ) 0.74 (d,  $J=8.1$  Hz, 3H,  $\text{CHCH}_3$ ), 2.21 (s, 1H, OH), 2.32 (s, 3H,  $\text{ArCH}_3$ ), 2.37 (s, 3H,  $\text{ArH}_3$ ), 3.03, 3.88 (AB quartet,  $J=18.6$  Hz, 2H,  $\text{ArCH}_2$ ), 3.95 (q,  $J=8.1$  Hz, 1H,  $\text{CHCH}_3$ ), 7.03-7.43 (m, 7H, ArH)

GC-MS 252 ( $\text{M}^+$ ), 234 ( $\text{M}^+-18$ ), 219, 203, 149, 105 (base), 91, 77

#### Z/E-1-Mesitoxy-1-Phenylpropene

The Z/E forms can not be separated. The sample collected from GC contained the Z/E isomers in a ratio of 1:4. The following spectroscopic data are derived from the spectra of the mixture.

$^1\text{H}$  NMR (250 MHz,  $\text{CDCl}_3$ )

Z-Isomer: 1.52 (d,  $J=8.1$  Hz, 3H,  $\text{CHCH}_3$ ), 2.18 (s, 3H, p-Mes- $\text{CH}_3$ ), 2.24 (s, 6H, o-Mes- $\text{CH}_3$ ), 5.19 (q,  $J=8.1$  Hz, 1H,  $\text{CHCH}_3$ ), 6.74-7.42 (m, 7H, ArH)

E-Isomer: 1.64 (d,  $J=8.1$  Hz, 3H,  $\text{CHCH}_3$ ), 2.22 (s, 6H, o-Mes- $\text{CH}_3$ ), 2.31 (s, 3H, p-Mes- $\text{CH}_3$ ), 4.38 (q,  $J=8.1$  Hz, 1H,  $\text{CHCH}_3$ ), 6.91-7.66 (m, 7H, ArH)

MS (Mixture) 252 ( $\text{M}^+$ ), 223, 147, 136 (base), 115, 105, 91, 77

#### **Products from $\alpha$ -Mesitylvalerophenone**

The ketone (0.30 g) in cyclohexane (500 ml) was irradiated to 100% ketone conversion by GC. The major product was isolated by GC at  $260^\circ\text{C}$  and characterized as Z-5,7-dimethyl-2-phenyl-1-propyl-2-indanol. A minor product was identified by GC-MS as 1-mesitoxy-1-phenylpentene. The formation of small amount of benzaldehyde was verified by irradiation of the ketone in the presence of 0.007 M dodecanthiol in benzene and coinjections with authentic sample on HPLC and GC. When irradiated in benzene and benzene with 1 M dioxane to 100% ketone conversion, a small peak on GC



(column #1, 165<sup>o</sup>c) was identified as 4,6-dimethyl-2-phenyl-2-indanol (the type II product) by coinjection with authentic sample on GC. The area ratio of this peak to Z-5,7-dimethyl-2-phenyl-1-propyl-2-indanol was 0.046 and 0.065 in benzene and benzene with 1 M dioxane respectively. However, in a quantum yield measurement in benzene with 1 M dioxane where irradiation was controlled at low ketone conversion, the relative amount of this peak to the indanol seemed much smaller than the above value, and was too small to be measured.

#### Z-5,7-Dimethyl-2-Phenyl-1-Propyl-2-Indanol

<sup>1</sup>H NMR (250 MHz, CDCl<sub>3</sub>) 0.93 (t, J=8.1 Hz, 3H, (CH<sub>2</sub>)<sub>2</sub>CH<sub>3</sub>), 1.10-2.01 (m, 4H, (CH<sub>2</sub>)<sub>2</sub>CH<sub>3</sub>), 2.07 (s, 1H, OH), 2.22 (s, 3H, ArCH<sub>3</sub>), 2.29 (s, 3H, ArH<sub>3</sub>), 3.25, 3.40 (AB quartet, J=16.6 Hz, 2H, ArCH<sub>2</sub>), 3.51 (dd, J<sub>1</sub>=4.7 Hz, J<sub>2</sub>=3.4 Hz, 1H, CHPr), 6.81-7.38 (m, 7H, ArH)

<sup>13</sup>C NMR (250 MHz, CDCl<sub>3</sub>) 14.54, 18.92, 21.01, 21.41, 32.52, 47.51, 54.00, 83.38, 122.21, 124.70, 126.47, 127.87, 129.20, 133.28, 136.13, 139.97, 141.37, 149.11

MS 280(M<sup>+</sup>), 262 (M<sup>+</sup>-18), 233, 218, 175, 146, 133, 105 (B<sub>base</sub>), 91, 77

IR (CCl<sub>4</sub>) 3610, 3090-2875, 1600, 1455, 1065, 1040

#### 1-Mesityoxy-1-Phenylpentene

The identification was based on the characteristic fragmentation of the enol ethers giving an ion peak at 136 in MS.

GC-MS 280 (M<sup>+</sup>), 223, 145, 136 (base), 115, 105, 91, 77

#### **Products from α-Mesitylisobutyrophenone**

The ketone (0.30 g) in cyclohexane (500 ml) was irradiated to 100% ketone conversion by HPLC. Two major products were isolated by GC at 180<sup>o</sup>c and identified as benzaldehyde and 2-mesitylpropene. The formation of



benzaldehyde was verified by irradiation of the ketone in the presence of 0.005 M dodecanthiol in benzene and coinjections with authentic sample on HPLC and GC.

### Benzaldehyde

**<sup>1</sup>H NMR (250 MHz, CDCl<sub>3</sub>)** 7.52-7.93 (m, 5H, ArH), 10.11 (s, 1H, CHO)

### 2-Mesitylpropene

**<sup>1</sup>H NMR (250 MHz, CDCl<sub>3</sub>)** 1.97 (s, 3H, =CCH<sub>3</sub>), 2.27 (s, 6H, o-Mes-CH<sub>3</sub>), 2.33 (s, 3H, p-Mes-CH<sub>3</sub>), 4.78 (d, J=2.1 Hz, 1H, vinyl H), 5.29 (d, J=2.1 Hz, 1H, vinyl H), 6.90 (s, 2H, ArH)

### **Products from α-Mesityl-α-Phenylacetophenone**

The ketone (0.30 g) in cyclohexane (500 ml) was irradiated to 100% ketone conversion by HPLC. Three major products were separated by GC at 270°C and identified by their spectroscopic data. The formation of small amount of benzaldehyde was verified by irradiation of the ketone in the presence of 0.007 M dodecanthiol in benzene and coinjections with authentic sample on HPLC and GC.

### Z-5,7-Dimethyl-1,2-Diphenyl-2-Indanol

**<sup>1</sup>H NMR (250 MHz, CDCl<sub>3</sub>)** 1.57 (s, 1H, OH), 1.83 (s, 3H, ArCH<sub>3</sub>), 2.37 (s, 3H, ArH<sub>3</sub>), 3.37, 3.50 (AB quartet, J=16.8 Hz, 2H, ArCH<sub>2</sub>), 4.66 (s, 1H, ArCHPh), 6.68-7.43 (m, 11H, ArH)

**<sup>13</sup>C NMR (250 MHz, CDCl<sub>3</sub>)** 19.27, 21.28, 48.70, 63.25, 83.09, 122.52, 124.88, 126.77, 127.44, 128.11, 128.68, 129.49, 129.70, 134.78, 137.46, 137.54, 138.59, 141.90, 147.81

**MS** 314 (M<sup>+</sup>), 296 (M<sup>+</sup>-18), 209, 105 (base), 91, 77

**IR (CDCl<sub>3</sub>)** 3560, 3090-2860, 1608, 1500, 1455, 1180, 1060



E-1-Mesitoxy-1,2-Diphenylethylene

**<sup>1</sup>H NMR (250 MHz, CDCl<sub>3</sub>)** 2.29 (s, 6H, o-Mes-CH<sub>3</sub>), 2.32 (s, 3H, p-Mes-H<sub>3</sub>), 5.43 (s, 1H, vinyl H), 7.00-7.60 (m, 12H, ArH)

**<sup>13</sup>C NMR (250 MHz, CDCl<sub>3</sub>)** 16.25, 20.76, 103.03, 117.79, 125.42, 126.41, 127.11, 127.91, 128.32, 128.62, 128.81, 129.23, 129.53, 129.70, 131.12

**MS** 314 (M<sup>+</sup>), 223, 209, 179, 178 (base), 136, 105, 91, 77

**IR (CDCl<sub>3</sub>)** 3560, 3070-2860, 1608, 1500, 1455, 1180, 1060

Z-1-Mesitoxy-1,2-Diphenylethylene

m.p. 97.5-100<sup>o</sup>c (recrystallized from hexane)

**<sup>1</sup>H NMR (250 MHz, CDCl<sub>3</sub>)** 2.28 (s, 3H, p-Mes-H<sub>3</sub>), 2.56 (s, 6H, o-Mes-CH<sub>3</sub>), 5.97 (s, 1H, vinyl H), 6.68-7.82 (m, 12H, ArH)

**<sup>13</sup>C NMR (250 MHz, CDCl<sub>3</sub>)** 17.10, 20.46, 111.30, 126.34, 127.11, 127.92, 128.23, 128.34, 128.81, 129.72, 132.75, 136.25, 136.59, 150.28, 153.63

**MS** 314 (M<sup>+</sup>), 223, 209, 179, 178, 136 (base), 105, 91, 77

**IR** 3080-2860, 1640, 1605, 1480, 1290, 1210, 1148, 1060

**α-Mesityl-α-Phenyl-p-Methoxyacetophenone**

The ketone (0.30 g) in benzene (500 ml) was irradiated to 100% ketone conversion by HPLC. Three major products were separated by preparative tlc with 5% ethyl acetate in hexane as eluent and identified by their spectroscopic data. The order of elution follows the E-enol ether, Z-enol ether closely behind, and indanol. The formation of small amount of p-methoxybenzaldehyde was verified by irradiation of the ketone in the presence of 0.007 M dodecanthiol in benzene and coinjections with authentic sample on HPLC and GC.

Z-5,7-Dimethyl-2-(p-Methoxyphenyl)-1-Phenyl-2-Indanol



**<sup>1</sup>H NMR (250 MHz, CDCl<sub>3</sub>)** 1.73 (s, 1H, OH), 1.85 (s, 3H, ArCH<sub>3</sub>), 2.38 (s, 3H, ArH<sub>3</sub>), 3.36, 3.48 (AB quartet, J=16.8 Hz, 2H, ArCH<sub>2</sub>), 3.82 (s, 3H, OCH<sub>3</sub>), 4.63 (s, 1H, ArCHPh), 6.65-7.42 (m, 11H, ArH)

**<sup>13</sup>C NMR (250 MHz, CDCl<sub>3</sub>)** 19.20, 21.25, 48.57, 55.20, 63.11, 82.92, 113.42, 122.49, 126.10, 127.34, 128.61, 129.50, 129.63, 134.73, 137.37, 137.70, 138.72, 139.99, 141.90

**MS** 344 (M<sup>+</sup>), 253, 209, 105, 91, 77, 43 (base)

**IR (CDCl<sub>3</sub>)** 3530, 3070-2845, 1610, 1500, 1250, 1180, 1035

**E-1-Mesitoxy-1-(p-Methoxyphenyl)-2-Phenylethylene**

**<sup>1</sup>H NMR (250 MHz, CDCl<sub>3</sub>)** 2.28 (s, 6H, o-Mes-CH<sub>3</sub>), 2.34 (s, 3H, p-Mes-H<sub>3</sub>), 3.86 (s, 3H, OCH<sub>3</sub>), 5.47 (s, 1H, vinyl H), 6.87-7.56 (m, 11H, ArH)

**<sup>13</sup>C NMR (250 MHz, CDCl<sub>3</sub>)** 17.10, 20.80, 55.24, 110.09, 113.34, 113.70, 124.29, 125.25, 126.04, 127.93, 128.31, 128.49, 128.64, 128.72, 129.49, 129.69, 130.55

**MS** 344 (M<sup>+</sup>), 135 (base), 105, 91, 77

**IR (CDCl<sub>3</sub>)** 3050-2870, 1640, 1610, 1515, 1480, 1250, 1210, 1175

**Z-1-Mesitoxy-1-(p-Methoxyphenyl)-2-Phenylethylene**

m.p. 95.5-97.5<sup>o</sup>c (recrystallized from methanol)

**<sup>1</sup>H NMR (250 MHz, CDCl<sub>3</sub>)** 2.19 (s, 3H, p-Mes-H<sub>3</sub>), 2.28 (s, 6H, o-Mes-CH<sub>3</sub>), 3.78 (s, 3H, OCH<sub>3</sub>), 5.91 (s, 1H, vinyl H), 6.71-7.81 (m, 11H, ArH)

**<sup>13</sup>C NMR (250 MHz, CDCl<sub>3</sub>)** 17.10, 22.67, 55.14, 110.09, 113.35, 124.37, 126.05, 127.93, 128.31, 128.49, 128.64, 128.88, 129.49, 129.69, 130.55, 132.67, 136.47

**MS** 344 (M<sup>+</sup>), 135 (base), 105, 91, 77

**IR (CDCl<sub>3</sub>)** 3040-2850, 1640, 1610, 1510, 1480, 1255, 1215, 1180

**Products from α-Mesityl-α-Phenyl-p-Cyanoacetophenone**

The ketone (0.30 g) in benzene (500 ml) was irradiated to 100% ketone



conversion by HPLC. Three major products were separated by preparative tlc with 7% ethyl acetate in hexane as eluent and identified by their spectroscopic data. The order of elution follows the E-enol ether, Z-enol ether closely behind, and indanol. The formation of small amount of p-cyanobenzaldehyde was verified by irradiation of the ketone in the presence of 0.007 M dodecanthiol in benzene and coinjections with authentic sample on HPLC and GC.

**Z-5,7-Dimethyl-2-(p-Cyanophenyl)-1-Phenyl-2-Indanol**

m.p. 168.7-170°C (recrystallized from methanol)

**<sup>1</sup>H NMR (250 MHz, CDCl<sub>3</sub>)** 1.72 (s, 1H, OH), 1.85 (s, 3H, ArCH<sub>3</sub>), 2.37 (s, 3H, ArH<sub>3</sub>), 3.38, 3.44 (AB quartet, J=16.8 Hz, 2H, ArCH<sub>2</sub>), 4.53 (s, 1H, ArCHPh), 6.88-7.61 (m, 11H, ArH)

**<sup>13</sup>C NMR (250 MHz, CDCl<sub>3</sub>)** 19.05, 21.24, 48.47, 63.02, 82.66, 110.58, 118.87, 122.45, 125.57, 127.79, 128.90, 129.29, 129.96, 131.96, 134.83, 136.83, 137.85, 138.07, 141.11, 153.49

**MS** 339 (M<sup>+</sup>), 209, 197, 130, 105, 91, 77, 43 (base)

**IR (CDCl<sub>3</sub>)** 3525, 3090-2860, 2225, 1610, 1495, 1456, 1250, 1090-1010

**E-1-Mesitoxy-1-(p-Cyanophenyl)-2-Phenylethylene**

**<sup>1</sup>H NMR (250 MHz, CDCl<sub>3</sub>)** 2.19 (s, 6H, o-Mes-CH<sub>3</sub>), 2.25 (s, 3H, p-Mes-H<sub>3</sub>), 5.51 (s, 1H, vinyl H), 6.83-7.62 (m, 11H, ArH)

**<sup>13</sup>C NMR (250 MHz, CDCl<sub>3</sub>)** 16.16, 20.76, 104.55, 126.28, 128.28, 128.95, 129.30, 129.71, 129.89, 130.53, 132.00, 134.76, 135.61, 140.00, 148.06, 152.02

**MS** 339 (M<sup>+</sup>), 248, 209, 204, 203, 136 (base), 105, 91, 77

**IR (CDCl<sub>3</sub>)** 3090-2860, 2225, 1635, 1475, 1200, 1137

**Z-1-Mesitoxy-1-(p-Cyanophenyl)-2-Phenylethylene**

m.p. 173-174.7°C (recrystallized from methanol)

**<sup>1</sup>H NMR (250 MHz, CDCl<sub>3</sub>)** 2.16 (s, 3H, p-Mes-H<sub>3</sub>), 2.23 (s, 6H, o-Mes-CH<sub>3</sub>),



6.04 (s, 1H, vinyl H), 6.69-7.79 (m, 11H, ArH)

$^{13}\text{C}$  NMR (250 MHz,  $\text{CDCl}_3$ ) 17.02, 20.45, 111.55, 113.70, 118.53, 127.21, 127.44, 127.64, 128.47, 129.13, 130.01, 131.82, 133.36, 135.35, 142.10, 149.82, 152.82

MS 339 ( $\text{M}^+$ ), 248, 209, 204, 203, 136 (base), 135, 105, 91, 77

IR ( $\text{CDCl}_3$ ) 3060-2840, 2220, 1630, 1475, 1205, 1138

### Products from $\alpha$ -Mesityl- $\alpha$ -Phenyl-2,4,6-Trimethylacetophenone

The ketone (0.30 g) in cyclohexane was irradiated to 100% ketone conversion by HPLC. The major product was isolated by tlc with 2% ethyl acetate in hexane and identified as 1,2-dimesityl-1,2-di-phenylethane. The formation of mesitaldehyde was verified by irradiation of the ketone in the presence of 0.007 M dodecanthiol in benzene and coinjection with authentic sample on HPLC and GC.

#### 1,2-Dimesityl-1,2-Diphenylethane (Two Diastereomers)

The two diastereomers can not be separated and the following spectra are from the ones of the mixtures. The identification was based on the comparison with literature data.<sup>118</sup>

##### Diastereomer (1)

$^1\text{H}$  NMR (250 MHz,  $\text{CDCl}_3$ ) 2.07 (s, 6H,  $\text{ArCH}_3$ ), 2.12 (s, 6H,  $\text{ArCH}_3$ ), 2.22 (s, 6H,  $\text{ArCH}_3$ ), 5.46 (s, 2H,  $\text{ArCHPh}$ ), 6.55-7.09 (m, 14H, ArH)

##### Diastereomer (2)

$^1\text{H}$  NMR (250 MHz,  $\text{CDCl}_3$ ) 2.10 (s, 6H,  $\text{ArCH}_3$ ), 2.21 (s, 6H,  $\text{ArCH}_3$ ), 2.31 (s, 6H,  $\text{ArCH}_3$ ), 5.48 (s, 2H,  $\text{ArCHPh}$ ), 6.72-7.24 (m, 14H, ArH)

MS 318 ( $\text{M}^+$ ), 209 ( $\text{M}^+ / 2$ )

### Products from $\alpha$ -Mesityl-2,4,6-Trimethylacetophenone



The ketone (0.30 g) in cyclohexane was irradiated to 100% ketone conversion by HPLC. The major product was isolated by GC at 250°C and identified as 1,2-dimesitylethane. The formation of mesitaldehyde was verified by irradiation of the ketone in the presence of 0.007 M dodecanthiol in benzene and coinjection with authentic sample on HPLC and GC.

### 1,2-Dimesitylethane

<sup>1</sup>H NMR (250 MHz, CDCl<sub>3</sub>) 2.27 (s, 3H, p-Mes-H<sub>3</sub>), 2.37 (s, 6H, o-Mes-CH<sub>3</sub>), 2.79 (s, 4H, ArCH<sub>2</sub>), 6.85 (s, 4H, ArH)

MS 266 (M<sup>+</sup>), 221, 204, 189, 161, 139, 133 (base), 117, 105, 91, 77

### **Products from α-Mesityl-o-Methylacetophenone**

The ketone (0.30 g) in cyclohexane was irradiated to 100% ketone conversion by GC. The NMR of the crude product showed the major products were 3,5-dimethyl-2-(o-tolyl)-2-indanol and 1,2-dimesityl-ethane. The products were isolated by GC at 260°C. 3,5-Dimethyl-2-(o-tolyl)-2-indanol partially dehydrates on the preparative GC and quantitatively dehydrates on the analytical GC. The formation of tolaldehyde was verified by irradiation of the ketone in the presence of 0.007 M dodecanthiol in benzene and coinjections with authentic sample on HPLC and GC.

### 3,5-Dimethyl-2-(o-tolyl)-2-Indanol

<sup>1</sup>H NMR (250 MHz, CDCl<sub>3</sub>) 2.26 (s, 3H, ArCH<sub>3</sub>), 2.32 (s, 3H, ArH<sub>3</sub>), 2.52 (s, 3H, o-CH<sub>3</sub>), 2.26, 3.62 (2 AB quartets, J=16.6 Hz, 4H, ArCH<sub>2</sub>), 6.87-7.62 (m, 6H, ArH)

<sup>13</sup>C NMR (250 MHz, CDCl<sub>3</sub>) 18.98, 21.18, 21.72, 46.49, 48.22, 83.60, 122.87, 125.56, 125.79, 127.33, 128.54, 129.06, 132.29, 133.88, 136.28, 136.58, 140.64, 143.08

MS 252 (M<sup>+</sup>), 234 (base, M<sup>+</sup>-18), 219, 204, 133, 119, 91, 77

IR (CCl<sub>4</sub>) 3600, 3060-2860, 1615, 1482, 1452, 1220, 1048



### Products from $\beta$ -(o-Tolyl)propiophenone

The ketone (0.30 g) in cyclohexane (500 ml) was irradiated for 14 days. The conversion was too low for any products to be isolated and identified, although there were peaks of products on GC.

### Products from $\beta$ -(o-Tolyl)isobutyrophenone

The ketone (0.30 g) in cyclohexane (500 ml) was irradiated for 14 days to approximately 25% ketone conversion by GC. The major product was isolated by GC at 260°C and identified as 3-methyl-1,2,3,4-tetrahydro-2-naphthol.

#### 3-Methyl-1,2,3,4-Tetrahydro-2-Naphthol

$^1\text{H}$  NMR (250 MHz,  $\text{CDCl}_3$ ) 0.77 (d,  $J=6.7$  Hz, 3H,  $\text{CHCH}_3$ ), 2.35 (s, 1H, OH), 2.37-2.81 (m, 3H,  $\text{ArCH}_2\text{CHCH}_3$ ), 2.95, 3.37 (AB quartet,  $J=17.3$  Hz, 2H,  $\text{ArCH}_2$ ), 3.58 (q,  $J=7.3$  Hz, 1H,  $\text{CHCH}_3$ ), 7.06-7.53 (m, 9H, ArH)

$^{13}\text{C}$  NMR (250 MHz,  $\text{CDCl}_3$ ) 15.87, 34.67, 36.83, 45.60, 74.81, 124.94, 124.95, 126.01, 126.14, 126.61, 128.28, 128.67, 129.34, 134.29, 136.20, 146.81

MS 238 ( $\text{M}^+$ ), 220 ( $\text{M}^+-18$ ), 205, 133, 105 (base), 91, 77

IR ( $\text{CDCl}_3$ ) 3510, 3060-2855, 1450, 1180, 1130

### Products from $\beta$ -Mesitylpropiophenone

The ketone (0.30 g) in methanol (500 ml) was irradiated for 18 days to 100% ketone conversion by GC. The major product was isolated by GC at 260°C and identified as 5,7-dimethyl-1,2,3,4-tetrahydro-2-naphthol.

#### 5,7-Dimethyl-1,2,3,4-Tetrahydro-2-Naphthol

$^1\text{H}$  NMR (250 MHz,  $\text{CDCl}_3$ ) 2.18 (s, 3H,  $\text{ArCH}_3$ ), 2.12 (s, 1H, OH), 2.26 (s, 3H,



ArCH<sub>3</sub>), 2.35-2.82 (m, 4H, ArCH<sub>2</sub>CH<sub>2</sub>), 2.94, 3.28 (AB quartet, J=17.5 Hz, 2H, ArCH<sub>2</sub>), 6.75-7.50 (m, 7H, ArH)

<sup>13</sup>C NMR (250 MHz, CDCl<sub>3</sub>) 19.35, 20.77, 23.72, 35.34, 43.85, 72.14, 124.84, 126.93, 127.63, 128.23, 128.56, 130.64, 133.32, 134.10, 135.13, 147.55

MS 252 (M<sup>+</sup>), 234 (M<sup>+</sup>-18), 219, 202, 143, 132, 115, 105 (base), 91, 77

IR (CDCl<sub>3</sub>) 3580, 3080-2860, 1445, 1225, 1175, 1100

### Products from β-Mesitylisobutyrophenone

The ketone (0.30 g) in cyclohexane (500 ml) was irradiated for 14 days to 100% ketone conversion by GC. The product was isolated by GC at 260°C and identified as 3,5,7-trimethyl-1,2,3,4-tetrahydro-2-naphthol.

#### 3,5,7-Trimethyl-1,2,3,4-Tetrahydro-2-Naphthol

<sup>1</sup>H NMR (250 MHz, CDCl<sub>3</sub>) 0.83 (d, J=7.1 Hz, 3H, CHCH<sub>3</sub>), 1.78 (s, 1H, OH), 2.27 (s, 3H, ArCH<sub>3</sub>), 2.30 (s, 3H, ArCH<sub>3</sub>), 2.38-2.82 (m, 3H, ArCH<sub>2</sub>CHCH<sub>3</sub>), 2.92, 3.48 (AB quartet, J=17.1 Hz, 2H, ArCH<sub>2</sub>), 6.77-7.55 (m, 7H, ArH)

<sup>13</sup>C NMR (250 MHz, CDCl<sub>3</sub>) 15.63, 19.36, 20.77, 32.22, 36.85, 45.87, 74.54, 124.90, 126.38, 127.56, 128.12, 128.58, 131.05, 133.73, 135.10, 136.00, 146.68

MS 266 (M<sup>+</sup>), 248 (M<sup>+</sup>-18), 233, 132, 117, 105 (base), 91, 77

IR (CDCl<sub>3</sub>) 3610, 3100-2840, 1605, 1490, 1450, 1180, 1075

### NMR Studies of Photoproducts from α-(2,4,6-Triisopropylphenyl)-acetophenone and α-(2,4,6-Triisopropylphenyl)acetophenone-d<sub>2</sub>

α-(2,4,6-Triisopropylphenyl)acetophenone 17 in benzene-d<sub>6</sub> in a Pyrex NMR tube was irradiated at 365 nm for 8 hr (sample #1), and 22 hr (sample #2). NMR showed that the area ratio of one of the methyl signals at C1 of the



indanol (0.78 ppm) to the  $\alpha$ -methylene signal of the remained ketone (4.32 ppm) was 1.08 (sample #1) and 1.35 (sample #2). The relative amount of the indanol to the ketone was then 0.72 (sample #1) and 0.90 (sample #2). The area ratio of the vinyl proton signal of the enol (6.13 ppm) to the same methyl signal of the indanol was 1/2.3 (sample #1) and 1/3.5 (sample #2), averaging 1/2.9.

$\alpha$ -(2,4,6-Triisopropylphenyl)acetophenone- $d_2$  17- $d_2$  in  $CCl_4$  in a Pyrex NMR tube was irradiated at 465 nm until the area ratio of the methyl signal (0.78 ppm) at C1 of the indanol to the ortho proton signal of the benzoyl group (8.10 ppm) in the remained ketone reached ca. 0.5 by 60 MHz NMR. The solvent was evaporated and  $CDCl_3$  was added. A 250 MHz NMR was then taken. The area ratio of the same signals was 0.527, indicating a ratio of 0.35 for the indanol and the remained ketone. The area ratio of the  $\alpha$ -methylene signal appearing at 4.45 ppm to the ortho proton signal of the benzoyl group in the ketone was 0.11.

The deuterium NMR of the irradiated sample was taken in  $CHCl_3$  on a Bruker WH-180 spectrometer with a 10 mm broadband probe.

## V. Irradiation in Solid State

Irradiation in solid state has been conducted in powder form or crystal. The ketones to be irradiated were first dissolved in spectral grade methylene chloride, and the resulting solutions were transferred onto small glass plates (2.5x1 cm) to form a liquid layer. The samples were air-dried, and then dried under vacuum. The glass plates were placed in pyrex tubes (100x13 mm) sealed with rubber septa. The samples were irradiated with a medium pressure mercury lamp filtered through an uranium sleeve for ketone 17 and



a Pyrex tube for the others, degassed by means of needles through the septa with argon gas during the reaction.

Alternatively, the ketones can be irradiated in crystalline form. A pyrex test tube (100x13 mm) was stretched and cut in the middle with a natural gas

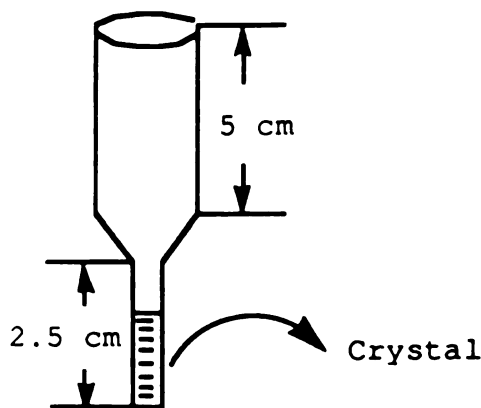


Figure 70

torch (Figure 70). Fine crystals of the ketones were placed in the sealed stretched end of the test tube, which was degassed and irradiated the same way as in the powder reactions with a Pyrex sleeve.

The products were dissolved in benzene and identified by a combination of coinjection with authentic samples on GC or HPLC and spectroscopic data. The product ratios were measured by GC or HPLC.

#### A. In Powder Form

The following ketones have been irradiated in powder form with the general procedure described above.



**$\alpha$ -(o-Tolyl)acetophenone**

The ketone was irradiated for 24 hr, and the product was identified as 2-phenyl-2-indanol by its identical  $^1\text{H}$  NMR spectrum with the authentic sample. The NMR was taken from the reaction mixture without separation.

 **$\alpha$ -(o-Tolyl)propiophenone**

The ketone was irradiated for 24 hr. Two of the products were identified by GC-MS and coinjection with authentic samples on GC as Z-1-methyl-2-phenyl-2-indanol and 2,3-di(o-tolyl)butane. The third product was isolated by GC at  $240^\circ\text{C}$  and characterized as  $\beta$ -(o-tolyl)propiophenone by its identical  $^1\text{H}$  NMR spectrum with the authentic sample. Benzaldehyde was identified by coinjection with the authentic sample. The product ratio was measured by GC. The irradiated sample (0.1 g) was dissolved in 2 ml benzene with 0.004 M heptadecane. Benzaldehyde was analyzed on column #4 at  $100^\circ\text{C}$ . The other components were analyzed on column #2 at  $145^\circ\text{C}$ . The relative area ratio of the components was as follows: indanol/18/(ArCHR) $_2$ /benzaldehyde = 5.07/1.00/1.77/1.20, which was then corrected by multiplying each number with the GC response factors listed in appendix for the individual compounds. The response factor for (ArCHR) $_2$  was estimated to be 0.944 by dividing its number of carbon atoms into 17 (the carbon number of heptadecane). The corrected relative ratio was given as indanol/18/(ArCHR) $_2$ /benzaldehyde = 6.03/1.40/1.67/3.08. The sum of the four numbers was 12.18. The percentage of product distribution was obtained by dividing each of the four numbers by 12.18.



### **$\alpha$ -Mesitylacetophenone**

The ketone was irradiated for 24 hr. 4,6-Dimethyl-2-phenyl-2-indanol and 1,2-dimesitylethane were identified by GC-MS and coinjection with authentic samples on GC. Dibenzil was identified by coinjection with the authentic sample on GC. The product ratio was measured by GC with column # 4 ( 100°C for 5 min and then raising the temperature manually ca. 10°C/min to 165°C). The relative area ratio of the products was indanol/(ArCH<sub>2</sub>)<sub>2</sub>/dibenzil = 41.94/16.94/1.00. The following carbon atom numbers of each compounds were divided into each number in the relative ratio. The carbon atom number was 16.5 for the indanol, 20 for (ArCH<sub>2</sub>)<sub>2</sub>, and 12 for dibenzil (single-oxygen-bonded carbon atom contributes only 0.5 and double-oxygen-bonded carbon atom contributes 0). The corrected ratio was then indanol/(ArCH<sub>2</sub>)<sub>2</sub>/dibenzil = 2.54/0.847/0.0833. The product percentages were obtained by dividing each of the corrected numbers by their sum (3.47).

### **$\alpha$ -(2,4,6-Triisopropylphenyl)acetophenone**

The ketone was irradiated for 48 hr with an uranium sleeve. The products were dissolved in CCl<sub>3</sub>D and characterized. The product ratio was measured by <sup>1</sup>H NMR. The area ratio of the indanol methyl signal at 0.78 ppm to the  $\alpha$ -methylene proton signal of the the ketone at 4.45 ppm was 0.055. The ratio of the vinyl proton signal of the Z-enol at 6.07 pm to the same methyl signal of the indanol was 3.04.

### **B. In Crystal**



The following ketones have been irradiated in crystal with the general procedure described above.

#### **$\alpha$ -(o-Tolyl)propiophenone**

The ketone was irradiated for 36 hr, and the products was identified by coinjection with authentic samples on GC as Z-1-methyl-2-phenyl-2-indanol,  $\beta$ -(o-tolyl)propiophenone and benzaldehyde. The product ratio was measured the same way as in the powder reaction. The uncorrected relative ratio was indanol/18/benzaldehyde = 14.03/1.00/2.70.

#### **$\alpha$ -Mesitylpropiophenone**

The ketone was irradiated for 15 hr to 100% conversion. The major product formed was identified as Z-1,5,7-trimethyl-2-phenyl-2-indanol by its identical  $^1\text{H}$  NMR spectrum taken from the crude product with the authentic sample. There were two small peaks appearing immediately after solvent peak on GC (column #2, 160°C). The area ratio of the indanol to the sum of the small peaks was 99/1.

#### **$\alpha$ -Mesitylvalerophenone**

The ketone was irradiated for 15 hr to 100% conversion. The major product formed was identified as Z-5,7-dimethyl-1-propyl-2-phenyl-2-indanol by its identical  $^1\text{H}$  spectrum taken from the crude product with the authentic sample.

A second experiment was conducted. The ketone was irradiated for 10.5



hr. The irradiation was stopped while the sample remained as crystal. The major product formed was identified as Z-5,7-dimethyl-1-propyl-2-phenyl-2-indanol by its identical  $^1\text{H}$  spectrum taken from the reaction mixture with the authentic sample. The area ratio of the indanol to the starting ketone on GC (column #2, 165 $^{\circ}\text{C}$ ) was 0.29, indicating a conversion of 23%. There were 5 small peaks on GC, two of which appeared immediately after solvent peak. The area ratio of the indanol to the sum of the small peaks was 11/1. One of the peak was identified as  $\alpha$ -mesitylacetophenone, and another 4,6-dimethyl-2-phenyl-2-indanol (type II products) by coinjection with authentic samples on GC. The area ratio of the two peaks to the indanol was 0.0165/1 and 0.0382/1 respectively, which was then corrected by the response factors listed in Appendix and became 0.0192/1 and 0.0422/1.

#### **$\alpha$ -Mesityl- $\alpha$ -Phenylacetophenone**

The ketone was irradiated for 10 days. Since the photoproducts were solid which remained where they were formed, preventing light from penetrating the sample, the reaction seemed to occur only on the surface of the sample. The NMR of the reaction mixture showed that the major product was Z-5,7-dimethyl-1,2-diphenyl-2-indanol (>90%). The enol ethers were not detected by NMR. The area ratio of the methyl signal of the indanol at 2.37 ppm to the ortho benzoyl proton signal of the starting ketone at 7.9 ppm was 1.35, indicating a conversion of 47%.

#### **VI. Irradiation in Cyclodextrin Complexes**

The cyclodextrin complexes of the ketones were prepared by the



following general procedure. The ketones (1 equiv, 0.05-0.20 g) were added to aqueous cyclodextrin solutions (1 equiv). The solutions were stirred overnight. The precipitated complexes were filtered, washed with ether, and dried at 65°C in an oven for 12 hr.  $\alpha$ -(o-Tolyl)propiophenone,  $\alpha$ -(o-tolyl)valerophenone,  $\alpha$ -(o-tolyl)-isobutyrophenone all formed complexes with  $\beta$ -cyclodextrin.  $\alpha$ -Mesitylpropiophenone,  $\alpha$ -mesitylvalerophenone did not form complexes with  $\beta$ -cyclodextrin, however they did form complexes with  $\gamma$ -cyclodextrin.

The saturated aqueous solutions of the complexes (approx. 0.05 g in 500 ml) were irradiated for 36 hr in an irradiator with a medium pressure mercury lamp under argon. The products were extracted with chloroform until no more products could be extracted, and identified by coinjection with authentic sample on GC.

#### **$\alpha$ -(o-Tolyl)isobutyropropiophenone**

All the products have very short retention times on GC with a Magabore DB210 column, indicating the products from cleavage. Benzaldehyde was identified by coinjection with authentic sample on GC.

#### **$\alpha$ -Mesitylpropiophenone**

The major product was Z-1,5,7-trimethyl-2-phenyl-2-indanol, and very small amount of E-5,7-Trimethyl-2-Phenyl-2-Indanol was also identified, by coinjection with authentic samples on GC. The Z/E ratio was 40/1.



## VII. Dynamic NMR Measurements

All the low temperature NMR studies were performed on a Bruker 250 MHz NMR spectrometer with the chosen solvent depending on the temperature ranges.  $\text{CDCl}_3$  was used for  $\alpha$ -mesitylvalerophenone. Acetone- $\text{d}_6$  was used for  $\alpha$ -mesitylpropiophenone. A mixture of  $\text{CD}_2\text{Cl}_2$  and methanol- $\text{d}_4$  (7:1) was used in the cases of  $\alpha$ -(*o*-tolyl)isobutyrophenone and  $\alpha$ -mesitylisobutyrophenone. A mixture of ethanol- $\text{d}_6$  and acetone- $\text{d}_6$  was used for  $\alpha$ -mesityl- $\alpha$ -phenylacetophenone.

The temperature ranges within which DNMR measurements were conducted was 170K-300K for  $\alpha$ -(*o*-tolyl)isobutyrophenone,  $\alpha$ -mesitylisobutyrophenone, and  $\alpha$ -mesityl- $\alpha$ -phenylacetophenone, 200K-320K for  $\alpha$ -mesitylpropiophenone, and 220K-350K for  $\alpha$ -mesitylvalerophenone.

Equation (2) was used to calculate the rotational rate constants at various temperatures.

The linewidths of the broadened merged peaks along with the differences in chemical shift of the separated signals were accessed. The linewidths were measured manually by means of a magnifying glass and a 0.5 mm ruler. For  $\alpha$ -(*o*-tolyl)isobutyrophenone, its  $\alpha$ -methyl signals were measured; for  $\alpha$ -mesitylpropiophenone,  $\alpha$ -mesitylvalerophenone, their mesityl *o*-methyl signals; for  $\alpha$ -mesitylisobutyrophenone, its  $\alpha$ -methyl as well as mesityl *o*-methyl signals; for  $\alpha$ -mesityl- $\alpha$ -phenylacetophenone, its *m*-mesityl proton signals, which was due to the difficulty in measuring its mesityl *o*-methyl signals caused by overlapping with the *p*-mesityl methyl signal.

The raw data are given in Appendix.



## VIII. Molecular Mechanism Calculations

The calculations were performed on an IBM PC with an enhanced graphics adaptor.

MMPMI, an advanced version of MM2 with MMP1 Pi subroutines incorporated for delocalized Pi electron systems by Allinger, was used for molecular mechanics calculations.

STRPI incorporated in MIO by Gilbert and Gajewski was used to generate the structural input for MMPMI.

The additional software were a 4027 emulator and Microsoft Pcp3 (V3.6).

Two dihedral angle drive options were available with MMPMI. The use of dihedral angle drive could insure the findings of all the local minima.

The calculations were generally done in the following way. A structural input was generated with MIO, and submitted to MMPMI for calculations. The resulting output structure was then reinput into MMPMI for a second calculation. The purpose of this procedure was to supply MMPMI with a better input structure. The second calculation was performed with a dihedral angle drive operating first regarding the  $C_{\alpha}$ -CO bond rotation; then this rotation was fixed at angles producing conformations with minimized energies, and a second dihedral angle drive was applied to the rotation of the  $\alpha$ -aryl group. Combinations of the two dihedral drives provided the conformations with energetic minima regarding  $C_{\alpha}$ -CO and  $C_{\alpha}$ -Ar bond rotations. Finally, these energy-minimized structures were used as inputs for calculations without dihedral angle drive for verifications.

For  $\beta$ -arylpropiophenones, there were three bond rotations that need to be examined,  $C_{\alpha}$ -CO,  $C_{\alpha}$ - $C_{\beta}$ , and  $C_{\beta}$ -Ar. The two dihedral drives were not



enough to do calculations with three angles fixed. Thus the third dihedral drive was done by rotating the  $\beta$ -aryl group without fixing the first two dihedral angles. The results showed that rotation of the  $\beta$ -aryl group did not change the first dihedral angles from where they were input, as was hoped.

## IX. X-Ray Crystallography

Samples of  $\alpha$ -mesityl-2,4,6-trimethylacetophenone,  $\alpha$ -mesityl-valerophenone, and  $\alpha$ -mesityl- $\alpha$ -phenylacetophenone were dissolved in ethanol in a vial. The resulted solution was then poured in a Petri dish, and allowed to stand for 2-3 days until the crystal started to grow. The solvent was removed by a disposable pipet, and the crystal was washed quickly with cold ethanol, and dried by air. The samples were submitted to Dr. D. Ward. The data collections were performed with Mo  $K_{\alpha}$  radiation ( $\lambda = 0.71073$  Å) on a Nicolet P3F diffractometer. The structures were solved by direct methods. The X-ray structures of the ketones are given in the result section (Figure 27-29), and the crystallographic parameters are presented in the appendix.



## Appendix



**Table 24. Kinetic Data of C<sub>α</sub>-CO Bond Rotation for α-(o-Tolyl)-isobutyrophenone**

$$\Delta\nu = 0.24 \text{ ppm} = 60 \text{ Hz}, \omega (300\text{K}) = 0.007 \text{ ppm}$$

T(K)	185	190	195	200
ω(ppm)	0.20	0.09	0.06	0.03
ω(Hz)	50	22.5	15	7.5
k(s <sup>-1</sup> )	156	282	399	896
1/Tx10 <sup>3</sup>	5.41	5.26	5.13	5.00
lnk	5.05	5.64	5.99	6.63

**Table 25. Kinetic Data of C<sub>α</sub>-Mes Bond Rotation for α-Mesityl-propiofenone**

$$\Delta\nu = 0.69 \text{ ppm} = 173 \text{ Hz}, \omega(320\text{K}) = 0.013 \text{ ppm}$$

T(K)	250	260	270	280	290
ω(ppm)	0.30	0.17	0.09	0.05	0.03
ω(Hz)	75	42.5	22.5	12.5	7.5
k(s <sup>-1</sup> )	723	1170	2117	3770	6260
1/Tx10 <sup>3</sup>	4.00	3.85	3.70	3.57	3.45
lnk	6.58	7.06	7.66	6.23	8.74



Table 26. Kinetic Data of C<sub>α</sub>-Mes Bond Rotation for α-Mesityl-valerophenone

$$\Delta\nu = 0.56 \text{ ppm} = 140 \text{ Hz}, \omega(330\text{K}) = 0.02 \text{ ppm}$$

T(K)	280	290	300	310	320
$\omega(\text{ppm})$	0.20	0.16	0.09	0.06	0.04
$\omega(\text{Hz})$	50	40	22.5	15	10
$k(\text{s}^{-1})$	625	827	1400	2070	3090
$1/T \times 10^3$	3.57	3.45	3.33	3.23	3.13
lnk	6.44	6.72	7.24	7.64	8.04

Table 27. Kinetic Data of C<sub>α</sub>-CO Bond Rotation for α-Mesityl-isobutyrophenone

$$\Delta\nu = 0.19 \text{ ppm} = 48 \text{ Hz}, \omega(300\text{K}) = 0.003 \text{ ppm}$$

T(K)	185	190	200	210
$\omega(\text{ppm})$	0.22	0.12	0.05	0.03
$\omega(\text{Hz})$	55	30	12.5	7.5
$k(\text{s}^{-1})$	89	152	305	489
$1/T \times 10^3$	5.41	5.26	5.00	4.76
lnk	4.49	5.02	5.72	6.19



Table 28. Kinetic Data of C<sub>α</sub>-Mes Bond Rotation for α-Mesityl-isobutyrophenone

$$\Delta\nu = 0.72 \text{ ppm} = 180 \text{ Hz}, \omega(300\text{K}) = 0.005 \text{ ppm}$$

T(K)	210	220	230	240
$\omega(\text{ppm})$	0.14	0.06	0.03	0.02
$\omega(\text{Hz})$	35	15	7.5	5
$k(\text{s}^{-1})$	1510	3410	6790	10200
$1/T \times 10^3$	5.41	5.26	5.13	5.00
$\ln k$	5.12	5.63	6.14	6.80

Table 29. Kinetic Data of C<sub>α</sub>-Mes Bond Rotation for α-Mesityl-α-Phenylacetophenone

$$\Delta\nu = 0.26 \text{ ppm} = 64 \text{ Hz}, \omega(300\text{K}) = 0.007 \text{ ppm}$$

T(K)	180	185	190	210	230
$\omega(\text{ppm})$	0.29	0.19	0.11	0.02	0.014
$\omega(\text{Hz})$	72.5	47.5	27.5	5	2.5
$k(\text{s}^{-1})$	125	184	273	1314	2616
$1/T \times 10^3$	5.56	5.41	5.26	4.76	4.35
$\ln k$	4.83	5.21	5.61	7.18	7.87



Table 30. Quenching Indanol Formation from  $\alpha$ -(o-Tolyl)-p-Methoxyacetophenone with 2,5-Dimethyl-2,4-Hexadiene in Benzene at 313 nm

HPLC analysis with ultrasphere Si column  
Hexane/ethyl acetate 95:5, 1.5 ml/min  
Methyl benzoate as internal standard (0.00264 M)

$[Q], 10^{-4} \text{ M}$	$A(\text{photo})/A(\text{std})$	$\Phi^0/\Phi$
0.000	0.782 (0.778, 0.786)	
0.880	0.641	1.20
1.76	0.492	1.59
3.51	0.399	1.96
4.33	0.348	2.25
5.20	0.310	2.52

[Ketone] = 0.015 M, [Indanol] = 0.000782 M

Table 31. Quenching Benzaldehyde Formation From  $\alpha$ -(o-Tolyl)-propiophenone with Naphthalene in Benzene with 0.007 M Dodecanthiol at 365 nm

HPLC analysis with ultrasphere Si column  
Hexane/ethyl acetate 99:1, 1.2 ml/min  
Octyl benzoate as internal standard (0.00726 M)

$[Q], 10^{-2} \text{ M}$	$A(\text{photo})/A(\text{std})$	$\Phi^0/\Phi$
0.00	0.726 (0.714, 0.738)	
1.36	0.407	1.78
2.72	0.228	3.18
5.45	0.120	6.05
8.17	0.0825	8.80
9.53	0.0727	9.99

[Ketone] = 0.042 M, [Benzaldehyde] = 0.00482 M



Table 32. Quenching Benzaldehyde Formation from  $\alpha$ -(o-Tolyl)-propiophenone with Naphthalene in Benzene with 0.007 M Dodecanthiol at 365 nm

HPLC analysis with ultrasphere Si column  
Hexane/ethyl acetate 99:1, 1.2 ml/min  
Octyl benzoate as internal standard (0.00810 M)

$[Q], 10^{-2} \text{ M}$	$A(\text{photo})/A(\text{std})$	$\Phi^0/\Phi$
0.00	0.698	
0.508	0.506	1.38
1.02	0.369	1.89
1.52	0.278	2.51
2.03	0.242	2.88
2.54	0.217	3.21

[Ketone] = 0.045 M, [Benzaldehyde] = 0.00517 M

Table 33. Quenching  $\alpha$ -(o-Tolyl)acetophenone Formation from  $\alpha$ -(o-Tolyl)valerophenone with 2,5-Dimethyl-2,4-Hexadiene in Benzene at 313 nm

GC analysis with column #1, 230°C  
Pentadecane as internal standard (0.00930 M)

$[Q], 10^{-1} \text{ M}$	$A(\text{photo})/A(\text{std})$	$\Phi^0/\Phi$
0.00	0.207 (0.207, 0.206)	
0.260	0.118	1.75
0.520	0.0807	2.56
0.780	0.0649	3.19
1.04	0.0533	3.88
1.56	0.0386	5.36

[Ketone] = 0.028 M, [Product] = 0.00222 M



Table 34. Quenching  $\alpha$ -(o-Tolyl)acetophenone Formation from  $\alpha$ -(o-Tolyl)valerophenone with 2,5-Dimethyl-2,4-Hexadiene in Benzene at 313 nm

GC analysis with column #1, 230°C  
Pentadecane as internal standard (0.00388 M)

$[Q], 10^{-2} \text{ M}$	$A(\text{photo})/A(\text{std})$	$\Phi^o/\Phi$
0.00	0.347 (0.362, 0.332)	
0.520	0.283	1.23
1.04	0.257	1.35
1.56	0.231	1.50
2.08	0.225	1.54
2.60	0.208	1.67
3.12	0.184	1.89

[Ketone] = 0.020, [Product] = 0.00155 M



Table 35. Quenching Benzaldehyde Formation from  $\alpha$ -(o-Tolyl)-isobutyrophenone with Naphthalene in Benzene with 0.007 M Dodecanthiol at 365 nm

HPLC analysis with ultrasphere Si column  
Hexane/ethyl acetate 99:1, 1.2 ml/min  
Octyl benzoate as internal standard (0.00718 M)

$[Q], 10^{-2} \text{ M}$	A(photo)/A(std)	$\Phi^0/\Phi$
0.00	0.814 (0.817, 0.811)	
0.942	0.401	2.02
1.88	0.248	3.31
2.83	0.184	4.42
3.77	0.143	5.69
4.71	0.124	6.56
5.65	0.104	7.83

[Ketone] = 0.035 M, [Benzaldehyde] = 0.00536 M

Table 36. Quenching Benzaldehyde Formation from  $\alpha$ -(o-Tolyl)-isobutyrophenone with Naphthalene in Benzene with 0.007 M Dodecanthiol at 365 nm

HPLC analysis with ultrasphere Si column  
Hexane/ethyl acetate 99:1, 1.2 ml/min  
Octyl benzoate as internal standard (0.00800 M)

$[Q], 10^{-2} \text{ M}$	A(photo)/A(std)	$\Phi^0/\Phi$
0.00	0.581 (0.572, 0.590)	
0.22	0.484	1.20
0.44	0.385	1.51
0.66	0.352	1.65
0.88	0.301	1.93
1.11	0.270	2.15

[Ketone] = 0.045 M, [Benzaldehyde] = 0.0042 M



Table 37. Quenching Indanol Formation from  $\alpha$ -Mesitylpropio-phenone with Naphthalene in Benzene at 365 nm

GC analysis with column #1, 250°C  
Octadecane as internal standard (0.00738 M)

$[Q], 10^{-2} \text{ M}$	A(photo)/A(std)	$\Phi^0/\Phi$
0.00	0.367 (0.370, 0.364)	
1.87	0.271	1.35
3.74	0.221	1.66
5.62	0.185	1.98
7.49	0.164	2.24
9.36	0.144	2.55
10.3	0.111	3.31

[Ketone] = 0.027 M, [Indanol] = 0.00290 M

Table 38. Quenching Indanol Formation from  $\alpha$ -Mesitylpropio-phenone with Naphthalene in Benzene at 365 nm

GC analysis with column #1, 250°C  
Octadecane as internal standard (0.00351 M)

$[Q], 10^{-1} \text{ M}$	A(photo)/A(std)	$\Phi^0/\Phi$
0.00	0.538 (0.551, 0.525)	
0.368	0.294	1.83
0.735	0.226	2.38
1.10	0.171	3.15
1.47	0.142	3.78

[Ketone] = 0.025 M, [Indanol] = 0.00202 M



**Table 39. Quenching Indanol Formation from  $\alpha$ -Mesitylvalerophenone with Naphthalene in Benzene at 365 nm**

GC analysis with column #1, 250°C  
Nonadecane as internal standard (0.00573 M)

$[Q], 10^{-1} \text{ M}$	A(photo)/A(std)	$\Phi^o/\Phi$
0.00	0.436 (0.432, 0.441)	
0.871	0.323	1.35
1.74	0.246	1.77
2.61	0.200	2.13
3.48	0.158	2.75
4.35	0.125	3.49
5.22	0.107	4.07
6.09	0.0915	4.77

[Ketone] = 0.033 M, [Indanol] = 0.00287



Table 40. Quenching Indanol Formation from  $\alpha$ -Mesitylvalerophenone with Naphthalene in Benzene at 365 nm

GC analysis with column #2, 165°C  
Nonadecane as internal standard (0.00718 M)

$[Q], 10^{-1} \text{ M}$	A(photo)/A(std)	$\Phi^0/\Phi$
0.00	0.551 (0.537, 0.564)	
0.964	0.381	1.45
1.93	0.284	1.94
2.89	0.228	2.42
3.85	0.190	2.90
4.82	0.160	3.44
5.78	0.132	4.17
6.75	0.112	4.92
8.67	0.0842	6.54
10.6	0.0687	8.02
12.5	0.00516	10.6

[Ketone] = 0.047 M, [Indanol] = 0.00455



Table 41. Quenching Benzaldehyde Formation from  $\alpha$ -Mesityl-isobutyrophenone with Naphthalene in Benzene with 0.007 M Dodecanthiol at 365 nm

HPLC analysis with ultrasphere Si column  
Hexane/ethyl acetate 99:1, 1.2 ml/min  
Octyl benzoate as internal standard (0.00688 M)

[Q], M	A(photo)/A(std)	$\Phi^0/\Phi$
0.000	0.290 (0.289, 0.284, 0.297)	
0.103	0.159	1.82
0.206	0.115	2.52
0.309	0.0904	3.21
0.412	0.0706	4.11
0.515	0.0588	4.74

[Ketone] = 0.022 M, [Benzaldehyde] = 0.00182 M

Table 42. Quenching Benzaldehyde Formation from  $\alpha$ -Mesityliso-butyrophenone with Naphthalene in Benzene with 0.007 M Dodecanthiol at 365 nm

HPLC analysis with ultrasphere Si column  
Hexane/ethyl acetate 99:1, 1.2 ml/min  
Octyl benzoate as internal standard (0.00663 M).

[Q], $10^{-1}$ M	A(photo)/A(std)	$\Phi^0/\Phi$
0.000	0.311 (0.301, 0.320)	
0.557	0.257	1.21
1.11	0.214	1.45
1.67	0.166	1.87
2.23	0.139	2.23

[Ketone] = 0.023 M, [Benzaldehyde] = 0.00188 M



Table 43. Quenching Indanol Formation from  $\alpha$ -Mesityl- $\alpha$ -Phenyl-acetophenone with 2,5-Dimethyl-2,4-Hexadiene in Benzene at 365 nm

HPLC analysis with ultrasphere Si column  
Hexane/ethyl acetate 99:1, 1.2 ml/min  
Methyl benzoate as internal standard (0.00870 M)

[Q], M	A(photo)/A(std)	$\Phi^0/\Phi$
0.00	0.257 (0.256, 0.258)	
0.167	0.225	1.14
0.334	0.200	1.29
0.500	0.179	1.44
0.834	0.151	1.71
1.00	0.132	1.95
1.57	0.104	2.47

[Ketone] = 0.033 M, [Indanol] = 0.00175 M



Table 44. Quenching Indanol Formation from  $\alpha$ -Mesityl- $\alpha$ -Phenyl-acetophenone with 2,5-Dimethyl-2,4-Hexadiene in Hexane at 365 nm

HPLC analysis with ultrasphere Si column  
Hexane/ethyl acetate 99:1, 1.2 ml/min  
Methyl benzoate as internal standard (0.00430 M)

[Q], M	A(photo)/A(std)	$\Phi^0/\Phi$
0.00	0.159	
0.265	0.140	1.14
0.529	0.103	1.54
0.793	0.0826	1.92
1.32	0.0712	2.24
1.59	0.0621	2.56

[Ketone] = 0.027, [Indanol] = 0.000539



The area ratios of the enol ethers (ketone 8, 9, 10) to the standards are given in a combined form for the Z and E isomers, and corrected by the response factors  $A(\text{photo})/A(\text{std}) = [A^E(\text{photo}) \times R_f^E + A^Z(\text{photo}) \times R_f^Z]/A(\text{std})$ . The ratios of Z/E isomers at different ketone conversions are given in table 64.

Table 45. Quenching Aryl Vinyl Ether Formation from  $\alpha$ -Mesityl- $\alpha$ -Phenylacetophenone with 2,5-Dimethyl-2,4-Hexadiene in Hexane at 365 nm

HPLC analysis with ultrasphere Si column  
Hexane/ethyl acetate 99:1, 1.2 ml/min  
Methyl benzoate as internal standard (0.00432 M)

$[Q]$ , M	$A(\text{photo})/A(\text{std})^a$	$\Phi^o/\Phi$
0.00	0.159 (0.158, 0.159)	
0.265	0.130	1.22
0.529	0.113	1.41
0.794	0.0957	1.66
1.06	0.0862	1.84
1.32	0.0772	2.05
1.59	0.0714	2.22
2.21	0.0574	2.77

[Ketone] = 0.027 M, [Enol Ether] = 0.000687



Table 46. Quenching Indanol Formation from  $\alpha$ -Mesityl- $\alpha$ -Phenyl-  
p-Methoxyacetophenone with Naphthalene in Benzene at  
365 nm

HPLC analysis with ultrasphere Si column  
Hexane/ethyl acetate 97:3, 1.2 ml/min  
Butyl p-methoxybenzoate as internal standard (0.00300 M)

$[Q], 10^{-1} \text{ M}$	A(photo)/A(std)	$\Phi^{\circ}/\Phi$
0.00	0.225 (0.227, 0.223)	
0.0133	0.149	1.51
0.0268	0.104	2.16
0.0399	0.0784	2.88
0.0532	0.0658	3.42
0.0665	0.0558	4.03

[Ketone] = 0.037 M, [Indanol] = 0.00196 M

Table 47. Quenching Indanol Formation from  $\alpha$ -Mesityl- $\alpha$ -Phenyl-  
p-Methoxyacetophenone with Naphthalene in Benzene  
at 365 nm

HPLC analysis with ultrasphere Si column  
Hexane/ethyl acetate 97:3, 1.2 ml/min  
Butyl p-methoxybenzoate as internal standard (0.00602 M)

$[Q], 10^{-1} \text{ M}$	A(photo)/A(std)	$\Phi^{\circ}/\Phi$
0.00	0.281 (0.275, 0.287)	
0.00984	0.170	1.65
0.0197	0.132	2.13
0.0295	0.115	2.44
0.0394	0.0926	2.88
0.0492	0.0849	3.31

[Ketone] = 0.047 M, [Indanol] = 0.00491 M



Table 48. Quenching Aryl Vinyl Ether Formation from  $\alpha$ -Mesityl- $\alpha$ -Phenyl-p-Methoxyacetophenone with Naphthalene in Benzene at 365 nm

HPLC analysis with ultrasphere Si column  
Hexane/ethyl acetate 97:3, 1.2 ml/min  
Butyl p-methoxybenzoate as internal standard (0.00300 M)

$[Q], 10^{-1} \text{ M}$	A(photo)/A(std)	$\Phi^0/\Phi$
0.00	0.231 (0.227, 0.235)	
0.0133	0.147	1.57
0.0268	0.108	2.14
0.0399	0.0846	2.73
0.0532	0.0731	3.16
0.0665	0.0605	3.82

[Ketone] = 0.037 M, [Enol Ether] = 0.000693 M

Table 49. Quenching Aryl Vinyl Ether Formation from  $\alpha$ -Mesityl- $\alpha$ -Phenyl-p-Methoxyacetophenone with Naphthalene in Benzene at 365 nm

HPLC analysis with ultrasphere Si column  
Hexane/ethyl acetate 97:3, 1.2 ml/min  
Butyl p-methoxybenzoate as internal standard [0.00602 M]

$[Q], 10^{-1} \text{ M}$	A(photo)/A(std)	$\Phi^0/\Phi$
0.00	0.272 (0.276, 0.268)	
0.00984	0.188	1.45
0.0197	0.137	1.98
0.0295	0.119	2.28
0.0492	0.0862	3.16

[Ketone] = 0.047 m, [Enol Ether] = 0.00164 M



Table 50. Quenching Aryl Vinyl Ether Formation from  $\alpha$ -Mesityl- $\alpha$ -Phenyl-p-Cyanoacetophenone with 2,5-Dimethyl-2,4-Hexadiene in Benzene at 365 nm

HPLC analysis with ultrasphere Si column  
Hexane/ethyl acetate 95:5, 1.2 ml/min  
Benzene as internal standard (0.00580 M)

$[Q], 10^{-1} \text{ M}$	A(photo)/A(std)	$\Phi^o/\Phi$
0.00	0.0729 (0.0747, 0.0712)	
0.244	0.0550	1.33
0.488	0.0452	1.61
0.732	0.0369	1.98
0.976	0.0341	2.14
1.22	0.0293	2.49
1.46	0.0264	2.76

[Ketone] = 0.015 M, [Enol Ether] = 0.000423 M



Table 51. Quenching Mesitaldehyde Formation from  $\alpha$ -Phenyl-2,4,6-Trimethylacetophenone with 2,5-Dimethyl-2,4-Hexadiene in Benzene with 0.007 M Dodecanthiol at 313 nm

HPLC analysis with ultrasphere Si column  
Hexane/ethyl acetate 99:1, 1.2 ml/min  
Octyl benzoate as internal standard (0.00938 M)

[Q], M	A(photo)/A(std)	$\Phi^0/\Phi$
0.00	0.737 (0.731, 0.744)	
0.127	0.577	1.28
0.253	0.387	1.90
0.380	0.294	2.50
0.506	0.261	2.82
0.633	0.218	3.40
0.760	0.193	3.82

[Ketone] = 0.021 M, [Mesitaldehyde] = 0.000465 M



Table 52. Quenching Indanol Formation from  $\alpha$ -Mesityl-o-Methyl-acetophenone with Naphthalene in Benzene at 365 nm

GC analysis with column #1, 250°C  
Nonadecane as internal standard (0.00600 M)

$[Q], 10^{-1} \text{ M}$	A(photo)/A(std)	$\Phi^o/\Phi$
0.00	0.472 (0.461, 0.483)	
0.125	0.352	1.34
0.251	0.311	1.52
0.376	0.274	1.72
0.501	0.230	2.05
0.626	0.217	2.18
0.752	0.193	2.45

[Ketone] = 0.040 M, [Indanol] = 0.00360 M

Table 53. Quenching Indanol Formation from  $\alpha$ -Mesityl-o-Methyl-acetophenone with Naphthalene in Benzene at 365 nm

GC analysis with column #1, 250°C  
Nonadecane as internal standard (0.00356 M)

$[Q], 10^{-1} \text{ M}$	A(photo)/A(std)	$\Phi^o/\Phi$
0.00	0.859	
0.775	0.687	1.25
1.55	0.636	1.35
2.33	0.511	1.68
3.10	0.452	1.90

[Ketone] = 0.033 M, [Indanol] = 0.00356 M



Table 54. Quenching Mesitaldehyde Formation from  $\alpha$ -Mesityl-2,4,6-Trimethylacetophenone with 2,5-Dimethyl-2,4-Hexadiene in Benzene with 0.007 M Dodecanthiol at 313 nm

HPLC analysis with ultrasphere Si column  
Hexane/ethyl acetate 99:1, 1.2 ml/min  
Octyl benzoate as internal standard (0.00864 M)

$[Q], 10^{-1} \text{ M}$	A(photo)/A(std)	$\Phi^0/\Phi$
0.000	1.95 (1.87, 2.03)	
0.383	1.71	1.14
0.765	1.45	1.34
1.15	1.12	1.74
1.53	0.941	2.07
2.30	0.632	3.09
3.44	0.504	3.87
4.59	0.470	4.15
5.74	0.404	4.83

[Ketone] = 0.021 M, [Mesitaldehyde] = 0.00113 M



Table 55. Quenching Mesitaldehyde Formation from  $\alpha$ -Mesityl-2,4,6-Trimethylacetophenone with 2,5-Dimethyl-2,4-Hexadiene in Benzene with 0.007 M Dodecanthiol at 313 nm

HPLC analysis with ultrasphere Si column  
Hexane/ethyl acetate 99:1, 1.2 ml/min  
Octyl benzoate as internal standard (0.00854 M)

$[Q], 10^{-1} \text{ M}$	A(photo)/A(std)	$\Phi^0/\Phi$
0.000	1.39 (1.40, 1.38, 1.40)	
0.220	1.19	1.17
0.440	1.12	1.25
0.659	1.01	1.38
0.879	0.913	1.53
1.10	0.874	1.59
1.32	0.809	1.72
1.76	0.645	2.16
2.20	0.525	2.65
2.42	0.451	3.09
3.08	0.366	3.81
3.74	0.346	4.03
4.40	0.315	4.42
5.06	0.296	4.71
6.37	0.254	5.48
7.20	0.234	5.95
7.92	0.215	6.48
8.64	0.208	6.70
9.36	0.190	7.33

[Ketone] = 0.020 M, [Mesitaldehyde] = 0.000789 M



Table 56. Quenching Mesitaldehyde Formation from  $\alpha$ -Mesityl- $\alpha$ -Phenyl-2,4,6-Trimethylacetophenone with 2,5-Dimethyl-2,4-Hexadiene in Benzene with 0.007 M Dodecanthiol at 313 n

HPLC analysis with ultrasphere Si column  
Hexane/ethyl acetate 99:1, 1.2 ml/min  
Butyl p-methoxybenzoate as internal standard (0.00730 M)

[Q], M	A(photo)/A(std)	$\Phi^0/\Phi$
0.000	0.583 (0.600, 0.561, 0.588)	
0.244	0.464	1.26
0.487	0.441	1.32
0.741	0.403	1.45
0.975	0.360	1.62
1.34	0.289	2.02
1.70	0.279	2.09

[Ketone] = 0.026 M, [Mesitaldehyde] = 0.00165 M



Table 57. Quenching Mesitaldehyde Formation from  $\alpha$ -Mesityl- $\alpha$ -Phenyl-2,4,6-Trimethylacetophenone with 2,5-Dimethyl-2,4-Hexadiene in Benzene with 0.007 M Dodecanthiol at 313 nm

HPLC analysis with ultrasphere Si column  
Hexane/ethyl acetate 99:1, 1.2 ml/min  
Butyl p-methoxybenzoate as internal standard (0.00681 M)

[Q], M	A(photo)/A(std)	$\Phi^0/\Phi$
0.000	0.510 (0.504, 0.516)	
0.394	0.389	1.31
0.788	0.295	1.73
1.18	0.256	1.99
1.97	0.196	2.60

[Ketone] = 0.028 M, [Mesitaldehyde] = 0.00135 M

Table 58. Quenching Tetralol Formation from  $\beta$ -(o-Tolyl)-isobutyrophenone with 2,5-Dimethyl-2,4-Hexadiene in Benzene at 313 nm

GC analysis with column #2, 155°C  
Eicosane as internal standard (0.00850 M)

[Q], M	A(photo)/A(std)	$\Phi^0/\Phi$
0.000	0.0254	
0.109	0.0143	1.78
0.218	0.00897	2.83
0.327	0.00715	3.60
0.435	0.00557	4.56
0.544	0.00470	5.39

[Ketone] = 0.059 M, [Tetralol] = 0.000250 M



Table 59. Quenching Tetralol Formation from  $\beta$ -Mesitylisobutyrophenone with 2,5-Dimethyl-2,4-Hexadiene in Benzene at 313 nm

GC analysis with column #3, temperature programming, 90°C for 5 min, 5°C/min to 160°C.  
Nonadecane as internal standard (0.00658 M)

$[Q], 10^{-1} \text{ M}$	A(photo)/A(std)	$\Phi^{\circ}/\Phi$
0.000	0.264 (0.274, 0.264)	
0.964	0.175	1.51
1.93	0.134	1.97
2.89	0.104	2.54
3.87	0.0864	3.06
4.82	0.0730	3.62

[Ketone] = 0.042 M, [Tetralol] = 0.00230 M

Table 60. Quenching Tetralol Formation from  $\beta$ -Mesitylisobutyrophenone with 2,5-Dimethyl-2,4-Hexadiene in Benzene at 313 nm

GC analysis with column #3, temperature programming, 90°C for 5 min, 5°C/min to 160°C.  
Nonadecane as internal standard (0.00706 M)

$[Q], 10^{-1} \text{ M}$	A(photo)/A(std)	$\Phi^{\circ}/\Phi$
0.000	0.222	
0.452	0.166	1.34
0.905	0.145	1.53
1.36	0.108	2.05
2.27	0.0899	2.47

[Ketone] = 0.046 M, [Tetralol] = 0.00207 M



**Table 61. Quenching Tetralol Formation from  $\beta$ -Mesitylpropio-phenone with 2,5-Dimethyl-2,4-Hexadiene in Benzene at 313 nm**

GC analysis with column #1, 160°C  
Eicosane as internal standard (0.00346 M)

[Q], M	A(photo)/A(std)	$\Phi^0/\Phi$
0.000	0.0751 (0.0738, 0.0764)	
0.113	0.0527	1.43
0.227	0.0376	2.00
0.340	0.0298	2.52
0.454	0.0234	3.21
0.567	0.0187	4.02

[Ketone] = 0.052 M, [Tetralol] = 0.000320 M



Table 62. GC Response Factors

<u>Compounds</u>	<u>Standard</u>	<u>Condition<sup>a</sup></u>	<u>R<sub>f</sub></u>
<u>Z-1-Methyl-2-Phenyl-2-Indanol</u>	Heptadecane	#1, 210 <sup>o</sup> c	1.19
<u>α-(o-Tolyl)acetophenone</u>	Pentadecane	#1, 230 <sup>o</sup> c	1.15
<u>Z-1,5,7-Trimethyl-2-Phenyl-2-Indanol</u>	Octadecane	#1, 250 <sup>o</sup> c	1.07
<u>E-1,5,7-Trimethyl-2-Phenyl-2-Indanol</u>	Octadecane	#1, 250 <sup>o</sup> c	1.07
<u>1-Mesitoxo-1-Phenylpropene</u>	Octadecane	#1, 250 <sup>o</sup> c	1.06
<u>Z-5,7-Dimethyl-2-Phenyl-1-propyl-2-Indanol</u>	Nonadecane	#1, 250 <sup>o</sup> c	1.15
<u>3,5-Dimethyl-2-(o-Tolyl)indene</u>	Nonadecane	#1, 250 <sup>o</sup> c	1.27
<u>3-Methyl-1,2,3,4-Tetrahydro-2-Tetralol</u>	Eicosane	#2, 155 <sup>o</sup> c	1.16
<u>5,7-Dimethyl-1,2,3,4-Tetrahydro-2-Tetralol</u>	Eicosane	#2, 160 <sup>o</sup> c	1.23
<u>3,5,7-Trimethyl-1,2,3,4-Tetrahydro-2-Tetralol</u>	Nonadecane	T Program <sup>b</sup>	1.32
	Heptadecane	#4, 100 <sup>o</sup> c	2.57
<u>Benzaldehyde</u>	Pentadecane	T Program <sup>c</sup>	2.16
<u>p-Methoxybenzaldehyde</u>	Pentadecane	T Program <sup>d</sup>	2.22
<u>p-Cyanobenzaldehyde</u>	Pentadecane	T Program <sup>d</sup>	2.18
<u>4,6-Dimethyl-2-Phenyl-2-Indanol</u>	Nonadecane	#2, 165 <sup>o</sup> c	1.27
<u>α-Mesitylacetophenone</u>	Nonadecane	#2, 165 <sup>o</sup> c	1.34

a. Column #, temperature. b. #3, 90<sup>o</sup>c for 5 min, 5<sup>o</sup>c/min to 160<sup>o</sup>c. c. #3, 70<sup>o</sup>c, for 8 min, 5<sup>o</sup>c/min to 130<sup>o</sup>c. d. #3, 80<sup>o</sup>c, for 8 min, 5<sup>o</sup>c/min to 130<sup>o</sup>c.



Table 63. HPLC Response Factors<sup>a</sup>

Compounds	Standard	R <sub>f</sub>
<u>2-(p-Methoxyphenyl)-2-Indanol<sup>b</sup></u>	Methyl Benzoate	0.379
<u>3,5-Dimethyl-2-phenyl-2-Indanol<sup>c</sup></u>	Methyl Benzoate	0.767
4,6-Diisopropyl-1,1-Dimethyl- <u>2-Phenyl-2-Indanol<sup>c</sup></u>	3,5-Dimethoxybenzonitrile	1.64
<u>Z-5,7-Dimethyl-1,2-Diphenyl-2-Indanol<sup>d</sup></u>	Methyl Benzoate	0.784
<u>E-1-Mesitoxyl-1,2-Diphenylethylene<sup>d</sup></u>	Methyl Benzoate	0.217
<u>Z-1-Mesitoxyl-1,2-Diphenylethylene<sup>d</sup></u>	Methyl Benzoate	0.115
Z-5,7-Dimethyl-2-(p-Methoxyphenyl)- <u>1-Phenyl-2-Indanol<sup>e</sup></u>	Butyl p-Methoxybenzoate	2.90
E-1-Mesitoxyl-1-(p-Methoxyphenyl)- <u>2-Phenylethylene<sup>e</sup></u>	Butyl p-Methoxybenzoate	0.391
Z-1-Mesitoxyl-1-(p-Methoxyphenyl)- <u>2-Phenylethylene<sup>e</sup></u>	Butyl p-Methoxybenzoate	0.328
Z-5,7-Dimethyl-2-(p-Cyanophenyl)- <u>1-Phenyl-2-Indanol<sup>f</sup></u>	p-Chlorobenzyl Cyanide	0.175
E-1-Mesitoxyl-1-(p-Cyanophenyl)- <u>2-Phenylethylene<sup>f</sup></u>	p-Chlorobenzyl Cyanide	0.0469
Z-1-Mesitoxyl-1-(p-Cyanophenyl)- <u>2-Phenylethylene<sup>f</sup></u>	p-Chlorobenzyl Cyanide	0.0224
	Methyl Benzoate	0.960
<u>Benzaldehyde<sup>d</sup></u>	Octyl Benzoate	0.914
<u>o-Tolaldehyde<sup>d</sup></u>	Octyl Benzoate	1.18
	Butyl p-Methoxybenzoate	0.388
<u>Mesitaldehyde<sup>d</sup></u>	Octyl Benzoate	0.0672



Table 63 (cont'd)

a. Ultrasphere Si column, ethyl acetate in hexane as eluent. b. 5%, 1.5 ml/min. c. 2%, 1.5 ml/min. d. 1%, 1.2 ml/min. e. 3%, 1.2 ml/min. f. 5%, 1.2 ml/min.



Table 64. Uncorrected HPLC Z/E Ratios of Aryl Vinyl Ethers

Aryl Vinyl Ether <sup>a</sup>	Absorbance (365 nm)	Z/E Ratio at Normal Conversion <sup>b</sup>	Z/E Ratio at Low Conversion <sup>b</sup>	Z/E Ratio at Equilibrium <sup>c</sup>
Z	7	0.025M/8%	0.1M/0.16%	
8 AVE E	47	10.9/1.0	2.3/1.0	10.8/1.0
Z	12	0.036M/8%	0.1M/0.09%	
2 AVE E	63	7.3/1.0	1.9/1.0	7.2/1.0
Z	1100	0.015M/6%	0.1M/0.10%	
10 AVE E	620	1.0/0.86	1.0/0.48	1.0/0.86

a. # AVE--aryl vinyl ethers from ketone #. b. Top--initial ketone concentration with conversion, bottom--Z/E ratio. c. Prolonged irradiation of isolated aryl vinyl ethers.







Table 65. Quantum Yields of Photoproducts from  $\alpha$ -Arylacetophenone Derivatives

		Actinometry <sup>j</sup>				
Ketone Product <sup>a</sup>	Solvent <sup>b</sup>	Analysis <sup>c</sup> [K] <sup>d</sup>	[Std] <sup>e</sup>	$f A_p/A_{std}$	[P] <sup>g</sup>	$[AP]^h i \times 10^2$
<u>1</u>	Indanol	Benzene	S	0.015 BC1/0.00264	0.778/0.786	7.78/7.86E-4 0.153
		Benzene	Con 1	0.023 C17/0.00236	0.417/0.421	1.17/1.18E-3 0.00795 2.41
		0.5M Pyr	Con 1	0.023 C17/0.00370	8.91/8.39E-2	3.92/3.69E-4 0.00835 2.50
		t-BuOH	Con 1	0.024 C17/0.00536	9.67/10.5E-2	6.68/6.17E-4 0.0119 3.61
	Indanol	MeCN/H <sub>2</sub> O	Con 1	0.022 C17/0.00412	0.151/0.158	7.42/7.73E-4 0.0119 3.61
<u>2</u>	Aldehyde	Benzene	S	0.022 BC8/0.00712	0.136/0.136	8.91/8.91E-4 0.00104 0.315
<u>2-d</u>	Indanol	Benzene	S	0.029 C17/0.00557	0.124/0.118	8.22/7.82E-4 0.00604 1.83
		Benzene	S	0.028 C15/0.00930	0.207/0.206	2.21/2.22E-3 0.0120 3.64
	Type II	MeOH	Con 2	0.026 C15/0.00504	0.219/0.205	1.27/1.19E-3 0.00202 0.612
<u>3</u>	Indanol	MeOH	Con 2	0.026 C15/0.00504	1.67/1.22E-2	9.67/7.06E-5 0.00202 0.612
<u>4</u>	Aldehyde	RSH	S	0.031 BC8/0.00734	0.386	0.00259 0.00205 0.621
		Benzene	S	0.070 C18/0.00692	0.713/0.744	5.28/5.51E-3 0.00733 2.22
	2M Diox	Con 3	0.069 C18/0.00798	0.651/0.635	5.56/5.42E-3	0.00328 0.994
	MeCN	Con 3	0.073 C18/0.0118	0.493/0.485	6.22/6.12E-3	0.00277 0.839



Table 65 (cont'd)

	Indanol	MeOH	Con 3	0.075	C18/0.00609	0.885/0.861	5.77/5.61E-3	0.00277	0.839
	Benzene	S	0.070	C18/0.00692	3.67/2.62E-2	2.69/1.92E-4	0.00733	2.22	
	2M Diox	Con 3	0.069	C18/0.00798	1.08/1.29E-2	9.14/10.9E-5	0.00328	0.994	
	Enol	MeCN	Con 3	0.073	C18/0.0118	5.09/5.27E-3	6.37/6.59E-5	0.00277	0.839
	Ethers	MeOH	Con 3	0.075	C18/0.00609	1.41/1.39E-2	1.03/1.02E-4	0.00277	0.839
5	Aldehyde	RSH	Con 4	0.060	BC8/0.00717	4.49/4.47E-2	2.94/2.93E-4	0.00583	1.77
	Benzene	S	0.034	C19/0.00544	0.386/0.391	2.41/2.45E-3	0.00653	1.98	
	2M Diox	S	0.077	C19/0.0110	0.744/0.718	9.41/9.08E-3	0.00825	2.50	
	MeCN	S	0.039	C19/0.00285	1.431/1.461	4.70/4.80E-3	0.00224	0.679	
	Indanol	MeOH	S	0.040	C19/0.00938	0.856/0.897	9.25/9.69E-3	0.00399	1.21
	Benzene	S	0.034	C19/0.00544	1.38/1.37E-2	7.51/7.45E-5	0.00653	1.98	
	2M Diox	S	0.077	C19/0.0110	1.20/1.08E-2	1.32/1.19E-4	0.00825	2.50	
	Enol	MeCN	S	0.039	C19/0.00285	1.16/1.08E-2	3.30/3.08E-5	0.00224	0.679
	Ethers	MeOH	S	0.040	C19/0.00938	6.66/7.00E-3	6.25/6.57E-5	0.00399	1.21
	Aldehyde	RSH	Con 4	0.045	MBC4/0.00528	2.49/2.61E-2	1.19/1.26E-4	0.00640	1.94
7	Aldehyde	RSH	S	0.041	BC8/0.00683	0.408/0.424	2.55/2.65E-3	0.00274	0.830



Table 65 (cont'd)

<u>Benzene</u>	S	0.0639	BC1/0.0125	3.67/3.55E-2	3.60/3.48E-4	0.00429	1.90			
<u>Hexane</u>	S	0.0337	BC1/0.00955	0.106/0.103	7.94/7.71E-4	0.0108	3.99			
<u>2M Diox</u>	S	0.0207	BC1/0.0122	00696	6.66E-4	0.00660	2.00			
<u>MeCN</u>	S	0.0515	BC1/0.020	9.59/9.50E-2	1.44/1.49E-3	0.00522	2.17			
<u>Indanol</u>	S	0.0216	BC1/0.00595	0.241/0.245	1.12/1.14E-3	0.00739	2.24			
<u>Hexane</u>	S	0.0337	BC1/0.00955	0.100/0.104	9.55/9.93E-4	0.0108	3.99			
<u>2M Diox</u>	S	0.0207	BC1/0.0122	00328	4.00E-4	0.00660	2.00			
<u>Enol</u>	S	0.0515	BC1/0.020	0.0228	4.56E-4	0.00522	2.17			
<u>Ethers</u>	S	0.0216	BC1/0.00595	8.24/8.18E-2	4.90/4.87E-4	0.00739	2.24			
							0.00911			
<u>8</u>	<u>Aldehyde</u>	<u>RSH</u>	<u>Con 4</u>	0.0211	BC1/0.0121	1.54/1.40E-2	1.79/1.63E-4	0.00679	4.52	
							9.15/8.92E-2	7.96/7.76E-4	0.00943	2.86
							0.0110			
							0.0092			
	<u>Benzene</u>	S	0.0370	MBC4/0.00300	0.227/0.223	1.97/1.94E-3	0.0068	8.18		
	<u>Indanol</u>	S	0.0361	MBC4/0.00687	5.50/5.62E-2	1.10/1.12E-3	0.00891	2.70		











Table 65 (cont'd)

17	Indanol	Dioxane	Con 6	0.0784	DMBN/0.0404	1.83/1.71E-2	1.21/1.13E-3	0.00720	7.56	0.00783
		Benzene	Con 6	0.0811	DMBN/0.0300	0.101/0.115	4.97/5.68E-3	0.00469	1.42	0.00987
17-d	Indanol	Dioxane	Con 6	0.0784	DMBN/0.0325	3.55/3.98E-2	1.89/2.12E-3	0.00720	7.56	0.00783

a. Aldehyde-aldehyde formed from the benzoyl radical in type I cleavage, type II-type II cleavage product. b. 0.5M pyr-benzene with 0.5 M pyridine, t-BuOH-t-butyl alcohol, MeCN/H<sub>2</sub>O-2% H<sub>2</sub>O in acetonitrile, MeOH-methanol, 2M Diox-benzene with 2 M dioxane, MeCN-acetonitrile. c. S-same as the condition listed for Stern-Volmer quenching data; Con 1-GC, column #1, 210°C; Con 2-GC, column #2, 155°C; Con 3-GC, column #2, 160°C; Con 4-HPLC, 1% ethyl acetate in hexane, 1.2 ml/min; Con 5-GC, column #3, temperature programming, 80°C for 8 min, increase to 130°C with a rate of 5°C/min, then to 189°C with a rate of 25°C, and hold for 15 min; Con 6-HPLC, 2% ethyl acetate in hexane, 1.5 ml/min. d. Concentration of starting ketone in M. e. BCl-methyl benzoate, BC8-octyl benzoate, MBC4--butyl p-methoxybenzoate, CBN--p-chlorobenzyl acetonitrile, DMBN-3,5-dimethoxybenzonitrile, Cl--straight chain hydrocarbon with i carbon atoms. f. Aera ratio of product to standard. g. Product concentration in M, two measurements separated by a slash, decimal point expressed in exponential form. h. Concentration of acetophenone in M. i. Light intensity in ein/l; for ketone 8, 9, 10, 17, corrected for absorbance difference at 365 nm. j. Concentration of valerophenone between 0.099-0.11 M.



Table 66. Quantum Yields<sup>a</sup> of Photoproducts from  $\beta$ -Arylpropiophenone Derivatives

	Ketones	Solvent	[K]	Std	A <sub>p</sub> /A <sub>std</sub>	[P]	Actinometry	
							[MAP]x10 <sup>3</sup>	I
19	Benzene	0.0628	C20/0.00736	2.25/2.27E-2	1.92/1.94E-4	8.76+6.94	0.982	
	2M Diox	0.0752	C20/0.00400	4.17/4.03E-2	1.93/1.87E-4	4.76+6.52+6.91	1.11	
						3.97+5.44+		
	MeCN	0.0794	C20/0.00956	1.52/1.49E-2	1.67/1.65E-4	2.48+2.59+4.53	1.19	
	MeOH	0.0758	C20/0.00934	3.30/3.16E-2	3.58/3.42E-4	2.58+7.28+8.67	1.16	
	Benzene	0.0704	C20/0.00626	3.41/3.21E-2	2.63/2.47E-4	9.28+8.54	1.11	
20	2M Diox	0.0699	C20/0.00435	5.22/5.37E-2	2.79/2.87E-4	7.15+8.83	0.999	
						3.97+5.44+		
	MeCN	0.0646	C20/0.0120	2.29/2.14E-2	3.38/3.16E-4	2.48+2.59+4.53	1.19	
	MeOH	0.0791	C20/0.00453	0.126/0.130	7.02/7.24E-4	9.28	0.580	
						4.29+4.16+2.70		
	Benzene	0.0673	C20/0.00393	6.01/6.21E-2	2.91/3.01E-4	+3.94+3.28+5.76	1.51	
20-d	2M Diox	0.0661	C20/0.00527	3.44/3.19E-2	2.23/2.07E-4	3.63+8.42+1.62	0.854	
	Benzene	0.0418	C19/0.00658	0.274/0.254	2.38/2.21E-3	9.20+7.44	1.04	



Table 66 (cont'd)

<u>2M Diox</u>	<u>0.0435</u>	<u>C19/0.00749</u>	<u>9.29/9.35E-2</u>	<u>9.19/9.24E-4</u>	<u>6.24</u>	<u>0.390</u>
					3.97+5.44+	
<u>MeCN</u>	<u>0.0483</u>	<u>C19/0.00595</u>	<u>0.230/0.207</u>	<u>1.81/1.63E-3</u>	<u>2.48+2.59+4.53</u>	<u>1.19</u>
<u>21 MeOH</u>	<u>0.0461</u>	<u>C19/0.00916</u>	<u>0.368/0.378</u>	<u>4.45/4.57E-3</u>	<u>6.24</u>	<u>0.390</u>
<u>Benzene</u>	<u>0.0468</u>	<u>C19/0.00871</u>	<u>0.114/0.122</u>	<u>1.31/1.40E-3</u>	<u>4.29+4.16+2.70</u>	<u>0.697</u>
<u>21-d 2M Diox</u>	<u>0.0460</u>	<u>C19/0.00927</u>	<u>0.128/0.129</u>	<u>1.57/1.58E-3</u>	<u>3.63+8.42+1.62</u>	<u>0.854</u>

a. Same analysis conditions as in the quenching studies.



**Table 67. X-Ray Crystallographic Parameters for  $\alpha$ -Mesitylvalerophenone 6**



Table of Bond Angles (in Degrees) for  
 $\alpha$ -mesitylvalerophenone

Atom1 -----	Atom2 -----	Atom3 -----	Angle -----
C2	C1	C6	120.2(2)
C1	C2	C3	120.4(2)
C2	C3	C4	119.7(2)
C3	C4	C5	120.4(2)
C4	C5	C6	120.9(2)
C1	C6	C5	118.5(2)
C1	C6	C7	123.4(2)
C5	C6	C7	118.1(2)
O1	C7	C6	119.9(2)
O1	C7	C8	120.3(2)
C6	C7	C8	119.7(2)
C7	C8	C9	115.0(1)
C7	C8	C18	110.3(2)
C9	C8	C18	113.5(2)
C8	C9	C10	121.5(2)
C8	C9	C14	119.6(1)
C10	C9	C14	118.8(1)
C9	C10	C11	119.6(2)
C9	C10	C15	123.3(1)
C11	C10	C15	117.2(2)
C10	C11	C12	122.1(2)
C11	C12	C13	117.8(2)
C11	C12	C16	120.8(2)
C13	C12	C16	121.4(2)



Table of Bond Angles (Continued) for  
 $\alpha$ -mesitylvalerophenone

Atom1 -----	Atom2 -----	Atom3 -----	Angle -----
C12	C13	C14	122.5(2)
C9	C14	C13	119.2(2)
C9	C14	C17	123.4(1)
C13	C14	C17	117.4(2)
C8	C18	C19	114.3(2)
C18	C19	C20	111.7(2)
C2	C1	H1	120.(1)
C6	C1	H1	119.(1)
C1	C2	H2	120.(1)
C3	C2	H2	120.(1)
C2	C3	H3	122.(2)
C4	C3	H3	119.(2)
C3	C4	H4	118.(2)
C5	C4	H4	121.(2)
C4	C5	H5	123.(1)
C6	C5	H5	116.(1)
C7	C8	H8	103.(1)
C9	C8	H8	108.8(9)
C18	C8	H8	105.3(9)
C10	C11	H11	117.(1)
C12	C11	H11	120.(1)
C12	C13	H13	120.6(8)
C14	C13	H13	116.8(8)
C10	C15	H15a	110.(2)



Table of Bond Angles (Continued) for  
 $\alpha$ -mesitylvalerophenone

Atom1 -----	Atom2 -----	Atom3 -----	Angle -----
C10	C15	H15b	114.(2)
C10	C15	H15c	109.(2)
H15a	C15	H15b	108.(2)
H15a	C15	H15c	110.(2)
H15b	C15	H15c	105.(2)
C12	C16	H16a	115.(1)
C12	C16	H16b	110.(1)
C12	C16	H16c	118.(2)
H16a	C16	H16b	108.(3)
H16a	C16	H16c	106.(2)
H16b	C16	H16c	98.(3)
C14	C17	H17a	112.(1)
C14	C17	H17b	117.(1)
C14	C17	H17c	116.(2)
H17a	C17	H17b	105.(2)
H17a	C17	H17c	105.(2)
H17b	C17	H17c	100.(2)
C8	C18	H18a	108.(1)
C8	C18	H18b	108.(1)
C19	C18	H18a	110.(1)
C19	C18	H18b	104.(1)
H18a	C18	H18b	112.(2)
C18	C19	H19a	106.(1)
C18	C19	H19b	108.(1)



Table of Bond Angles (Continued) for  
 $\alpha$ -mesitylvalerophenone

Atom1 -----	Atom2 -----	Atom3 -----	Angle -----
C20	C19	H19a	107.(1)
C20	C19	H19b	111.(1)
H19a	C19	H19b	112.(2)
C19	C20	H20a	113.(2)
C19	C20	H20b	110.(2)
C19	C20	H20c	112.(2)
H20a	C20	H20b	101.(2)
H20a	C20	H20c	103.(2)
H20b	C20	H20c	117.(2)

-----  
Numbers in parentheses are estimated standard deviations  
in the least significant digits.







Table of Bond Distances (in Angstroms) for  
 $\alpha$ -mesitylvalerophenone

Atom1	Atom2	Distance
-----	-----	-----
O1	C7	1.216(3)
C1	C2	1.391(3)
C1	C6	1.387(3)
C2	C3	1.380(4)
C3	C4	1.375(4)
C4	C5	1.375(4)
C5	C6	1.396(3)
C6	C7	1.491(3)
C7	C8	1.537(3)
C8	C9	1.530(2)
C8	C18	1.539(3)
C9	C10	1.402(2)
C9	C14	1.411(3)
C10	C11	1.392(2)
C10	C15	1.518(3)
C11	C12	1.380(3)
C12	C13	1.379(3)
C12	C16	1.517(2)
C13	C14	1.390(2)
C14	C17	1.512(3)
C18	C19	1.512(3)
C19	C20	1.536(3)
C1	H1	0.94(2)
C2	H2	0.95(2)



Table of Bond Distances (Continued) for  
 $\alpha$ -mesitylvalerophenone

Atom1	Atom2	Distance
C3	H3	0.98(3)
C4	H4	1.04(3)
C5	H5	0.98(2)
C8	H8	1.02(2)
C11	H11	1.04(2)
C13	H13	0.94(2)
C15	H15a	0.93(2)
C15	H15b	1.03(2)
C15	H15c	1.00(3)
C16	H16a	1.02(3)
C16	H16b	0.92(3)
C16	H16c	0.96(3)
C17	H17a	0.91(2)
C17	H17b	1.03(3)
C17	H17c	0.99(2)
C18	H18a	1.01(2)
C18	H18b	1.06(2)
C19	H19a	1.11(2)
C19	H19b	0.99(2)
C20	H20a	1.01(3)
C20	H20b	1.04(2)
C20	H20c	0.96(3)

Numbers in parentheses are estimated standard deviations  
in the least significant digits.



Table of Torsion Angles in Degrees  
for  $\alpha$ -mesitylvalerophenone

Atom 1 -----	Atom 2 -----	Atom 3 -----	Atom 4 -----	Angle -----
C6	C1	C2	C3	-0.90 ( 0.32)
C2	C1	C6	C5	0.21 ( 0.30)
C2	C1	C6	C7	-177.28 ( 0.19)
C1	C2	C3	C4	0.53 ( 0.35)
C2	C3	C4	C5	0.53 ( 0.37)
C3	C4	C5	C6	-1.23 ( 0.36)
C4	C5	C6	C1	0.85 ( 0.32)
C4	C5	C6	C7	178.47 ( 0.20)
C1	C6	C7	O1	162.30 ( 0.20)
C1	C6	C7	C8	-14.45 ( 0.28)
C5	C6	C7	O1	-15.20 ( 0.29)
C5	C6	C7	C8	168.05 ( 0.18)
O1	C7	C8	C9	128.94 ( 0.19)
O1	C7	C8	C18	-0.86 ( 0.26)
C6	C7	C8	C9	-54.32 ( 0.24)
C6	C7	C8	C18	175.88 ( 0.17)
C7	C8	C9	C10	-51.69 ( 0.23)
C7	C8	C9	C14	131.10 ( 0.17)
C18	C8	C9	C10	76.52 ( 0.22)
C18	C8	C9	C14	-100.69 ( 0.20)
C7	C8	C18	C19	-169.38 ( 0.17)
C9	C8	C18	C19	60.00 ( 0.23)
C8	C9	C10	C11	-176.15 ( 0.16)
C8	C9	C10	C15	4.71 ( 0.27)



Table of Torsion Angles (Continued)  
for  $\alpha$ -mesitylvalerophenone

Atom 1 -----	Atom 2 -----	Atom 3 -----	Atom 4 -----	Angle -----
C14	C9	C10	C11	1.08 ( 0.25)
C14	C9	C10	C15	-178.06 ( 0.17)
C8	C9	C14	C13	177.01 ( 0.15)
C8	C9	C14	C17	-2.45 ( 0.25)
C10	C9	C14	C13	-0.28 ( 0.26)
C10	C9	C14	C17	-179.74 ( 0.16)
C9	C10	C11	C12	-0.94 ( 0.29)
C15	C10	C11	C12	178.25 ( 0.18)
C10	C11	C12	C13	-0.05 ( 0.29)
C10	C11	C12	C16	179.35 ( 0.19)
C11	C12	C13	C14	0.90 ( 0.28)
C16	C12	C13	C14	-178.50 ( 0.18)
C12	C13	C14	C9	-0.74 ( 0.27)
C12	C13	C14	C17	178.76 ( 0.17)
C8	C18	C19	C20	176.52 ( 0.19)
C6	C1	C2	H2	174.65 ( 1.44)
H1	C1	C2	C3	-177.81 ( 1.27)
H1	C1	C2	H2	-2.26 ( 1.93)
H1	C1	C6	C5	177.14 ( 1.27)
H1	C1	C6	C7	-0.35 ( 1.29)
C1	C2	C3	H3	179.36 ( 1.65)
H2	C2	C3	C4	-175.02 ( 1.44)
H2	C2	C3	H3	3.81 ( 2.20)
C2	C3	C4	H4	-173.91 ( 1.65)



Table of Torsion Angles (Continued)  
for  $\alpha$ -mesitylvalerophenone

Atom 1 -----	Atom 2 -----	Atom 3 -----	Atom 4 -----	Angle -----
H3	C3	C4	C5	-178.34 ( 1.60)
H3	C3	C4	H4	7.22 ( 2.31)
C3	C4	C5	H5	-176.65 ( 1.47)
H4	C4	C5	C6	173.01 ( 1.68)
H4	C4	C5	H5	-2.41 ( 2.25)
H5	C5	C6	C1	176.58 ( 1.37)
H5	C5	C6	C7	-5.80 ( 1.38)
O1	C7	C8	H8	-112.88 ( 0.88)
C6	C7	C8	H8	63.87 ( 0.89)
H8	C8	C9	C10	-166.60 ( 0.98)
H8	C8	C9	C14	16.19 ( 1.00)
C7	C8	C18	H18a	67.44 ( 1.19)
C7	C8	C18	H18b	-54.21 ( 1.20)
C9	C8	C18	H18a	-63.18 ( 1.20)
C9	C8	C18	H18b	175.17 ( 1.20)
H8	C8	C18	C19	-58.86 ( 1.01)
H8	C8	C18	H18a	177.96 ( 1.54)
H8	C8	C18	H18b	56.31 ( 1.55)
C9	C10	C11	H11	-177.88 ( 1.20)
C15	C10	C11	H11	1.31 ( 1.22)
C9	C10	C15	H15a	-158.44 ( 1.54)
C9	C10	C15	H15b	-36.72 ( 1.56)
C9	C10	C15	H15c	80.30 ( 1.44)
C11	C10	C15	H15a	22.40 ( 1.56)







Table of Torsion Angles (Continued)  
for  $\alpha$ -mesitylvalerophenone

Atom 1 -----	Atom 2 -----	Atom 3 -----	Atom 4 -----	Angle -----
C11	C10	C15	H15b	144.12 ( 1.54)
C11	C10	C15	H15c	-98.86 ( 1.44)
H11	C11	C12	C13	176.81 ( 1.24)
H11	C11	C12	C16	-3.79 ( 1.27)
C11	C12	C13	H13	-175.76 ( 1.16)
C16	C12	C13	H13	4.84 ( 1.19)
C11	C12	C16	H16a	-70.13 ( 1.95)
C11	C12	C16	H16b	167.20 ( 1.70)
C11	C12	C16	H16c	56.34 ( 2.21)
C13	C12	C16	H16a	109.25 ( 1.95)
C13	C12	C16	H16b	-13.42 ( 1.71)
C13	C12	C16	H16c	-124.28 ( 2.20)
H13	C13	C14	C9	176.04 ( 1.11)
H13	C13	C14	C17	-4.46 ( 1.13)
C9	C14	C17	H17a	-177.68 ( 1.47)
C9	C14	C17	H17b	-56.53 ( 1.40)
C9	C14	C17	H17c	61.75 ( 1.55)
C13	C14	C17	H17a	2.84 ( 1.49)
C13	C14	C17	H17b	124.00 ( 1.39)
C13	C14	C17	H17c	-117.73 ( 1.54)
C8	C18	C19	H19a	59.85 ( 1.08)
C8	C18	C19	H19b	-60.85 ( 1.32)
H18a	C18	C19	C20	-61.51 ( 1.09)
H18a	C18	C19	H19a	-178.17 ( 1.51)



—  
Nu  
in



Table of Torsion Angles (Continued)  
for  $\alpha$ -mesitylvalerophenone

Atom 1	Atom 2	Atom 3	Atom 4	Angle
H18a	C18	C19	H19b	61.12 ( 1.70)
H18b	C18	C19	C20	59.30 ( 1.12)
H18b	C18	C19	H19a	-57.36 ( 1.53)
H18b	C18	C19	H19b	-178.06 ( 1.70)
C18	C19	C20	H20a	-177.52 ( 1.63)
C18	C19	C20	H20b	-65.83 ( 1.68)
C18	C19	C20	H20c	65.91 ( 1.93)
H19a	C19	C20	H20a	-61.50 ( 2.04)
H19a	C19	C20	H20b	50.19 ( 2.08)
H19a	C19	C20	H20c	-178.07 ( 2.27)
H19b	C19	C20	H20a	61.66 ( 2.17)
H19b	C19	C20	H20b	173.35 ( 2.19)
H19b	C19	C20	H20c	-54.91 ( 2.40)

Numbers in parentheses are estimated standard deviations  
in the least significant digits.



Table 68. X-Ray Crystallographic Parameters for  $\alpha$ -Mesityl-2,4,6-Trimethyl-acetophenone 14

Table of Bond Angles (in Degrees) for  
1,2-Dimesitylethanone

Atom1 -----	Atom2 -----	Atom3 -----	Angle -----
C2	C1	C6	118.9(2)
C2	C1	C15	119.6(3)
C6	C1	C15	121.5(2)
C1	C2	C3	122.2(3)
C2	C3	C4	117.9(3)
C2	C3	C16	121.1(3)
C4	C3	C16	121.0(3)
C3	C4	C5	122.0(3)
C4	C5	C6	119.0(3)
C4	C5	C17	119.6(3)
C6	C5	C17	121.4(2)
C1	C6	C5	119.9(2)
C1	C6	C7	119.7(2)
C5	C6	C7	120.4(2)
O1	C7	C6	121.5(2)
O1	C7	C8	122.1(2)
C6	C7	C8	116.4(2)
C7	C8	C9	115.4(2)
C8	C9	C10	120.5(2)
C8	C9	C14	120.2(2)
C10	C9	C14	119.3(2)
C9	C10	C11	118.9(3)
C9	C10	C18	121.9(2)
C11	C10	C18	119.1(3)
C10	C11	C12	122.6(3)
C11	C12	C13	117.4(3)
C11	C12	C19	121.8(3)
C13	C12	C19	120.9(3)
C12	C13	C14	122.1(3)
C9	C14	C13	119.6(3)
C9	C14	C20	121.4(2)
C13	C14	C20	119.0(2)



Table of Bond Angles (Continued) for  
1,2-Dimesitylethanone

Atom1 -----	Atom2 -----	Atom3 -----	Angle -----
C1	C2	H2	119.0
C3	C2	H2	118.9
C3	C4	H4	118.9
C5	C4	H4	119.1
C7	C8	H8a	108.2
C7	C8	H8b	107.7
C9	C8	H8a	108.5
C9	C8	H8b	107.4
H8a	C8	H8b	109.5
C10	C11	H11	118.8
C12	C11	H11	118.6
C12	C13	H13	118.6
C14	C13	H13	119.3
C1	C15	H15a	109.8
C1	C15	H15b	109.0
C1	C15	H15c	109.5
C1	C15	H15d	109.7
C1	C15	H15e	109.7
C1	C15	H15f	109.0
H15a	C15	H15b	109.5
H15a	C15	H15c	109.5
H15a	C15	H15d	140.5
H15a	C15	H15e	57.0
H15a	C15	H15f	55.3
H15b	C15	H15c	109.5
H15b	C15	H15d	55.2
H15b	C15	H15e	141.2
H15b	C15	H15f	57.4
H15c	C15	H15d	57.1
H15c	C15	H15e	55.5
H15c	C15	H15f	141.4
H15d	C15	H15e	109.5
H15d	C15	H15f	109.5
H15e	C15	H15f	109.5
C3	C16	H16a	109.8
C3	C16	H16b	109.6
C3	C16	H16c	109.0
C3	C16	H16d	109.7
C3	C16	H16e	109.2
C3	C16	H16f	109.5
H16a	C16	H16b	109.5
H16a	C16	H16c	109.5
H16a	C16	H16d	140.4
H16a	C16	H16e	57.6
H16a	C16	H16f	54.7
H16b	C16	H16c	109.5
H16b	C16	H16d	54.6
H16b	C16	H16e	141.2
H16b	C16	H16f	57.9



Table of Bond Angles (Continued) for  
1,2-Dimesitylethane

Atom1 -----	Atom2 -----	Atom3 -----	Angle -----
H16c	C16	H16d	57.7
H16c	C16	H16e	55.0
H16c	C16	H16f	141.5
H16d	C16	H16e	109.5
H16d	C16	H16f	109.5
H16e	C16	H16f	109.5
C5	C17	H17a	109.6
C5	C17	H17b	109.3
C5	C17	H17c	109.5
H17a	C17	H17b	109.5
H17a	C17	H17c	109.5
H17b	C17	H17c	109.5
C10	C18	H18a	109.9
C10	C18	H18b	109.4
C10	C18	H18c	109.1
H18a	C18	H18b	109.5
H18a	C18	H18c	109.5
H18b	C18	H18c	109.5
C12	C19	H19a	109.8
C12	C19	H19b	109.3
C12	C19	H19c	109.4
C12	C19	H19d	110.2
C12	C19	H19e	109.1
C12	C19	H19f	109.1
H19a	C19	H19b	109.5
H19a	C19	H19c	109.5
H19a	C19	H19d	140.0
H19a	C19	H19e	56.2
H19a	C19	H19f	55.9
H19b	C19	H19c	109.5
H19b	C19	H19d	56.0
H19b	C19	H19e	141.6
H19b	C19	H19f	56.7
H19c	C19	H19d	56.1
H19c	C19	H19e	56.6
H19c	C19	H19f	141.5
H19d	C19	H19e	109.5
H19d	C19	H19f	109.5
H19e	C19	H19f	109.5
C14	C20	H20a	109.2
C14	C20	H20b	109.8
C14	C20	H20c	109.4
H20a	C20	H20b	109.5
H20a	C20	H20c	109.5
H20b	C20	H20c	109.5

-----  
Numbers in parentheses are estimated standard deviations  
in the least significant digits.



Table of Bond Distances (in Angstroms) for  
1,2-Dimesitylethanone

Atom1	Atom2	Distance
-----	-----	-----
O1	C7	1.200(3)
C1	C2	1.391(4)
C1	C6	1.393(4)
C1	C15	1.509(4)
C2	C3	1.381(4)
C3	C4	1.381(4)
C3	C16	1.512(4)
C4	C5	1.388(4)
C5	C6	1.401(4)
C5	C17	1.514(4)
C6	C7	1.503(4)
C7	C8	1.515(4)
C8	C9	1.518(4)
C9	C10	1.399(4)
C9	C14	1.390(4)
C10	C11	1.393(4)
C10	C18	1.511(4)
C11	C12	1.375(4)
C12	C13	1.382(4)
C12	C19	1.512(4)
C13	C14	1.390(4)
C14	C20	1.511(4)



Table of Bond Distances (Continued) for  
1,2-Dimesitylethanone

Atom1	Atom2	Distance
-----	-----	-----
C2	H2	0.95
C4	H4	0.95
C8	H8a	0.95
C8	H8b	0.95
C11	H11	0.95
C13	H13	0.95
C15	H15a	0.95
C15	H15b	0.95
C15	H15c	0.95
C15	H15d	0.95
C15	H15e	0.95
C15	H15f	0.95
C16	H16a	0.95
C16	H16b	0.95
C16	H16c	0.95
C16	H16d	0.95
C16	H16e	0.95
C16	H16f	0.95
C17	H17a	0.95
C17	H17b	0.95
C17	H17c	0.95
C18	H18a	0.95
C18	H18b	0.95
C18	H18c	0.95
C19	H19a	0.95
C19	H19b	0.95
C19	H19c	0.95
C19	H19d	0.95
C19	H19e	0.95
C19	H19f	0.95
C20	H20a	0.95
C20	H20b	0.95
C20	H20c	0.95

-----  
Numbers in parentheses are estimated standard deviations  
in the least significant digits.



**Table 69. X-Ray Crystallographic Parameters for  $\alpha$ -Mesityl- $\alpha$ -Phenylacetophenone 8**

**Table of Bond Angles (in Degrees) for  
2-Mesityl-1,2-diphenylethanone**

Atom1 -----	Atom2 -----	Atom3 -----	Angle -----
C2	C1	C6	120.4(4)
C1	C2	C3	120.1(6)
C2	C3	C4	120.3(5)
C3	C4	C5	120.6(4)
C4	C5	C6	119.7(6)
C1	C6	C5	119.0(4)
C1	C6	C7	122.5(4)
C5	C6	C7	118.6(5)
O1	C7	C6	120.2(4)
O1	C7	C8	121.4(4)
C6	C7	C8	118.3(5)
C7	C8	C9	114.4(4)
C7	C8	C15	117.1(4)
C9	C8	C15	111.5(3)
C8	C9	C10	120.6(4)
C8	C9	C14	121.4(4)
C10	C9	C14	117.9(4)
C9	C10	C11	121.2(5)
C10	C11	C12	120.3(5)
C11	C12	C13	119.2(5)
C12	C13	C14	121.2(5)
C9	C14	C13	120.1(5)
C8	C15	C16	123.6(5)
C8	C15	C20	117.5(4)
C16	C15	C20	118.9(5)
C15	C16	C17	119.4(5)
C15	C16	C21	123.0(5)
C17	C16	C21	117.5(5)
C16	C17	C18	122.3(5)
C17	C18	C19	118.3(6)
C17	C18	C22	121.5(5)
C19	C18	C22	120.2(6)
C18	C19	C20	121.2(5)
C15	C20	C19	119.9(5)
C15	C20	C23	121.5(5)
C19	C20	C23	118.7(5)



Table of Bond Angles (Continued) for  
2-Mesityl-1,2-diphenylethanone

Atom1 -----	Atom2 -----	Atom3 -----	Angle -----
C2	C1	H1	120.3
C6	C1	H1	119.3
C1	C2	H2	120.1
C3	C2	H2	119.9
C2	C3	H3	119.8
C4	C3	H3	119.8
C3	C4	H4	119.5
C5	C4	H4	119.9
C4	C5	H5	120.7
C6	C5	H5	119.6
C7	C8	H8	100.9
C9	C8	H8	106.9
C15	C8	H8	104.4
C9	C10	H10	118.9
C11	C10	H10	119.9
C10	C11	H11	120.2
C12	C11	H11	119.5
C11	C12	H12	120.1
C13	C12	H12	120.7
C12	C13	H13	119.1
C14	C13	H13	119.7
C9	C14	H14	119.0
C13	C14	H14	120.8
C16	C17	H17	119.5
C18	C17	H17	118.2
C18	C19	H19	119.4
C20	C19	H19	119.3
C16	C21	H21a	109.6
C16	C21	H21b	108.5
C16	C21	H21c	110.3
C16	C21	H21d	109.4
C16	C21	H21e	110.4
C16	C21	H21f	108.6
H21a	C21	H21b	109.5
H21a	C21	H21c	109.5
H21a	C21	H21d	141.1
H21a	C21	H21e	55.7
H21a	C21	H21f	56.8
H21b	C21	H21c	109.5
H21b	C21	H21d	56.8
H21b	C21	H21e	141.1
H21b	C21	H21f	55.7
H21c	C21	H21d	55.7
H21c	C21	H21e	56.8
H21c	C21	H21f	141.1
H21d	C21	H21e	109.5
H21d	C21	H21f	109.5
H21e	C21	H21f	109.5
C18	C22	H22a	110.6



Table of Bond Angles (Continued) for  
2-Mesityl-1,2-diphenylethanone

Atom1	Atom2	Atom3	Angle
-----	-----	-----	-----
C18	C22	H22b	108.9
C18	C22	H22c	108.9
C18	C22	H22d	108.3
C18	C22	H22e	110.0
C18	C22	H22f	110.1
H22a	C22	H22b	109.5
H22a	C22	H22c	109.5
H22a	C22	H22d	141.0
H22a	C22	H22e	57.8
H22a	C22	H22f	54.7
H22b	C22	H22c	109.5
H22b	C22	H22d	54.7
H22b	C22	H22e	141.0
H22b	C22	H22f	57.8
H22c	C22	H22d	57.8
H22c	C22	H22e	54.7
H22c	C22	H22f	141.0
H22d	C22	H22e	109.5
H22d	C22	H22f	109.5
H22e	C22	H22f	109.5
C20	C23	H23a	109.9
C20	C23	H23b	109.6
C20	C23	H23c	108.9
H23a	C23	H23b	109.5
H23a	C23	H23c	109.5
H23b	C23	H23c	109.5

-----  
Numbers in parentheses are estimated standard deviations  
in the least significant digits.



Table of Bond Distances (in Angstroms) for  
2-Mesityl-1,2-diphenylethanone

Atom1	Atom2	Distance
O1	C7	1.231(7)
C1	C2	1.381(6)
C1	C6	1.389(8)
C2	C3	1.354(7)
C3	C4	1.375(9)
C4	C5	1.376(7)
C5	C6	1.386(6)
C6	C7	1.506(6)
C7	C8	1.514(6)
C8	C9	1.521(6)
C8	C15	1.528(7)
C9	C10	1.386(7)
C9	C14	1.380(6)
C10	C11	1.379(6)
C11	C12	1.367(8)
C12	C13	1.360(8)
C13	C14	1.390(6)
C15	C16	1.393(7)
C15	C20	1.398(7)
C16	C17	1.382(9)
C16	C21	1.522(9)
C17	C18	1.366(9)
C18	C19	1.381(8)
C18	C22	1.512(10)
C19	C20	1.384(8)
C20	C23	1.499(7)



Table of Bond Distances (Continued) for  
2-Mesityl-1,2-diphenylethanone

Atom1	Atom2	Distance
C1	H1	0.95
C2	H2	0.95
C3	H3	0.95
C4	H4	0.95
C5	H5	0.95
C8	H8	0.95
C10	H10	0.95
C11	H11	0.95
C12	H12	0.95
C13	H13	0.95
C14	H14	0.95
C17	H17	0.95
C19	H19	0.95
C21	H21a	0.95
C21	H21b	0.95
C21	H21c	0.95
C21	H21d	0.95
C21	H21e	0.95
C21	H21f	0.95
C22	H22a	0.95
C22	H22b	0.95
C22	H22c	0.95
C22	H22d	0.95
C22	H22e	0.95
C22	H22f	0.95
C23	H23a	0.95
C23	H23b	0.95
C23	H23c	0.95

Numbers in parentheses are estimated standard deviations  
in the least significant digits.



Table of Torsion Angles in Degrees  
for 2-Mesityl-1,2-diphenylethanone

Atom 1	Atom 2	Atom 3	Atom 4	Angle
C9	C8	C15	C20	81.24 ( 0.49)
C8	C9	C10	C11	173.84 ( 0.48)
C14	C9	C10	C11	-3.26 ( 0.77)
C8	C9	C14	C13	-175.05 ( 0.47)
C10	C9	C14	C13	2.02 ( 0.75)
C9	C10	C11	C12	2.47 ( 0.86)
C10	C11	C12	C13	-0.35 ( 0.88)
C11	C12	C13	C14	-0.87 ( 0.86)
C12	C13	C14	C9	0.02 ( 1.27)
C8	C15	C16	C17	175.03 ( 0.41)
C8	C15	C16	C21	-3.76 ( 0.68)
C20	C15	C16	C17	-0.74 ( 0.64)
C20	C15	C16	C21	-179.52 ( 0.43)
C8	C15	C20	C19	-175.18 ( 0.37)
C8	C15	C20	C23	4.54 ( 0.56)
C16	C15	C20	C19	0.85 ( 0.60)
C16	C15	C20	C23	-179.44 ( 0.39)
C15	C16	C17	C18	-0.43 ( 0.73)
C21	C16	C17	C18	178.42 ( 0.46)
C16	C17	C18	C19	1.47 ( 0.73)
C16	C17	C18	C22	-178.05 ( 0.48)
C17	C18	C19	C20	-1.35 ( 0.68)
C22	C18	C19	C20	178.18 ( 0.44)
C18	C19	C20	C15	0.21 ( 0.65)
C18	C19	C20	C23	-179.52 ( 0.40)



Table of Torsion Angles in Degrees (continued)  
 2-Mesityl-1,2-diphenylethanone

Atom 1 -----	Atom 2 -----	Atom 3 -----	Atom 4 -----	Angle -----
C6	C1	C2	C3	-1.41 ( 0.86)
C2	C1	C6	C5	2.35 ( 0.82)
C2	C1	C6	C7	-178.23 ( 0.51)
C1	C2	C3	C4	-0.24 ( 0.85)
C2	C3	C4	C5	0.92 ( 0.84)
C3	C4	C5	C6	0.06 ( 0.77)
C4	C5	C6	C1	-1.66 ( 0.80)
C4	C5	C6	C7	178.89 ( 0.49)
C1	C6	C7	O1	-171.90 ( 0.53)
C1	C6	C7	C8	3.44 ( 0.76)
C5	C6	C7	O1	7.53 ( 0.77)
C5	C6	C7	C8	-177.13 ( 0.47)
O1	C7	C8	C9	5.87 ( 0.72)
O1	C7	C8	C15	-127.31 ( 0.51)
C6	C7	C8	C9	-169.41 ( 0.44)
C6	C7	C8	C15	57.41 ( 0.60)
C7	C8	C9	C10	87.40 ( 0.58)
C7	C8	C9	C14	-95.60 ( 0.56)
C15	C8	C9	C10	-136.82 ( 0.48)
C15	C8	C9	C14	40.18 ( 0.62)
C7	C8	C15	C16	39.87 ( 0.59)
C7	C8	C15	C20	-144.30 ( 0.41)
C9	C8	C15	C16	-94.58 ( 0.51)

-----  
 Numbers in parentheses are estimated standard deviations  
 in the least significant digits.



Table of Torsion Angles in Degrees  
for 1,2-Dimesitylethanone

Atom 1	Atom 2	Atom 3	Atom 4	Angle
-----	-----	-----	-----	-----
C6	C1	C2	C3	0.90 ( 0.39)
C15	C1	C2	C3	-177.54 ( 0.25)
C2	C1	C6	C5	-2.56 ( 0.37)
C2	C1	C6	C7	178.03 ( 0.23)
C15	C1	C6	C5	175.85 ( 0.25)
C15	C1	C6	C7	-3.56 ( 0.37)
C1	C2	C3	C4	1.17 ( 0.39)
C1	C2	C3	C16	179.85 ( 0.25)
C2	C3	C4	C5	-1.62 ( 0.40)
C16	C3	C4	C5	179.69 ( 0.26)
C3	C4	C5	C6	0.00 ( 0.44)
C3	C4	C5	C17	178.34 ( 0.26)
C4	C5	C6	C1	2.13 ( 0.38)
C4	C5	C6	C7	-178.46 ( 0.23)
C17	C5	C6	C1	-176.19 ( 0.25)
C17	C5	C6	C7	3.22 ( 0.38)
C1	C6	C7	O1	78.99 ( 0.34)
C1	C6	C7	C8	-99.95 ( 0.28)
C5	C6	C7	O1	-100.42 ( 0.32)
C5	C6	C7	C8	80.64 ( 0.31)
O1	C7	C8	C9	-3.06 ( 0.37)
C6	C7	C8	C9	175.88 ( 0.22)
C7	C8	C9	C10	-96.44 ( 0.28)
C7	C8	C9	C14	81.65 ( 0.29)
C8	C9	C10	C11	177.45 ( 0.22)
C8	C9	C10	C18	-3.38 ( 0.36)
C14	C9	C10	C11	-0.64 ( 0.35)
C14	C9	C10	C18	178.52 ( 0.24)
C8	C9	C14	C13	-177.17 ( 0.22)
C8	C9	C14	C20	2.59 ( 0.36)
C10	C9	C14	C13	0.94 ( 0.36)
C10	C9	C14	C20	-179.31 ( 0.24)
C9	C10	C11	C12	-0.75 ( 0.38)
C18	C10	C11	C12	-179.94 ( 0.32)
C10	C11	C12	C13	1.78 ( 0.38)
C10	C11	C12	C19	-178.48 ( 0.24)
C11	C12	C13	C14	-1.47 ( 0.38)
C19	C12	C13	C14	178.79 ( 0.24)
C12	C13	C14	C9	0.14 ( 0.39)
C12	C13	C14	C20	-179.62 ( 0.24)



### References

1. Jablonski, A. Z. Physik. 1935, 94, 38
2. Cowen, D. O.; Drisko, R. L. "Elements of Organic Photochemistry", Academic Press, New York, N. Y. 1969
3. a. Wagner, P. J.; Kochevar, I. J. Am. Chem. Soc. 1968, 90, 2232  
b. Clark, W. D.; Litt, A. D.; Steel, C. J. Am. Chem. Soc. 1969, 91, 5413  
c. Herkstroeter, W. G.; Jones, L. B.; Hammond, G. S. J. Am. Chem. Soc. 1966, 88, 4777
4. a. Rentzepis, P.; Mitschke, C. T. Anal. Chem. 1970, 42, 20A  
b. Hochstrasser, R. M. Acc. Chem. Res. 1968, 1, 266
5. a. Wagner, P. J. Acc. Chem. Res. 1971, 4, 168  
b. Wagner, P. J.; Hammond, G. S. J. Am. Chem. Soc. 1966, 88, 1245  
c. Lamola, A. A.; Hammond, G. S. J. Chem. Phys. 1965, 43, 2129
6. Turro, N. J. "Morden Molecular Photochemistry", Benjamin-Cummings, Menlo Park, Ca. 1978
7. Wagner, P. J. in "Rearrangements in Ground and Excited Molecules", Academic Press, New York, N. Y. 1980, V3, 381
8. Wagner, P. J. Topics in Curr. Chem. 1976, 66, 1
9. a. Yang, N. C.; McClure, D. S.; Murov, S. L.; Houser, J. J.; Dusenberry, R. J. Am. Chem. Soc. 1967, 89, 5466  
b. Yang, N. C.; Dusenberry, R. L. J. Am. Chem. Soc. 1968, 90, 5899
10. Wagner, P. J.; Kemppainen, A. E.; Schott, H. N. J. Am. Chem. Soc. 1968, 95, 5604
11. Wagner, P. J.; Thomas, M. J.; Harris, E. J. Am. Chem. Soc. 1976, 98, 7675
12. Zimmerman, H. E. Adv. Photochem. 1963, 1, 183



13. Gray, P.; Williams, A. *Chem Rev.* **1959**, *59*, 239
14. Walling, C.; Padwa, A. J. *Am. Chem. Soc.* **1963**, *85*, 1593, 1597
15. Lewis, F. D.; Magyar, J. G. *J. Org. Chem.* **1972**, *37*, 2102
16. Baum, A. A.; J. *Am. Chem. Soc.* **1972**, *94*, 6866
17. a. Dalton, J. C.; Dawes, K.; Turro, N. J.; Weiss, D. S.; Barltrop, J. A.; Coyle, J. D. *J. Am. Chem. Soc.* **1971**, *93*, 7213  
 b. Dalton, J. C.; Pond, D. M.; Weiss, D. S.; Lewis, F. D.; Turro, N. J. *J. Am. Chem. Soc.* **1970**, *92*, 2564
18. Yang, N. C.; Feit, E. D.; Hui, M. H.; Turro, N. J.; Dalton, J. C. *J. Am. Chem. Soc.* **1970**, *92*, 6974
19. Barltrop, J. A.; Coyle, J. D. "Excited States in Organic States", Wiley, New York, N. Y. **1975**
20. Wagner, P. J. McGrath, J. M. *J. Am. Chem. Soc.* **1972**, *94*, 3849
21. Heine, H. -G. *Justus Liebigs Ann. Chem.* **1970**, *732*, 105
22. Murov, S. L. *Handbook of Photochemistry*, Marcel Dekker, New York, N. Y. **1973**
23. a. Norrish, R. G. W.; Bamford, C. H. *Nature* **1936**, *138*, 1016  
 b. Norrish, R. G. W.; Bamford, C. H. *Nature* **1937**, *140*, 195  
 c. Norrish, R. G. W. *Trans. Faraday Soc.* **1937**, *33*, 1521
24. a. Heine, H. -G.; Hartmann, W.; Kory, D. R.; Magyar, J. G.; Hoyle, C. E.; McVey, J. K.; Lewis, F. D. *J. Org. Chem.* **1974**, *39*, 691  
 b. Lewis, F. D.; Hoyle, C. H.; Magyar, J. G. *J. Org. Chem.* **1975**, *40*, 488  
 c. Lewis, F. D.; Magyar, J. G. *J. Am. Chem. Soc.* **1973**, *95*, 5973
25. a. Ciamician, G.; Silber, P. *Chem. Ber.* **1900**, *33*, 2911  
 b. Ciamician, G.; Silber, P. *Chem. Ber.* **1901**, *34*, 1530
26. a. Walling, C.; Gibian, M. J. *J. Am. Chem. Soc.* **1965**, *87*, 3361  
 b. Padawa, A. *Tetrahedron Lett.* **1964**, 3465



27. a. Hammond, G. S.; Leermakers, P. A. J. *Am. Chem. Soc.* **1962**, *84*, 207  
b. Yang, N. C.; Shani, A. *Chem. Commun.* **1971**, 815  
c. Wagner, P. J.; Ersfeld, D. A. *J. Am. Chem. Soc.* **1976**, *78*, 4515
28. a. Wagner, P. J.; Hammond, G. S. *Adv. Photochem.* **1968**, *5*, 21  
b. Turro, N. J.; Lee, C. G. *Mol. Photochem.* **1972**, *4*, 427
29. a. Kropp, P. J. *J. Am. Chem. Soc.* **1969**, *91*, 5783  
b. Agosta, W. C.; Smith, A. B. *J. Am. Chem. Soc.* **1971**, *93*, 5513
30. a. Wagner, P. J.; Hammond, G. S. *J. Am. Chem. Soc.* **1965**, *87*, 4009  
b. Dougherty, T. J. *ibid.* **1965**, *87*, 4011
31. Salem, L. *J. Am. Chem. Soc.* **1974**, *96*, 3486
32. a. Wagner, P. J. *Acc. Chem. Res.* **1983**, *16*, 461  
b. Winnik, M. A. *Chem. Rev.* **1981**, *81*, 491
33. Lewis, F. D.; Johnson, R. W.; Kory, D. R. *J. Am. Chem. Soc.* **1974**, *96*, 6100
34. Alexander, E. C.; Uliana, J. A. *J. Am. Chem. Soc.* **1974**, *96*, 6090
35. Wagner, P. J.; Meador, M. A. *J. Am. Chem. Soc.* **1983**, *103*, 4484
36. Paul, H.; Small, R. D.; Scaiano, J. C. *J. Am. Chem. Soc.* **1978**, *100*, 4520
37. Meador, M. A.; Wagner, P. J. *J. Am. Chem. Soc.* **1983**, *105*, 4484
38. a. Lappin, G. R.; Zannucci, S. J. *Org. Chem.* **1971**, *36*, 1808  
b. Pappas, S. P.; Pappas, B. C.; Blackwell, J. E., Jr. *J. Org. Chem.* **1967**, *32*, 3066  
c. Pappas, S. P.; Zehr, R. D. *J. Am. Chem. Soc.* **1971**, *93*, 7112  
d. Pappas, S. P.; Alexander, J. E.; Zehr, R. D. *J. Am. Chem. Soc.* **1974**, *96*, 6928
39. Lewis, F. D.; Johnson, R. W.; Johnson, D. E. *J. Am. Chem. Soc.* **1974**, *96*, 6090



40. Wagner, P. J. J. Photochem. 1979, 10, 387
41. Zwicker, E. F.; Grossweiner, L. J.; Yang, N. C. J. Am. Chem. Soc. 1963, 85, 2671
42. Huffman, K. R.; Lov, M.; Ullman, E. F. J. Am. Chem. Soc. 1965, 87, 5417
43. a. Chen, C. P. Ph.D. Dissertation, Michigan State University 1977  
b. Wagner, P. J.; Chen, C. P. J. Am. Chem. Soc. 1976, 98, 239  
c. Hagg, R.; Wirz, J.; Wagner, P. J. Helv. Chim. Acta 1977, 60, 2595
44. Das, P. K.; Encinas, M. V.; Small, R. D.; Scaiano, J. C. J. Am. Chem. Soc. 1979, 101, 6965
45. Matsuura, T.; Kitaura, Y. Tetrahedron 1969, 25, 4487
46. Hart, H.; Giguere, R. J. J. Am. Chem. Soc. 1983, 105, 7775
47. Hart, H.; Lin, L. -T. W. Tetrahedron Lett. 1985, 26, 575
48. Heine, H. -G. Tetrahedron Lett. 1971, 1473
49. Thomas, J. M.; Morsi, S. E.; Desvergne, J. P. Adv. Phys. Org. Chem. 1977, 15, 63
50. Turro, N. J.; Gratzel, M.; Braun, A. N. Angew. Chem., Int. Ed. Engl. 1980, 19, 675
51. Whitten, D. G.; Russel, R. C.; Schmehl, R. H. Tetrahedron 1982, 38, 2455
52. Ramamurthy, V.; Ramnath, N.; Ramesh, V. J. Photochem. 1985, 31, 73
53. a. Appel, W. K.; Greenhough, T. J.; Scheffer, J. R.; Trotter, J.; Walsh, L. J. Am. Chem. Soc. 1980, 102, 1158  
b. ibid. 1980, 102, 1160
54. Scheffer, J. R. Acc. Chem. Res. 1980, 13, 283
55. Aoyama, T.; Hasegawa, T.; Watabe, M.; Shiraishi, H.; Omote, Y. J.



- Org. Chem. 1978, 43, 419
56. Aoyama, T.; Hasegawa, T.; Omote, Y. J. Am. Chem. Soc. 1979, 101, 5343
  57. a. Wagner, P. J.; Zepp, R. G.; Liu, K.; Thomas, M.; Lee, T.; Turro, N. J. J. Am. Chem. Soc. 1976, 98, 8125  
b. Ogata, Y.; Takagi, K. J. Org. Chem. 1974, 39, 1385
  58. Scheffer, J. R.; Trotter, J.; Omkaram, N.; Evans, S. V.; Ariel, S. Mol. Cryst Liq. Cryst. 1986, 134, 169
  59. Scheffer, J. R.; Dzakpasu, A. A. J. Am. Chem. Soc. 1978, 100, 2163
  60. Appel, W. K.; Jiang, Z. Q.; Scheffer, J. R.; Walsh, L. J. Am. Chem. Soc. 1983, 105, 5354
  61. Atwood, J. L.; Davies, J. E. D.; Mac Nicol, D. D.; Eds. "Inclusion Compounds", Academic Press, London, 1984, Vol. 1-3
  62. Reddy, G. D.; Usha, G.; Ramanathan, K. V.; Ramamurthy, V. J. Org. Chem. 1986, 51, 3085
  63. a. Baretz, B. H.; Turro, N. J. J. Am. Chem. Soc. 1983, 105, 1309  
b. Turro, N. J.; Kraeutler, B.; Anderson, D. R. *ibid.* 1979, 101, 7435  
c. Turro, N. J.; Weed, G. C. *ibid.* 1983, 105, 1861  
d. Turro, N. J.; Mattay, J. J. Am. Chem. Soc. 1981, 103, 4200
  64. Frederick, B.; Johnston, L. T.; Mayo, P. D.; Wong, S. K. Can. J. Chem. 1984, 62(3), 403
  65. Wagner, P. J.; Leavitt, R. A. J. Am. Chem. Soc. 1973, 95, 3669
  66. Wagner, P. J.; Kelso, P. A.; Kemppainen, A. E.; Haug, A.; Graber, D. R. Mol. Photochem. 1970, 2, 81
  67. Stermitz, F. R.; Nicodem, D. E.; Muralidharan, V. P.; O'Donnell, C. M. Mol. Photochem. 1970, 2, 87
  68. Whitten, D. G.; Punch, W. E. Mol. Photochem. 1970, 2, 77



69. Netto-Ferreira, J. C.; Leigh, W. J.; Scaiano, J. C. *J. Am. Chem. Soc.* **1985**, 107, 2617
70. a. Binsch, G. *Top. Stereochem.* **1968**, 3, 97  
b. Ivanova, T. M.; Kugatova-Shemyakina, G. P. *Russ. Chem. Rev.* **1970**, 39, 510
71. Sandstrom, J. *Dynamic NMR Spectroscopy*, Academic Press, London **1982**, 78
72. Westheimer, F. H. "Steric Effects in Organic Chemistry", Newman, M. S. Ed., Wiley, New York, N. Y. **1956**
73. a. Allinger, N. L. *Adv. Phys. Org. Chem.* **1976**, 13  
b. Altona, C.; Farber, D. H. *Topics in Curr. Chem.* **1974**, 45, 1
74. Pappas, S. P.; Zehr, R. D.; Blackwell, Jr., J. E. *J. Heterocyclic Chem.* **1970**, 1215
75. Lewis, F. D.; Hilliard, T. A. *J. Am. Chem. Soc.* **1972**, 94, 385
76. a. Wagner, P. J.; Kelso, P. A.; Kemppainen, A. E.; Zepp, R. G. *J. Am. Chem. Soc.* **1972**, 94, 7506  
b. Meador, M. A. Ph.D. Dissertation, Michigan State University **1983**
77. Farnia, G.; Marcuzzi, F.; Melloni, G.; Sandona, G.
78. Knorr, R.; Ernst, L.; Friedrich, R.; Reibig, H. *-U. Chem. Ber.* **1981**, 114, 1592
79. Wagner, P. J.; Meador, M. A. *J. Am. Chem. Soc.* **1984**, 106, 3684
80. Measured by Dr. J. C. Scaiano at the NRC of Canada
81. Wagner, P. J. in "Creation and Detection of the Excited State", Marcel Dekker, New York, N. Y. **1971**, vol 1A, 173
82. Stothers, J. B.; Lauterbur, P. C. *Can. J. Chem.* **1964**, 42, 1563
83. Bartle, K. D.; Hallas, G.; Hepworth, J. D. *Org. Magn. Reson.* **1975**, 7,



154

84. Silverstein, R. M.; Bassler, G. C.; Morrill, T. C. "Spectrometric Identification of Organic Compounds", Wiley, New York, N. Y. 1980
85. Braude, E. A.; Sondheimer, F. J. Chem. Soc. 1955, 3754
86. Jeffe, H. H.; Orchin, M. "Theory and Applications of Ultraviolet Spectroscopy", John Wiley and Sons, Inc. Fourth Printing 1966, 415
87. a. Rutherford, K. G.; Wassenaar, S.; Brien, J. F.; Fung, D. P. C. Can. J. Chem. 1971, 49, 4116
- b. Tournier, H.; Longeray, R.; Dreux, J. Bull. Soc. Chim. Fr. 1972, 3216
88. a. Scheffer, R. J. Acc. Chem. Res. 1980, 13, 283
- b. Lowry, T. H.; Richardson, K. S. "Mechanism and Theory in Organic Chemistry", Harper & Row Publishers, New York, 2<sup>nd</sup> Ed. 1981, 569
89. Scaiano, J. C.; Leigh, W. J.; Meador, M. A.; Wagner, P. J. J. Am. Chem. Soc. 1985, 107, 5806
90. Clark, W. D. K.; Litt, A. D.; Steel, C. Chem. Commun. 1969, 1087
91. Lutz, H.; Lindgust, L. Chem. Commun. 1971, 493
92. Scaiano, J. C.; Wagner, P. J. J. Am. Chem. Soc. 1984, 106, 4626
93. Wagner, P. J.; Kochever, I.; Kemppainen, A. E. J. Am. Chem. Soc. 1972, 94, 7489
94. See the discussion of photoenolization of  $\alpha$ -(triisopropylphenyl)acetophenone in this thesis
95. a. Biali, S. E.; Rappoport, Z. J. Am. Chem. Soc. 1985, 107, 1007
- b. Kaftory, M.; Biali, S. E.; Rappoport, Z. J. Am. Chem. Soc. 1985, 107, 1701
96. Saltiel, J. Org. Photochem. 1972, 3, 1







97. a. Saltiel, J. J. Am. Chem. Soc. 1967, 89, 1036  
b. Saltiel, J. J. Am. Chem. Soc. 1968, 90, 6394  
c. Hammond, G. S.; Sattlel, J.; Lamola, A. A.; Turro, N. J.; Pradshaw, J. S.; Cowan, R. C.; Vogt, V.; Dalton, C. J. Am. Chem. Soc. 1964, 86, 3197
98. Hart, H. Private Communication
99. Cohen, S, G.; Stein, N.; Chao, H. M. J. Am. Chem. Soc. 1968, 90, 521
100. Davidson, R. S.; Lambech, P. F. Chem Commun. 1968, 511
101. Wagner, P. J.; Truman, R. J.; Puchalski, A. E.; Wake, R. J. Am. Chem. Soc. 1986, 108, 7727
102. Walling, C.; Gibian, M. J. J. Am. Chem. Soc. 1974, 96, 5644
103. Gordon, A. J.; Ford, R. A. "The Chemist's Companion", Wiley, New York, N. Y. 1972
104. Perrin, D. D.; Armarego, W. L. F.; Perrin, D. R. "Purification of Laboratory Chemicals", 2<sup>nd</sup> Ed., Pergamon Press, FGR 1980
105. Siebert, E. J. Ph.D. Dissertation, Michigan State University 1981
106. Nahm, K. Ph.D. Dissertation, Michigan State University 1987
107. Wagner, P. J.; Kemppainen, A. E. J. Am. Chem. Soc. 1968, 90, 5896
108. J. Am. Chem. Soc. 1976, 98, 6232
109. Cavaleriro, J. A. S.; Kenner, G. W.; Smith, K. M. J. Chem. Soc. Perkin I 1974, 1188
110. Olsen, R. Private Communication
111. Fuson, R. C.; Armstrong, L. J.; Chadwick, D. H.; Kneisley, J. W.; Rowland, S. R.; Shenk, W. J.; Soper, Q. F. J. Am. Chem. Soc. 1945, 67, 386
112. Wyman, D. P.; Kanfman, P. R. J. Org. Chem. 1964, 29, 1956
113. Lutz, R. E.; Hinkley, D. F. J. Am. Chem. Soc. 1950, 72, 4091



114. Fuson, R. C.; Corse, J.; McKeever, C. H. J. Am. Chem. Soc. 1940, 62, 3250
115. Fonken, G. S.; Johbson, W. S. J. Am. Chem. Soc. 1952, 74, 831
116. Mcloskey, A. C.; Fonken, G. S.; Kluiber, R. W.; Johnson, W. S. Org. Syn., Rev. Ed. 4, 261
117. Mcwilliam, D. C.; Balasubramanian, T. R.; Kuivila, H. G. J. Am. Chem. Soc. 1978, 100, 6407
118. Luh, T. Y.; Lee, K. S.; Tam, S. W. J. Organomet. Chem. 1981, 219(3), 345